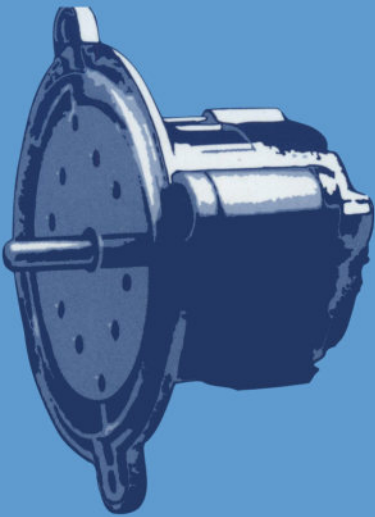
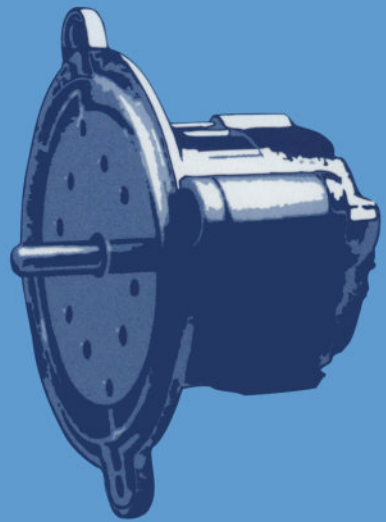




POWER AND ENERGY SERIES 26

SMALL ELECTRIC MOTORS



**Helmut Moczala,
Jürgen Draeger,
Hermann Krauß,
Helmut Schock and
Siegfried Tillner**

The Institution of Electrical Engineers

IEE POWER AND ENERGY SERIES 26

Series Editors: Professor A. T. Johns
Dr A. Ter-Gazarian
D. F. Warne

SMALL ELECTRIC MOTORS

Other volumes in this series:

- Volume 1 **Power circuits breaker theory and design**
C. H. Flurscheim (Editor)
- Volume 2 **Electric fuses** A. Wright and P. G. Newbery
- Volume 3 **Z-transform electromagnetic transient analysis in high-voltage networks** W. Derek Humpage
- Volume 4 **Industrial microwave heating** A. C. Metaxas and R. J. Meredith
- Volume 5 **Power system economics** T. W. Berrie
- Volume 6 **High voltage direct current transmission** J. Arrillaga
- Volume 7 **Insulators for high voltages** J. S. T. Looms
- Volume 8 **Variable frequency AC motor drive systems** D. Finney
- Volume 9 **Electricity distribution network design** E. Lakervi and E. J. Holmes
- Volume 10 **SF₆ switchgear** H. M. Ryan and G. R. Jones
- Volume 11 **Conduction and induction heating** E. J. Davies
- Volume 12 **Overvoltage protection of low-voltage systems** P. Hasse
- Volume 13 **Statistical techniques for high-voltage engineering**
W. Hauschild and W. Mosch
- Volume 14 **Uninterruptible power supplies** J. D. St. Aubyn and J. Platts (Editors)
- Volume 15 **Principles of digital protection** A. T. Johns and S. K. Salman
- Volume 16 **Electricity economics and planning** T. W. Berrie
- Volume 17 **High voltage engineering and testing** H. M. Ryan (Editor)
- Volume 18 **Vacuum switchgear** A. Greenwood
- Volume 19 **Electrical safety: a guide to the causes and prevention of electrical hazards** J. Maxwell Adams
- Volume 20 **Electric fuses, 2nd Edn.** A. Wright and P. G. Newbery
- Volume 21 **Electricity distribution network design, 2nd Edn.**
E. Lakervi and E. J. Holmes
- Volume 22 **Artificial intelligence techniques in power systems**
K. Warwick, A. Ekwue and R. Aggarwal (Editors)
- Volume 23 **Financial and economic evaluation of projects in the electricity supply industry** H. Khatib
- Volume 24 **Power system commissioning and maintenance practice**
K. Harker
- Volume 25 **Engineers' handbook of industrial microwave heating**
R. J. Meredith

SMALL ELECTRIC MOTORS

Prof. Dr.-Ing. Helmut Moczala

Prof. Dr.-Ing. Jürgen Draeger

Prof. Dr.-Ing. Hermann Krauß

Dipl.-Ing. Helmut Schock

Dipl.-Ing. Siegfried Tillner

Translated by Eur. Ing. D. H. Hopewell

English edition published by: The Institution of Electrical Engineers,
London, United Kingdom

English edition © 1998: The Institution of Electrical Engineers

Elektrische Kleinmotoren
originally published in German by Expert Verlag, 1987

German edition © 1987: Expert Verlag, 7044 Ehningen bei Böblingen, Germany

This publication is copyright under the Berne Convention and the Universal Copyright Convention. All rights reserved. Apart from any fair dealing for the purposes of research or private study, or criticism or review, as permitted under the Copyright, Designs and Patents Act, 1988, this publication may be reproduced, stored or transmitted, in any forms or by any means, only with the prior permission in writing of the publishers, or in the case of reprographic reproduction in accordance with the terms of licences issued by the Copyright Licensing Agency. Inquiries concerning reproduction outside those terms should be sent to the publishers at the undermentioned address:

The Institution of Electrical Engineers,
Michael Faraday House,
Six Hills Way, Stevenage,
Herts. SG1 2AY, United Kingdom

While the authors and the publishers believe that the information and guidance given in this work is correct, all parties must rely upon their own skill and judgment when making use of it. Neither the author nor the publishers assume any liability to anyone for any loss or damage caused by any error or omission in the work, whether such error or omission is the result of negligence or any other cause. Any and all such liability is disclaimed.

The moral right of the authors to be identified as authors of this work has been asserted by him/her in accordance with the Copyright, Designs and Patents Act 1988.

British Library Cataloguing in Publication Data

A CIP catalogue record for this book
is available from the British Library

ISBN 0 85296 921 X

Printed in England by Redwood Books, Trowbridge

Contents

Foreword	xiii
Acknowledgments	xv
1 Drives with small motors	1
<i>H. Moczala</i>	
1.1 Economic significance of small motors	3
1.2 Small motors and driven devices	4
1.3 Demands on small motors	9
1.3.1 Compatibility with the energy source	9
1.3.2 Torque	9
1.3.3 Speed	9
1.3.4 Efficiency	10
1.3.5 Maintenance	10
1.3.6 Motor construction	10
1.3.7 Mechanical vibrations	11
1.3.8 Interference fields	11
1.3.9 Price	11
1.4 Function principles of small motors	11
1.5 Overview of small motors	14
2 Operation of the multiphase induction motor	17
<i>J. Draeger</i>	
2.1 Introduction	17
2.2 Operation of the induction machine	18
2.2.1 Rotating and alternating fields	18
2.2.2 Derivation of a rotating field from a polyphase winding	21
2.2.3 Torque generation	23

2.2.3.1	Uniform rotating field	23
2.2.3.2	Elliptic rotating fields	28
2.2.4	Current characteristics	29
2.2.5	Speed control possibilities	34
2.3	Single-phase motors	37
2.3.1	Externally started motor	37
2.3.2	Motor with a resistive auxiliary winding	38
2.3.3	The capacitor start and run motor (csar motor)	39
2.3.3.1	The two-winding motor	39
2.3.3.2	Three-winding motors	42
3	Operation and application of polyphase induction motors	45
	<i>S. Tillner</i>	
3.1	Introduction	45
3.2	The two-winding csar motor	47
3.2.1	Theoretical principles	47
3.2.2	Operating characteristics of a two-winding csar motor	51
3.2.3	Motors with input voltage selection	54
3.3	The three-winding csar motor	55
3.4	Choice between the two-winding and three-winding motor	55
3.5	In-service supply voltage tolerances	56
3.6	Comparison of csar motor and 3-phase motor	57
3.7	Motors with starter windings	57
3.7.1	Run-up characteristics of the resistive auxiliary phase motor	58
3.7.2	Starting characteristics of capacitor-start motors	59
3.7.3	Double capacitor motors	61
3.8	Application of multiwinding induction motors	61
3.8.1	Motors for central heating circulating pumps	61
3.8.2	Washing machine drives	61
3.8.3	Main drives for photocopiers	64
3.8.4	Oil-burner motors	64
4	Shaded-pole induction motors	65
	<i>S. Tillner</i>	
4.1	Introduction	65
4.2	Operation of the shaded-pole motor	65
4.3	Field distribution and harmonic fields	67
4.4	Construction of shaded-pole motors	69
4.5	Operational performance of shaded-pole motors	70
4.5.1	Operating characteristics and technical data	70
4.5.2	Comparison of the operating characteristics of the shaded-pole motor and the capacitor start and run induction motor (csar motor)	72
4.5.3	Losses and efficiency	72

4.6	Design and dimensioning of shaded-pole motors	73
4.6.1	Winding conformity	73
4.6.2	Influence of the rotor resistance	75
4.6.3	Shaded-pole arc and shaded-pole winding resistance	75
4.7	Applications of shaded-pole motors	75
4.7.1	Applications of shaded-pole motors with unsymmetrical construction	76
4.7.2	Shaded-pole motors as fan motors	77
4.7.3	Shaded-pole motors for washing machine spinners	78
5	Synchronous motors	81
	<i>H. Moczala</i>	
5.1	Summary of possible synchronous motor constructions	81
5.2	Permanent magnets	83
5.2.1	The permanent magnetic circuit	83
5.2.2	Permanent magnetic materials	84
5.3	Principles of synchronous motor function	85
5.3.1	Motors with permanent magnet rotors	85
5.3.2	Motors with hysteresis rotors	88
5.3.3	Motors with reluctance rotors	90
5.4	Construction of synchronous motors	90
5.4.1	Motors with permanent magnet rotors	90
5.4.2	Motors with hysteresis rotors	96
5.4.3	Motors with reluctance rotors	96
5.5	Characteristics	98
5.6	Applications	101
6	Universal motors	103
	<i>J. Draeger</i>	
6.1	Introduction	103
6.2	Construction	103
6.3	Operating principles	106
6.3.1	Magnetic flux distribution	106
6.3.2	Induced voltages and terminal voltage	108
6.3.3	Torque and power	109
6.3.4	Commutation	111
6.3.5	Brushes	114
6.4	Operational performance	115
6.4.1	Operating characteristics	115
6.4.2	Speed control	117
6.4.2.1	Variation of the terminal voltage U	117
6.4.2.2	Changing the supply frequency f	118
6.4.2.3	Changing the excitation flux ϕ_{lh} through field winding taps	118
6.4.2.4	Changing the series resistance $R_A + R_E$	119

6.5	Radio–TV interference	120
6.6	Applications	120
7	Direct current motors	123
	<i>H. Moczala</i>	
7.1	Basic principles	123
7.2	Direct current linear motors without commutators	124
	7.2.1 Operating performance	124
	7.2.2 Types of construction	125
7.3	Rotating direct current motors	128
	7.3.1 Principal construction	128
	7.3.2 Operating performance	129
	7.3.3 Armature reaction	133
	7.3.4 Commutation	134
	7.3.5 Speed control	135
	7.3.6 Rotating direct current motor designs	135
	7.3.6.1 Motors with standard forms of construction	135
	7.3.6.2 Motors with flux concentration	137
	7.3.6.3 Motors with cup rotors	137
	7.3.6.4 Motors with disc rotors	138
7.4	Properties	141
7.5	Applications	142
8	Electronic circuits for small electric motors	145
	<i>H. Schock</i>	
8.1	Introduction	145
8.2	Active electronic components for driving motors	145
	8.2.1 Diodes	146
	8.2.2 Thyristors	146
	8.2.2.1 The thyristor	146
	8.2.2.2 GTO (gate turnoff thyristor)	147
	8.2.2.3 MCT (MOS controlled thyristor)	147
	8.2.2.4 Triac, diac	147
	8.2.3 Transistors	148
	8.2.3.1 Bipolar transistors	148
	8.2.3.2 Unipolar (MOS) transistors	150
	8.2.3.3 IGBT	151
	8.2.4 Integrated circuits	153
8.3	Motor control	154
	8.3.1 Circuits with alternating voltage	154
	8.3.2 Direct current circuits	155
8.4	Examples	159
	8.4.1 Control circuit for a bipolar two-winding stepper motor	159
	8.4.2 Washing machine controller	162

9	Brushless direct current motors	165
	<i>H. Moczala</i>	
9.1	Technical solutions for brushless direct current motors	165
9.2	Principal construction and behaviour	166
9.3	Types of construction	173
9.3.1	Design variants	173
9.3.2	Motor windings and energising circuits	174
9.3.3	Position indicators	176
9.3.4	Speed setting and control	177
9.4	Motor designs and constructions	178
9.4.1	Internal rotor motors and airgap windings	178
9.4.2	Internal rotor motor with slotted stator	181
9.4.3	Motors with disc stators	183
9.4.4	Two-coil motors	185
9.4.5	Linear motors	187
9.5	Properties	190
9.6	Applications	192
9.7	Outlook	193
10	Stepper motors – principles and applications	197
	<i>H. Krauss</i>	
10.1	Introduction	197
10.2	Modes of operation	198
10.2.1	Principle of function	198
10.2.2	Static performance of stepper motors	199
10.2.2.1	Static torque curve	199
10.2.2.2	Step angle accuracy	202
10.2.3	Dynamic performance	204
10.2.3.1	Torque/step frequency performance	204
10.2.3.2	Acceleration and braking	206
10.2.3.3	Optimal frequency for average velocities	208
10.2.3.4	Single step and step sequence	210
10.2.3.5	Stopping the stepper motor	212
10.3	Electrical control circuitry	214
10.3.1	Methods of control	214
10.3.1.1	Unipolar drive	214
10.3.1.2	Bipolar drive	215
10.3.1.3	Five-phase motor drive	217
10.3.2	Semiconductor power switch with inductive load	217
10.3.3	Control circuits	219
10.3.3.1	Switching stages	219
10.3.3.2	Circuits for producing the switching sequences	222
10.3.3.3	Control circuits for acceleration and braking	222
10.3.3.4	Digital step sequence control	223

10.3.3.5	Stepper motor with closed-loop drive	225
10.3.3.6	Step division – microstep drive	225
10.4	Basic system for stepper motor drives	227
10.4.1	Drives with the facilities of acceleration, braking, variable stepping frequency and reversibility	227
10.4.2	Positioning drive in combination with a counter	227
10.4.3	Drive with step frequency variation via a voltage/frequency converter	228
10.4.4	Drive with microprocessor control	229
10.5	Choice criteria for stepper motors	229
10.5.1	Forms of construction	229
10.5.1.1	Two-stator motor	229
10.5.1.2	Hybrid stepper motor	230
10.5.1.3	Construction of a 5-phase hybrid stepper motor	231
10.5.1.4	Disc magnet stepper motors	232
10.5.2	Example of choosing a stepper motor	234
10.6	Summary of important stepper motor concepts	235
11	Measurements in small drive systems	241
	<i>J. Draeger</i>	
11.1	Introduction	241
11.2	Sampling functions	242
11.3	Current, voltage, power	243
11.4	Speed of rotation	246
11.4.1	Analogue speed measurement	246
11.4.2	Incremental rotation measurement	246
11.5	Torque	251
11.5.1	Total loss methods	254
11.5.2	Direct methods	256
11.5.3	Indirect methods	259
11.6	Mechanical power	260
11.7	Temperature	261
11.8	Interference field strength	261
12	Vibration and noise problems in small drives	263
	<i>J. Draeger</i>	
12.1	Introduction	263
12.2	Sound field quantities	263
12.3	Subjective sensitivity to noise	267
12.4	Noise measurement	268
12.5	Vibration (oscillation) measurement	270
12.6	Vibration and noise excitation	273
12.7	Vibration and noise reduction	276

12.7.1 Methods at the noise source	276
12.7.2 Insulation and vibration isolation	276
12.7.3 Sound damping	280
12.7.4 Technical solutions	283
Index	287

Foreword

Small electric motors are installed as drive elements in many types of consumer equipment and also in the industrial sector, and increasingly find application in almost all branches of industry for manufacture. Their purpose is to reduce manual labour and increase comfort, as well as enabling rationalisation in industry. Their maximum output power is regarded in most instances as being around 1kW. In this power range the small motor manufacturer offers a wide variety of special motors to meet the requirements of many different driven devices. Technical knowledge of small motors is extensive. It has led to high quality small drives and also to a large number of different kinds of motor.

This makes it impossible in my view to produce in one volume an account that has any claim of being complete. If the material is reduced to its essential minimum, however, a selection should be possible such that the widest possible area of interest may be addressed. The number of small motor specifiers is large, and it is principally for these people that the book has been written. For those specialists whose concern is the development, manufacture or marketing of small motors, a comprehensive overview is provided here, stretching beyond the confines of their individual specialisations.

Through numerous well attended series of lectures on small electrical machines at the Technical Academy Esslingen a lively interest was established, not least because the lectures were aimed at a large number of motor specifiers and users. The experience and stimulation derived from those lectures contributed significantly to the production of this book.

It is well recognised that much effort is being put into the development of new types of drive elements which may be listed under the general heading of 'actuators'. Actuators operate in accordance with various physical or chemical principles but are still very much in the development phase. Therefore, this book is restricted to a study of small electrical machines that

work on electro-dynamic principles and are generally mass-produced. The various function principles of small motors, summarised in Fig. 1.9, form the basis for the division of material for study: Chapters 2–5 discuss rotating field machines, and 6 and 7 commutator machines. Present developments, in particular the increasing involvement of electronics, are treated in the Chapters on electronic components, brushless DC motors and stepper motors.

In this book the relationship between the motor and its driven load is kept constantly in view. The final two Chapters are concerned with measurements and noise problems. The depth of treatment, which is limited by space restrictions, has been gauged to suit the requirements of the specifier user. Sufficient information is given about physical principles with mathematical support to enable the selection of the appropriate motor for the application, taking into account the demands of the driven devices, reliability, safety and at the same time the cost-effectiveness of the choice. The individual Chapters of the book have been written independently by specialists. Although indispensable standards were laid down, the differing styles of the authors are quite clearly recognised. The resultant nonuniformity seems to me to be a small price to pay for the advantage of having up to date material from the best informed sources.

This book is the second edition. Although the original is only five years old, rapid technical change has made necessary the revision, extension and sometimes complete replacement of many of the sections.

Finally, I should like to thank my co-authors for their constructive co-operation. In spite of the demands of their professional employment they were always prepared to contribute to the lectures at the Technical Academy Esslingen, to keep their subjects up to date and to produce their sections for the book.

Helmut Moczala
Meschede

Acknowledgments

Translator's acknowledgments

I would like to thank my wife, Margaret, for her patience and for her acceptance of the delay in what should have been my retirement, and for helping me with the frustrating and tedious, but necessary, task of renumbering the index. I also thank Mrs Angela Bergmann, translator/interpreter for ABB Automatisierungsanlagen Cottbus GmbH, for her invaluable help with typing and checking the more difficult passages, and without whose involvement and encouragement this project would certainly have been abandoned.

Publisher's acknowledgment

The publisher would like to acknowledge the contribution of John G. W. West, Consulting Engineer, in reviewing this translation.

Chapter 1
Drives with small motors

Helmut Moczala

Small electric motors are devices used in drives in the power range up to about 10^3 W. In this book the distinction found elsewhere between small and miniature motors is not made. Even the 10^3 W value given above does not represent an absolute limit. For example, brushless direct current (DC) motors are now manufactured with power ratings up to 2×10^5 W.

There is a wide variety of small motors, each design being tailored to meet the special demands made by the driven device. In this way these motors are in contrast with high powered motors, particularly 3-phase induction motors, which are largely built to standard specifications.

Small motors work according to various function principles, and motors which work according to a given principle have many application-orientated forms of construction. For example, single-phase capacitor start and run (csar) motors are used for driving, amongst many other things, oil burners and central heating pumps. Because of the quite different needs of the devices being driven, the motor constructions are distinctly different, even for motors which have the same power rating and which run at the same speed.

The oil-burner motor (Figure 1.1) is characterised by its short length that makes for a compact burner unit. After the blower wheel has been mounted on the motor shaft, it can be mounted directly onto the burner housing via the large flange. The bearing housing at the nondrive end is formed to enable the mounting of the oil pressure pump. Ball bearings ensure long running, low maintenance service.

Central heating circulating pumps have weak points owing to the necessary pump seals. These weak points can be avoided by a special design of pump motor (Figure 1.2). As can be seen in the cross-sectional drawing of Figure 1.3, motor rotor 1 is totally surrounded by the circulating water. Stator 3, however, is reliably isolated from the water by split casing 3, which extends from the motor flange through to the nondrive end. In this way the need for

2 *Small electric motors*

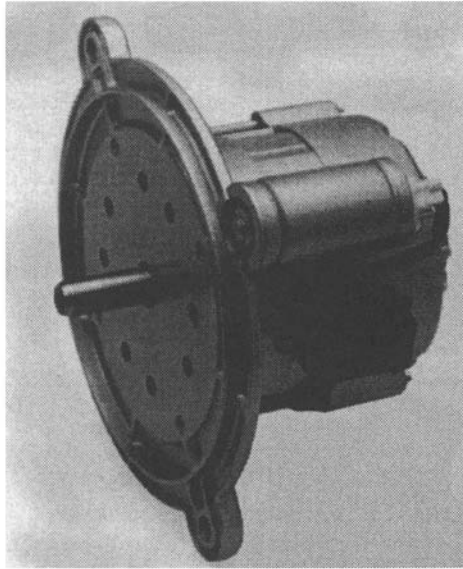


Figure 1.1 Oil-burner motor (35 W, 2800 rev/min) with the start and run capacitor mounted on the flange

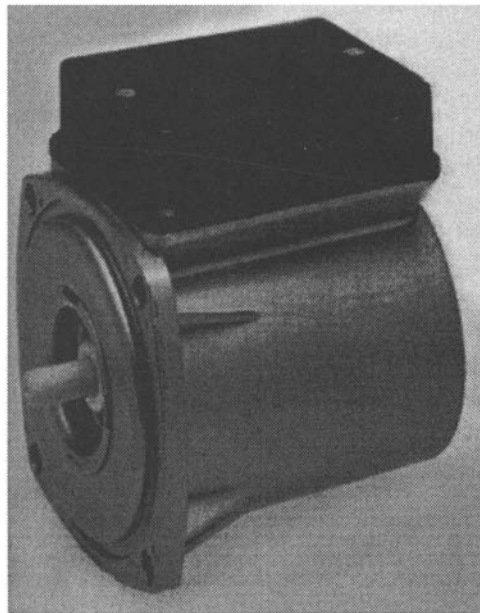


Figure 1.2 Motor for central heating water pump (50 W, 2400 rev/min) with start and run capacitor in attached compartment
(Courtesy: AEG)

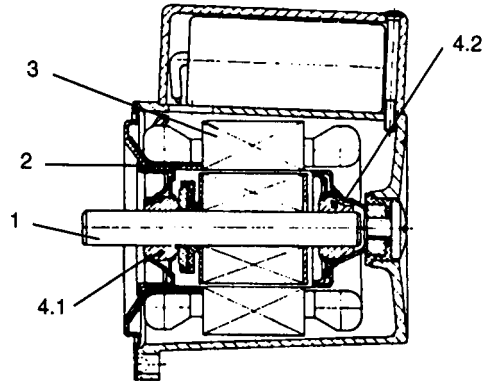


Figure 1.3 Longitudinal section through a central heating water pump motor.

- | | |
|----------------|--------------------------|
| 1 motor rotor | 3 stator |
| 2 split casing | 4 self aligning bearings |
- (Courtesy: AEG)

failure-prone, sliding contact seals is avoided and all seals are between nonmoving parts. The rotor must, of course, be corrosion-resistant to the hot water. The ceramic self-aligning bearings 4.1 and 4.2 are lubricated by the hot water.

As the above example indicates, the optimum solution to a drive problem calls for consideration of the driving motor and the driven device, i.e. the complete drive, as a single unit.

1.1 Economic significance of small motors

The development and construction of special small motors for various applications is in most cases viable only when these special motors can be sold in large quantities. There is in fact a huge market for these motors because small motors are found in all branches of industry and in many households. It is not difficult to identify 20 to 30 small motor applications in the average household, ranging from electric toothbrushes to washing machines to central heating pumps.

The production value of all electric motors – and accessories – in the year 1990 in the former West Germany amounted to 6.77×10^9 DM. The proportion of small motors (polyphase AC motors < 375 W, single-phase AC motors, universal motors and DC motors < 375 W) accounted for 2.58×10^9 DM or 38%. As the production value chart (Figure 1.4) shows, small motors in 1975 accounted for 0.97×10^9 DM or 25% of the total of all rotating machines – motors and generators – being manufactured. In particular, the development of DC motors has taken the market by storm in the intervening time.

4 Small electric motors

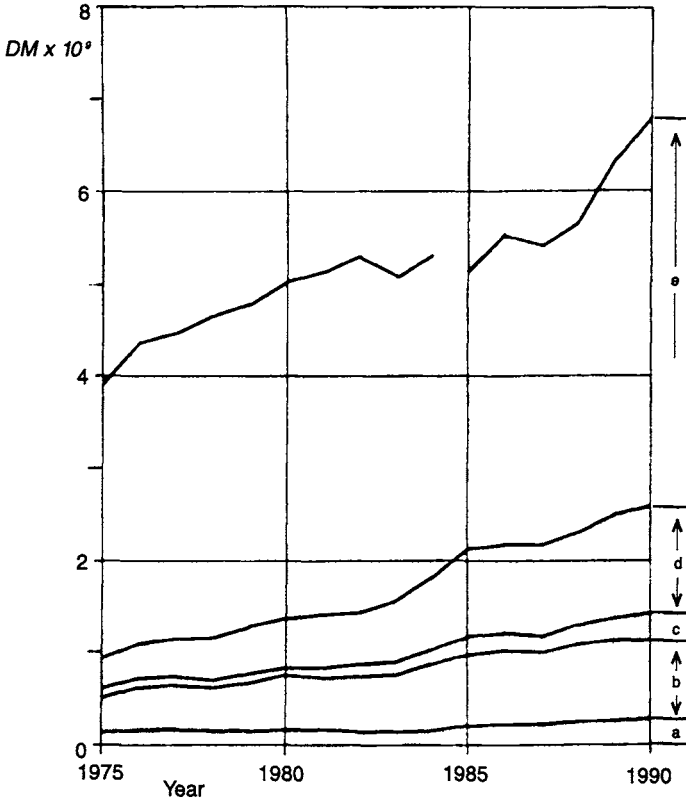


Figure 1.4 Production value of electric motors in former West Germany from 1975 to 1990

- a polyphase AC motors;
- b single phase AC motors;
- c universal motors;
- d DC motors;
- e total

(Source: ZVEI, Fachverband Elektrische Antriebe)

In 1990 there were 74.4 million small motors manufactured, compared with 41 million in 1975 (Figure 1.5). The average price per unit in 1990 was about 34.7 DM.

1.2 Small motors and driven devices

Small motors are conceived as converters that change the electrical energy delivered to the terminals into mechanical energy to be transferred to the driven device via the motor shaft. Because the efficiency of these processes involving small motors is usually much less than 100%, the motor delivers, in

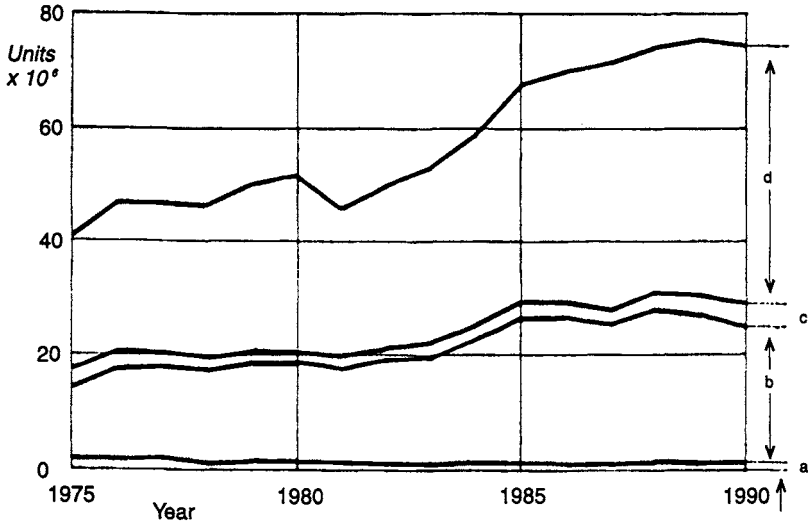


Figure 1.5 Production quantities of small electric motors in former West Germany from 1975 to 1990

- a polyphase AC motors < 375 W;
- b single phase AC motors;
- c universal motors;
- d DC motors < 375 W

(Source: ZVEI, Fachverband Elektrische Antriebe)

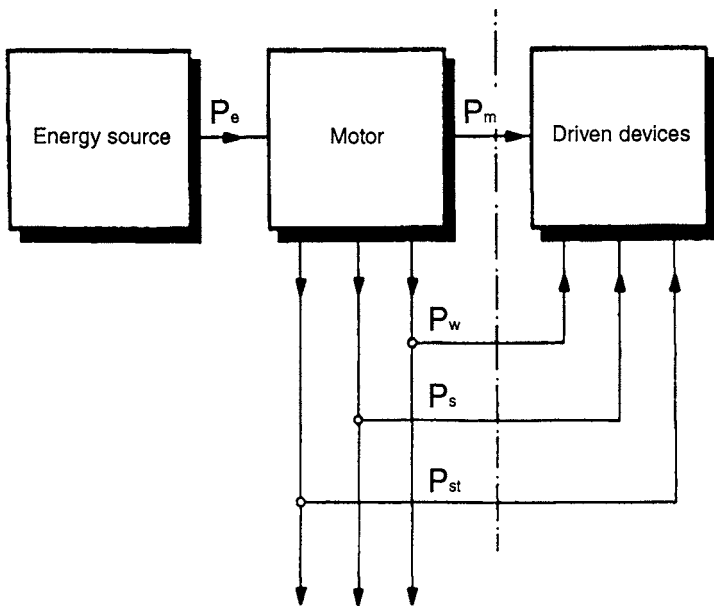


Figure 1.6 Energy flow between source, motor, driven devices and surroundings

6 Small electric motors

addition to the mechanical power P_m , energy in the form of heat, sound and mechanical vibrations, and electrical and magnetic alternating fields.

For a small drive (Figure 1.6) all forms of energy output from the motor must be taken into account. For the motor:

$$P_e = P_m + P_w + P_s + P_{st} \quad (1.1)$$

in which

P_e = input power to the motor

P_m = shaft output mechanical power

P_w = heat loss

P_s = sound and vibration loss

P_{st} = output interference electric and magnetic field power.

The motor efficiency is derived from the mechanical shaft output power

$$\eta = \frac{P_m}{P_e} \quad (1.2)$$

The mechanical output power is related to speed n_m and torque M_m :

$$P_m = 2\pi n_m M_m = \omega_m M_m \quad (1.3)$$

where the quantity ω_m is called the angular velocity, and

$$\omega_m = 2\pi n_m \quad (1.4)$$

The mechanical power from the motor, after the end of the start and run-up process, is equal to the power absorbed by the driven device P_i :

$$P_m = \omega_m M_m = P_i = \omega_i M_i \quad (1.5)$$

When the interconnection between motor and load is such that there is no speed transformation, then:

$$\omega_m^* = \omega_i^* \quad (1.6)$$

$$M_m^* = M_i^* \quad (1.7)$$

Every driven device (load) has a torque requirement M_i which is dependent on the angular velocity ω_i . In Figure 1.7 the $M_i(\omega_i)$ characteristic of a fan is shown as a broken line. In this case the torque requirement M increases with the square of the angular velocity ω_i . The motor also has a characteristic torque M_m as a function of angular velocity ω_m , as is shown in Figure 1.7 for the $M_m(\omega_m)$ characteristic of a shaded-pole motor by the continuous curve.

The fan previously mentioned is to be coupled to the output shaft of this motor. At the instant of switching on the power the run-up starts with $\omega_m = \omega_i = 0$. Because at first the motor torque M_m is greater than the load's requirement M_i , the angular velocity $\omega_m (= \omega_i)$ increases in accordance with the basic mechanical law

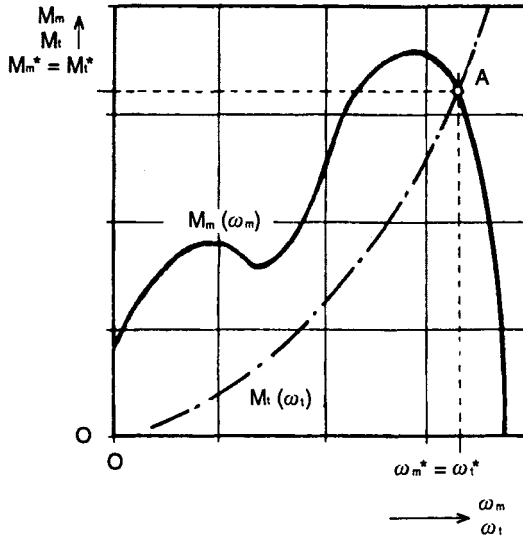


Figure 1.7 Characteristic $M_t(\omega_t)$ of a fan (broken line) and characteristic $M_m(\omega_m)$ of a shaded-pole motor (continuous line)

$$J \frac{d\omega_m}{dt} = M_m - M_t \tag{1.8}$$

where J is the total moment of inertia of the rotating system with reference to the motor shaft.

The starting phase is over when $d\omega_m/dt$ becomes zero, and the steady-state condition of eqn. 1.7 is satisfied.

In Figure 1.7 the steady state shown is the stable working point A, which is at the intersection of the drive and load characteristic curves.

Figure 1.8 shows the interaction of the shaded-pole motor already discussed and a fan with a greater torque input requirement. Here we see three intersections of the motor and fan characteristics: B, C and D. Following the previous considerations, a run-up from standstill can only reach point B. If the motor torque is increased afterwards by, say, increasing the input voltage, the motor speed is increased and point D can be reached and held after the removal of the overvoltage. A drive with characteristics as in Figure 1.8a is unsatisfactory because two working points B and D are possible. Working point C cannot be achieved and held because it is unstable. The slightest change in load torque causes the speed to rise to point D or to fall to point B.

The $M_m(\omega_m)$ characteristics depict the average torques of time-varying cyclic functions. Figure 1.8b shows, for example, the instantaneous torque (over ~13 ms at 50 Hz) transferred from the stator to the rotor of a shaded-pole motor running at working point E (see Figure 1.8a). In addition to the

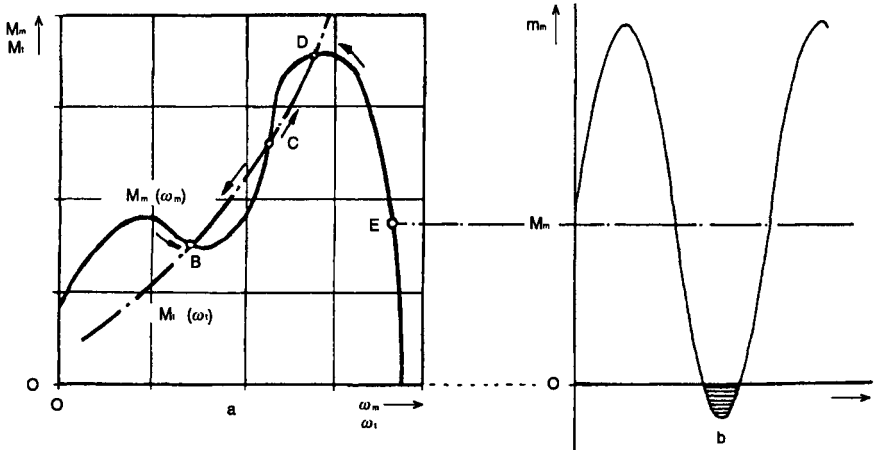


Figure 1.8 (a) Characteristic $M_f(\omega)$ of a fan (broken line) and the characteristic $M_m(\omega_m)$ of a shaded-pole motor (continuous line); (b) instantaneous value $m_m(t)$ of the torque of a shaded-pole motor at operating point E

average torque M_m there are also strong vibration torques at double the mains frequency that can be large enough to produce short duration braking torques (shaded area). Because of the drive moments of inertia, these torque vibrations have only a small effect on the speed of rotation.

In the power balance of the motor (see eqn. 1.1) the second term after the mechanical power P_m is the heat loss P_w . P_s and P_{st} may be considered to be negligible in the power balance equation because

$$P_w \gg P_s + P_{st} \tag{1.9}$$

Therefore the equation for heat loss simplifies to:

$$P_w = P_e - P_m = P_e(1 - \eta) \tag{1.10}$$

That part of the input power which is not converted into mechanical power is considered to be lost as heat.

The heat loss in the motor leads to additional heating of the driven device, particularly so when the drive is totally enclosed. Also, as a safety measure, it must be ensured that a temperature rise does not cause damage to the motor or the driven device.

Although the powers involved in the mechanical and acoustic vibration and in the electric and magnetic fields are numerically negligible, their effects on the driven load can be a severe nuisance.

Mechanical vibrations in the motor originating from alternating magnetic forces, rotor dynamic imbalance, vibrating bearing housings, etc. contribute only minimally to the acoustic power radiated from the motor surface. Far more serious is the disturbance caused in the driven load owing to vibrations in sympathy with those generated in the motor, giving rise to increased noise.

Magnetic and electric AC fields generated in the motor, although of low intensity, can cause severe interferences in sensitive pick-up devices (e.g. gramophone or magnetic heads) that, together with pre-amplifiers, form a part of the driven system.

1.3 Demands on small motors

From the above considerations the demands that must be made of small motors may be listed. The following is a summary of the more important considerations:

1.3.1 Compatibility with the energy source

The following energy sources are available for small motors:

- AC mains
- DC mains, particularly in vehicles
- batteries and accumulators for mains-independent drives.

AC mains delivers voltages from 110 V to 240 V at 50 Hz or 60 Hz. In most cases only single-phase connection is possible; only in special cases is a 3-phase supply available. Small motors must be formed so that they work acceptably given input voltages which range from -15% to $+6\%$ relative to their rated voltages.

DC motors are powered conveniently from voltages between 5 V and 24 V. In mains-independent drives it should be noted that the use of dry batteries is only economic if the batteries can be discharged down to 60% of their initial voltage.

1.3.2 Torque

A small motor must not only develop the necessary starting torque, but it must also provide torque during the run-up in excess of the load torque requirement in order to enable a rapid run-up. If there is a saddle in the motor torque speed curve, the lowest point of the saddle must be greater than the load torque at that speed. Otherwise the system will be 'left hanging' at a speed lower than that intended. Load friction is much greater at low temperatures owing to the viscosity/temperature characteristic of the lubricant. This fact must be taken into account when the starting performance is being calculated.

1.3.3 Speed

In rotating field motors the speed n_m is related to the AC supply frequency f and the number of pole pairs p in the motor. The equation for the synchronous speed n_s

$$n_s = \frac{f}{p} \quad (1.11)$$

is applicable.

Consequently only certain specific synchronous speeds are attainable. For the higher power motors $p = 1$ or 2 , i.e. 2- or 4-pole designs are preferred, whilst for lower power applications higher numbers of pole pairs attract greater interest.

Rotating field motors are not judged by their speed only, but by their dependence on supply voltage and load torque. When the demand for constant speed is high, synchronous motors are used, whose rotors turn in synchronism with the rotating field.

Commutator motors can be constructed for rotating at any reasonable speed. They are also of interest when AC supplies are used and high power can be achieved through high speed. Demands for constant speed can be met by incorporating mechanical or electronic control systems.

1.3.4 Efficiency

High efficiencies are not normally demanded from AC motors on account of the relatively low cost of the energy supplied. On account of dwindling energy resources, however, this view is being reconsidered. Nevertheless, when the driven load can withstand only a limited amount of heat flow from the AC motor, the motor efficiency may not be allowed to fall below a minimum value. The requirements from DC motors are quite different, when they are supplied from batteries. On account of the very high cost of battery energy, high efficiency is expected from these motors.

1.3.5 Maintenance

In general small motors should not require maintenance. Therefore they must have the same life expectancy as the driven load. The lifetime of a rotating field motor is that of its bearings. An expectancy of 10^4 h from motors fitted with plain bearings is quite normal. Brushes and commutators determine the lifetime of commutator motors. When the requirements are high the mechanical commutation may be replaced by systems using electronic components.

1.3.6 Motor construction

The motor should be as small and light as possible for its task. The materials used must withstand the temperature stresses adequately. Climatic influences – humidity, in particular – must not be allowed to have corrosive effects that detract from the performance of the motor.

1.3.7 Mechanical vibrations

A very low noise level is demanded from many kinds of drive. It is not absolutely necessary to provide a low vibration expensive motor. It is often more appropriate to fit an economically priced motor whose disturbing mechanical vibrations can be 'isolated' from the driven load.

1.3.8 Interference fields

The effects of electromagnetic interference fields emanating from the motor on sensitive pick-ups and amplifying devices in the vicinity of the driven load may be reduced in certain ways:

- by placing the motor and the pick-up devices as far away from each other as possible
- by adjusting the motor aspect so that the field component is a minimum in the direction of the pick-up device
- by putting adequate screening between the motor and the pick-up device.

Disturbances caused by motor current variations over the power supply lines must be blocked appropriately with the help of electrical filters.

1.3.9 Price

Whilst the first requirement from a small electric motor used in an industrial situation is reliability, in domestic appliances there is the absolute necessity of keeping the price to a minimum. This condition can only be met when the motor is built in as an integral irreplaceable part of the whole appliance.

1.4 Function principles of small motors

The various demands on small motors can only be met by there being a variety of motor structures.

Whilst AC motors may take the form of rotating field motors with no electrical contact with the rotor, the commutation arrangements cannot be dispensed with in DC motors. By variations on the two basic principles of 'rotating field motor' and 'commutator motor', a broad spectrum of small motors adaptable to the particular demands of the driven devices may be derived.

In all the motor variants, the common feature is the torque resulting from the magnetic fields in an airgap. In practice, however, it is advantageous to look at rotating field motors and commutator motors from other vantage points:

- In the rotating field motor, the starting point is a spatially rotating magnetic field that takes the rotor along with it.

- In commutator motors, the forces acting on current-carrying conductors in magnetic fields are considered.

Figure 1.9 gives an overview of the more important types of small motor. For rotating field motors that produce a more or less complete rotating field there are five winding variants shown:

- 3-phase motor with a three-coil winding connected in star
- single-phase motor with a three-coil winding connected in delta and a phase-shifting capacitor (Steinmetz circuit)
- single-phase motor with a two-coil winding, comprising a main phase and a capacitor auxiliary phase
- single-phase motor with a two-coil winding, comprising a main phase and a resistive auxiliary phase
- shaded pole motor.

Whilst a near perfect circular rotating field is achieved in the 3-phase motor, only a very poor rotating field can be attained in a shaded pole motor. Because there is seldom a 3-phase supply available for energising small motor drives, it is necessary to make do with a highly elliptic rotating field.

Depending upon the demands made on the motor, one of several rotor types may be called into service:

- squirrel cage rotor (induction motor)
- permanent magnet rotor (synchronous motor)
- hysteresis rotor (synchronous motor)
- reluctance rotor (synchronous motor).

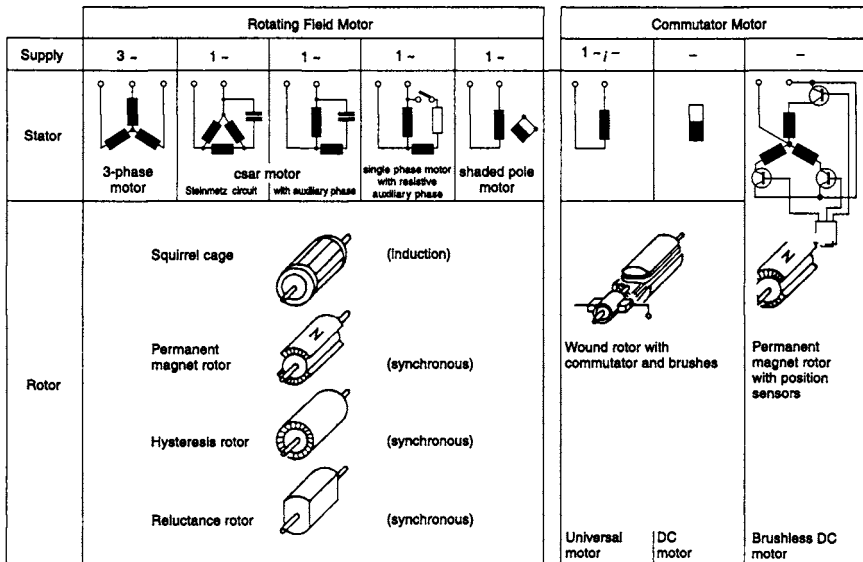


Figure 1.9 *Function principles of the more important types of small motor*

Induction motor rotors comprise mostly a high conductivity cage embedded in a set of iron stampings. Induced currents build up in the cage when it is rotating more slowly than the synchronous rotating field. These currents and the rotating field acting together develop the motor torque. Consequently, synchronous running of the rotor and the field is not possible because then no rotor currents would be induced.

The permanent magnet rotor, which has the same number of poles as the stator, locks into synchronism with the stator's rotating field and trails this field by an angle that depends on the load torque. This angle increases with load torque up to a limiting value. If this limiting value is exceeded, then the rotor falls out of step and then produces only vibrating alternating torques.

These vibrating torques arise when the motor is first energised, i.e. when the rotor is at a standstill and the field is rotating. A start is only possible if the rotor can be accelerated up to synchronous speed quickly enough. In general, this is possible only in slow running, i.e. multipole, motors.

The reluctance rotor performs similarly. This one has airgap variations or soft magnetic poles between which the airgap, which is bounded by the stator and rotor contours, is widened appreciably. The rotor is therefore characterised by varying airgaps or varying magnetic resistances (reluctances). As with the permanent magnet rotor, the reluctance rotor seeks to align itself with the magnetic axis of the rotating field, and to turn with it. The starting problems are similar to those of the permanent magnet rotor. In high speed reluctance motors, the starting torque is provided by an induction motor type squirrel cage rotor which by virtue of its reluctance properties 'springs into synchronism'.

In contrast, no such starting problems are experienced with the hysteresis rotor. This is made of permanent magnet material whose coercive force is so small that the material is magnetised cyclically by the rotating field. At synchronous speed there is no magnetic cycling, so the motor then behaves as a synchronous motor. During run-up the rotor is magnetised cyclically in such a way that its magnetic axis rotates in synchronism with the magnetising field. In this way a torque is developed in the motor during the run-up until synchronism is achieved. Hysteresis motors can be built for any synchronous speed and they need no auxiliary starting means.

Commutator motors are driven principally from direct voltage, from which no rotating field can be generated. The torque comes from the interaction of current-carrying loops and a constant magnetic field. The loops are continuously changing position relative to the field. The supply of current through the loops must be arranged so that the torques developed always have the same algebraic sign.

In the classical DC motor, the loops in combination with the commutator form the rotor, and the constant field is fixed spatially. The source voltage is applied to the commutator via brushes. In small DC motors, these days, the constant field is developed by a permanent magnet.

In universal motors, the stator winding develops the spatially fixed magnetic field. In accordance with its name, the universal motor may be driven from an AC or a DC supply when it is ensured that the directions of stator and rotor currents reverse simultaneously, for example in a series connected motor.

These days universal motors are driven almost exclusively from the AC mains supply. Because, in contrast to rotating field motors, they can be designed to run at any required speed, they have gained importance where high power motors with a low demand on material are needed. In such situations very high speeds of rotation are selected so that the torque may be relatively low and the motor dimensions are small compared with rotating field motors of comparable power rating. Portable household appliances that demand high power, e.g. vacuum cleaners, coffee grinders, kitchen machinery, etc., are normally fitted with universal motors as the drive components.

The disadvantage of the classical commutator motor is the mechanical sliding contact, which limits the life and gives rise to noise and electrical interference. This disadvantage can be overcome through the inclusion of electronic switches in place of the mechanical commutator. The method is to switch currents in stator coils by means of transistors and to provide a permanent magnet rotor. Because the transistor control is related to the rotor position, just as armature current is controlled by commutation in the classical commutator motor, the basic properties of the 'brushless' DC motor are no different from those of the mechanically commutated DC motor.

Figure 1.9, which shows just the more important principles of small motor function, is not complete, of course. It omits, for example, stepper motors, which resemble in their construction multipole multiwinding rotating field motors with permanent magnet or reluctance rotors. In contrast to rotating field motors, these are not energised from the a.c mains but from current pulses through electronic circuits. Because these motors make one angular step per impulse they are used for converting impulse sequences into proportional angular movements.

As well as small motors which work according to the principles discussed above, a new range of drive types is appearing which exploit other physical phenomena such as magnetostrictive or inverse piezoelectric effects. There are also motors using thermo-bimetallic strips, memory alloying or extensible materials, and finally there are electrochemical linear motors. These motors are frequently named actuators.

Also, rotating travelling wave motors with piezoceramic elements are under development.

1.5 Overview of small motors

Looking at Figure 1.9 should not lead one to the conclusion that every small motor has a cylindrical rotor that turns inside the stator. In fact, there are

many modes of construction that are not to be found amongst the larger machines. As well as motors with internal rotors (Figure 1.10*a*) there are cup-rotors (*b*), disc rotors (*c*) and external rotors (*d*) to be found. In linear motors, which have recently entered into the low power business, there is the division between long stator (*e*) and short stator (*f*) designs. Which of these various forms is used depends on, amongst other things, the desired moment of inertia of the rotor. Manufacturing considerations can also be a deciding factor.

As well as the forms shown in Figure 1.10, there are other special designs which make particularly simple small motors possible. Only unsymmetrical stator stampings or multiclaw constructions with a single stator coil which are components of fully effective motors are mentioned here.

Some idea of the possible number of motor variants can be derived by 'multiplying' the types of Figure 1.9 by the forms of Figure 1.10. Of course, not all the hundreds of possible variants are of particular technical interest. On the other hand, parameters not discussed so far, such as pole-pair number, output power and input voltage, increase the number of motor types manufactured.

There has in the past been no shortage of effort towards arranging the small motors available on the market in tabular form. These tables rapidly lose any value in the face of turbulent development, so an up-to-date listing is not attempted here. Nevertheless, a few general guidelines seem to be in order:

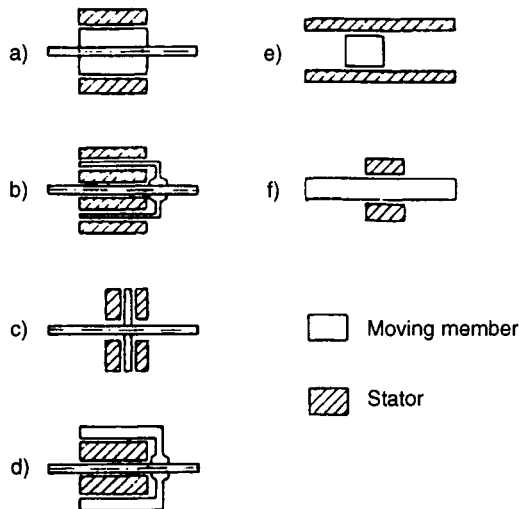


Figure 1.10 Construction forms of the more important small motors
a internal rotor motor; *b* cup rotor motor; *c* disc rotor motor; *d* external rotor motor; *e* linear motor with long stator; *f* linear motor with short stator

- In general, rated power and speed go in step. For example, multipole synchronous motors have low power output, whereas fast rotating commutator motors serve the high power end of the range.
- The nominal power ranges for single-phase csar motors and for commutator motors are comparable. Csar motors offer long life and higher reliability, whilst high speed commutator motors are small and light.
- The preferred speed range for commutator motors lies between 3000 and 20,000 rev/min.
- Shaded-pole motors with concentrated mains energised windings are made with power ratings up to about 100 W.

Of course, there are specific applications for the various types of small motors; e.g. induction motors with resistive auxiliary phases are used only for freezer compressors. An overview of present-day applications is deliberately avoided here because such an overview could have only temporary validity. The relentless force towards producing ever better and ever cheaper drives makes it necessary to be reconsidering continuously the drive concepts and their relationship to the motor function principles to be applied.

Chapter 2

Operation of the multiphase induction motor

Jürgen Draeger

2.1 Introduction

A notable feature of induction motors, including polyphase motors, is their very simple construction, as can be seen from Figure 2.1, which illustrates two dismantled 3-phase induction motors. Their being relatively inexpensive and needing little maintenance as well as their being operable directly from the 3-phase mains supply without needing intermediate circuitry has led to the widespread use of induction motors.

In this chapter, the operation, performance and applications of 3-phase and single-phase mains-energised induction motors are discussed. In addition, a fundamental consideration is given to the rules concerning rotating and alternating fields, to their generation in polyphase windings and to their function in induction motors.

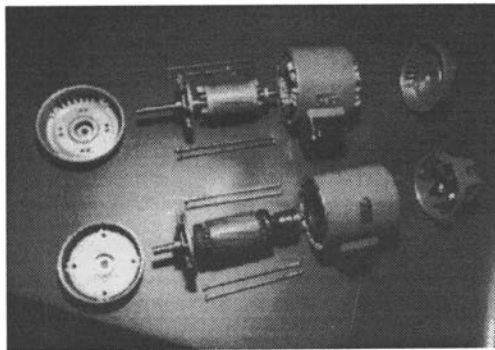


Figure 2.1 Components of polyphase induction motors with short-circuit (cage) and slip-ring (wound) rotors

2.2 Operation of the induction machine

2.2.1 Rotating and alternating fields

In a polyphase induction motor the stator windings are laid in slots which are uniformly distributed around the periphery. The essentials of a 3-phase, 2-pole machine are shown in cross-section in Figure 2.2. At first, the magnetomotive force (MMF) distribution resulting from a current i flowing through a stator coil is considered in detail. Figure 2.3 shows the spatial MMF distribution b over a linearly developed stator as a function of the spatial parameter x when $i = \text{const}$. The resultant stepped waveform is not easily expressed mathematically because of the discontinuities. However, any periodic function such as the function $b(x)$ shown here may be expressed as a sinusoidal function with the same period and with a number of harmonics, and hence as a continuous function. Owing to the odd and even symmetry in the function $b(x)$, only the odd harmonic, $m = 1, 3, 5, \dots$, exist. The number of pole-pairs in each component field corresponds to the harmonic number $p = m$. To describe the basic action it is admissible to limit the consideration to the fundamental, $m = 1$, component of the MMF function $b_1(x)$. Consequently, in the examination of the effect of the field, its spatial distribution may always be described as sinusoidal. The time-dependent sinusoidal variation of the supply voltage at angular frequency ω results in the winding current i being similarly periodic in time. Consequently the positions of the null points in the function $b_1(x)$ are fixed. A periodically varying field, whose spatial distribution of zeros and maxima is fixed, is called an alternating field.

The space- and time-dependent MMF distribution $b_1(x, t)$ of the fundamental component with peak field amplitude B_1 and pole span τ is given as

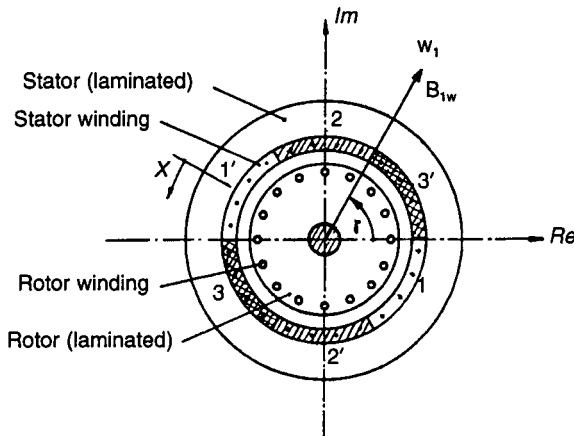


Figure 2.2 Cross-section of a 3-phase 2-pole induction machine

$$b_1(x, t) = B_1 \sin\left(\frac{\pi x}{\tau}\right) \cos \omega t \quad (2.1)$$

To describe a sinusoidally distributed field in space, it is sufficient to know its peak magnitude B_1 , and the direction of the axis of the field. Both are represented in an Argand diagram vector \mathbf{B}_{1w} which lies in the direction of the field's axis and whose length is B_1 (see Figure 2.2).

If the angle between the field's axis and the Argand-diagram real axis is γ , then \mathbf{B}_{1w} is expressed as

$$\mathbf{B}_{1w} = B_1 \exp j\gamma \quad (2.2)$$

The instantaneous value of field magnitude and its vector direction is expressed as:

$$\mathbf{b}_{1w} = \mathbf{B}_{1w} \cos \omega t = B_1 \exp j\gamma \cos \omega t \quad (2.3)$$

We now consider rotating the stator counter-clockwise mechanically at an angular velocity ω_1 . The vector \mathbf{B}_{1w} is rotated at this same ω_1 . A field whose maxima and zeros move as time passes is called a rotating field. Because, in this case, the rotating field vector \mathbf{B}_{1d} changes its direction relative to the reference direction by the angle $\omega_1 t$ in time t , the expression for the rotating field vector is

$$\mathbf{B}_{1d} = \mathbf{B}_{1w} \exp j\omega_1 t \quad (2.4)$$

If, in particular, $i = \text{const.}$, and hence $\omega = 0$ and $\cos \omega t = 1$, the expression for the instantaneous value of the rotating field is

$$\mathbf{b}_{1d} = B_1 \exp j\gamma \exp j\omega_1 t \quad (2.5)$$

The field amplitude has constant magnitude B_1 , and \mathbf{b}_{1d} is described as a uniform (circular) rotating field. The space- and time-dependent instantaneous value of \mathbf{b}_{1d} is expressed by

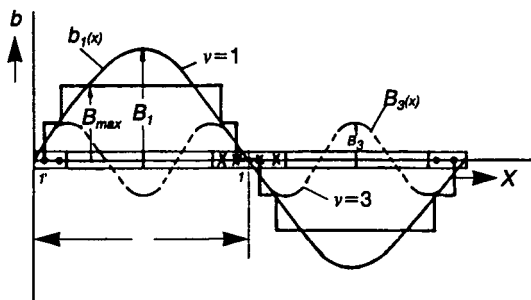


Figure 2.3 Spatial MMF distribution of the airgap field and its resolution into fundamental and harmonic components.

$$\mathbf{b}_{1d}(x, t) = B_1 \sin\left(\frac{\pi x}{\tau} - \omega_1 t - \gamma\right) \tag{2.6}$$

When two circular rotating fields \mathbf{B}_{11d} and \mathbf{B}_{12d} with different amplitudes B_{11d} and B_{12d} but with the same angular velocity ω_1 are working together, the result in accordance with Figure 2.4a is the vector sum of the component fields \mathbf{B}_{1rd} and it is also a uniform rotating field.

If the circular rotating fields \mathbf{B}_{11d} and \mathbf{B}_{12d} rotate in opposite senses but at equal speeds of rotation, i.e. ω_1 and $-\omega_1$, then the end point of \mathbf{B}_{1rd} describes an ellipse with major axis $B_{11d} + B_{12d}$ and minor axis $B_{11d} - B_{12d}$. This is an elliptic (nonuniform) rotating field in the rotation sense of the stronger of the two components. In the special case $B_{11d} = B_{12d}$, the end point of the resulting $B_{1rd} = 2B_{11d} \exp j\gamma \cos \omega_1 t = b_{1w}$ describes a straight line. It is an alternating field with amplitude double that of the uniform rotating field.

Because the sum of an arbitrary number of uniform rotating fields having the same angular velocity and rotating in the same sense is itself a uniform rotating field in that sense, the following general statements may be made. When an arbitrary number of uniform rotating fields with arbitrary magnitudes and senses of rotation but with the same angular speed ω_1 are added, the result is an elliptic rotating field. Special cases are: a uniform rotating field when the sum of the fields rotating in one of the senses is zero; and an alternating field when the sums of the counter-rotating fields are equal.

Conversely, any elliptic field may be substituted by two uniform rotating fields, counter-rotating with equal angular speeds but with different amplitudes. An alternating field may be substituted by two counter-rotating equal magnitude circular rotating fields, each having half the magnitude of the alternating field.

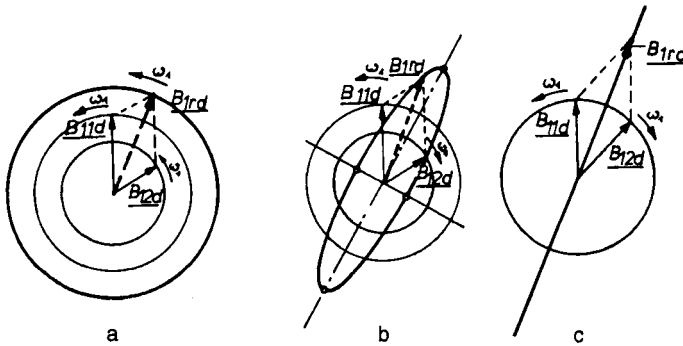


Figure 2.4 Resulting rotating field \underline{B}_{1rd} from the addition of: (a) two uniform fields rotating in the same sense; (b) two different counter-rotating uniform fields; (c) two equal counter-rotating uniform fields

2.2.2 Derivation of a rotating field from a polyphase winding

When several windings are arranged so that their field axes have different directions, and the windings are energised with currents which have different phases but the same frequency, the result is a rotating field. The form of the resultant field is easily determined when the alternating field in each winding is substituted by a pair of counter-rotating uniform fields, each having one-half of the magnitude of the alternating field, as discussed in Section 2.2.1. For coil 1 in Figure 2.5 the instantaneous magnetic field, in accordance with eqns. 2.2 and 2.4 is

$$\mathbf{b}_{1w} = \frac{B_1}{2} \exp j\gamma_1 \exp j\omega_1 t + \frac{B_1}{2} \exp j\gamma_1 \exp -j\omega_1 t \quad (2.7)$$

The alternating fields of all n stator coils may be expressed in this manner. Terms containing $\exp j\omega_1 t$ adding up to the direct uniform rotating field, and similarly terms containing $\exp -j\omega_1 t$ for the counter-rotating field, may be gathered. Phase angles of the currents in the n coils, relative to coil 1 current, may be expressed by φ_2 to φ_n , respectively, and then

$$\begin{aligned} \mathbf{B}_{1rd} = & \frac{1}{2} \exp j\omega_1 t \exp j\gamma_1 [B_{11} + B_{12} \exp j(\gamma_2 - \gamma_1) \exp -j\varphi_2 \\ & + \dots + B_{1n} \exp j(\gamma_n - \gamma_1) \exp -j\varphi_n] \\ & + \frac{1}{2} \exp(-j\omega_1 t) \exp j\gamma_1 [B_{11} + B_{12} \exp j(\gamma_2 - \gamma_1) \exp(-j\varphi_2) \\ & + \dots + B_{1n} \exp j(\gamma_n - \gamma_1) \exp j\varphi_n] \end{aligned} \quad (2.8)$$

Note that, throughout the two main terms in eqn. 2.8, the coil axis direction vectors $\exp j\gamma_1$ etc. are identical in both, whereas the current derived vectors $\exp -j\omega_1 t$, $\exp -j\varphi_2$, etc. have opposite algebraic signs every time.

In general, when the contents of the two square bracketings are unequal, \mathbf{B}_{1rd} is an elliptic rotating field, which becomes the sought-after uniform

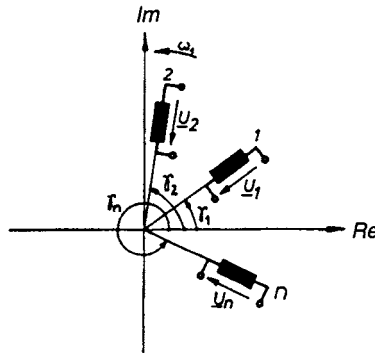


Figure 2.5 Arrangement of n stator coils

rotating field when the contents of one of them adds up to zero. In particular, when $B_{11} = B_{12} = \dots B_{1n} = B_1$, the magnitudes of the alternating fields are equal. The contents within a set of square brackets becomes zero when its elements form a symmetrical star. This condition is satisfied in general when, for the k th coil, $1 < k \leq n_1$,

$$\gamma_k - \gamma_1 \mp \varphi_k = \pm \frac{2\pi}{n} (k-1) \rightarrow \frac{\gamma_k - \gamma_1}{k-1} \mp \frac{\varphi_k}{k-1} = \pm \frac{2\pi}{n} = \text{const.} \quad (2.9)$$

Given a two-winding stator, $n = 2$ and $k = 2$, a uniform rotating field is generated when:

$$\gamma_2 - \gamma_1 \mp \varphi_2 = \pm \pi \quad (2.10)$$

An important special case is $\gamma_2 - \gamma_1 = 90^\circ$ and $\varphi_2 = 90^\circ$. The second square bracket contents in eqn. 2.8 become

$$B_1 [1 + \exp j90^\circ \exp j90^\circ] = 0$$

and the first square bracket contents become

$$B_1 [1 + \exp j90^\circ \exp j90^\circ] = 2B_1.$$

This corresponds to there being 90° spatial displacement between the two stator coils, and 90° phase displacement between their currents.

In this case,

$$\mathbf{B}_{1nt} = B_1 \exp j\gamma_1 \exp j\omega_1 t \quad (2.11)$$

Other combinations of $\gamma_2 - \gamma_1$, and φ_2 , adding up to 180° , produce a uniform rotating field, but it is weaker.

Similarly, for a three-winding stator, $n = 3$ and $k = 2$ or 3 , a circular rotating field is generated when

$$\gamma_2 - \gamma_1 \mp \varphi_2 = \pm \frac{2\pi}{3} \quad (2.12)$$

and

$$\gamma_3 - \gamma_1 \mp \varphi_3 = \pm \frac{4\pi}{3} \quad (2.13)$$

An important special case is

$$\begin{aligned} \gamma_2 - \gamma_1 = 60^\circ & & \varphi_2 = 60^\circ \\ \gamma_3 - \gamma_1 = 120^\circ & & \varphi_3 = 120^\circ \end{aligned} \quad (2.14)$$

The appearance of 60° in the discussion may cause concern. However, when practical stator windings and electrical connections to them are considered, it can be seen that eqn. 2.14 is in accordance with the normal 3-phase motor stator.

Substitution of the angles in eqn. 8.14 into eqn. 2.8, when $n = 3$, produces

$$\mathbf{B}_{1rd} = \frac{3}{2} B_1 \exp j\gamma_1 \exp j\omega_1 t \quad (2.15)$$

Here again, other combinations of winding layouts and current phase angles give rise to weaker uniform rotating fields.

A visual impression of the generation of the rotating field is obtained if, for a chosen instant, e.g. when the current in coil 1 peaks, the instantaneous fields of the three coils are indicated each by a pair of counter-rotating field vectors, as shown in Figure 2.6. The clockwise rotating vectors cancel and the counter-clockwise rotating vectors coincide and add up to a field strength of $1.5 B_1$.

Similarly, Figure 2.7 shows the resultant field of a 2-phase winding in which the spatial displacement of the field axes and the phase displacement of the energising currents do not correspond. The result is an elliptic rotating field.

In both cases, the direction of rotation of the field is reversed by means of interchanging the voltages supplied to two coils.

2.2.3 Torque generation

Polyphase motor windings generally generate elliptic rotating fields. Because every elliptic rotating field can be substituted by two counter-rotating uniform fields, whose effects may be linearly superimposed in unsaturated machines, that which follows pays attention to the effects of uniform rotating fields.

2.2.3.1 Uniform rotating field

The cause of the rotating field, and its magnitude in accordance with the law of induction, is the voltage system connected to the stator winding. The rotating field must turn at a speed such that the induced electromotive force

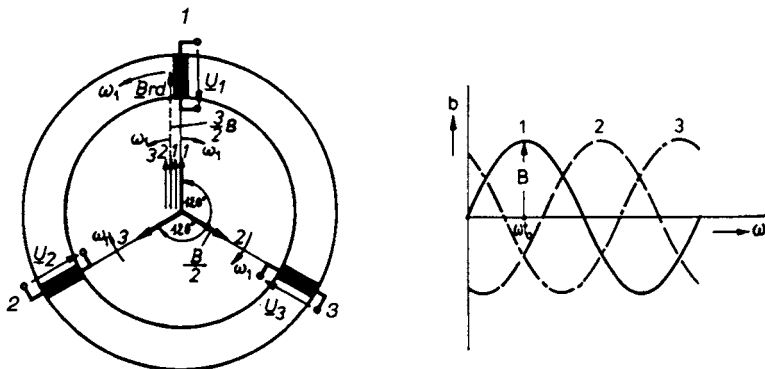


Figure 2.6 Uniform rotating field generation in a symmetrically constructed 3-coil machine, when connected to a symmetrical 3-phase mains supply

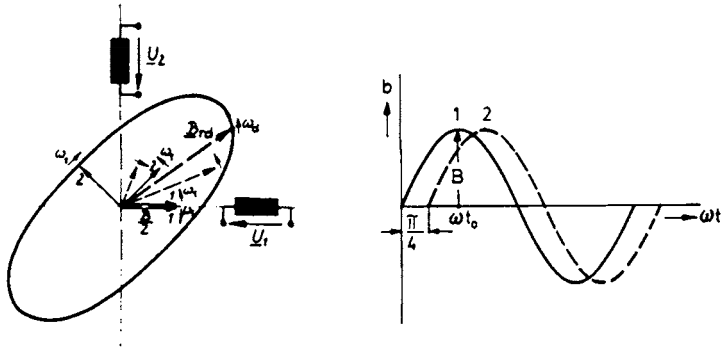


Figure 2.7 *Rotating field generation in a two-coil machine.*

(EMF) in each stator coil equals the supply voltage minus the internal voltage drop.

Thus, its speed of rotation is derived from the mains frequency f_1 . When there are p pole-pairs, the synchronous speed of the rotating field is n_1 , where:

$$n_1 = \frac{f_1}{p} \tag{2.16}$$

Higher order fields – resulting from harmonics in the MMF waveform – have correspondingly lower synchronous speeds on account of their greater numbers of pole-pairs.

The rotating field passes through the rotor iron stampings whose uniformly distributed slots hold the polyphase rotor winding. When the rotating field links the conductors of a stationary rotor, a voltage U_{q20} at frequency f_1 is induced in the rotor winding, its magnitude depending on the stator/rotor winding turns ratio. The machine acts as a transformer. In order to minimise the magnetising current, the airgap is designed to be $\delta = 0.1\text{--}0.5$ mm. When the rotor turns with speed n in the direction of the rotating field or with speed $-n$ in the counter direction, the induced rotor voltage has frequency

$$f_2 = (n_1 \mp n)p = f_1 \mp np = n_2 p \tag{2.17}$$

where n_2 is the relative angular speed between that of the rotating field and that of the rotor. In this manner the induction machine acts as a frequency changer. The induction machine is also a phase changer if the number of rotor winding coils m_2 differs from the number of stator winding coils m_1 , in which case an m_2 -phase set of voltages is induced in the rotor winding.

If the rotor windings are closed, via slip-rings, in the case of the wound rotor motor or by short-circuit rings at the ends of massive rotor bars in the case of the squirrel cage motor, a rotor current I_2 flows whose phase relative to the induced rotor voltage U_2 depends on the rotor winding resistance R_2 and the leakage reactance $X_2 = 2\pi f_2 L_{\sigma 2}$ per coil. The rotor polyphase currents

develop a rotating field at speed $n_2 + n = n_1$ so that, together with the stator rotating field, it develops a constant torque M in the rotor equal to the reaction torque in the fixed stator. The motor torque M thus developed provides the load torque M_L so that, in accordance with the laws of dynamics, and given that the moment of inertia of the rotor plus load, referred to the motor shaft, is J ,

$$M - M_L = J \frac{d\omega}{dt} = 2\pi J \frac{dn}{dt} \tag{2.18}$$

during the run-up.

As speed n increases, f_2 , U_2 and consequently I_2 decrease. On reaching $n = n_1$, $I_2 = 0$ and therefore $M = 0$. In the motor mode, no further acceleration is possible. In practice the machine, running as a motor, always turns at a speed less than n_1 because even on no-load the friction loss torque remains to be developed. The rotor runs at less than synchronous speed by a load-dependent fraction called the slip s ,

$$s = \frac{n_1 - n}{n_1} = 1 - \frac{n}{n_1} = \frac{n_2}{n_1} = \frac{f_2}{f_1} \tag{2.19}$$

The induction motor runs asynchronously. The torque is easily calculated from a consideration of the power budget in conjunction with Figure 2.8.

The stator rotating field power P_{D1} , which is the mains input power P_1 minus the stator copper and iron losses P_{v1} , is split into the mechanical power P_m and the rotor electrical power P_{D2} . P_m is then reduced by an amount P_{VR} , the friction power loss. P_{D2} comprises secondary mains power drawn out of the slip-rings, P_2 , and the rotor (heat) power loss P_{v2} .

The gross torque M is derived from the stator rotating field power P_{D1} and the synchronous speed n_1 :

$$P_{D1} = 2\pi n_1 M \tag{2.20}$$

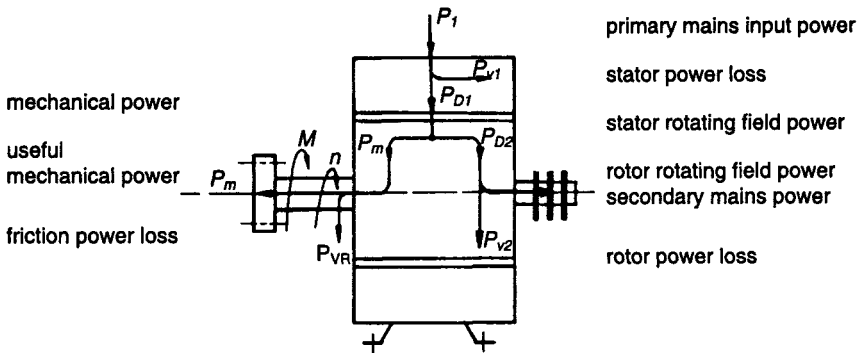


Figure 2.8 Division of power

The mechanical power P_m is:

$$P_m = 2\pi nM = \frac{n}{n_1} P_{D1} = (1-s)P_{D1} \quad (2.21)$$

and the rotor electrical power is

$$P_{D2} = P_{D1} - P_m = \left(1 - \frac{n}{n_1}\right) P_{D1} = sP_{D1} \quad (2.22)$$

Thus, the key to the proportions of power transferred to the rotor is the slip. The induction motor rotor is either completely short-circuited or loaded with resistors via slip-rings. In both cases, the power in the rotor circuit is converted entirely into heat, so that $P_{D2} = P_{V2}$. It follows that

$$P_{V2} = sP_{D1} = 2\pi n_1 Ms \quad (2.23)$$

from which

$$M = \frac{P_{V2}}{s2\pi n_1} \quad (2.24)$$

Given low-loss rotor stampings, the rotor power loss may be considered to be entirely within the rotor winding and any present external rotor circuit resistors. Given a resistance R_2 per rotor winding circuit carrying current I_2 , and m_2 windings

$$P_{V2} = m_2 I_2^2 R_2 \quad (2.25)$$

I_2 is derived from the rotor winding induced voltage U_2 , the rotor circuit resistance R_2 and the rotor leakage inductance $L_{\sigma 2}$ as

$$I_2 = \frac{U_2}{\sqrt{R_2^2 + (\omega_2 L_{\sigma 2})^2}} = \frac{U_2}{\sqrt{R_2^2 + s^2 (\omega_1 L_{\sigma 2})^2}} \quad (2.26)$$

$\omega_1 L_{\sigma 2} = X_{\sigma 2}$ is the rotor leakage reactance at standstill when $f_2 = f_1$. U_2 is proportional to the slip and the rotor open-circuit induced voltage at standstill U_{q20} , i.e. $U_2 = sU_{q20}$, so that I_2 becomes:

$$I_2 = \frac{sU_{q20}}{\sqrt{R_2^2 + s^2 X_{\sigma 2}^2}} = \frac{U_2}{\sqrt{\left(\frac{R_2}{s}\right)^2 + X_{\sigma 2}^2}} \quad (2.27)$$

From eqns. 8.24, 8.25 and 8.27 it follows that

$$M(s) = \frac{m_2}{2\pi n_1} \frac{U_{q20}^2}{\left(\frac{R_2}{s}\right)^2 + X_{\sigma 2}^2} \frac{R_2}{s} \quad (2.28)$$

In motors not affected by skin-effects and deep rotor bars (e.g. slip-ring motors) all the quantities in eqn. 2.28 except s are machine constants.

When eqn. 2.28 is rearranged,

$$M(s) = \frac{m_2 U_{q20}^2 R_2}{2\pi n_1} \frac{s}{R_2^2 + (sX_{\sigma 2})^2} \tag{2.28a}$$

Inspecting this equation and the M -curve of Figure 2.9 shows that:

- For small s , positive (motoring) or negative (generating), $M(s)$ is approximately proportional to s
- $M(s)$ has a peak value M_k for a particular slip s_k .

At higher values of s , $M(s)$ decreases in spite of increasing rotor current. The reason is the increasing phase displacement between I_2 and U_2 as the rotor frequency increases, with a consequent reduction in the rotor power P_{w2} (see also eqn. 2.20). An important working parameter is the starting torque M_A at standstill ($s = 1$).

The machine can only run as a generator when the necessary reactive current for stator magnetisation is available, i.e. when the stator is connected to a live mains supply.

Figure 2.9 also shows the torque components resulting mainly from the 5th and 7th MMF components of the symmetrical 3-phase stator winding. In some circumstances, a saddle occurs in the total $M(s)$ characteristic. 3rd-harmonic MMF components cancel in a 3-phase machine but may occur in 2-phase motors.

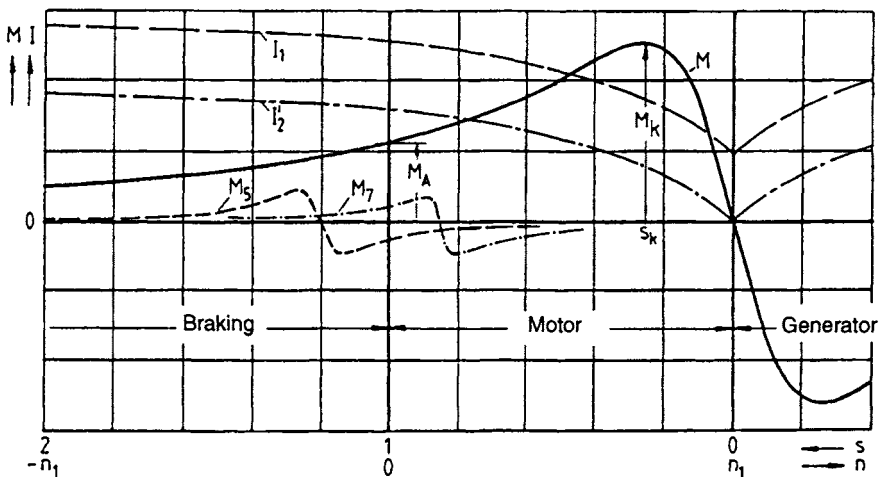


Figure 2.9 Torque-speed characteristic $M(s)$ and corresponding stator and rotor currents $I_1(s)$ and $I_2'(s)$.

Harmonic torques of order 5 and 7

By differentiating eqn. 2.28a with respect to s , it follows that the slip s_k , at which peak torque M_k is developed, is

$$s_k = \frac{R_2}{X_{\sigma 2}} \tag{2.29}$$

and the peak torque, derived from eqn. 2.28, is

$$M_k = \pm \frac{m_2}{2\pi n_1} \frac{U_{q20}}{2X_{\sigma 2}} \tag{2.30}$$

M_k is independent of R_2 , and dependent on $X_{\sigma 2}$ only, whereas s_k is adjustable via R_2 or $X_{\sigma 2}$. Dividing eqn. 2.28 by eqn. 2.30 and substituting from eqn. 2.29 gives the simple and elegant Kloss formula,

$$\frac{M(s)}{M_k} = \frac{2}{\frac{s}{s_k} + \frac{s_k}{s}} \tag{2.31}$$

which enables the complete $M(s)$ characteristic to be derived from s_k and M_k .

2.2.3.2 Elliptic rotating fields

If the rotating field is elliptic, resulting from, for example, an unsymmetrical supply, the supply may be resolved into counter-rotating components U_m and U_g , where $U_m > U_g$. When the components are connected to the stator windings of two identical machines, mechanically coupled as in Figure 2.10, torques M_m and M_g are developed in the rotors, which turn in the sense of the stronger torque M_m .

The output torque from the machine set is $M = M_m + M_g$; the positive sign takes account of the vector directions and hence the algebraic signs of the two torques. Calculation of M_m and M_g is as in Section 2.2.3.1.

Motor I with torque M_m runs as a motor with slip s , and motor II with torque M_g runs as a brake with slip $2 - s$. The component - and composite - torque/slip characteristics are shown in Figure 2.11. The backwards-rotating uniform field reduces the output torque from the machine set and prevents it from running at synchronous speed n_1 at no load. The attainment of a satisfactory overall motoring torque is dependent on the braking torque being small.

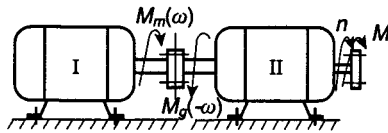


Figure 2.10 *Two machines that are equivalent to a machine with an elliptic rotating field*

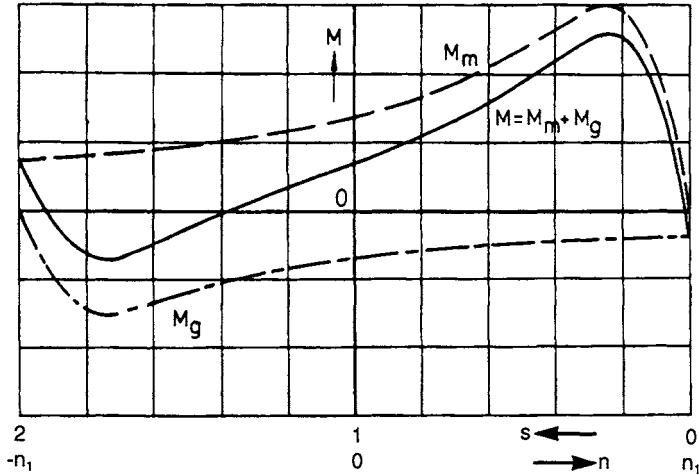


Figure 2.11 Torque produced from an elliptic rotating field

Separating the elliptic rotating field into circular rotating components is useful for considering and deriving M_m and M_g , but it obscures a serious nuisance effect in the true single-rotor machine. Counter-rotating fields in the stator induce rotor currents I_{2m} and I_{2g} which are also counter-rotating, and these currents produce their own counter-rotating rotor fields. As already discussed in Section 2.2.3.1, interactions between fields derived from U_m and I_{2m} (similarly U_g and I_{2g}) produce constant torques. However, interactions between fields derived from counter rotating U_m and I_{2g} (similarly U_g and I_{2m}) produce alternating torques at twice the mains supply frequency, and they do not normally cancel. These alternating torques can have the same order of magnitude as the constant torques, and generate structural noise via the motor frame mountings.

2.2.4 Current characteristics

The input current I_1 to the stator includes the field magnetising current I_μ lagging the input voltage by 90° and the small in-phase current I_{Fe} for the stator iron losses. Both currents are components of the measurable no-load current I_{10} .

When the rotor is mechanically loaded, the rotor current is I_2 and a current I_1^* , in addition to I_{10} , flows in the stator winding. The law of induction requires that the stator MMF θ_1 and the rotor MMF θ_2 must cancel because the airgap rotating field depends only on the supply voltage U_1 and not on the loading on the machine.

Therefore, when the machine is mechanically loaded,

$$I_1 = I_{10} + I_1^* \tag{2.32}$$

I_1^* is proportional to I_2 , and I_2 depends on the slip in accordance with eqn. 2.27. As the slip increases, R_2/s becomes small compared with $X_{\sigma 2}$, so that I_2 tends to the limit $U_{q20}/X_{\sigma 2}$ when s is large. A simple overview of the current characteristics of the induction motor is obtained by considering the single-phase equivalent circuit of Figure 2.12, which resembles that of a transformer, whose secondary winding is loaded with a variable resistor $R_2'(1-s)/s$, whose heat dissipation equals the mechanical power output from the rotor.

Transformation from the m_2 -phase rotor winding with N_2 turns per phase and the ξ_2 winding factor to the m_1 -phase stator winding with parameters N_1 and ξ_1 , respectively, for rotor/stator MMF balance, gives

$$I_2' = \frac{m_2 N_2 \xi_2}{m_1 N_1 \xi_1} I_2 \tag{2.33}$$

and the corresponding power balance conditions give

$$R_2' = \frac{m_1 (N_1 \xi_1)^2}{m_2 (N_2 \xi_2)^2} R_2 \tag{2.34}$$

and

$$X_{\sigma 2}' = \frac{m_1 (N_1 \xi_1)^2}{m_2 (N_2 \xi_2)^2} X_{\sigma 2} \tag{2.35}$$

In a practical machine, $R_1 \ll X_{\sigma 1}$ and $R_{Fe} \gg X_h$. A useful, and not harmful, approximation is to delete R_1 and R_{Fe} from Figure 2.12, thus producing the much simpler Figure 2.13.

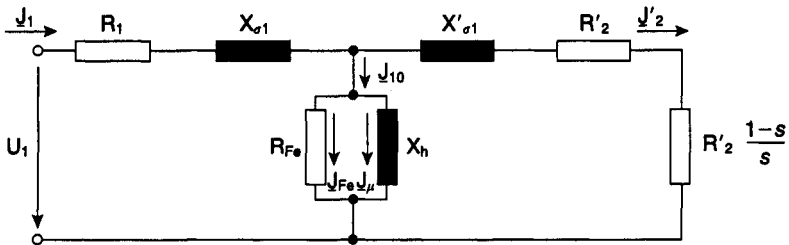


Figure 2.12 Equivalent circuit referred to the stator winding

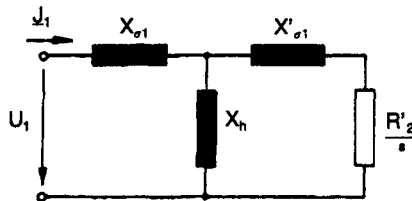


Figure 2.13 Simplified equivalent circuit

Expressing the impedance of a pure inductor in the form jX and analysing the circuit of Figure 2.13, specifying U_1 as the stator winding element voltage, the current $I_1(s)$ in this element is:

$$I_1(s) = U_1 \frac{jR'_2 - s(X'_{\sigma 2} + X_h)}{j(X_{\sigma 1} + X_h)R'_2 - s(X_{\sigma 1}X'_{\sigma 2} + X_{\sigma 1}X_h + X'_{\sigma 2}X_h)} \quad (2.36)$$

Thus the locus of the tip of the phasor $I_1(s)$ describes a circular path (primary current diagram) in the complex number plane, as is shown in principle in Figure 2.14.

The slip corresponding to each point on the semicircle is determined as follows.

The point $s = 1$ is determined from Figure 2.13 and eqn. 2.36. The line joining $s = 1$ and $s = \infty$ is extended so that it intersects an arbitrarily chosen line which runs in the direction of the tangent to the circle through $s = \infty$, i.e. vertically. The vertical line $01s$ in Figure 2.14 is called the slip line. The point of intersection is marked $s = 1$, and the line is graduated linearly between points 0 and 1. The chord from any chosen point on the semicircle to the point $s = \infty$ intersects the slip line, and the value of s may be read off the scale.

Other working quantities, as well as input current I_1 , may be read off the circle diagram.

The gross power transferred to the rotor P_1 , the synchronous speed n_1 , the number of stator phase winding elements m_1 and the torque M are related by

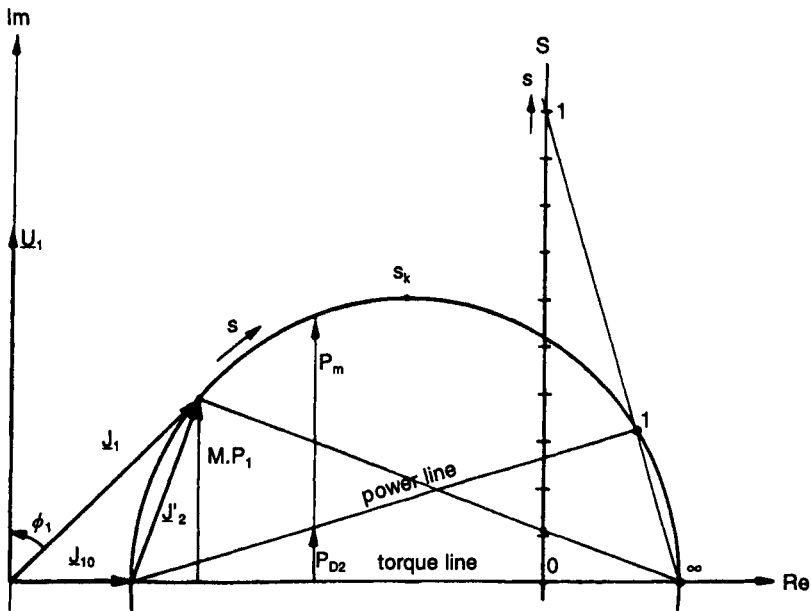


Figure 2.14 Primary current diagram

$$P_1 = 2\pi n_1 M = m_1 I_1 U_1 \cos \phi_1 \propto I_1 \cos \phi_1 \tag{2.37}$$

so that

$$M = \frac{m_1 U_1}{2\pi n_1} I_1 \cos \phi_1 \propto I_1 \cos \phi_1 \tag{2.38}$$

The vertical displacement between the designated torque line and the semicircle is proportional to the input power and the torque. The peak torque occurs at slip s_k , whose point is the highest on the semicircle.

The vertical displacement P_1 , proportional to the input power, is divided into mechanical power P_m and rotor electrical power P_{D2} by the power line.

The magnitudes of $I_1(s)$ and $I_2'(s)$ are included in Figure 2.9. The working characteristics of a 370 W squirrel cage motor for slip from 0 to s_k are depicted in Figure 2.15. The no-load current is relatively high, owing to the airgap between the stator and rotor. The operating range, after start and run-up, is considered to be between $s = 0$ and $s = s_k$, so that the overload capacity, defined as the pull-out torque M_k divided by the nominal full-load torque M_N is $M_k/M_N = 1.5-2.5$.

The nominal full-load slip is about 5%.

If it is necessary to limit the very high starting current, this can be achieved in a slip-ring motor by having switchable resistances R_v connected to the slip-rings. These resistors are switched out sequentially as speed increases. The increased rotor resistance $R_2 + R_v$ increases the pull-out slip s_k but leaves the pull-out torque M_k unchanged. As eqn. 2.31 shows, a greater starting torque is obtainable with less rotor current I_2 by means of increasing the rotor circuit resistance and, with it, the rotor circuit power loss P_{v2} .

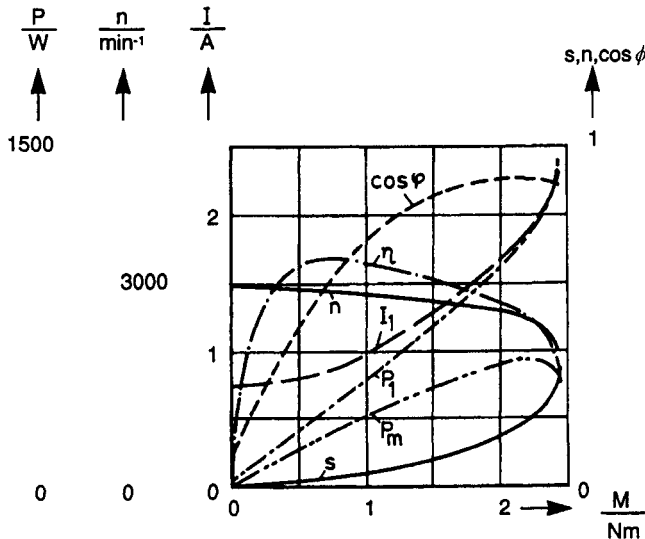


Figure 2.15 Working characteristics of a 3-phase squirrel cage induction motor (370 W)

Figure 2.16 shows how the torque characteristics are influenced by switching R_v .

With squirrel cage motors, no external variation of rotor resistance is possible. A choice of rotor bar profiles enables an increase in rotor power loss, and hence equivalent rotor resistance by exploiting rotor frequency dependent flux penetration (skin) effects in the rotor. Figure 2.17 shows the characteristics owing to various rotor bar profiles. The effect of having a double cage rotor normally found only in the larger machines is included. If the starting current is still too high, the initial voltage connected to the stator must be reduced by means of series resistors, autotransformers or star-start

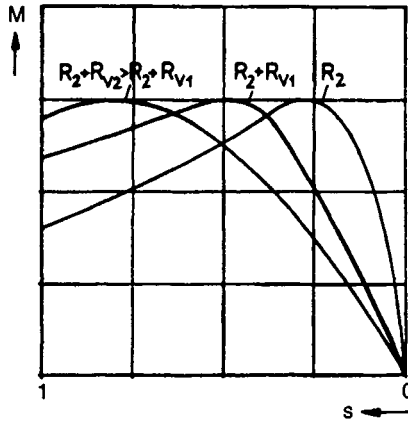


Figure 2.16 $M(s)$ with switched R_v

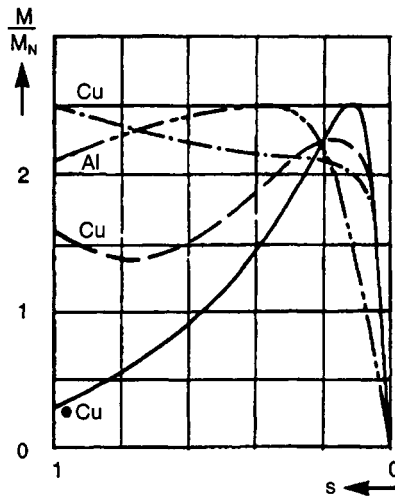


Figure 2.17 $M(s)$ with various rotor bar forms

delta-run connection of the stator windings. Noting eqn. 2.28, $M \approx U_{q20}^2$ and neglecting stator losses, it follows that the torque developed is proportional to the square of the voltage applied to the stator.

2.2.5 Speed control possibilities

The speed of an induction motor may be varied by changing the synchronous speed $n_1 = f_1/p$ or by changing the slip by either altering the airgap flux per pole

$$\Phi_1 = \frac{1}{N_1 \xi_1} \frac{m_1}{2} \int u_1 dt \quad (2.39)$$

or by varying the rotor resistance R_2 . It is also possible to energise the stator and rotor of a slip-ring machine from independent supplies at frequencies f_1 and f_2 , making it a double-fed induction machine. Thus, there are the following technical possibilities:

Changing the number of pole pairs p by switching the stator winding. Changing the number of pole pairs changes the synchronous speed $n_1 = f_1/p$ in whole-number steps so that the characteristics shown in Figure 2.18 are applicable.

Changing the mains frequency f_1 through a rotary or electronic converter-inverter. A smooth change of synchronous speed $n_1 = f_1/p$ is possible. If the motor pull-out torque is to be held constant, the inverter voltage must be proportional to its frequency (see Figure 2.19). The technical complication and expense of this method is considerable.

Changing the rotor circuit resistance R_2 in a slip-ring motor changes the pull-out slip s_K but not the synchronous speed n_1 (Figure 2.20). Therefore, speed control is possible only when there is a load torque on the motor. When the

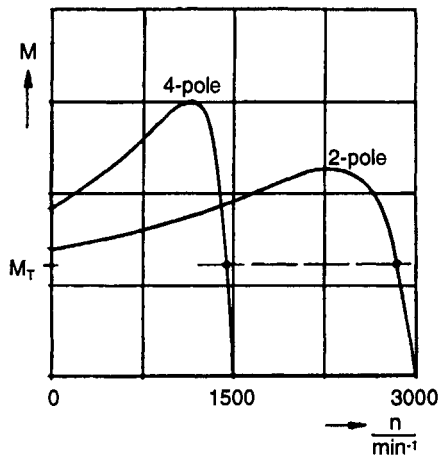


Figure 2.18 $M(n)$ with pole changing

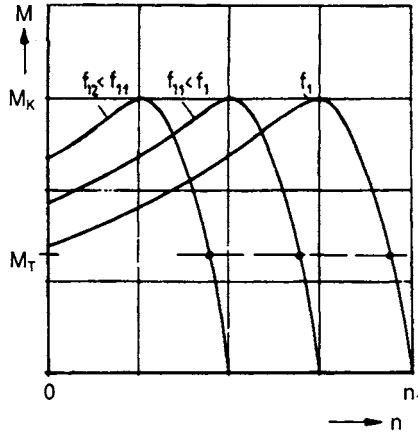


Figure 2.19 $M(n)$ with mains frequency changing

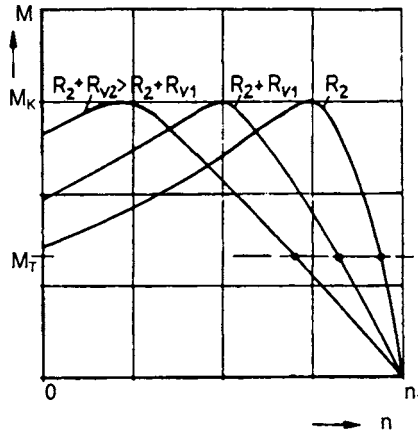


Figure 2.20 $M(n)$ with rotor resistance changing

speed reduction is large the efficiency is low owing to the large slip. This kind of speed control is normally used only for starting.

Changing the flux ϕ_1 by changing $\int u_1 dt$. This is possible by either changing the magnitude of U_1 with a transformer or, technically preferable, by connecting phase controlled antiparallel thyristor pairs or triacs into the mains supply lines. As the torque at a given value of slip is proportional to ϕ_1^2 , the torque-slip characteristic is lowered with decreasing flux as shown in Figure 2.21. Speed variation at a given torque by means of slip variation is possible as far as the pull-out slip s_K . If a wide speed range is envisaged, a special rotor with high R_2 is needed. Keeping the thermal capacity of the machine in mind, it is necessary to reduce the load at the lower speeds or to increase the machine size. For these reasons and because of the relatively poor efficiency, this kind

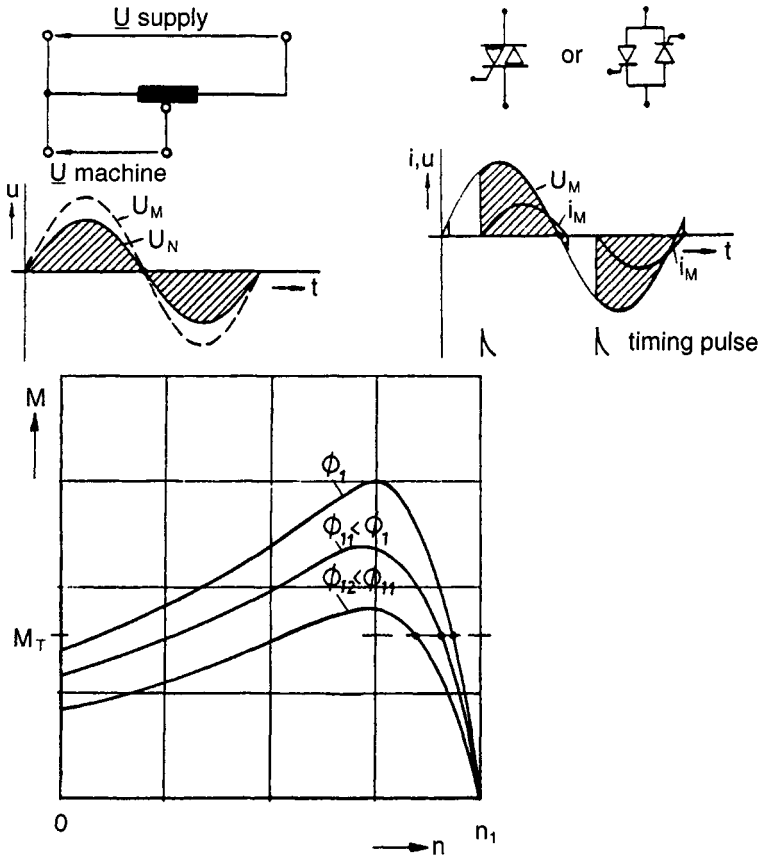


Figure 2.21 $M(n)$ by varying the airgap flux

of speed control – except for motor starting – is restricted to machines rated up to 3 kW.

Changing the rotor frequency f_2 in a double-fed machine. The stator rotating field with speed $n_1 = f_1/p$ interacts with the rotor rotating field with speed $n_2 = \pm f_2/p$ (depending upon the phase sequence), and a constant torque M is developed only when the two fields rotate at the same speed. Therefore, at rotor speed n , $n_1 = n + n_2$. (see eqns. 2.17 and following).

The induction motor becomes a synchronous motor running at speed

$$n = n_1 - n_2 = \frac{f_1 \mp f_2}{p} \tag{2.40}$$

When $f_2 = 0$ the rotor speed is constant, $n = n_1$. When the stator and rotor fields rotate at the same speed and in the same sense, i.e. when $f_1 = f_2$, the rotor speed is $n = 0$. When the stator fields have the same frequency but are counter-rotating, the rotor speed is $n = 2n_1$.

2.3 Single-phase motors

Frequently, particularly in domestic premises, there is only a single-phase supply available. It is then necessary to provide different R/X ratios in at least two of the stator windings to produce a phase shift between the two fields so that there is a rotating field.

In a motor with an auxiliary winding, this is achieved by increasing the winding resistance or by changing the reactance by connecting a capacitor in series with the winding. The operation of these machines, together with that of the externally started motor with only one winding, is discussed below in greater detail.

2.3.1 Externally started motor

The operation of a machine which has only a single stator winding is best understood if it is considered as having two equal counter-rotating uniform rotating fields, which develop torques M_m and M_g in opposite senses, and these torques are added in the rotor. In Figure 2.22 the direct torque M_m and the reverse torque M_g and their resultant sum M are shown as a function of slip. Thus, the motor develops an asynchronous torque except at standstill and off-load running. It must be started by some external means (thrown), and it runs up to speed in the direction thrown. The no-load speed is less than the synchronous speed. Because the reverse torque is significant at all speeds, the vibration torque at twice the mains frequency \hat{m}_p can also be large.

Figure 2.23 shows the asynchronous torque and the vibration torque relative to normal full-load torque for a 90 W motor. If the motor must start and run up independently, at least one extra winding is necessary so that some rotating field can be generated.

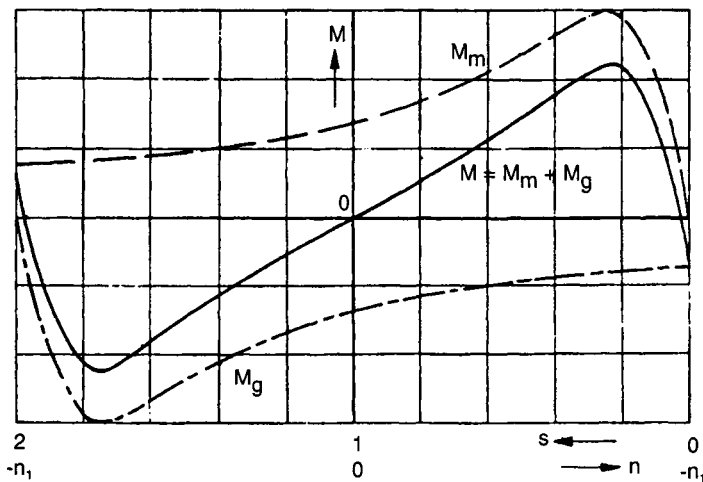


Figure 2.22 Torque developed in a one-winding motor

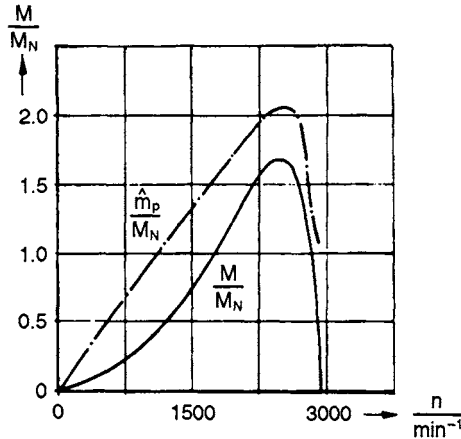


Figure 2.23 Vibration torque \hat{m}_p and asynchronous torque M relative to full-load torque M_N in a 90 W motor

2.3.2 Motor with a resistive auxiliary winding

In addition to the main winding H_a , there is an auxiliary winding H_i displaced spatially by 90 electrical degrees which, because of the high power loss in its series resistance R , must be switched out after run-up by means of a relay, centrifugal switch, thermal- or hand-operated switch (see Figure 2.24). The motor then runs with the single winding. The corresponding torque/speed run-up performance is shown in Figure 2.26. As the phasor diagram of the supply voltage and the currents (Figure 2.25) shows, the phase angle β between the starting currents is much less than 90° , so that only an elliptic rotating field can be generated. The torque is as shown in Figure 2.11. The starting torque depends on the machine design and is normally 1–1.5 M_N . The vibration torque is as shown in Figure 2.23 for the externally started motor.

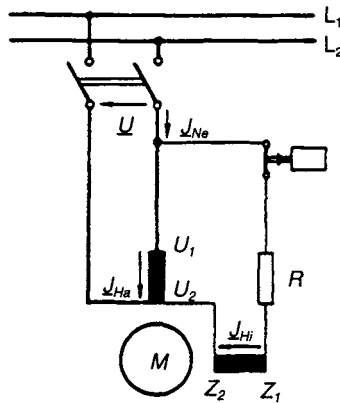


Figure 2.24 Circuit of a motor with resistive auxiliary winding

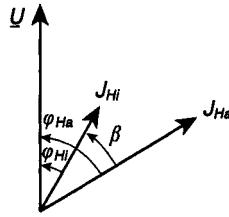


Figure 2.25 Phasor diagram of the stator currents

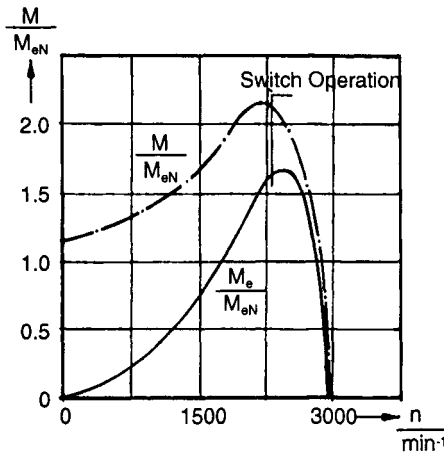


Figure 2.26 Torque/speed characteristics of the motor with resistive auxiliary winding relative to the full-load torque of the motor running on the main winding only

2.3.3 The capacitor start and run motor¹ (csar motor)

2.3.3.1 The two-winding motor

In the two-winding csar motor the auxiliary winding is set 90 electrical degrees spatially from the main winding and is supplied through a series-connected capacitor (see Figure 2.27). As the phasor diagram of voltages and currents, Figure 2.28, shows, a 90° phase advance between the two-winding currents is possible, given the correct capacitor value C . A uniform rotating field results when the MMFs of the two windings Θ_{Ha} and Θ_{Hi} have the same magnitude and a phase displacement of 90°. Given effective winding turns $N_{Ha}\xi_{Ha}$ and $N_{Hi}\xi_{Hi}$ this symmetry is achieved when the condition $\varphi_{Ha} = \varphi_{Hi} = \varphi_s$ is met; implying a transformation ratio r , where:

¹This motor, with its long descriptive title, is mentioned many times in this Chapter and the next. Therefore, frequent use is made of the easily written, read and said abbreviation, csar

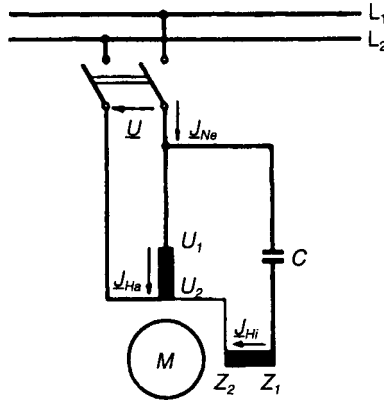


Figure 2.27 Circuit of a csar motor

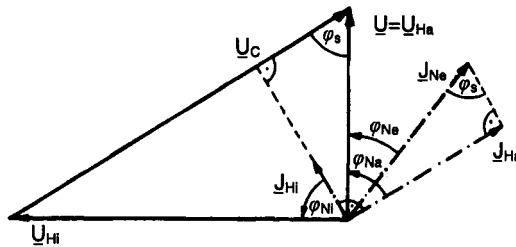


Figure 2.28 Phasor diagram of a loaded symmetrically matched csar motor

$$r = \frac{N_{Hi} \xi_{Hi}}{N_{Ha} \xi_{Ha}} = \frac{U_{Hi}}{U_{Ha}} = \frac{I_{Ha}}{I_{Hi}} = \tan \phi_s \tag{2.41}$$

The capacitance of C is

$$C = \frac{I_{Ha} \cos \phi_s}{U \omega \tan \phi_s} = \frac{I_{Ha}}{U \omega r \sqrt{1+r^2}} = \frac{I_{Nr}}{U \omega (1+r^2)} \tag{2.42}$$

The capacitor terminal voltage is

$$U_C = \frac{U}{\cos \phi_s} \tag{2.43}$$

which is obviously always greater than the supply voltage U.

Symmetry, i.e. a uniform rotating field, occurs for only one load – once r and C have been fixed. For all other loads, the rotating field is elliptic and, consequently, there is a vibrating torque. This is shown clearly in Figure 2.29. Conversely however, for a given required working point, the appropriate values of r and C for symmetry can be derived and provided.

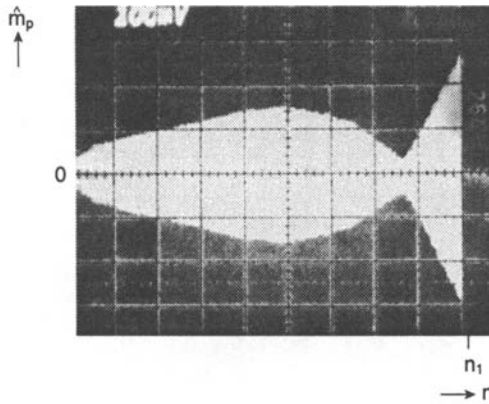


Figure 2.29 Oscillating torque amplitude in a csar motor (test result)

An important motor parameter is its starting torque M_A . The M_A can be comparable to that of a 3-phase motor of similar size when capacitance C is high. M_A is a maximum when the area of the parallelogram with adjacent sides J_{Ha} and J_{Hi} is a maximum (see Figure 2.28).

Because the auxiliary winding current is high when C is high, motors with high starting torques have their auxiliary windings switched out during run-up or their capacitor values switched down – in double capacitor motors – so that the motor runs symmetrically (see Figure 2.30). The auxiliary winding circuit includes R , L and C in series so that the component voltages – particularly across C – become greater than the supply voltage. Figure 2.31 gives an example of how the capacitor voltage U_c depends on the speed n .

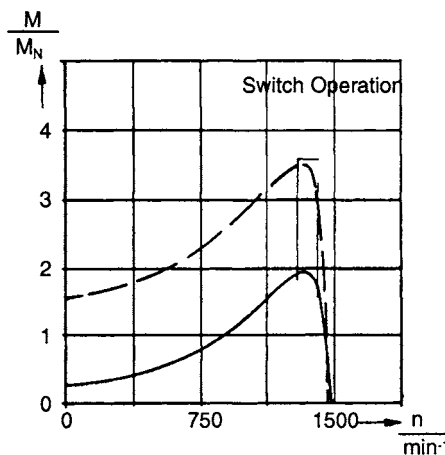


Figure 2.30 $M(n)$ of a double capacitor motor: one permanently connected and one switched out centrifugally

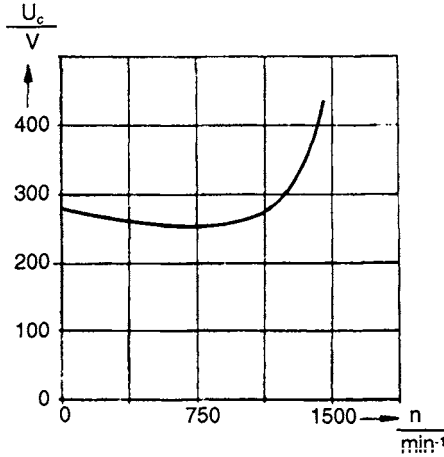


Figure 2.31 $U_c(n)$ of a csar motor capacitor with motor ratings 180 W, 220 V and $r = 1.5$

Metal-paper capacitors are used in permanently connected circuits and motor-electrolytic capacitors are used in circuits which include centrifugally operated cut-out switches.

2.3.3.2 Three-winding motors

Three-phase motors with either delta- or star-connected windings may also be run as symmetrical single-phase motors at specific speeds by means of connecting in the appropriate capacitors (see Figure 2.32).

The starting torques $M(s)$ are quite small, however, in comparison with 3-phase working, as Figure 2.33 shows. The necessary start and run capacitance is considerably more than that needed in the two-winding motor. The three-winding motors with this circuit are used only when 1-phase and 3-phase working is specified.

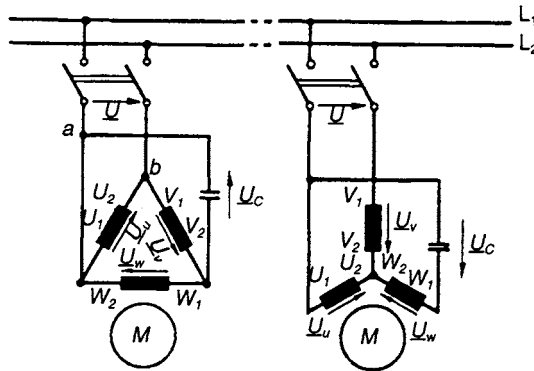


Figure 2.32 Steinmetz circuit

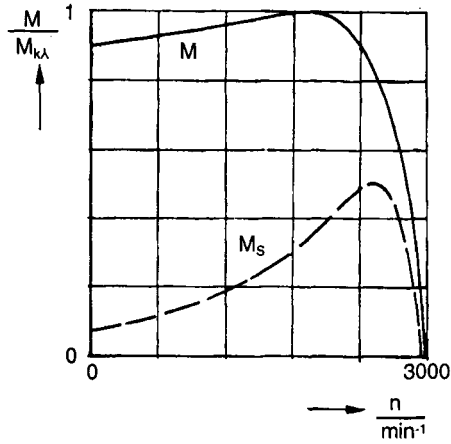


Figure 2.33 Torque $M(s)$ in the Steinmetz circuit and $M(n)$ when energised from the 3-phase supply

Chapter 3

Operation and application of polyphase induction motors

S. Tillner

3.1 Introduction

The polyphase induction motor, on account of its simple construction, its freedom from maintenance and its adaptability, has become the most frequently used of all motors. This is particularly so in industry, where the polyphase induction motor has become the standard 3-phase powered motor applied to the widest range of drives. Standard 3-phase motors have power ratings from about 60 W upwards. The manufacturers produce motors to suit the load requirements, mains voltages, operating times and starting requirements.

In the motor driven household appliance market, in central heating systems, house, garden and office appliances, two- or three-winding induction motors, adapted for running off single-phase mains and having a wide range of constructions, are used extensively. Pure 3-phase motors powered by 3-phase supplies are used in exceptional cases, e.g. for driving the pump in a large oil-fired boiler. An overview of the principal applications for, and power output required from, single-phase induction motors is given in Figure 3.1. The demands made on the motors differ considerably in the various applications quoted.

A lawn-mower motor should have the highest possible pull-out torque and the lowest possible weight. The utilisation factor is high and they are intensively fan cooled. Their starting torque requirement is relatively low.

The dimensioning of motors for hot water circulating systems is done with the highly unfavourable temperature conditions in mind. No ventilation is possible. Water temperatures up to 110°C and even higher temperatures within the motor are involved. The motor torque must be very smooth, with little vibration, otherwise motor vibrations are transmitted directly from the motor body into the piping system.

Each of the two- or three-winding motor circuits shown in Figure 3.2 has applications, depending upon the task in hand. The most frequently used is the two-winding csar¹ circuit (a).

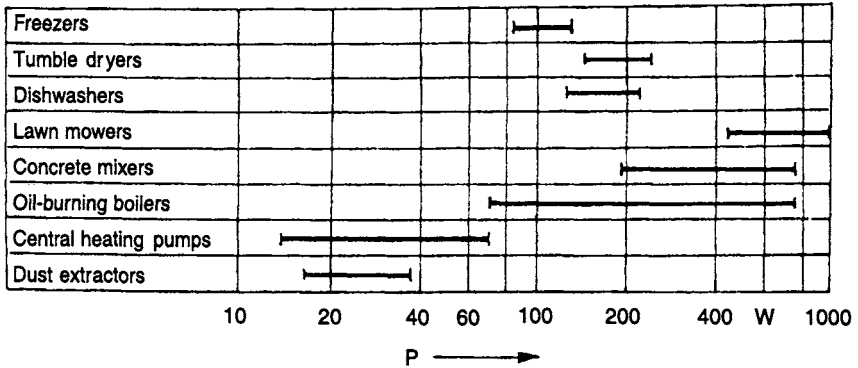


Figure 3.1 Examples of the applications of multiwinding induction motors in domestic appliances

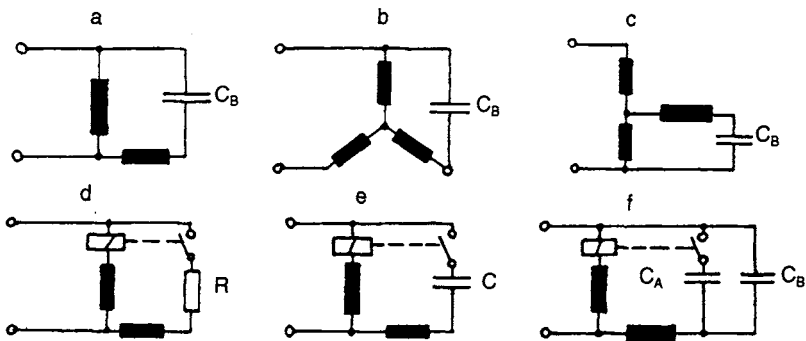


Figure 3.2 Workable winding layouts and circuits for the two- or three-winding induction motors running from a single phase supply

- a csar motor, two windings
- b csar motor, three windings
- c csar motor, T-circuit
- d resistive auxiliary phase motor
- e capacitor start motor
- f double capacitor motor

In Chapter 2 the operation of the induction motor was discussed according to the rotating field theory. The 3-phase induction motor energised from a symmetrical 3-phase supply has a uniform rotating field at all working points. The various forms of single-phase motors have in common that the airgap field is elliptic and that this field can be expressed as the sum of

¹In this chapter, the frequently mentioned capacitor start and run motor is abbreviated to csar motor.

superimposed direct and reverse uniform rotating fields. If the motor works from mains frequency f with slip s , then the direct rotating field B_M induces rotor currents with frequency sf , and for $1 > s > 0$ the driving torque M_m is developed. The reverse rotating field B_g induces rotor currents with frequency $(2 - s)f$, and a braking torque M_g is developed. The resulting output torque is²

$$M = M_m - M_g$$

As well as the asynchronous constant torque in the single-phase induction motor, there is an oscillating torque at twice the mains frequency owing to interaction between the direct rotating stator field B_M and the reverse rotating field produced by the rotor currents, and similarly between the reverse rotating stator field B_g and the direct rotating field produced by the rotor currents. The magnitude of the oscillating torque is dependent on the slip. The oscillating torques can often cause disturbing mechanical vibrations in the appliance. Isolating these vibrations is often an important mechanical design consideration.

3.2 The two-winding csar motor

3.2.1 Theoretical principles

The most frequently used single-phase powered induction motor is the two-winding csar motor, the reason being that, when it runs with its rated load, its performance approximates to that of a symmetrically powered 3-phase motor with its uniform rotating field. Figure 3.3 shows the winding layout of a two-winding 2-pole motor with 16 stator slots. Each winding occupies four slots per pole ($q = 4$) and the two complete windings are mutually displaced spatially by one-half a pole pitch.

The performance of the motor is determined by the currents in both windings depending on their magnitudes and the phase angle between them. Given the windings shown in Figure 3.3, there is a uniform rotating field when the MMFs in the two windings have equal magnitudes ($I_1 w_1 = I_2 w_2$) and when, for the specified sense of rotation, I_1 lags I_2 by 90° of phase angle.

The aim of the design is that, under rated running conditions, and in combination with the start and run capacitor C , the uniform rotating field condition is approximated as closely as possible.

An analysis of the performance of a single-phase energised multiwinding induction motor is made by means of utilising symmetrical components. An elliptic rotating airgap field can be resolved mathematically into direct and reverse uniform rotating components. Alternatively, a spatially symmetrically

²This torque equation relates to the scalar magnitudes of the three torques. In the equation $M = M_m + M_g$ of Section 2.2.3.2 the vectors of the torques are related.

wound machine can be considered to be energised by simultaneously applied direct and reverse rotating voltage supplies. This is now shown for a motor as in Figure 3.3, with two completely similar windings ($w_1 = w_2$). Figure 3.4a shows the voltages and phasor diagram of the direct voltage system. The voltage across coil 2 leads that on coil 1 by 90° of phase angle, indicated on the diagram as being multiplied by j . Figure 3.4b shows the reverse rotating system. The voltage across coil 2 lags that on coil 1 by 90° , indicated as multiplication by $-j$. The sums of these two component systems, as shown in Figure 3.4c, are the total voltages across coils 1 and 2. In the csar motor circuit, there is an impedance Z_v in series with coil 2, a capacitor.

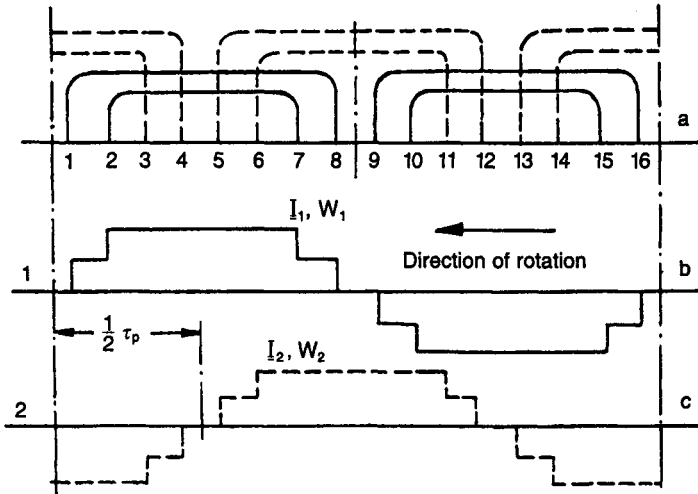


Figure 3.3 (a) spatial winding layout in a two-winding csar motor; (b) main winding MMF function; (c) auxiliary winding MMF function

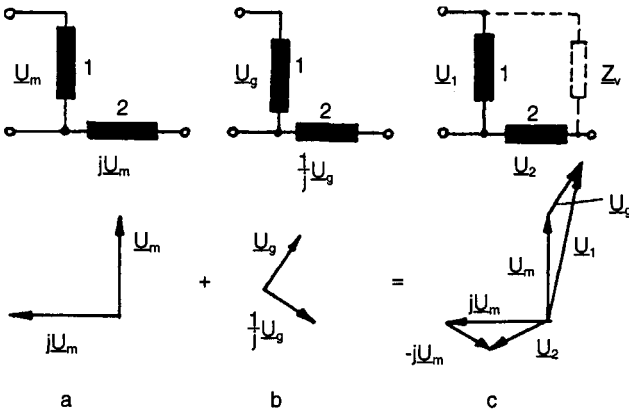


Figure 3.4 Representation in principle of the symmetrical components in the 2-phase system

In the analysis that follows, consideration is given to windings with unequal numbers of turns. Subscripts *HA* and *HI* apply, respectively, to the main and auxiliary windings. The turns per winding *w* with winding factor ξ appear in the expression for the transformation ratio:

$$r = \frac{w_{HI} \xi_{HI}}{w_{HA} \xi_{HA}}$$

The following equations connecting voltages and currents are then applicable (see also Figure 3.5):

Main winding voltage $\mathbf{U}_{HA} = \mathbf{U}_m + \mathbf{U}_g$

Auxiliary winding voltage $\mathbf{U}_{HI} = jr(\mathbf{U}_m - \mathbf{U}_g)$

Main winding current $\mathbf{I}_{HA} = \mathbf{I}_m + \mathbf{I}_g$

Auxiliary winding current $\mathbf{I}_{HI} = \frac{j}{r}(\mathbf{I}_m - \mathbf{I}_g)$

For each of the two symmetrical voltage components, reference can be made again to the straightforward 3-phase motor with its familiar equivalent circuit, Figure 3.6.

For each value of slip a direct impedance \mathbf{Z}_m and a reverse impedance \mathbf{Z}_g can be derived from the equivalent circuit. The principal difference between these two impedances is owing to the two effective rotor resistances. These are R_2'/s for the direct component and $R_2'/(2-s)$ for the reverse component system. The admittances to the two component voltages are:

$$\mathbf{Y}_m = \frac{1}{\mathbf{Z}_m} \quad \mathbf{Y}_g = \frac{1}{\mathbf{Z}_g}$$

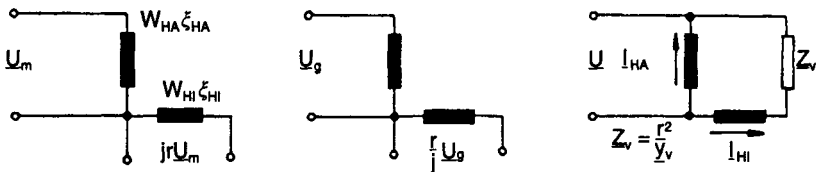


Figure 3.5 Symmetrical components of the voltage system at the two-winding induction motor.

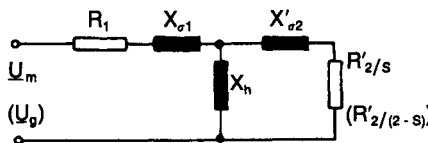


Figure 3.6 Equivalent circuit of the induction motor with symmetrical component voltage supplies U_m and U_g

Using the relationship derived from Figure 3.5c,

$$\mathbf{U} = \mathbf{U}_{HI} + \mathbf{I}_{HI} \mathbf{Z}_V$$

and applying the transformation ratio r to calculate the transformed admittance for \mathbf{Z}_v ,

$$\mathbf{Y}_V = r^2 / \mathbf{Z}_V$$

It can be shown, after a few algebraic reductions, that

$$\frac{\mathbf{U}_m}{\mathbf{U}} = \frac{\mathbf{Y}_g + \mathbf{Y}_v(1 - j/r)}{\mathbf{Y}_m + \mathbf{Y}_g + 2\mathbf{Y}_v} \quad \text{and} \quad \frac{\mathbf{U}_g}{\mathbf{U}} = \frac{\mathbf{Y}_m + \mathbf{Y}_v(1 + j/r)}{\mathbf{Y}_m + \mathbf{Y}_g + 2\mathbf{Y}_v}$$

The asynchronous torque is then calculated from the rotating field power for each symmetrical component of voltage. It must be recognised that the direct component produces a direct driving torque and the reverse component produces a braking torque. The asynchronous torque of the motor is derived as

$$M = \frac{2p}{\omega} \left[I_m^2 \operatorname{Re}(\mathbf{Z}_m - R_1) - I_g^2 \operatorname{Re}(\mathbf{Z}_g - R_1) \right]$$

The vibration torque at twice the mains frequency is, according to

$$M_p = \frac{2p}{\omega} \operatorname{Re} \left[\mathbf{I}_m \mathbf{I}_g (\mathbf{Z}_m - \mathbf{Z}_g) \exp j2\omega t \right]$$

The amplitude of the vibration torque corresponds to the length of the phasor and is written as:

$$\hat{M}_p = \frac{2p}{\omega} \left| \mathbf{I}_m \mathbf{I}_g (\mathbf{Z}_m - \mathbf{Z}_g) \right|$$

The vibration torques disappear when $\mathbf{Z}_m - \mathbf{Z}_g = 0$, i.e. at standstill, and when $I_g = 0$, i.e. when the reverse current symmetrical component disappears.

Symmetrical drive (uniform rotating field condition): A uniform rotating field arises when the reverse rotating voltage system disappears, i.e. when

$$\mathbf{Y}_m + \mathbf{Y}_v(1 - j/r) = 0$$

For a series capacitor C in the auxiliary circuit branch,

$$\mathbf{Y}_v = j\omega C$$

The condition for the symmetrical drive is then

$$\mathbf{Y}_m = \omega C (1/r - j)r^2$$

$$\omega C = Y_m \frac{1}{r\sqrt{1+r^2}}$$

A phasor diagram representation of the symmetrical operation of a two-winding motor relating voltages and currents is given in Figure 3.7 for $r = 1$ and $r > 1$. It is seen that, when $r = 1$, and symmetrical drive conditions are achieved, $\cos \phi = 1$. From the diagram Figure 3.7c and the substitutions $r = U_{HI} / U_{HA} = \tan \Psi$, relations that can be directly read off are:

$$I_{HI} = I_c = U_c \omega C \qquad \phi = 2\Psi - 90^\circ$$

$$\omega C U_N / \cos \Psi = I_N \cos \Psi$$

$$C = \frac{I_N}{\omega U_N} \cos^2 \Psi = \frac{I_N}{\omega U_N} \frac{1}{1+r^2}$$

Thus, it is a simple matter to determine the necessary start and run capacitance for a motor with specified parameters. For a two-winding motor with rated output power 44 W, efficiency $\eta = 0.5$, wound for 220 V working and a winding turns ratio $r = 1.25$, the calculated results are:

$$\psi = 51.6^\circ \quad \phi = 12.6^\circ \quad I_N = 0.41 \text{ A} \quad C = 2.3 \mu\text{F}$$

3.2.2 Operating characteristics of a two-winding csar motor

The operating characteristics of a two-winding csar motor can be appreciated from Figure 3.8. Those of a motor with a power rating 45 W are plotted against a base of speed. Asynchronous torque, amplitude of the vibration torque at twice the mains frequency and the per-unit direct and reverse rotating symmetrical voltage components are shown. In accordance with the aim of the design – optimum performance at rated power – it is noted that the reverse voltage symmetrical component and the vibration torque each have a minimum in the region of the speed at full load. From this load down to the no-load condition the vibration torque amplitude rises steeply, so that in many applications it is necessary to include vibration absorption means in the mechanical design.

Figure 3.9 shows the locus diagrams in the complex number plane of main-winding current, auxiliary winding current and supply current for the motor

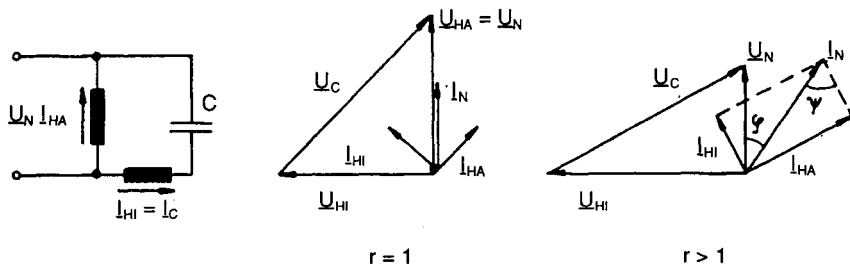


Figure 3.7 Phasor diagram of voltages and currents for symmetrical drive in a two-winding csar motor for $r = 1$ and $r > 1$

of Figure 3.8 operating in the motoring range $0 \leq s \leq 1$. In this example, the typical result occurs, in that the auxiliary winding current is greater when the motor is running light ($s = 0$) than when it is stationary ($s = 1$). In contrast,

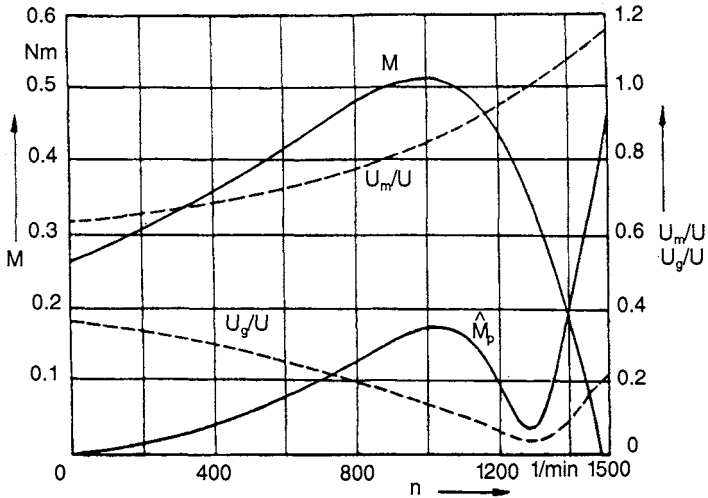


Figure 3.8 Operating characteristics of a two-winding capacitor motor (asynchronous torque, M , amplitude of the 100 Hz vibration torque, \hat{M}_p , and symmetrical components of the voltage system plotted against speed)

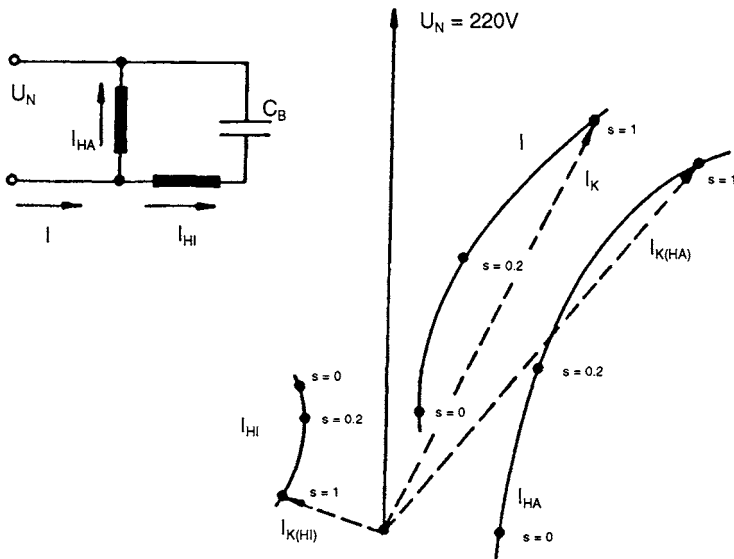


Figure 3.9 Locus diagrams of mains current, main winding and auxiliary winding currents for the motor of Figure 3.8

the main winding current rises steeply with increasing slip. During light running the heating in the auxiliary winding is usually greater than that in the main winding. Under high slip conditions, $s \rightarrow 1$, there is considerable heating in the main winding and the provision of thermal overload protection must be considered in the design.

The current loci may be determined simply by measuring the three currents I_{HA} , I_{HT} and I together with the power so that the phase angles ϕ may be calculated. When the effective winding turns ratio r is known, it is a simple matter to determine the operating point for symmetrical running.

Fig 3.10 shows a further set of characteristics of the motor of Figure 3.8. This time, speed n , heating power loss P_v , efficiency η and capacitor voltage U_c are plotted against torque.

The heating power loss P_v is greater on light load than on full load. In practice, therefore, csar heating power loss measurements are frequently done at light load.

The capacitor voltage U_c is greatest when the motor is running off load, and the capacitor must be specified accordingly.

Table 3.1 gives an overview of the technical data for a number of two-winding csar motors.

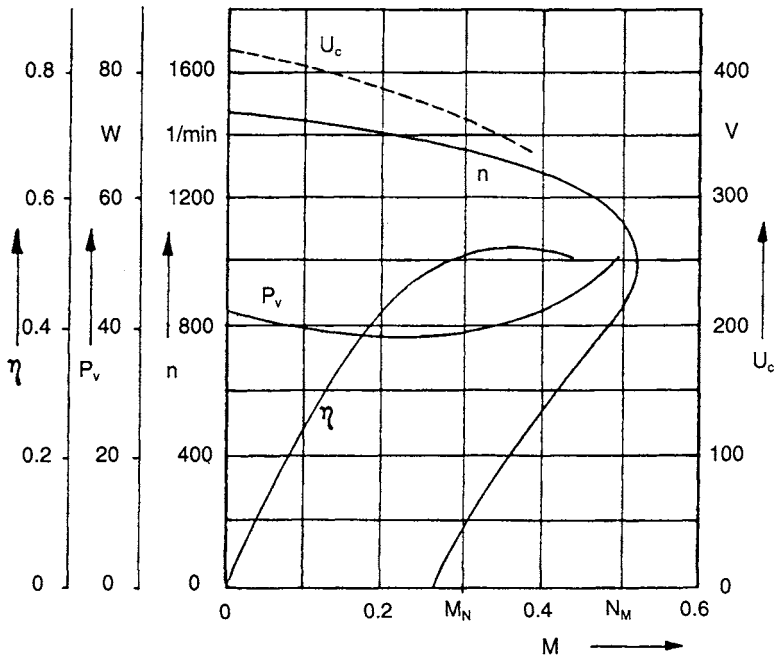


Figure 3.10 Operating characteristics of a two-winding csar motor (speed n , heating power loss P_v , efficiency η and capacitor voltage U_c as functions of torque M)

Table 3.1 *Technical data of a number of two-winding csar motors, with rated voltage 220 V, 50 Hz*

D_a = stator stamping external diameter; l_e = rotor core (iron) length; p = no. of pole pairs; M = starting torque; M_K = stalling (pull-out) torque

Cat. no.	D_a (mm)	l_e (mm)	p	P_2 (W)	n (rev/min)	M_A (Ncm)	M_K (Ncm)	η	C (μ F)
1	68	25	1	18	2600	6	11	0.40	1.0
2	68	56	1	40	2600	15	24	0.47	3.0
3	85	56	1	120	2600	38	72	0.57	5.0
4	102	40	1	180	2800	53	152	0.58	6.0
5	130	45	1	600	2850	50	400	0.67	12
6	85	38	2	40	1250	27	47	0.50	2.5
7	85	56	2	60	1250	35	65	0.52	3.0
8	117	32	2	210	1370	100	250	0.61	10
9	117	50	2	330	1390	132	407	0.63	12

3.2.3 Motors with input voltage selection

In special cases, motors with a 1:2 input voltage selection option are manufactured (e.g. for 110/220 V). Both the main winding and the auxiliary winding comprise two identical coils for series/parallel (high voltage/low voltage, respectively) connection. A different capacitor is required for each circuit, the lower voltage circuit requiring four times the capacitance.

Sometimes a voltage selection option of 1:2 is achieved by means of a T-circuit. Only the main winding is made up with two coils. Given low voltage input, the two main winding coils are connected in parallel, and the auxiliary winding plus series capacitor branch is also connected in parallel with the two parallel connected main winding coils. This is no different from the normal motor circuit. Given high voltage input the main winding coils are connected in series and the auxiliary winding with series capacitor branch is connected in parallel with one of the main winding coils. Hence, the currents in the two main winding coils are unequal. The operating characteristics of the high voltage circuit are less favourable. The voltage selection switching is much simpler (and only one capacitor is needed), but the motor can then only be used in applications where the demand for starting torque is low.

3.3 The three-winding csar motor

The layout of the stator winding is the same as in a three-phase motor; the motor is driven in accordance with Figure 3.2c (Steinmetz circuit). The performance is similar, in most respects, to that of the two-winding motor. There are certain differences, however, in view of the different layout.

Figure 3.11 shows the circuit and the voltage and current phasor diagram for a csar motor, whose windings are star-connected, when it is loaded for symmetrical running. The current through winding *v* is the capacitor current and is 90° phase advanced on the capacitor voltage $U_C = U_{VW}$. It follows that, for symmetrical running, the phase angle between voltage and current for each individual winding is 60° and that the phase angle between the supply voltage U_N and the input current I_N is 30°.

The capacitance of C for symmetrical running is derived from

$$C = \frac{I_{sym}}{\omega U_N}$$

For symmetrical running the three-winding csar motor capacitor voltage is the same as the supply voltage and hence 30–40% less than that for a two-winding motor with winding turns ratio $r = 1.1-1.3$ (as is usually the case). However, the capacitance in the case of the three-winding motor is greater by a factor 2.5–3.

3.4 Choice between the two-winding and three-winding motor

The choice between a two-coil or a three-coil winding often turns on manufacturing considerations – for example, whichever winding is the more practicable for the number of slots in the available stator stampings. Other reasons can be the requisite capacitance and its voltage rating, voltage selection or reversibility. A comparison of the implications is given in Table 3.2.

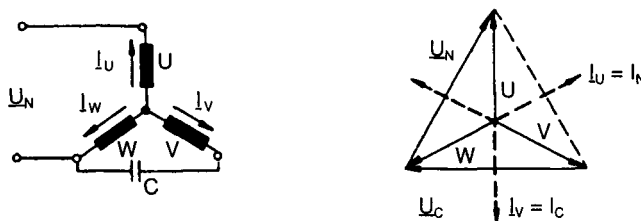


Figure 3.11 Phasor diagram of voltages and currents in a three-winding csar motor loaded for symmetrical running

Table 3.2 Some guidance towards the choice between a two-winding and three-winding motor

	Two-winding	Three-winding
Winding details	$r = 1-1.3$ depending on the slot patterns	Symmetrical
Capacitance	C	$C = 2.5-3.5 C$
Capacitor voltage	$1.8-2.3 U_N$	$1-1.3 U_N$
Reversal with the same characteristics in both directions	Two-pole switch for windings with $r \neq 1$	Single-pole switch
Voltage selection 2:1	8 terminals 2 capacitors T-circuit 4 terminals 1 capacitor	10 terminals 2 capacitors

In practice the two-winding csar motor is preferred, because it is usually the more cost-effective on account of the capacitor. An advantage of the three-winding motor is that the switching for motor reversal is much simpler, as Table 3.2 indicates.

3.5 In-service supply voltage tolerances

Because motors are energised from mains supplies whose voltages vary, and because the start and run capacitor has a $\pm 10\%$ manufacturing tolerance on C , the question arises: what influence do these variables have on motor performance when the design is based on the rated voltage and nominal capacitance?

First, the torque characteristic and the heating effects must be considered. Given a supply voltage variation from 0.9 to $1.06 U_N$, the worst torque characteristics occur at $0.9 U_N$ and $0.9 C$. The worst heating occurs for $1.06 U_N$ and $1.1 C$. Vibration torque at twice the mains frequency is worst at the other 'corner points', i.e. $0.9 U_N$ with $1.1 C$ and $1.06 U_N$ with $0.9 C$.

The following data have been determined for a two-winding csar motor with rated power output 160 W:

Rated voltage = 230 V (50 Hz), Capacitance = 7.0 μF
 Torque = 0.6 Nm at 2700 rev/min

Vibration torque developed

- at U_N and C : 0.01 Nm
- at $1.06 U_N$ and $0.9 C$: 0.22 Nm
- at $0.9 U_N$ and $1.1 C$: 0.20 Nm

For critical applications, a tightening of capacitor tolerance could be considered.

3.6 Comparison of csar motor and 3-phase motor

A comparison between the technical data of csar motors and 3-phase motors with the same frame size is given in Table 3.3. The motors compared here have the same stator stamping.

Table 3.3 Comparison of csar motors with three phase motors

1, 2 (csar)		csar motors				
3, 4 (tp)		three phase motors				
No.	D_a (mm)	l_e (mm)	P_2 (W)	n (rev/min)	M_A (Nm)	M_K (Nm)
1	130	45	370	2750	0.9	2.8
2	130	63	550	2800	1.2	4.5
3	130	45	550	2850	5.8	6.0
4	130	63	800	2880	9.2	9.5

3.7 Motors with starter windings

Single-phase motors with auxiliary-start windings are called into play when starting demands are heavy, i.e. when the starting torque must be appreciably more than the full-load running torque. There is a choice between capacitor-start motors and resistive auxiliary winding motors. The motor starts and accelerates with the auxiliary winding circuit switched in. At a speed approximating to pull-out torque/slip the auxiliary circuit is switched out, for example by the release of a relay that monitors the main winding current, or by a PTC (positive temperature coefficient) resistor. The motor then runs as a single-winding machine. In general, the auxiliary winding has a lower material cost owing to its shorter-term thermal requirements.

The motor, however, running as a single-winding machine, has far less impressive running characteristics than the csar motor. The vibration torque at twice the mains frequency has the same order of magnitude as the pull-out torque. Also, the efficiency is lower, and it can only be improved by the use of considerably more copper for the main winding.

3.7.1 Run-up characteristics of the resistive auxiliary phase motor

For there to be a starting torque, there must be a phase difference between the currents in the two coils at standstill. This is achieved in the resistive auxiliary phase motor by, for example, using finer wire for the coil or by adding some bifilar (magnetically ineffective) turns, so that its resistance is increased appreciably. Figure 3.12 shows the operating characteristics of a resistive auxiliary phase motor, the phasor diagram for the currents at standstill being shown in Figure 3.13.

In the following example, the power distribution at standstill is given as:

Short-circuit input power	$P_{1k} = 1800 \text{ W}$
Copper loss in main winding	$P_{cuHA} = 370 \text{ W}$
Copper loss in auxiliary winding	$P_{cuHI} = 1070 \text{ W}$
Iron loss ³	$P_{Fe} \approx 20 \text{ W}$

This means that, out of the 1800 W short-circuit input power, about 80% is dissipated as copper loss in the stator rotor windings. The auxiliary winding is severely stressed thermally. In this case the auxiliary winding temperature rises at the rate of about 17°C/s. The rotating field power corresponding to a starting torque of 0.6 Nm accounts for only about 10% of the short-circuit

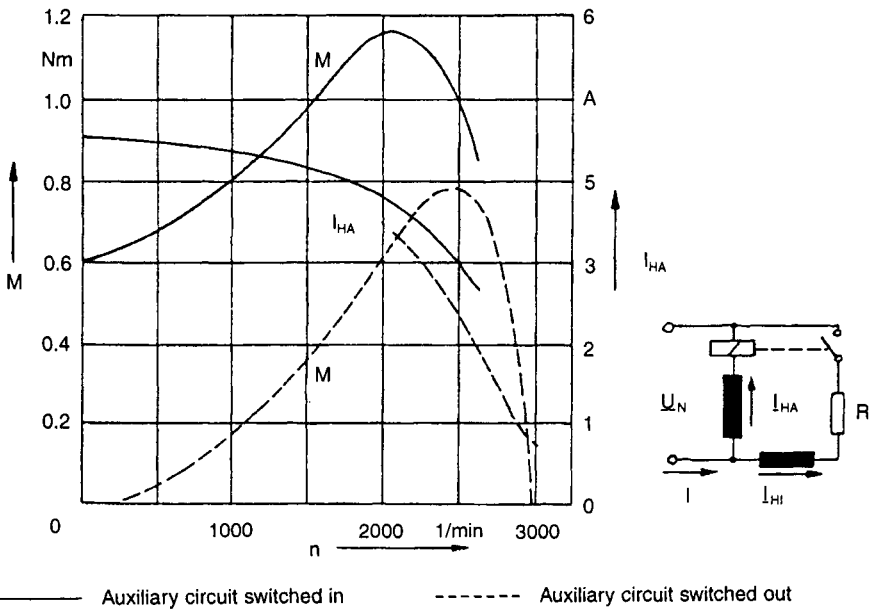


Figure 3.12 Operating characteristics of resistive auxiliary phase motors

³There is a 340 W discrepancy in the power balance. This is mainly rotor copper loss which is, normally, not directly measurable.

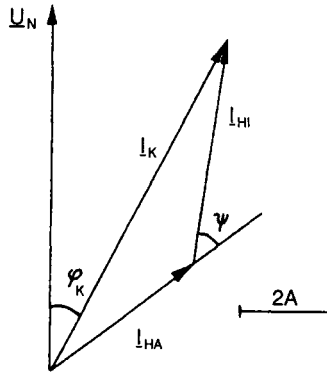


Figure 3.13 Phasor diagram of the starting currents in the resistive auxiliary phase motor (from the example of Figure 3.12)

input power. For this reason the power ratings of standard production auxiliary phase motors are kept less than 250 W.

A typical application: compressor motor in a refrigerating appliance. The motor is built into the refrigerant circuit. What matters most is a good efficiency under standard working conditions. To this end the main winding is designed to have low MMF harmonic content and it occupies two-thirds of the stator slots. The main winding stator slots are enlarged to accommodate more copper, which is necessary for achieving the desired efficiency. Under standard working conditions, an efficiency of about 65% can be achieved. In freezer motors the auxiliary winding is usually taken out of circuit by means of a positive temperature characteristic resistor.

3.7.2 Starting characteristics of capacitor-start motors

The power balance under starting conditions is considerably better in the capacitor-start motor than it is in the resistive auxiliary phase motor. A significantly better phase shift between the main winding and the auxiliary winding currents is achieved. Figure 3.14 shows the torque-speed characteristics of a capacitor-start motor with a closed and open auxiliary phase circuit. Figure 3.15 is the phasor diagram for the starting currents. During starting the power balance is typically:

Short-circuit input power	$P_K = 425 \text{ W}$
Copper loss in main winding	$P_{cuHA} = 155 \text{ W}$
Copper loss in auxiliary winding	$P_{cuHI} = 80 \text{ W}$
Iron loss	$P_{Fe} \approx 10 \text{ W}$
Rotor power (not directly measurable)	$\approx 180 \text{ W}$

For the motor with starting torque $M_A = 0.4 \text{ Nm}$, the rated mechanical power output is about 125 W or about 30% of the input power on starting. In comparison with the resistive auxiliary phase motor, the capacitor-start motor

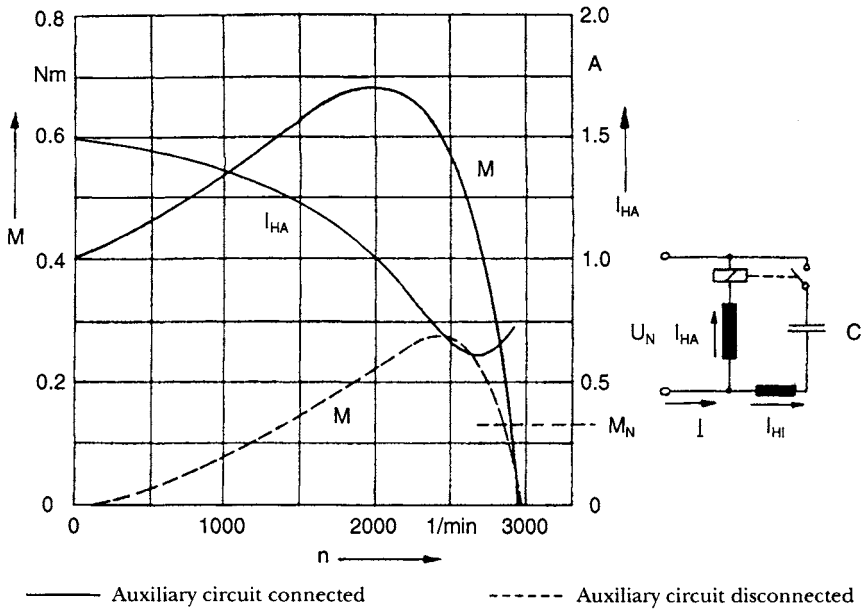


Figure 3.14 Characteristics of a capacitor-start motor

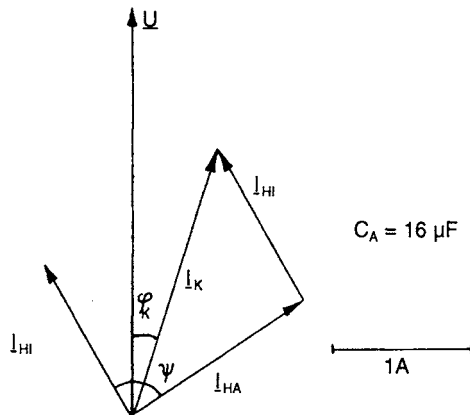


Figure 3.15 Phasor diagram of the starting currents in a capacitor-start motor (circuit, Figure 3.14)

develops about three times the starting torque for a given input starting power. A nonpolarised electrolytic capacitor is often used in the briefly energised auxiliary phase circuit. This capacitor is physically smaller than the metallised paper capacitors for a given capacitance.

3.7.3 Double capacitor motors

Alternatively, double capacitor motors may be installed when the starting conditions are difficult, i.e. in applications where the starting torque must be greater than the full-load running torque. The double capacitor motor can be designed for optimum efficiency, speed regulation and low-vibration running at full-load torque output without the need to compromise for good starting characteristics. Starting and accelerating characteristics are then optimised by appropriate choice of the starting capacitor.

3.8 Application of multiwinding induction motors

It becomes clear from the examples that follow that the mechanical construction of a motor is developed specifically to suit the application. Examples of mass-produced motors are chosen.

3.8.1 Motors for central heating circulating pumps

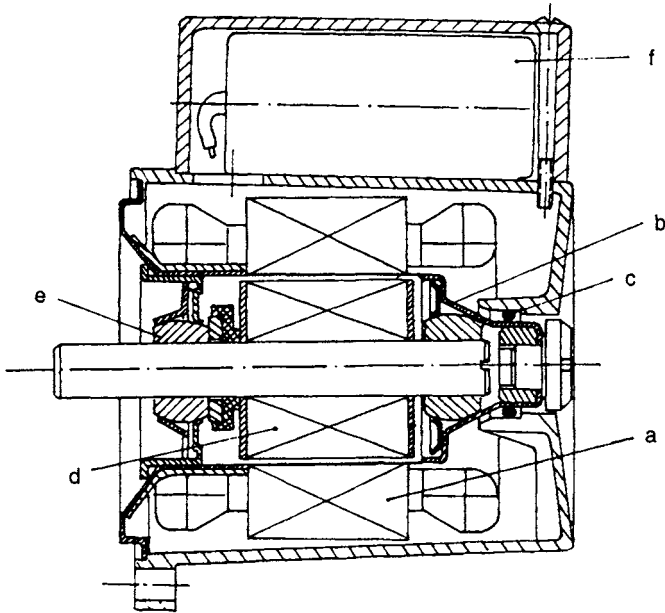
Drive motors for central heating circulating pumps are specially constructed castor motors. Figure 3.16 shows the longitudinal cross-section through a pump motor with split-case design. The stator and rotor regions are separated by a split case made of nonmagnetic steel. This split case is rigidly connected to the stator lamination assembly at its inside diameter and, at the same time, it holds the motor bearings. Pump motors are now usually fitted with a ceramic shaft and ceramic self-aligning bearings. The thrust washer behind the bearing at the shaft output end is also ceramic. The rotor cage is normally copper and the rotor body is encapsulated in a shell of corrosion-proof material.

Pump motors are thermally highly stressed (no ventilation, and contact with water at temperatures up to 110°C). There are pump motors manufactured in which the stators are encapsulated in a quartz-and-resin compound to improve heat conduction and raise the power rating.

Vibration-free running is essential for pump motors, otherwise 100 Hz hum is transmitted throughout the entire piping system. It is necessary to ensure that the on-load duty of the motor brings it as close as possible to symmetrical running conditions.

3.8.2 Washing machine drives

Although the electronically controlled series-wound commutator-motor presents the most frequently used solution for modern washing machines, the application of pole-changing induction motors is mentioned briefly. 2/12, 2/16 and 2/24 pole motors are encountered. The washing machine drive, with a drum speed of 50 to 55 rev/min, is achieved by means of the



*Figure 3.16 Longitudinal section through a central heating circulating pump
a stator lamination set; b split case; c gasket (O-ring); d rotor body;
e self-aligning bearing; f start and run capacitor*

appropriate multipole motor and belt reduction drive between the motor and drum. The motor is switched to two-pole working for spinner drive. The greater the pole-change ratio, the larger and heavier the motor. A comparison between induction motor drives and the increasingly used electronically controlled series commutator motor drive is given in Table 3.4.

Table 3.4 Technical data for washing machine drives: pole-changing induction motor (IM); universal series commutator motor (UM).

Motor	Motor speed, rev/min	Belt drive ratio	Spin speed, rev/min	Motor weight, kg
2/12 pole IM	450/2900	7.5:1	~ 400	10
2/16 pole IM	330/2900	5.8:1	~500	12
2/24 pole IM	220/2900	3.9:1	~700	15
Controlled UM	660/15000	12.5:1	~1200	6

Washing machines with pole-change motors are still encountered in southern Europe. Other solutions include pole-change motors in combination with phase shift control and speed regulation for increasing the speed ratio between wash and spin, giving a higher spin top speed.

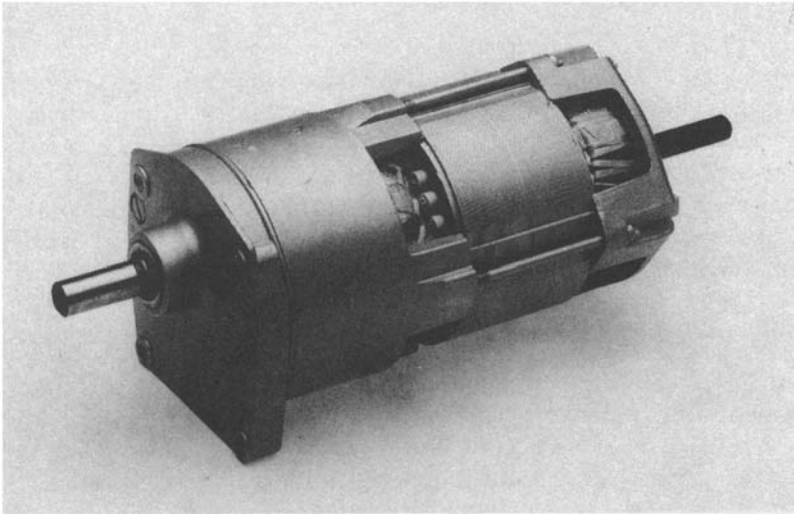


Figure 3.17 Integral motor-gearbox unit

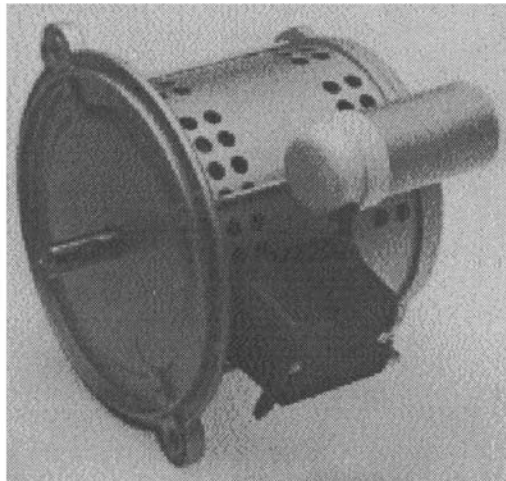


Figure 3.18 Oil-burner motor

A method much used in the past is worth mentioning. It uses a 2/4 pole motor and a two-speed gearbox so that an overall speed change from 7.5 to 1 for spinning and washing, respectively, is obtainable.

Now, particularly in central Europe, the induction motor has been replaced, in the main, by the electronically controlled universal series commutator motor, capable of achieving spinner speeds up to 1500 rev/min.

3.8.3 Main drives for photocopiers

The main drives for photocopiers are built in some cases as integral motor-gearbox units. The motor is a two-winding csar motor with power rating 100–300 W loaded to run with a low vibration torque under steady-state conditions.

The starting torque is usually greater than the full-load running torque. Importance is attached to a swift run-up. Therefore the motors are often provided with two capacitors. Life expectancy for the gearbox is expected to be between 2000 and 3000 working hours.

3.8.4 Oil-burner motors

Motors for oil-burners are constructed according to VDE 0530 and are provided with a flange according to DIN 42023. The blower wheel is connected to the flange end of the motor shaft. The nondrive end is constructed for mounting the oil pump that is driven via a coupling.

The motor power is related to the required 'burn' and can be between 100 and 800 W. Oil-burner motors are normally two-winding csar motors with externally mounted capacitors. For special applications oil-burner motors are made for direct connection to the 3-phase supply. Figure 3.18 shows a high power oil-burner motor.

Chapter 4
Shaded-pole induction motors

S. Tillner

4.1 Introduction

Millions of shaded-pole induction motors are made every year, with power ratings from a fraction of a watt to about 150 W. Applications are generally in small electrical appliances that require only a few watts of power, e.g. for driving heater fans or slide projector fans. In the household appliance market shaded-pole motors are used in washing machines as discharge pump motors and in cookers as fan motors in large quantities. In ironing machines, these motors are used with reduction gearing for driving the rollers. The direct drive to the drum of a washing machine for spinning has become a classical application for larger two- or four-pole shaded-pole motors with power ratings from 60 to 150 W. The motor is also used in vending machines for driving the fans and in combination with gearing and linkages for selecting and delivering the goods.

The construction of the shaded-pole motor is simple, particularly with respect to the windings. Large quantity production and extensive automation results in a favourable price per unit, and the shaded-pole motor often offers the most cost-effective solution to a drive problem. Their disadvantages compared with, say, capacitor start and run motors should be considered, however – namely their low efficiency and very often their unfavourable torque–speed characteristics.

4.2 Operation of the shaded-pole motor

The shaded-pole motor is a single-phase induction motor with the simplest possible structure, characterised by prewound stator coils fitted over laminated poles and transformer-coupled short-circuited auxiliary windings. These surround a part of the pole and normally take the form of a massive copper ring. This construction produces an elliptic rotating field in the airgap. This field acts on and turns the squirrel cage rotor.

The physical principles of the shaded-pole motor are more easily seen if, at first, the rotor cage is considered to be open-circuit. The development of the magnetic flux phasor diagrams proceeds from considering Figure 4.1*a*.

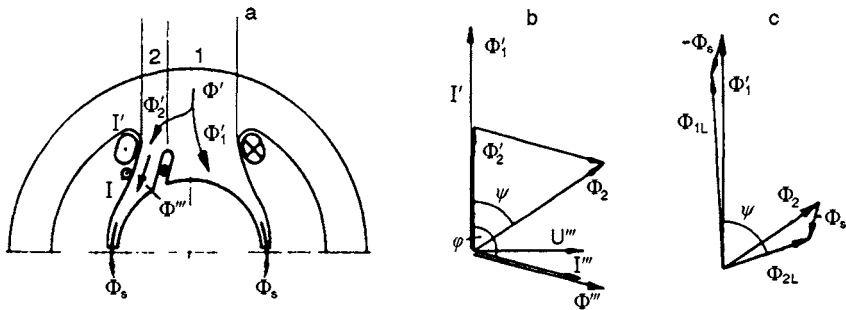
Current I' flows through the main winding, which has w turns. The auxiliary winding, which surrounds a part of the pole, is coupled to the main winding with mutual inductance M_{13} and carries current I''' . The voltage induced in the shaded-pole winding is

$$U''' = -j\omega M_{13}I'$$

and it lags the current I' by 90° . The impedance of the shaded-pole winding is inductive ($R''' + j\omega L'''$) so that the shaded-pole current I''' lags behind the voltage U''' . The shaded-pole current I''' lags behind the main current I' by the phase angle φ .

The component flux phasor diagrams are given in Figure 4.1 *b, c*. The main winding current I' causes the flux Φ' . The component Φ'_1 occupies pole section 1 and the component Φ'_2 occupies pole section 2. Flux Φ''' resulting from the shaded-pole winding current I''' is present in pole section 2 only. Thus the total in section 2, $\Phi_2 = \Phi''' + \Phi'_2$, lags behind the flux Φ'_1 in the pole section 1 by the angle ψ . Spatially the fluxes in the two pole sections are displaced by 90 electrical degrees. The rotating flux peak occurs first in the main pole and then in the shaded pole and thus the squirrel cage rotor turns in this sense, counter-clockwise in Figure 4.1*a*.

In Figure 4.1*c* account is also taken of the leakage flux Φ_s , which runs from each main pole to the neighbouring shaded pole and bypasses the rotor. Leakage flux reduces the magnitudes of both the main fluxes but, at the same time, increases the phase angle between them. This is a significant feature in motors which have 'stamped leakage bridges' (see Sections 4.4 and 4.6).



open-circuit rotor

Figure 4.1 Schematic diagram of the shaded-pole motor with open circuit rotor winding (a) and the principal phasor diagrams of the magnetic flux components (b, c)

4.3 Field distribution and harmonic fields

Owing to the stator construction, with its concentrated wound coils fixed around salient poles, the airgap field distribution has a significant spatial harmonic content. Figure 4.2a shows the airgap MMFs resulting from currents I' and I''' , spatially and at one instant of time. The spatial distributions are rectangular and stretch over pole span c' for the main winding and pole span c''' for the auxiliary shaded-pole winding. c' and c''' are arcs, shown as liner developments in Figure 4.2a.

Fourier analysis of the MMF distributions produces the following expressions for the fundamental magnetic field components:

Alternating field resulting from I' :

$$b_1' = B_1' \cos \omega t$$

where

$$B_1' = \mu_0 \frac{4}{\pi} \frac{I' w \sqrt{2}}{\delta} \sin\left(\frac{c' \pi}{t_p 2}\right)$$

Alternating field resulting from I''' :

$$b_1''' = B_1''' e^{j\beta t} \cos(\omega t + \varphi)$$

where

$$B_1''' = \mu_0 \frac{4}{\pi} \frac{I''' \sqrt{2}}{\delta} \sin\left(\frac{c''' \pi}{t_p 2}\right)$$

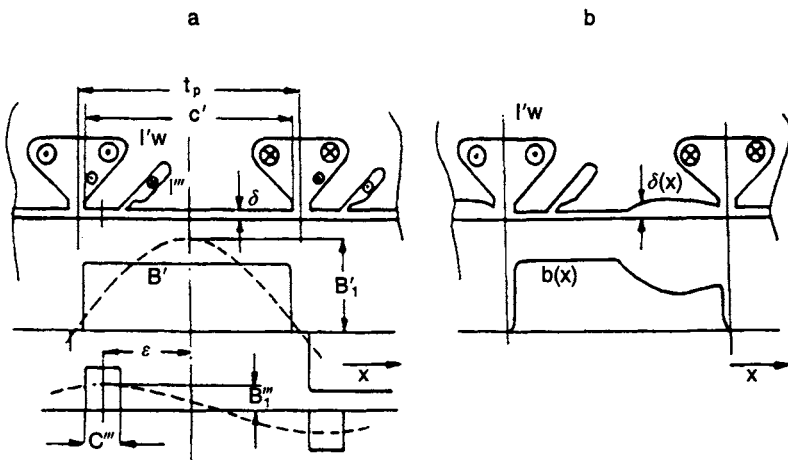


Figure 4.2 Flux density distribution owing to: (a) main winding and a uniform airgap; (b) main winding and a nonuniform airgap for the reduction of harmonic content

Each of the above alternating fields may be expressed as the sum of two uniform rotating fields, with opposite directions of rotation, and magnitudes equal to half of the magnitudes of the alternating fields. The resulting clockwise (cw) and counter-clockwise (ccw) fields may be expressed as

$$\mathbf{B}_{1ccw} = \frac{1}{2} \left\{ B_1' + B_1''' e^{j(\phi + t\epsilon)} \right\} e^{j\omega t}$$

and

$$\mathbf{B}_{1cw} = \frac{1}{2} \left\{ B_1' + B_1''' e^{-j(\phi - t\epsilon)} \right\} e^{-j\omega t}$$

The airgap field thus derived is a highly elliptic rotating field.

Amongst the spatial harmonic fields the third harmonic is particularly significant. From the Fourier analysis of what is practically a square wave MMF function (see Figure 4.2*a*) it follows that, for excitation I' , the spatial third harmonic field amplitude is

$$B_3' = \mu_0 \frac{4}{3\pi} \frac{I'w\sqrt{2}}{\delta} \sin\left(\frac{3c'\pi}{t_p 2}\right)$$

and for the shaded-pole MMF, derived from current I''' ,

$$B_3''' = \mu_0 \frac{4}{3\pi} \frac{I'''w\sqrt{2}}{\delta} \sin\left(\frac{3c'''\pi}{t_p 2}\right)$$

Inspection of the expressions for B_3' and B_3''' shows that they have the same order of magnitude.

The third harmonic MMF component gives rise to rotating fields at one-third synchronous speed, and this results in a saddle in the torque/speed characteristic, particularly in the larger shaded-pole motors, so it is necessary to provide means for improving the field distribution graph. A frequently chosen method is the provision of a nonuniform airgap which is made wider on the main pole side of the slot. Numerous airgap contours have been developed, such as that shown in Figure 4.2*b*. In some designs there are stepped contours and there may be flux saturation at the pole tips.

The above discussions left out all consideration of the influence of the rotor current. Interaction between the highly nonsinusoidal MMF distribution and the rotor current is very complicated. Literature on this subject is extensive.

Figure 4.3 shows the torque/speed characteristic of a shaded-pole motor M and the four calculated torque components due to direct- and counter-rotating fundamental and third harmonic MMF components.

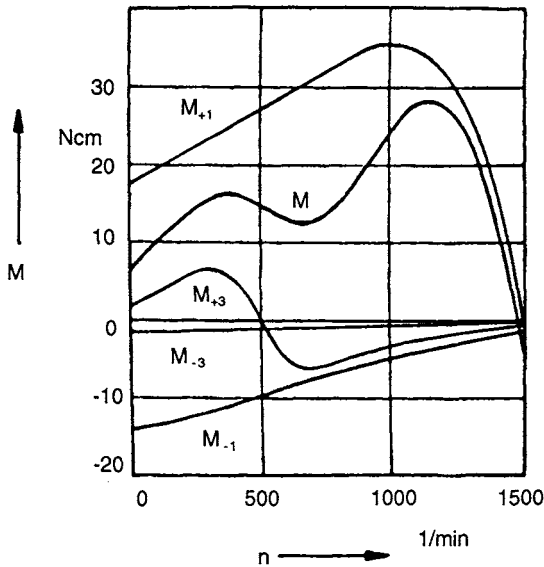


Figure 4.3 Fundamental and harmonic torque components (direct- and counter-rotating) and the resultant characteristic of a 4-pole shaded-pole motor

4.4 Construction of shaded-pole motors

There are many stator stamping shapes for shaded-pole motors on offer, and many designs are strongly influenced by manufacturing considerations. The version shown in Figure 4.4a with solid 'leakage flux inserts' is seldom found in modern production. The pole gaps are closed with these inserts after the coils have been put in place.

In the version of Figure 4.4c the leakage flux is limited by the arrangement of gaps and slots in the stator stampings. The versions with 'stamped leakage bridges' (Figs. 4.4b, d, e) are preferred for smaller motors, up to about 20 W. The core pack is made up of two parts, pressed together after the externally prepared mass-produced coil has been placed over the pole core.

The unsymmetrical version, Figure 4.4d, finds widespread application owing to its low manufacturing cost, e.g. for its simple, machine wound coil on a plastic former. When this motor is built into an appliance, care must be taken to ensure that no other steel parts are in close proximity because flux leakage could reduce its power output.

In the larger shaded-pole motors, the one piece stamping, Figure 4.4c or f, is preferred, because then the winding can be done economically by robots. Also, larger machines require windings with fewer turns of thicker wire and hence enable more favourable manufacturing conditions. Numerous stamping designs (Figs. 4.4d and e) include two shaded-pole slots per main pole. Improved running characteristics are achieved with this arrangement.

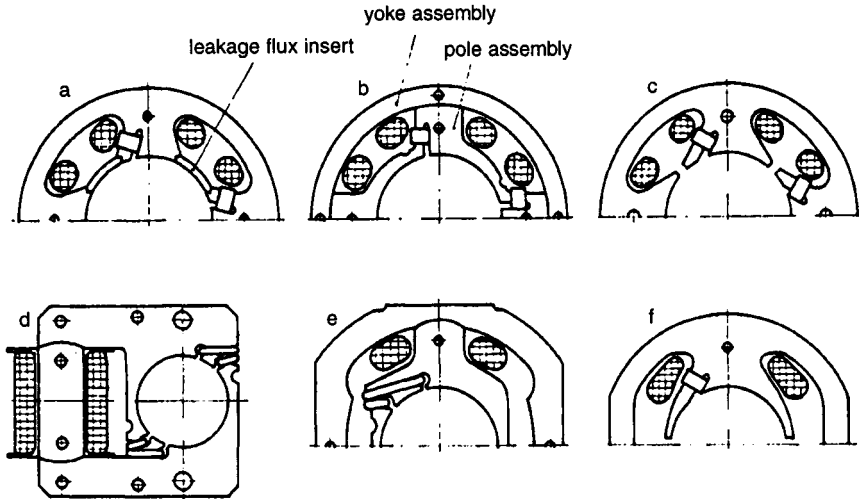


Figure 4.4 *Shaded-pole motor versions (explanations in the text)*

4.5 Operational performance of shaded-pole motors

4.5.1 Operating characteristics and technical data

The operating characteristics of a 50 W nominal power output motor are given in Figure 4.5. Speed, current, input power and efficiency are plotted against a base of torque. The ratio of short-circuit current to full load current I_K/I_N is about 1.7 in this example. In the smaller shaded-pole motors with powers 1–3 W this ratio can be about 1.2–1.3, and this means that these motors can be stalled for long periods without the need for thermal overload protection.

It is mentioned that, as with all induction motors, the shaded-pole motor has a torque output that varies according to the square of the supply voltage. Particular aspects are dealt with in Section 4.6.1.

Table 4.1 gives an overview of the power ratings and parameters, including dimensions of available shaded-pole motors. The following groups are chosen:

1. Two-pole shaded-pole motors with unsymmetrical construction as in Figure 4.4d and with stamping dimensions 63.5×63.5 mm.
2. Two-pole shaded-pole motors with rounded construction, as in Figure 4.4e, f, with various stamping dimensions designated by their external diameters and bore diameters.
3. Four-pole shaded-pole motors with rounded construction, as in Figure 4.4b, c.

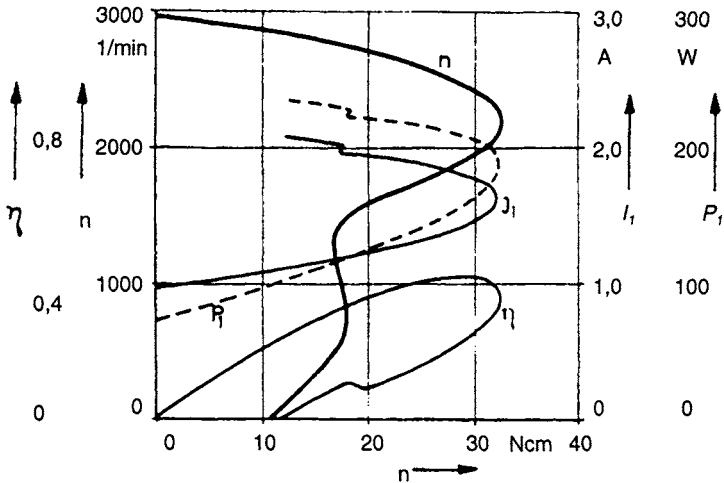


Figure 4.5 Operating characteristics of a 2-pole shaded-pole motor, with nominal power rating 50 W at 220 V supply voltage

Table 4.1 Technical data of standard pattern shaded-pole motors

		D_1	l_e	P_2	P_1	M_A	M_K	M_n	n_n
		(mm)	(mm)	(W)	(W)	(Ncm)	(Ncm)	(Ncm)	(rev/min)
1	63.5 × 63.5	31.6	16	3.3	19	1.5	2.2	1.2	2600
		31.6	20	5.0	25	1.9	3.0	1.8	2600
		31.6	30	7.5	38	3.1	4.4	2.8	2600
		31.6	45	11.0	55	4.4	6.5	4.0	2630
2	58 φ	25.0	16	1.2	12	0.4	0.9	0.5	2300
	75 φ	31.6	22	5.0	25	1.8	3.2	1.9	2500
	75 φ	31.6	35	10.0	40	3.0	6.0	3.7	2600
	136 φ	55.0	38	120.0	400	28.0	78.0	43.0	2680
3	68 φ	38	20	4.5	24	2.0	5.5	3.4	1270
	68 φ	38	38	10.0	50	8.0	12.0	7.3	1300
	80 φ	46	38	20.0	70	10.0	23.0	14.7	1300
	136 φ	74	20	55.0	240	18.0	85.0	39.0	1350

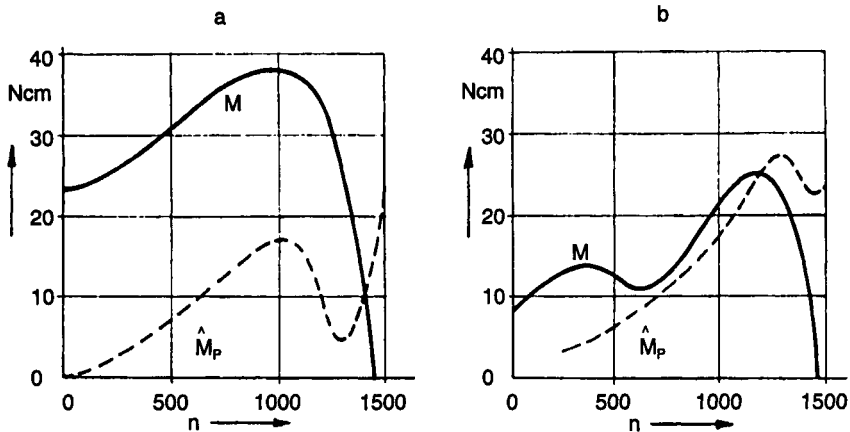


Figure 4.6 Drive torque and hum torque as a function of speed in (a) a csar motor and (b) a shaded-pole motor with the same dimensions

4.5.2 Comparison of the operating characteristics of the shaded-pole motor and the capacitor start and run induction motor (csar motor)

Torque/speed characteristics and double mains frequency hum torque are compared in Figure 4.6, with speed as the base parameter, between (a) the csar motor and (b) the shaded-pole motor, the two motors having the same overall dimensions and temperature rise above ambient. The graphs relate to 4-pole motors with 80 mm core diameter, the shaded-pole motor having the core shape of Figure 4.4c.

A comparison of the torque/speed characteristics shows that, in this case, the shaded-pole motor has only about 30% of the starting torque and about 60% of the stall (pull-out) torque of the csar motor. In addition the speed/torque characteristic of the shaded-pole motor exhibits a distinct saddle or dip during run-up owing to the third harmonic component in the MMF waveform. Regarding the double mains frequency hum torque, it has to be recognised that the csar motor working around normal full-load conditions is close to the uniform rotating field state, and thus the hum torque is minimal. In the shaded-pole motor, however, when running between the off-load and stall (pull-out) torque states, the hum torque has the same order of magnitude as the stall (pull-out) torque.

4.5.3 Losses and efficiency

Table 4.2 gives some idea of the efficiency of shaded-pole motors compared with csar motors. In the power range up to about 10 W, in which the majority of motors are shaded-pole, the efficiency of these motors is 20% or even less.

The following losses occur in the shaded-pole motor:

- stator iron loss P
- main winding copper loss P_{Cu1}
- shaded-pole ring copper loss P_{Cu3}
- I^2R loss in the rotor P_{v2}
- friction loss P_R

Table 4.2 Efficiency of shaded-pole motors compared with csar motors

Power P_2	Shaded-pole motor	Csar motor
1 W	0.1	
10 W	0.22 ... 0.3	ca. 0.4
50 W	0.30 ... 0.35	0.4 ... 0.5
100 W	0.32 ... 0.4	0.55 ... 0.65

Only the main winding copper loss can be determined by direct measurement. Shading ring copper loss is determined by replacing the usual solid copper ring – in a few prototype units – with a multiturn insulated winding with the same cross-sectional area. Its current and resistance are then measured. Stator iron losses are measured in a motor with open-circuited shading rings and a cageless rotor. When the friction loss is known, the remaining loss out of the total is principally the rotor copper loss. Table 4.3 shows the division of losses in two shaded-pole motors with different power ratings. It is observed that the copper losses in the main and shaded-pole windings are of the same order of magnitude. Rotor copper loss is considerable. Packing the main winding space full, with some difficulty, has only a slightly beneficial influence on efficiency and temperature rise.

Table 4.3 Loss distribution in a shaded-pole motor

Example		1	2
Power input, W	P_1	31	190
Stator iron loss, W	P_{Fe}	4	9
Copper loss (main winding), W	P_{Cu1}	4	26
Shaded-pole winding loss, W	P_{Cu3}	6.5	24
Rotor loss, W	P_{v2}	7	54
Friction loss, W	P_R	1	54
Power output, W	P_2	8.5	75
Efficiency	η	0.27	0.39

4.6 Design and dimensioning of shaded-pole motors

4.6.1 Winding conformity

In general, motors in electrical appliances must conform to the standard specifications, typically, VDE 0700. These state that the appliance must

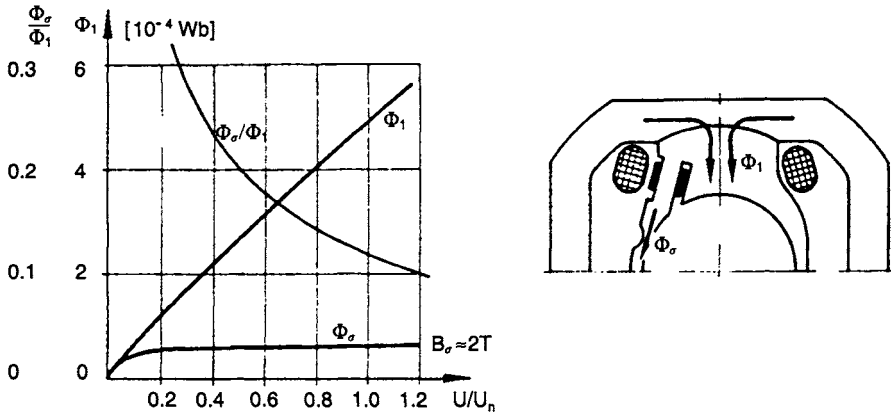


Figure 4.7 Stray flux and total flux in a motor with 'leakage bridges'

operate satisfactorily when the applied voltage is 85% of the nominal supply voltage and, at the other extreme, the specified top temperature must not be exceeded when the applied voltage is 106% of the nominal.

Conformity of the shaded-pole motor in the appliance is easily achieved in that, given the available motor with appropriate frame size, the reference voltage which meets both conditions is ascertained. The number of winding turns for the nominal supply voltage is then calculated by normal voltage transformation methods. If the temperature rise is too great, even with a full winding, a longer core, for instance, is necessary.

The torque of a shaded-pole motor – as with all induction motors – is proportional to the square of the input voltage. In motors with 'stamped leakage bridges', the following considerations apply:

- (a) The dependence of torque on voltage can be greater than quadratic. Figure 4.7 shows how, in a motor with 'stamped leakage bridges', the total flux Φ_1 , the leakage flux Φ_σ and the ratio Φ_σ/Φ_1 depend upon U/U_N . The leakage bridge is already saturated at low input voltage and the leakage flux remains virtually constant as the input voltage increases, the leakage flux density being about 2.2 T. The flux that determines the torque varies according to $\Phi_L(1 - \Phi_\sigma/\Phi_1)$. Given this expression, the dependency of torque on supply voltage can be approximated by an exponent. For the case before us, and in the voltage range $U/U_N = 0.85-1.0$, the exponent is about 2.4.
- (b) When the main pole airgap is contoured (Figure 4.2b) to reduce the saddle in the torque/speed characteristic and there are saturation zones at normal voltages, the field distribution can be voltage-dependent and as a result the benefit of the saddle effect can decrease at lower input voltages.

4.6.2 Influence of the rotor resistance

As in all induction motors, the torque/speed characteristic of a shaded-pole motor can be affected by changing the rotor resistance. Increasing the rotor resistance (e.g. by fitting smaller section end-rings to the rotor cage, or altering the alloy in the case of cast rotor cages) produces an increased starting torque. This effect applies to both the forward and reverse rotating fields and so the increase in starting torque is small, and there is usually a worsening of stall-torque, steady-state speed regulation and efficiency. Therefore, this method of increasing the starting torque and accelerating torque is only applicable in particular circumstances.

Figure 4.8 shows the torque/speed characteristics of a shaded-pole motor with normal rotor resistance and with the resistance increased by 70%. In the interest of optimising the performance of the shaded-pole motor, it is usual to incorporate low resistance rotors.

4.6.3 Shaded-pole arc and shaded-pole winding resistance

The dimensioning of the shaded-pole arc and the shaded-pole winding resistance has been the subject of much study and development because these parameters have considerable influence on the performance of the motor. In Figure 4.9 the influence of the shaded-pole arc and the shaded-pole winding resistance R''' on the starting torque M_A and on the stall torque M_K are depicted, given that the light load running losses remain unchanged.

4.7 Applications of shaded-pole motors

When shaded-pole motors are to be used, their properties, as described in detail in Section 4.5, must be considered. The relatively low starting torque

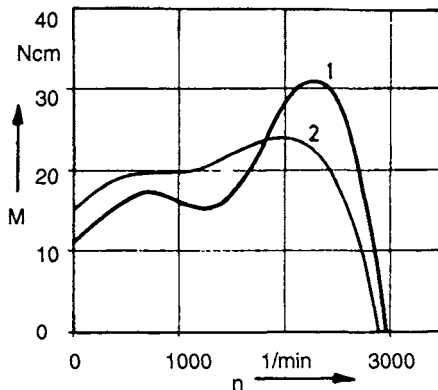


Figure 4.8 Torque/speed characteristic of a shaded-pole motor with rotor resistance R (1) and $1.7R$ (2)

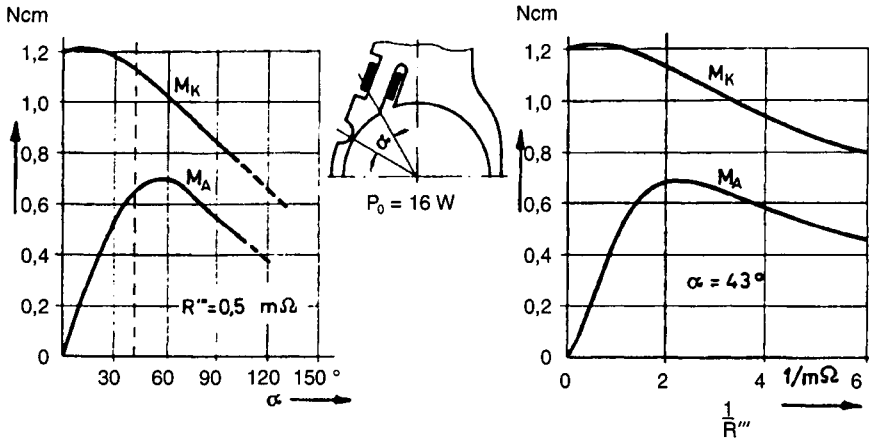


Figure 4.9 Influence of the shaded-pole arc and the conductance of the shaded-pole winding on the performance of a small shaded-pole motor
 a Change of shaded-pole arc
 b Change of shaded-pole winding resistance
 M_A = starting torque
 M_K = stall (pull-out) torque

often limits the applications. In many cases the heat dissipation is a problem when, for example, there is no possibility of good fan cooling.

In many situations attention must be paid to the double mains frequency hum torque, in the form of vibration absorbing mountings. Careful layout is required. Inertia of the motor and load, and the torsion constant of the motor suspension, result in angular vibrations. Hum torque isolation is most effective when the natural frequency of angular vibration is less than one-third of the excitation frequency. In this way, annoying hum from the apparatus can be avoided. Shaded-pole motor-driven fans in large chest freezers being suspended from steel springs is an example of this solution to a problem.

4.7.1 Applications of shaded-pole motors with unsymmetrical construction

The unsymmetrical construction of shaded-pole motors shown in Figure 4.4d is offered to the world market by many manufacturers of 1–20 W motors. There are many applications for motors with this construction, e.g. discharge pumps in washing machines and dishwashers, fan motors in electric cookers, drive motors for small appliances (slide projectors), motors for diverse drive applications in photocopiers and dispensing machines, and often in combination with miniature transmission systems.

In these motors, the windings are put onto plastic spools and are very simple and robust, and class F and H insulation can be achieved

economically. This is a requirement for motors which have to work at high temperatures, such as fan motors in electric cookers.

Putting the windings onto plastic spools offers simple solutions to the following:

- voltage selection using series-parallel coil connections
- tapped windings for driving fan motors at two speeds without the need for a series resistance
- using the motor field windings as a transformer by putting an isolated secondary winding on the stator separated from the main winding by an insulating card.

Motors of this construction are usually fitted with vertical-bearing covers and sintered plain bearings, and frequently with 'longlife bearings' with a particularly large lubricant reservoir and special means against lubricant leakage. In special circumstances, rolling contact bearings are fitted.

4.7.2 Shaded-pole motors as fan motors

Small fans: The category of small fans with an output power of 1 to 2 W includes hot air fans, hair dryers, air moisteners and extractor fans. Also, there are many types of apparatus which require internal fans. They are usually constructed as shown in Figure 4.10. The round shape is necessary so that the motor can be placed inside the fan body, and it is cooled by the fan. These motors are produced by the hundred-thousand, and the manufacturing processes are highly automated.

Refrigerators and freezers: In refrigerators and freezers, 4-pole shaded-pole motors are fitted. The common structure shown in Figure 4.10 has power

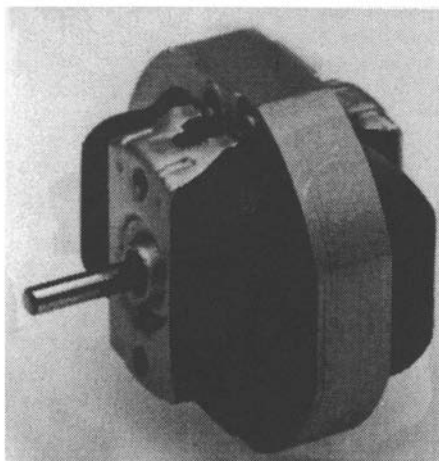


Figure 4.10 Shaded-pole motor for a small fan

ratings of 2–8 W, and the fans are axial. Often the motors have a closed construction and are fitted with longlife bearings and vibration damping mountings.

Extractor hoods: Extractor hoods are designed to move 200–300 m³/h air with a static pressure of 1 m bar. A proven means is the use of the capacitor start and run induction motor with external rotor. However, many internal rotor shaded-pole motors are used as an alternative. The technical requirements are often stepless speed control or switched speed selection (e.g. 2400–1900–1400 rev/min). From the characteristics of the 25 W motor depicted in Figure 4.11, it can be seen that speed setting by means of switching the input voltage is possible but with severe limitations.

4.7.3 Shaded-pole motors for washing machine spinners

These are usually 2-pole shaded-pole motors with power ratings up to about 150 W.

The direct-drive washing-machine spinner with a shaded-pole motor rigidly coupled to the drum is a typical example of adapting the motor and the appliance to work together as a unit. The critical drive problem occurs during run-up, with imbalance owing to unfavourable distribution of the washing load. The motor drum is elastically coupled to a subframe in the body shell. Because of imbalance, the motor drum oscillates vigorously during run-up. The 'critical speed' region under 400 rev/min, at which mechanical resonance occurs, must be swept through quickly so that the drum does not strike the body shell. At this speed there must be sufficient acceleration torque being developed by the motor. The 2-pole shaded-pole motor reaches

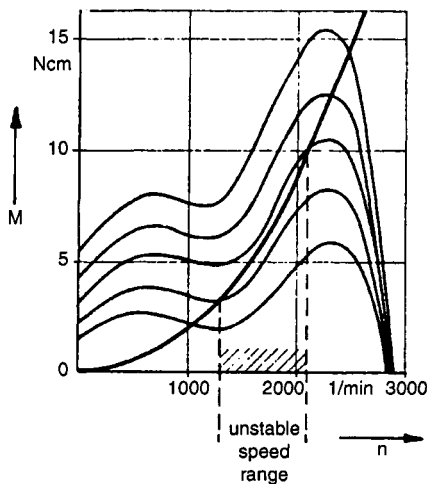


Figure 4.11 *Torque/speed characteristics of a fan drive*

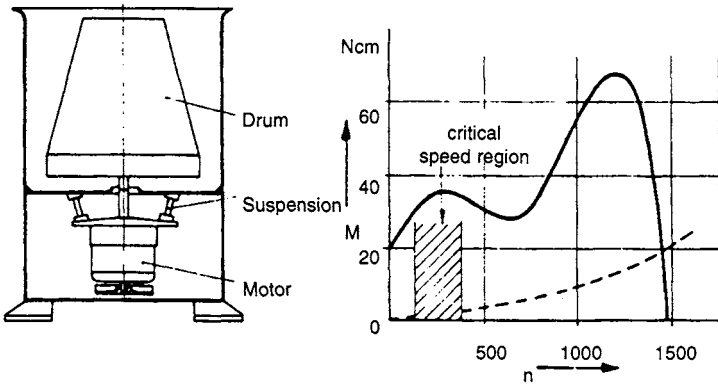


Figure 4.12 Washing-machine spinner direct-drive assembly and speed/torque characteristic

its first torque peak at this speed, owing to the third-harmonic content in the MMF distribution. This speed occurs before the saddle in the torque/speed characteristic (see Figure 4.12).

Chapter 5
Synchronous motors

Helmut Moczala

Synchronous motors are used predominantly in AC circuits when a constant speed is required that is independent of load torque and supply voltage. The speed n_s of the motor is dependent only on the mains frequency f and the number of pole-pairs p in accordance with the formula

$$n_s = \frac{f}{p} \quad (5.1)$$

Multipole synchronous motors with a capacitive auxiliary phase are also found, however, in slow speed drives on account of their low turning speed, relatively high torque and easy reversibility, when no importance is attached to synchronous running.

5.1 Summary of possible synchronous motor constructions

Synchronous motors are mostly rotating field motors in which the rotor has the same number of poles as the stator and turns synchronously with the rotating field. Synchronous motors with purely single-phase excitation are rarely encountered. Figure 5.1 gives a summary of the principal possibilities for the make-up of synchronous motors.

Various forms of stator are produced for generating a satisfactory rotating field. The principles are similar to those applicable to induction motors, namely:

- 3-phase winding for connection to a 3-phase supply
- 3-phase winding with a phase-shifting capacitor for connection to a single-phase supply
- 2-phase winding comprising a main coil and an auxiliary coil energised via a series capacitor

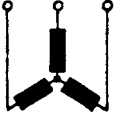
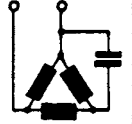
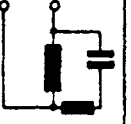
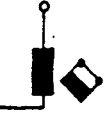

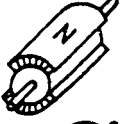
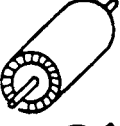
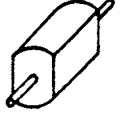
Supply	3 ~	1 ~	1 ~	1 ~	1 ~
Stator					
	three-phase motor	Single-phase capacitor m. Steinmetz circuit	Single-phase capacitor m. with auxiliary phase	shaded pole motor	single phase motor
Rotor	<p>Permanent magnet rotor  (synchronous)</p> <p>Hysteresis rotor  (synchronous)</p> <p>Reluctance rotor  (synchronous)</p>				

Figure 5.1 *Functional principles of the synchronous motor*

- a shaded-pole
- a single coil winding.

Whereas the 3-phase wound, 3-phase energised motor has a nearly perfect uniform rotating field under all working conditions, the shaded-pole motor field is highly elliptic. Motors with a single coil winding, which can only have an alternating field, need external starting provision.

Various stators may be combined with a choice of rotors, namely:

- permanent magnet rotor
- hysteresis rotor
- reluctance rotor.

Many stator/rotor combinations are possible. Also, rotor cages, as used in induction motors, appear in synchronous motors to enable starting, run-up and lock-in.

On account of the importance of the role played by permanent magnetic materials in synchronous motors, the following Section is devoted to a discussion of the properties of these materials.

5.2 Permanent magnets

5.2.1 The permanent magnetic circuit

Figure 5.2 shows a schematic representation of a permanent magnet circuit. The magnetic flux Φ from the permanent magnet 1 flows, via the soft iron pole-pieces 2.1 and 2.2, through the airgap 3. Assuming that there is no flux leakage and that all the flux Φ emerging from the permanent magnet 1 passes through the airgap 3, it follows that

$$\Phi = A_m B_m = AB \quad (5.2)$$

where B_m is the flux density in the permanent magnet and B is that in the airgap.

The circuit, when assembled, is fully magnetised by means of an MMF pulse θ which is unidirectional and starts and finishes at $\theta = 0$. In accordance with the closed magnetic circuit theorem (Ampere's law),

$$\theta = \oint H \cdot dl = H_m l_m + H\delta = 0 \quad (5.3)$$

where H_m and H are the magnetising intensities (in A/m) in the permanent magnet and airgap, respectively.

Eqn. 5.3 is valid under the assumptions that the magnetic potential drops in the soft iron pole pieces are negligible and that flux leakage is also negligible.

From eqns 5.2 and 5.3, and the relation $B = \mu_0 H$ in the airgap, it follows that

$$B_m = -\mu_0 H_m \frac{l_m}{\delta} \frac{A}{A_m} \quad (5.4)$$

This equation relating the permanent magnetic material parameters B_m and H_m establishes the so-called working line, which is dependent only on the

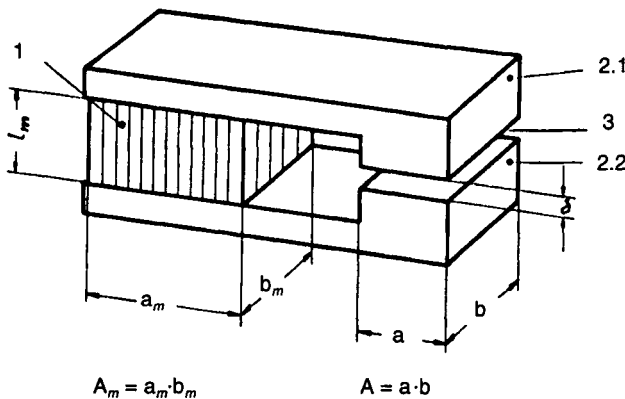


Figure 5.2 Permanent magnetic circuit

geometry of the magnetic circuit and not on the magnetic material's properties.

The relationship between B_m and H_m is the hysteresis curve for the material, and the demagnetisation curve in the second quadrant, as shown in Figure 5.3, has particular significance. The intersection of the working line and the demagnetisation curve is the working point P. The permanent magnet material's working flux density B_{mP} may be read off the diagram, and the airgap flux density B is then derived from eqn. 5.2. In practice, corrections (reductions) must be made because – owing to magnetic flux leakage – not all of the permanent magnet's flux passes through the airgap.

If the airgap is increased from δ to δ^* , the working line has a lower gradient, and a new working point P* with a lower flux density is established. This flux density reduction is permanent in the material, and reclosing the airgap to the original δ achieves only a partial recovery to a new working point P' and flux density $B_{mP'}$. $B_{mP'}$ depends on the 'physics' of the magnetic material and is not readily calculable.

Irreversible flux changes can also occur in the magnetic circuit as a result of strong neighbouring unfavourably directed fields. For a constant airgap the result is a parallel shift to the left of the working line.

5.2.2 *Permanent magnetic materials*

Characterisation of permanent magnetic materials is achieved by stating the remanent flux density B_{mr} and the coercive force H_{mc} . B_{mr} and H_{mc} occur where the demagnetisation curve cuts the vertical axis and the horizontal axis, respectively.

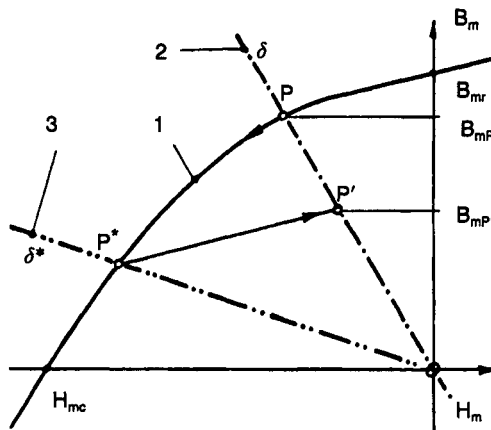


Figure 5.3 Working point of the permanent magnetic circuit

- 1 Demagnetisation curve $B_m(H_m)$
- 2 Working line for airgap δ
- 3 Working line for airgap $\delta^* > \delta$

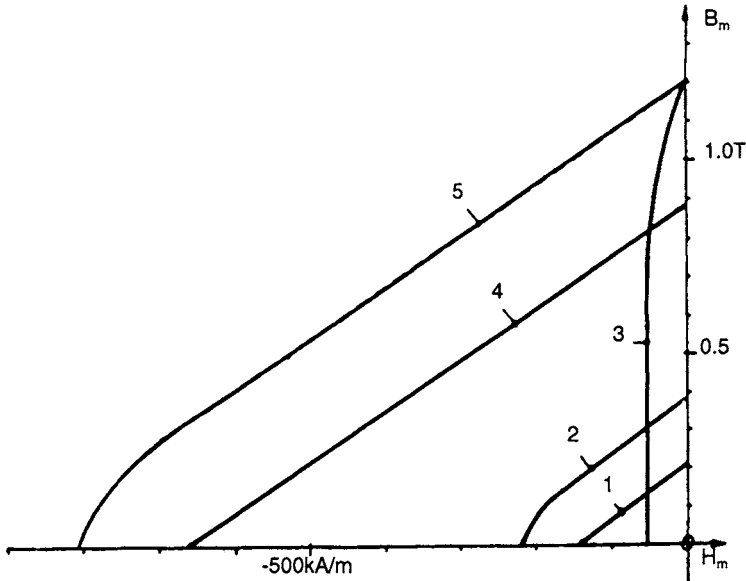


Figure 5.4 Demagnetisation curves $B_m(H_m)$ of: (1) hard ferrite, isotropic; (2) hard ferrite, anisotropic; (3) Alnico, anisotropic; (4) rare earth – cobalt; (5) neodymium-iron-boron

Figure 5.4 shows a number of permanent magnet material demagnetisation curves. A figure of merit of the material is the area under this curve. Amongst the commercially available materials, anisotropic Alnico 3 and neodymium-iron-cobalt 5 have the highest remanent flux densities, whilst materials 4 and 5 have the highest coercive forces. On account of their high cost, materials 3, 4 and 5 are only used for high specification motors. The hard ferrite sintered materials (1 and 2) and isotropic Alnico are more economical. Permanent magnets using neodymium-iron-boron, with their superior magnetic qualities, are susceptible to corrosion and must be restricted to a top working temperature of 150°C .

5.3 Principles of synchronous motor function

5.3.1 Motors with permanent magnet rotors

The permanent magnet rotor is the one most often used in synchronous motors. When running synchronously, the rotor magnetic axis trails the stator's rotating field axis by an angle β , which is dependent on the load torque M_r . The relationship is easily seen from a consideration of Figure 5.5 in which, instead of being developed by a polyphase winding system, the rotating field comes from a DC electromagnet which is rotated mechanically

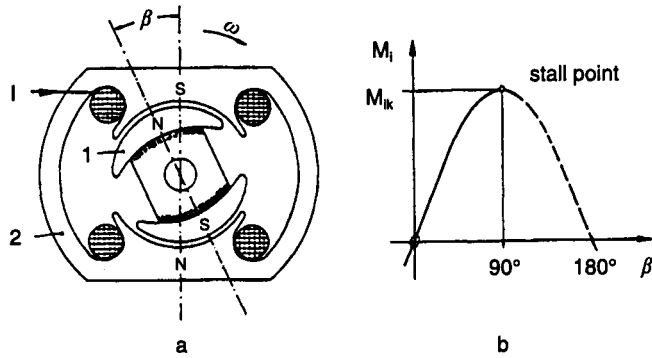


Figure 5.5 Development of the synchronous torque
 a Electromagnet – permanent-magnet coupling
 b Synchronous torque as a function of the load angle $M_i(\beta)$

at angular velocity ω . In this ‘magnetic coupling’ the load angle β increases as the ‘internal torque’ M_i increases. M_i is the torque developed between stator and rotor. The physically realisable torque from the motor output shaft must be less than M_i owing to unavoidable losses, e.g. friction.

The equation for the internal torque M_i is

$$M_i = k \Phi I \sin \beta \tag{5.5}$$

in which Φ is the airgap flux, I the winding current and k a constant for the motor.

The torque M_i reaches its maximum value when $\beta = 90^\circ$ and becomes the pull-out torque M_{ik} . If this torque is exceeded, the ‘magnetic coupling’ can no longer hold onto the rotor and it rotates relative to the field axis. As a consequence of the continuously increasing β , a sinusoidally varying torque with average value zero results – ‘The synchronous motor rotor falls out of step’.

This vibrating torque also occurs when the motor is switched on, i.e. when the stator field rotates and the rotor is stationary. A start and run-up is generally only possible when a supplementary asynchronous torque is first developed by means of a squirrel cage or hysteresis material rotor.

The supplementary starting arrangement may be dispensed with if it is possible to accelerate and synchronise the rotor very quickly, i.e. within a half period of the supply voltage. This is possible for multipole slow speed motors.

The equivalent circuit and phasor diagram of a synchronous motor is shown in Figure 5.6. The supply voltage U exceeds the induced voltage U_q in the winding by the sum of the resistive and reactive voltage drops in the winding when it is carrying the current I .

Thus,

$$U = U_q + R_1 I + j X_{l\sigma} I \tag{5.6}$$

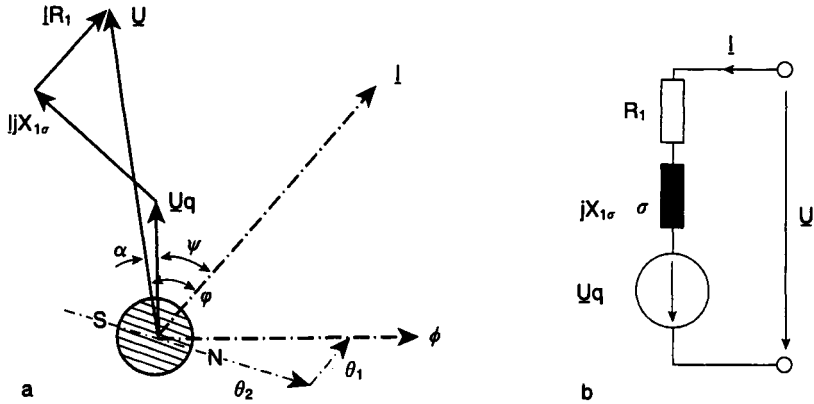


Figure 5.6 (a) Phasor diagram of the synchronous motor; (b) equivalent circuit of the synchronous motor

In this equation R_1 and $X_{1\sigma}$ are, respectively, the resistance and the synchronous reactance of the stator winding. The induced voltage U_q is derived partly from the permanent magnetic rotor's movement and partly from the stator flux linkage. In small synchronous motors, leakage flux has an unfavourable influence, so that only a fraction of the permanent magnet's flux links the stator winding.

For these reasons and on account of the fact that in low power motors the voltage drop in the winding is a large part of the supply voltage (when compared with the larger machines), it must be accepted that the induced voltage U_q is small compared with the supply voltage U .

From Figure 5.6a, resolving in the direction of I .

$$U \cos \varphi = U_q \cos \psi + IR_1$$

Multiplication by the current I gives:

$$UI \cos \varphi = U_q I \cos \psi + I^2 R_1$$

Here, $UI \cos \varphi$ is the electrical power from the supply, P_e , $U_q I \cos \psi$ is the 'internal' mechanical power transferred to the rotor P_{mi} (this power is not all available at the output shaft owing to bearing friction and other braking effects), and $I^2 R_1$ is the copper loss P_{cu} ,

$$P_e = P_{mi} + P_{cu} \quad (5.7)$$

The 'inner efficiency' η_i of the motor, relating to the rotor power P_{mi} is

$$\eta_i = \frac{P_{mi}}{P_e} = \frac{U_q \cos \psi}{U \cos \varphi} \quad (5.8)$$

Because in low power synchronous motors the ratio U_q/U is not good, a high value of efficiency η_i is not to be expected. Finally, the overall efficiency $\eta = P_m/P_e$ is even smaller owing to friction losses.

5.3.2 Motors with hysteresis rotors

Synchronous motors with hysteresis rotors display fundamentally different characteristics to those with permanent magnet rotors, particularly with respect to starting characteristics.

The rotor materials used in these motors have lower coercive force than the permanent magnet materials: $H_c = 4\text{--}50$ kA/m compared with more than 50 kA/m for Alnico (see Figure 5.4). Because of their position between the soft iron and the hard magnetic materials, they are referred to here as medium iron or hysteresis materials.

In contrast to the permanent magnet rotor, the hysteresis rotor gets its magnetisation from the stator after the motor is switched on. For this to be achieved from the available stator MMF it is necessary to use the medium magnetic materials for the hysteresis rotor.

For a consideration of the run-up action, let the starting point be that the stator-derived 2-pole rotating field penetrates the hysteresis rotor. If the rotor is turning at less than synchronous speed, the rotor becomes magnetised around its BH loop at the slip rate $n_s - n$.

As well as producing eddy current losses, the magnetic cycling in the rotor generates hysteresis losses, which depend on the magnetic properties of the material and the magnitude of the imposed field. The hysteresis energy ΔW_h per magnetic cycle absorbed by the rotor can be calculated by integrating throughout the rotor volume elements but, as the hysteresis curve has no suitable mathematical expression, an exact calculation of ΔW_h is very difficult.

Figure 5.7 shows a hysteresis curve $B_m(H_m)$ and the induction curve $B_m(t)$, which results from imposing a sinusoidally varying $H_m(t)$ on the material. $B_m(t)$ is clearly not sinusoidal but it can be seen to have a time lag behind $H_m(t)$. The angle δ between the positive-going zero crossings of H_m and B_m is a measure of this lag and is known as the hysteresis angle. δ cannot safely be called a phase angle owing to the different waveforms of the two functions. This hysteresis angle is to a great extent independent of frequency.

It is easily appreciated that there are energy losses in the hysteresis material, when a piece of the material lies motionless in the field of a loss-free coil, energised with alternating current. Current and H_m are in phase, whereas the induced voltage is 90° ahead of B_m . Because the voltage across the coil, when measured, is only $(90^\circ - \delta)$ ahead of the current, it follows that the coil absorbs in-phase current and hence power from the supply to provide the hysteresis loss.

When a hysteresis rotor is magnetically cycled by a rotating field, the elements of the rotor experience time displacement as discussed above between their B_m and H_m functions. Given a 2-pole field, the hysteresis angle between the H_m and B_m axes can also have a spatial interpretation.

At standstill ($n = 0$) the hysteresis rotor delivers no mechanical power but the stator transfers the hysteresis loss power $P_{ho} = n_s \Delta W_h$ over the airgap. This airgap power P_{ho} does not change when the rotor begins to turn because the

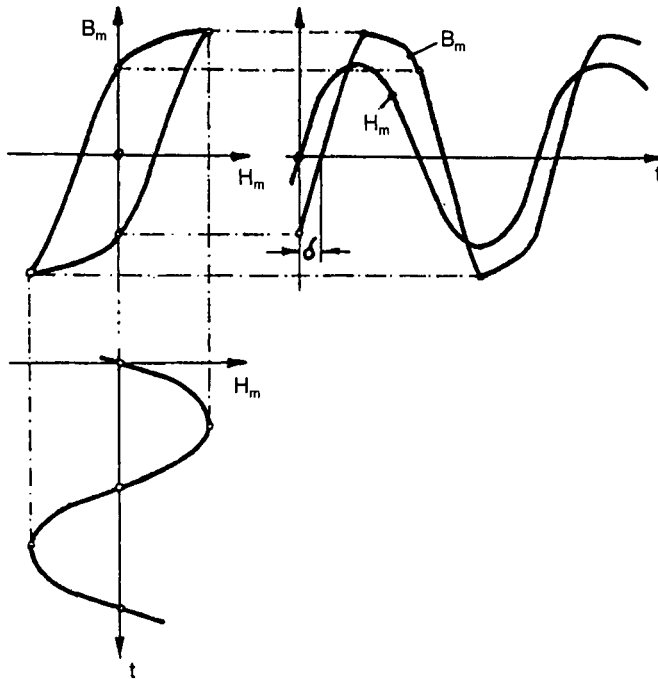


Figure 5.7 Derivation of the hysteresis angle δ

magnetic action in the airgap is the same as at standstill: the rotating field turns at synchronous speed n_s and the rotor behaves magnetically as at standstill, with the hysteresis angle being independent of speed. The hysteresis loss is less than at standstill owing to the lower cycling frequency $n_s - n$, the difference being converted into mechanical power $P_{mi} = 2\pi n M_i$,

The power balance equation is

$$P_{ho} = n_s \Delta W_h = (\eta_s - n) \Delta W_h + 2\pi n M_i \quad (5.9)$$

from which

$$M_i = \frac{\Delta W_h}{2\pi} \quad (5.9a)$$

Thus, at subsynchronous speeds, a constant torque that is independent of speed is to be expected.

At synchronous speed, the hysteresis motor displays the same properties as the motor with a permanent magnet rotor, except that the medium-iron rotor machine slips out of synchronism when the pull-out torque is exceeded and runs subsynchronously, as discussed above. The rotor returns to magnetic hysteresis cycling and to a subsynchronous speed that depends on the load characteristics.

Alternatively, in the case of slight overload, the rotor may repeatedly pull into and out of synchronism with an attendant vibrating torque or flutter (sometimes called microslip). Whereas permanent magnet synchronous motors may be loaded up to a load angle approaching 90°, only about 20° can be achieved in a hysteresis motor before the onset of slip and magnetic cycling.

5.3.3 *Motors with reluctance rotors*

Reluctance rotors are specially contoured so that airgap variations relative to the round stator occur in pairs, giving soft magnetic poles. The number of rotor poles corresponds to that of the stator. The varying airgaps and the corresponding airgap reluctance have given the name to this rotor. As with the permanent magnet rotor, the reluctance rotor seeks to align itself with the rotating stator field. Start and run-up problems are similar to those of permanent magnet rotors.

5.4 Construction of synchronous motors

Here one finds various types of construction which owe their existence not only to the different physical principles described above but also to many original design ideas. Besides the well-known internal rotor motors, there are many external rotor motors on the market. Special claw-pole constructions have been developed for multipole slow running motors.

5.4.1 *Motors with permanent magnet rotors*

Figure 5.8 shows the rotors of two synchronous motors, which differ from induction motor rotors in so far that permanent magnets are built into the rotors. The left rotor is 4-pole and the right is 6-pole. The ferrite magnets used, with their high coercive forces, have the advantage over Alnico in that they are not demagnetised by the stator field when placed in opposition. The squirrel cage is required for start and run-up.

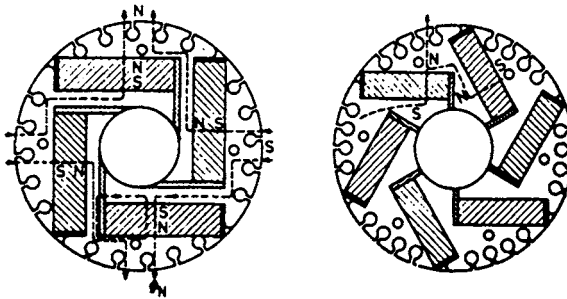


Figure 5.8 *Cross-section through the rotors of 4- and 6-pole Siemosyn motors*

The stators of the motors have the same number of pole-pairs as the rotors and they resemble those made for induction motors.

As well as these solutions for higher power motors, we find capacitor motors around the 10 W power level whose synchronisation is achieved by laterally magnetised discs placed alongside the induction rotor.

One manufacturer offers a 2-pole split pole stator with a permanent magnet rotor together with a hysteresis rotor for start and run-up.

The special construction of a low-speed permanent magnet synchronous motor with two windings is shown in Figure 5.9. This motor comprises two separate 16-pole stators and two rotors mounted on the same shaft.

Each stator has just one coil for exciting its 16 teeth which form a part of the press-formed stator halves. The pole teeth of the two stators are electrically displaced by 90 electrical degrees so that the pole teeth of the one stator are opposite to the rotor poles at the same time as the pole teeth of the other rotor are opposite to the rotor slots.

On account of the two motors being magnetically completely isolated, no uniform rotating field is obtainable on connection to two phase-shifted voltages. Each motor develops a pulsating torque. At synchronous speed the torques of the motors are characterised by equal drive torques and equal vibrating torques at double the mains frequency. If the two stator coils are energised with supplies that have 90° phase displacement, the two drive torques add, giving the sum for the driving torque, whereas the two vibrating torques cancel. From the outside this then appears to be an ideal uniform rotating field motor.

The phase shift between the two winding currents, when connection is made to a single phase supply, is achieved by means of a capacitor *C*. Figure 5.10 shows how reversal of rotation can be achieved with a single changeover switch.

The motor shown here has no ancillary equipment for starting and run-up. On account of the slow synchronous running speed, only a small acceleration is required to bring the rotor to synchronous speed within a half period of

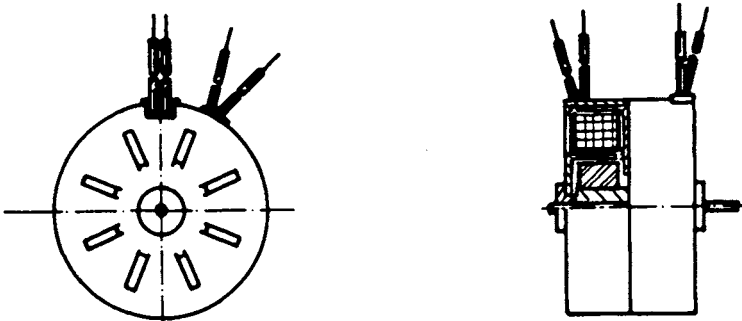


Figure 5.9 Synchronous motor with permanent magnet rotor and capacitor auxiliary phase for connection to a single-phase supply

the supply voltage. The motor is capable of developing the necessary torque for this acceleration without ancillary equipment.

An independent start is, however, not generally possible when higher synchronous speeds are required or when masses with high moment of inertia are rigidly coupled to the rotor. Figure 5.11 shows the typical double stator motor construction quite clearly.

Motors designs with three adjacent stator assemblies are produced for connecting to a 3-phase supply. Alongside these designs, motors as already described but with special windings and added electronic circuits are also finding applications as stepper motors.

Figure 5.12 shows the cross-section through a single-phase motor. Only one half-casing is shown, whilst the concentric coil that surrounds all the pole teeth and the rotor are not shown. The pole teeth that are pressed out of the casing and bent inwards form two sets consisting of the main pole teeth 2 and



Figure 5.10 Circuit for the generation of the phase-shifted voltages for the synchronous motor of Figure 5.9

The changeover switch serves to provide rotation reversal

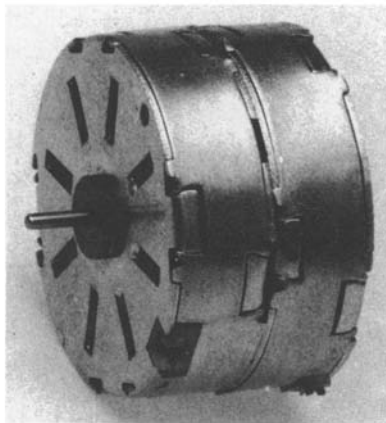


Figure 5.11 Synchronous motor with permanent magnet rotor and capacitor auxiliary phase

Output power = 0.24 W, 375 rev/min
(Courtesy: AEG)

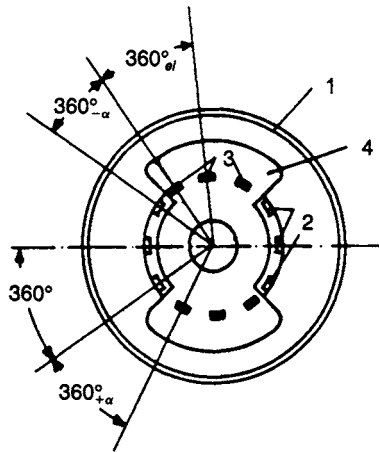


Figure 5.12 Section through a single-phase synchronous motor with main and auxiliary pole teeth

- 1 Half casing
 - 2 Main pole teeth
 - 3 Auxiliary pole teeth
 - 4 Copper plate (short-circuit winding)
- (The coils and the permanent magnet rotor are not shown)

the auxiliary pole teeth 3. The alternating magnetic flux in the auxiliary pole teeth lags that in the main pole teeth on account of the copper plate 4 which produces the shaded-pole effect. Thus we find in this motor a situation similar to that in the 2-phase motor already discussed in connection with Figure 5.9. There are pole tooth groups, which are characterised by mutually phase displaced fluxes, but with the difference that the two groups are arranged to face each other in sectors in the same casing. The auxiliary poles are displaced relative to the regularly distributed main poles by the spatial angle α . To derive the best constant torque from the 24-pole rotor, the sum of the displacement angle α (in electrical degrees) and the phase angle between the main pole and auxiliary pole fluxes should add up to 180° , thus meeting the condition for producing a uniform rotating field in rotating field motors. Figure 5.13 shows the construction details of a 16-pole motor in this class.

The older variant of a single-phase synchronous motor (Figure 5.14) is characterised by the classical split-pole arrangement. In this 8-pole motor each auxiliary pole next to the main pole is surrounded by a copper short-circuit plate in order to arrive at the required phase-lagging flux.

Figure 5.15 shows a similar motor in longitudinal section. The stator short-circuit plates close to the split winding can be seen clearly. The rotor poles are made up of iron claws; the rotor magnet is therefore magnetised axially. To ensure a consistent sense of rotation it may be necessary to build in a reverse rotation barrier; it depends on the quality of the rotating field achieved. Motors as depicted in Figure 5.12 need no such barrier.

Multipole synchronous motors of the type described, which are characterised by interlaced magnetic parallel pole teeth and a common spool exciting all the poles, are particularly suitable not only for low speed running but also for high torque output which, for a given magnetic material, is, in theory, proportional to the number of pole pairs.

Occasionally other multipole permanent magnet rotor motors are encountered whose field excitation is purely alternating. These motors can only start and run in the correct sense with the help of a mechanical device. In its simplest form this comprises a spring and ratchet wheel. In the event of

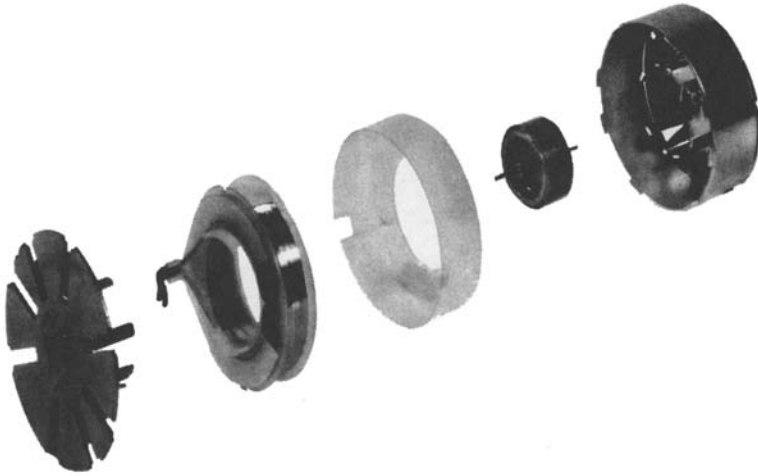


Figure 5.13 Exploded view of a single-phase synchronous motor with main and auxiliary pole teeth and permanent magnet rotor
Power output = 0.1 W; 375 rev/min
(Courtesy: AEG)

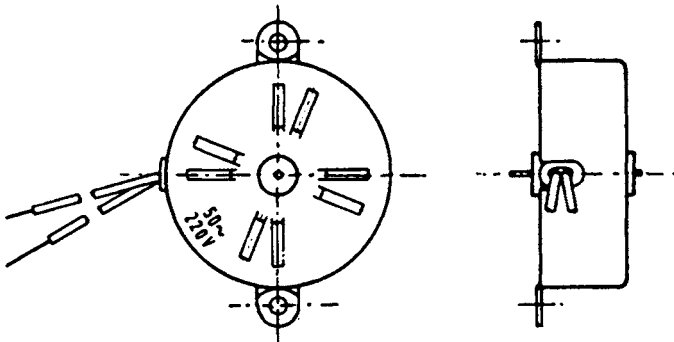


Figure 5.14 Single-phase synchronous motor with split-pole and permanent magnet rotor

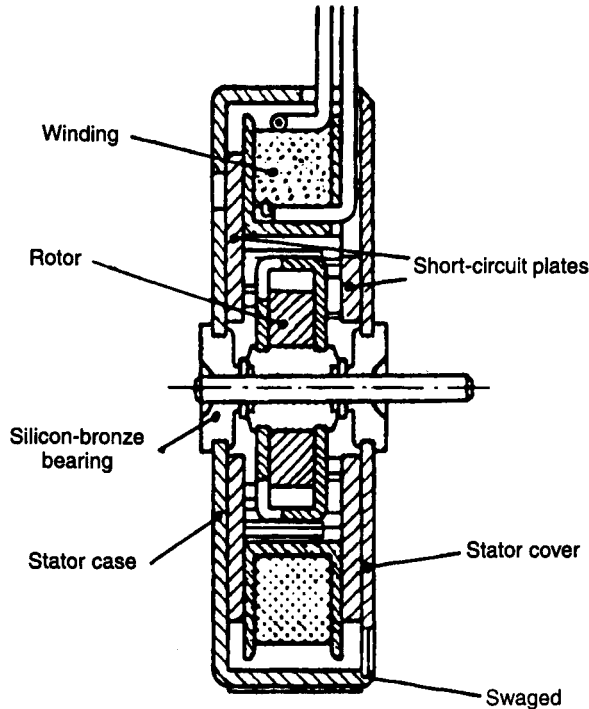


Figure 5.15 Section through a single-phase synchronous motor with shaded poles and a permanent magnet rotor

a false start (in the wrong sense) the spring is compressed by the pulsating rotor and it assists in pushing the rotor in the right direction on the next half cycle of the supply.

The purely alternating field principle has been exploited in recent developments, and even in some 2-pole motors. The cylindrical diametrically magnetised permanent magnet rotor turns within a stator with airgap variations (Figure 5.16). In the zero current state the magnetic axis of the rotor lines up with the pole axis of the stator at the angle of asymmetry shown. After switching on, the rotor starts oscillating with increasing amplitude because of the lack of symmetry until it locks into synchronism. This may occur in either direction of rotation.

The motor finds application only where the direction of rotation is immaterial as, for example, in centrifugal pumps. In order not to hinder the oscillatory start-up, the pump wheel is connected to the rotor axle via slack strings. Because hard ferrite rotors are largely corrosion-resistant, they may be separated from the stator by a split casing (Figure 3.16) and be integral with the pump wheel, thus avoiding the problems of sliding seals.

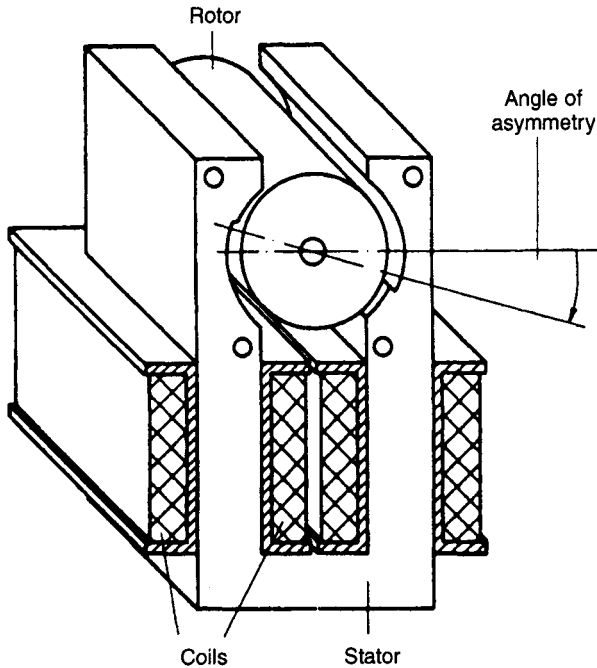


Figure 5.16 Two-pole, alternating field synchronous motor

5.4.2 Motors with hysteresis rotors

The hysteresis motor with a 3-phase winding (Figure 5.17) is characterised by its internal stator and external rotor. The high rotor moment of inertia, consequent upon its outside position, should give rise to particularly smooth running. The construction of this kind of motor is shown clearly in Figure 5.18.

The schematic representation (Figure 5.19) and the practical design (Figure 5.20) of a 2-pole shaded-pole hysteresis motor are given. Improvement of the rotating field is achieved by three short-circuit windings on each shaded pole as shown in Figure 5.20.

As well as the hysteresis motors with the low pole-pair numbers described above, multipole shaded-pole motors with a central winding and pole claws and with inner or outer rotors have been developed.

5.4.3 Motors with reluctance rotors

Reluctance motors frequently resemble induction motors in their construction. The rotors merely show irregularities, to enable the extra reluctance torque to be produced. In special hysteresis motors, to ensure synchronous running, the reluctance effect is used as well. In these multipole

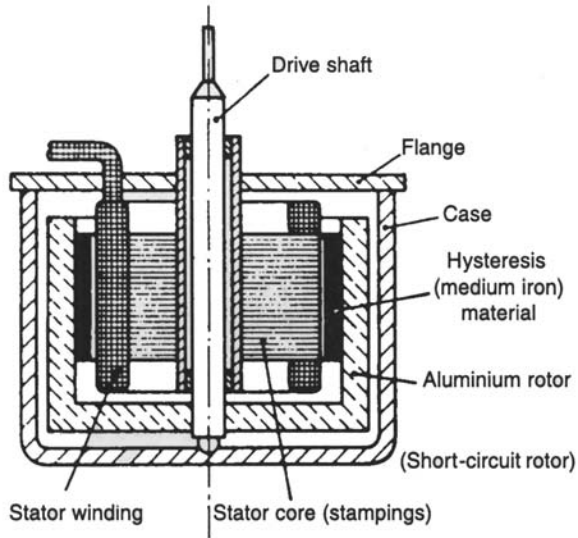


Figure 5.17 Section through a synchronous motor with an external hysteresis rotor

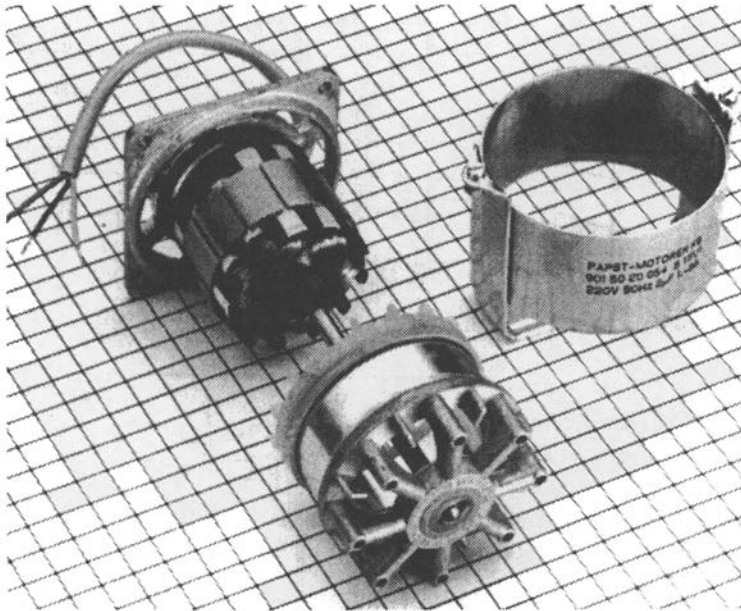


Figure 5.18 Construction of a single-phase synchronous motor with capacitor auxiliary phase and external hysteresis rotor
3.5 W, 1500 rev/min
(Courtesy: Papst)

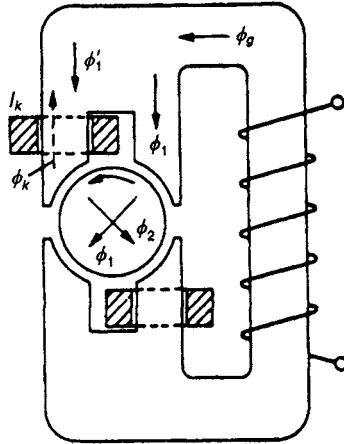


Figure 5.19 *Schematic diagram of a single-phase synchronous motor with shaded poles and a hysteresis inner rotor*

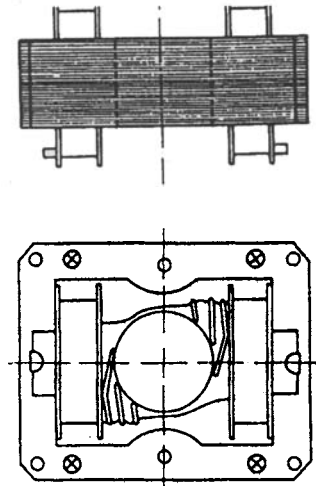


Figure 5.20 *Construction of a modern shaded-pole hysteresis motor*
The rotor is not shown

motors a regular pattern of windows is stamped around the circumference of the hysteresis ring.

5.5 Characteristics

Synchronous motors are fitted principally with permanent magnet or hysteresis rotors. Reluctance rotors play a lesser role. For a given motor set of

dimensions, the permanent magnet rotor motor delivers appreciably more torque than that with the hysteresis rotor. On the other hand, the hysteresis rotor motor has no starting problems because it can also develop induction motor torque.

A permanent magnet synchronous motor must be brought up to synchronous speed within a half period of the mains supply after switching on, if no provision for developing asynchronous torque is provided.

Only the smallest inertia loads may be rigidly coupled to these motors if an independent start is demanded. This is, of course, not the case for hysteresis motors.

Reluctance motors are generally fitted with squirrel cages to facilitate starting. They lock into synchronous running in a jerky manner. In contrast with hysteresis motors, reluctance motors are just as unsuited to asynchronous running under overload as are permanent magnet synchronous motors.

At the upper end of the power range, 50 W–30 kW, there are motors with deep pole permanent magnets for (direct) connection to the 3-phase supply available (Siemosyn and Siemotron motors). The rotors are as shown in Figure 5.8.

Fast running capacitor motors, whose induction rotors are synchronised through permanent magnets, and shaded-pole motors with permanent magnet rotors and hysteresis components for ensuring run-up are found in the power range up to 50 W.

Slow running permanent magnet motors are built with a capacitor auxiliary phase, or as 3-phase motors, with speeds from 250 to 600 rev/min and powers up to about 25 W. As shaded-pole motors they can deliver powers of up to about 1 W.

As Figure 5.21 shows, a torque M_s at synchronous speed is available from these low power synchronous motors. M_s is greater than the 'run-up' torque M_E over a wide range of supply voltages. M_E is the load torque that can be drawn from the motor without preventing the 'locking into synchronism'. The torque shown in Figure 5.21 is referred to the output shaft of a gear-train turning at 1 rev/min. The gear-train is coupled to the motor for measurement purposes.

It is quite clear that the 'run-up' torque must be less than the synchronous torque, because during running up to synchronism the rotor requires an accelerating torque that is then no longer available at the output shaft.

Two-, 4- and 6-pole hysteresis motors, manufactured with external rotors, can deliver powers up to about 70 W, whilst the multipole, mostly 16-pole, variants are only built for power outputs of milliwatts. Figure 5.22 shows the speed-torque characteristics of a 2-pole shaded-pole hysteresis motor (see Figure 5.20). The numbers 1, 2, 3 relate to different hysteresis materials. The available torque from standstill up to synchronous speed stays approximately constant. Compared with a shaded-pole induction motor with the same body size (curve 4), the hysteresis motors develop less torque.

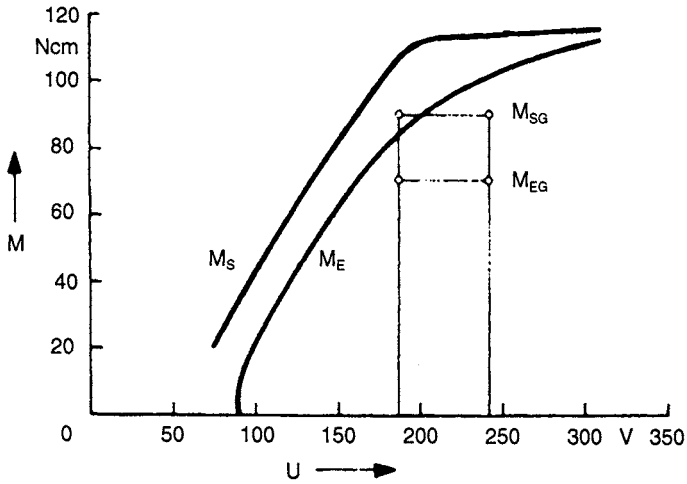


Figure 5.21 Dependence of synchronous torque M_S and 'run-up' torque M_E of a shaded-pole synchronous motor with permanent magnet rotor on the mains voltage U
 M_{SG} and M_{EG} are guaranteed values

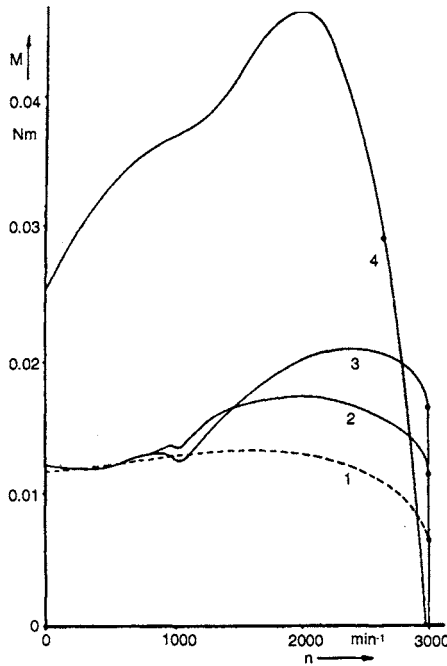


Figure 5.22 Characteristics $M(n)$ of a 2-pole synchronous motor, as in Figure 5.20, with various hysteresis materials 1, 2 and 3
 Curve 4 is that of a motor with an induction rotor

Reluctance motors with two or four poles, often designed to have external rotors, have power outputs up to 100 W. Their characteristics are like those of asynchronous motors, when the region near to synchronism is left out.

5.6 Applications

Motors which run at constant speed, independent of load, are necessary for many drive applications. However, these requirements have long been met by means other than synchronous motors.

Synchronous motors are losing their importance because:

- other, electronically energised, motors can be held at constant speed, and also this speed is adjustable
- clocks and timers are being equipped in increasing numbers with electronic components in place of synchronous motor – gearbox combinations
- in automatic apparatus, motor-driven programme switches can be replaced with electronic circuits.

Nevertheless, there remains a number of applications for which the synchronous motor provides the most economic solution. This applies to programmers in automatic washing machines and dishwashers. Also, simple clock-operated switches cannot be made without synchronous motors.

In slow speed drives, multipole multiwinding synchronous motors are installed on account of their low turning speed, their relatively high torque and their easy reversibility, and not on account of their synchronous running characteristics.

Chapter 6
Universal motors

Jürgen Draeger

6.1 Introduction

Universal motors are commutator machines. They may be driven from AC or DC mains. Their speed of rotation is limited only by the mechanical strength of the rotor and the bearings and the useful brush lifetime.

Universal motors driven from single-phase AC mains run at speeds from 3000 rev/min to 25 000 rev/min and have powers up to 1200 W. The less expensive induction motors are limited in speed by their operating principles and the mains frequency. In the following pages the construction, operation, performance and application possibilities of the universal motor are discussed.

6.2 Construction

The stator and rotor (armature) are both wound on stacks of stampings, each stamping being 0.5–0.7 mm thick on account of there being alternating magnetic fields in both the stator and rotor. The armature coils which start and finish on two adjacent commutator bars are connected in series and uniformly distributed around the armature in 8–18 half-open slots, usually as short-pitch coils at two levels. There is a voltage distribution throughout the armature over the commutator and fixed brushes. To reduce the voltage between commutator bars that are to be momentarily connected by the brushes, the coils are centre-tapped and the centre taps are connected to intermediate bars, so that the number of bars is twice the number of coils. The brush width is about 1.3–1.8 times that of a commutator bar. By skewing the slots by one slot pitch the airgap reluctance (magnetic resistance) is made very much less, depending on the position of the armature relative to the stator.

The stator winding surrounds the salient stator poles, which extend out to the 0.3–0.5 mm-wide airgap. The pole-pair number is normally $p = 1$. The airgap is constant over the greater part of its arc but it may be almost doubled towards the edges of the pole shoes for the sake of an improved on-load flux distribution and reduced noise. The commutating poles and compensating winding, normal in the larger series machines, are not designed into the smaller machines.

Figs. 6.1 and 6.2 show cross-sections and details of universal motors. The interaction of the airgap field b between the stator and armature, which is developed by the field winding, and the current i in the armature winding produces a torque

$$m \sim ib \tag{6.1}$$

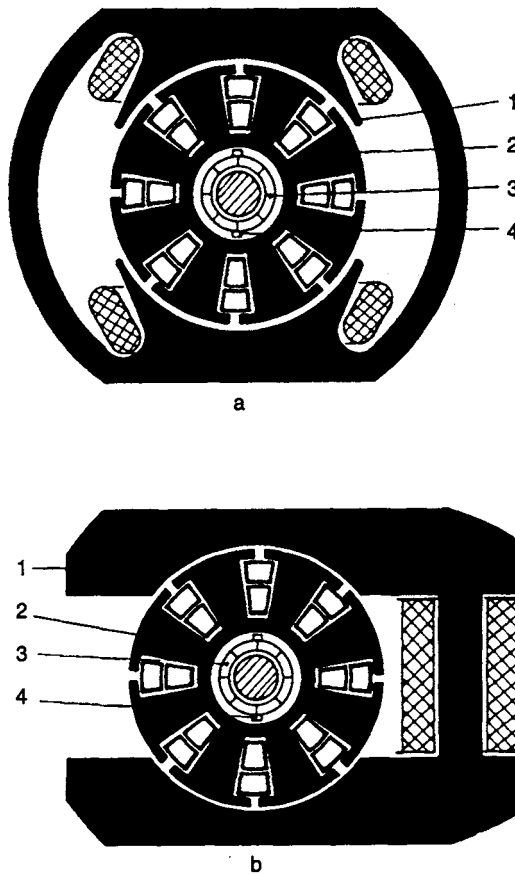


Figure 6.1 Cross-section through (a) symmetrical ($P > 200\text{ W}$) and (b) unsymmetrical ($P < 200\text{ W}$) universal motor
 1 Stator pole; 2 armature; 3 commutator; 4 brush

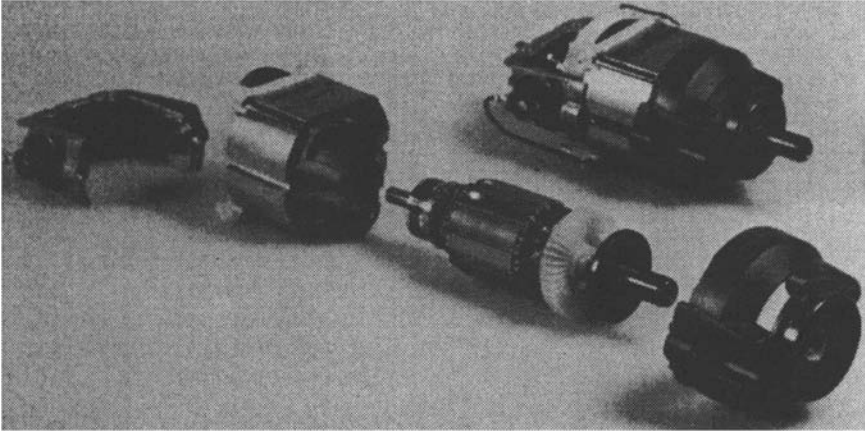


Figure 6.2 Details of a universal motor
(Courtesy: Vorwerk)

In particular, if i and b are sinusoidal, then the average value of the torque is

$$M \sim IB \cos \varphi \quad (6.2)$$

where I and B are the RMS values of the current and flux density at the same frequency and φ is the phase between the alternating quantities. If I and B do not have the same frequency, M is always zero.

Therefore, a machine which is to be connected to the AC mains cannot have a permanent magnet field. The phase angle should be as close to $\varphi = 0$ as possible (see eqn. 6.2) to obtain the best average torque.

This is achieved by connecting the field winding in series with the armature. Parallel connection of the two windings, given the necessarily highly inductive field winding and the low inductance armature winding, leads to a relatively large angle φ . Thus, AC commutator motors are only connected for series operation. Because the direction of current flow through a given armature conductor must reverse between passing each pole alternately, a commutator or current switching device is necessary between the armature winding and the supply. The construction of the machine is like that of the DC series motor. Therefore, in principle, it is possible to use the same machine as a universal AC/DC motor.

In the main consideration of the running performance, only the fundamental components of the waveforms of the alternating voltages, currents and magnetic fields will be analysed. Speed-dependent periodic changes in the rotor winding currents will not be considered. The DC series-connected motor will be considered as a special case, with supply frequency $f = 0$.

6.3 Operating principles

6.3.1 Magnetic flux distribution

Fig 6.3 shows the linear development of a machine as in Figure 6.1a, and the airgap distributions of:

- armature MMF Θ_A resulting from armature current I_A
- flux density B_A corresponding to MMF Θ_A
- flux density B_E resulting from the stator field excitation current I_E (=armature current I_A).

The brush axis is turned through an angle β from the magnetic neutral axis ($B_E = 0$) in the opposite sense to the armature rotation to assist commutation. B_A and B_E are superimposed to give B_R the flux density distribution in a loaded machine. The influence of armature MMF on the field distribution is called armature reaction. It causes:

- a distortion of the excitation field towards the pole shoe edge
- a reduction of the pole flux on account of the nonlinear magnetisation characteristic of the ferromagnetic circuit (saturation of the iron laminations)
- a load-dependent displacement of the neutral zone, at which B_R is zero.

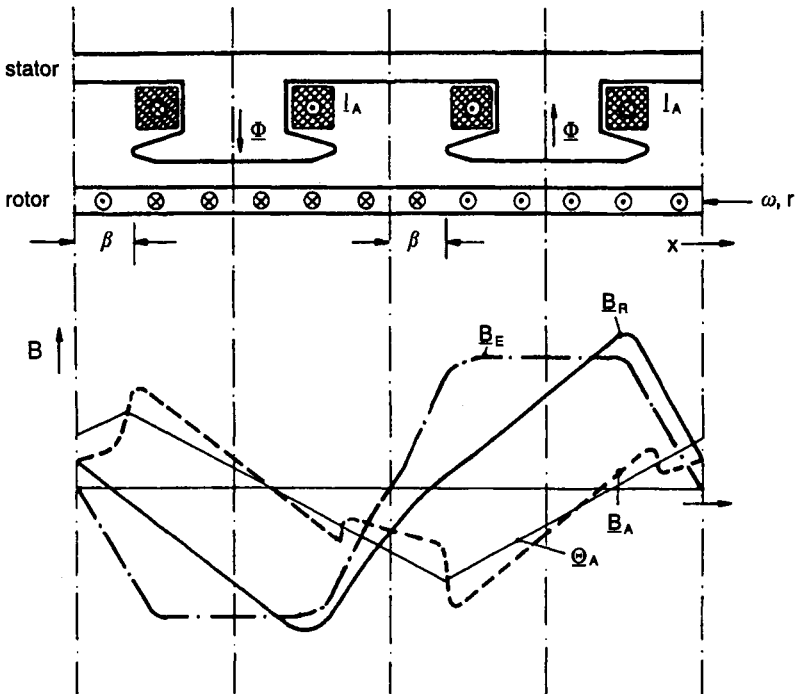


Figure 6.3 Magnetic induction distribution in the airgap of a 2-pole machine

The equivalent circuit of the series motor, for the purpose of determining the effects of the fluxes, is shown in Figure 6.4. The component fluxes, armature flux ϕ_A in the direction of the brush axis and stator flux ϕ_E in the direction of the motor field axis link N_A and N_E turns, respectively.

The machine is driven from the mains voltage U . The armature current I_A generates the armature winding flux ϕ_A and the stator excitation winding generates ϕ_E which, when somewhat reduced by the amounts of the stray fluxes $\phi_{A\sigma}$ and $\phi_{E\sigma}$, make up the resultant flux in the airgap. This flux is ϕ_{lh} resolved into two component fluxes, mutually at right angles, depicted as in the direct (longitudinal) axis and ϕ_{qh} in the quadrature axis of the machine.

Assuming that component fluxes may be added in an unsaturated machine,

$$\phi_h = \phi_E - \phi_{E\sigma} - (\phi_A - \phi_{A\sigma}) \sin \beta \quad (6.3)$$

and

$$\phi_{qh} = (\phi_A - \phi_{A\sigma}) \cos \beta \quad (6.4)$$

where ϕ_{lh} is generated by MMF $I_E N_E - I_A N_A \sin \beta$ and ϕ_{qh} is generated by MMF $I_A N_A \cos \beta$.

In small machines under running conditions the direct (longitudinal) axis is highly saturated so that changes in load current change ϕ_{lh} only slightly.

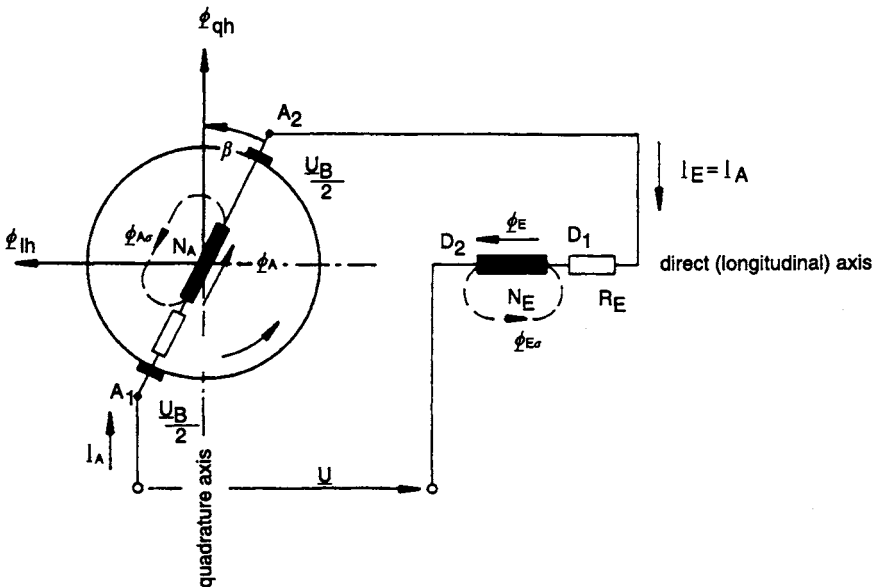


Figure 6.4 Equivalent circuit of the series motor

6.3.2 Induced voltages and terminal voltage

Voltage is induced in the armature winding as a result of armature rotation in the airgap field, and also by transformer action owing to the alternating airgap flux.

U_{qr} is the symbol for the component induced by armature rotation at speed n . Current, voltage and flux symbols relate to the RMS values for current and voltage and for the peak value of the fundamental component of flux,

$$U_{qr} = \frac{1}{\sqrt{2}} cn\phi_{lh} \left(1 - \frac{2\beta}{\pi}\right) = \frac{1}{\sqrt{2}} c_R n\phi_{lh} \quad (6.5)$$

where $c = 2pz/2a$, a machine constant, in which z is the number of conductors around the armature, p the number of pole-pairs and $2a$ the number of parallel paths through the armature winding.

The transformed voltage U_{qt} , given $\omega = 2\pi f$, where f = supply frequency, is

$$U_{qt} = \frac{1}{\sqrt{2}} j\omega N_A (\phi_{qh} \cos \beta - \phi_{lh} \sin \beta) \quad (6.6)$$

Taking the working resistances of the armature winding and that of the field winding R_A and R_E , respectively, and the brush voltage drop U_B into consideration, the terminal voltage becomes

$$\begin{aligned} U &= I_A R_E + \frac{1}{\sqrt{2}} j\omega N_E (\phi_{E\sigma} + \phi_{lh}) + I_A R_A \\ &+ \frac{1}{\sqrt{2}} j\omega N_A (\phi_{A\sigma} + \phi_{qh} \cos \beta - \phi_{lh} \sin \beta) \\ &+ \frac{1}{\sqrt{2}} c_R n\phi_{lh} + U_B \end{aligned} \quad (6.7)$$

The brush voltage drop, as Figure 6.5 shows, is a nonlinear function of the current and depends on the brush material. A better overview of the voltage relationships is given in Figure 6.6, in which the voltages U_B have been neglected.

The total active power in the machine is

$$P_w = |I_A| |U_{qr}| + |I_A|^2 (R_A + R_E) \quad (6.8)$$

The first term is the mechanical power developed and the second is the winding copper loss. No attention has been paid to the iron losses, the losses resulting from armature turns short-circuited by the brushes, nor to the effects of the flux harmonics.

When the supply is a direct voltage, $f = 0$, the RMS values of current and voltage are replaced by the constant values I and U , and the RMS flux $\phi/\sqrt{2}$ is replaced by the constant flux ϕ .

Eqs. 6.5 and 6.7 for the alternating current motor reduce to

$$U_{qr} = c_R n\phi_{lh} \quad (6.9)$$

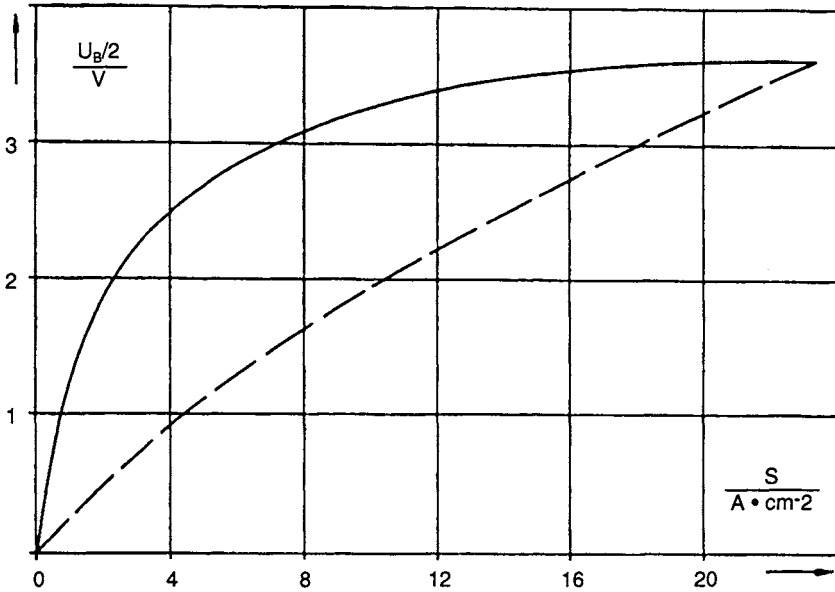


Figure 6.5 Brush voltage drop U_B as a function of the current density s
 — static characteristics
 ---- dynamic characteristics

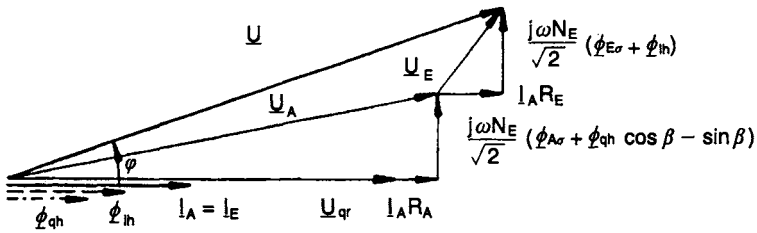


Figure 6.6 Phasor diagram of a universal motor on load

and

$$U = I_A(R_A + R_E) + c_R n \phi_{lh} + U_B \tag{6.10}$$

6.3.3 Torque and power

From eqn. 6.8 the internally developed mechanical power is

$$P_{mi} = |I_A| |U_{qr}| \tag{6.11}$$

From eqn. 6.5 and the given speed n , the internal average torque is

$$M_i = \frac{P_{mi}}{2\pi n} = \frac{|I_A| |U_{qr}|}{2\pi n} = \frac{c_R}{2\pi\sqrt{2}} |\phi_{lh}| |I_A| \tag{6.12}$$

Because, in a magnetically unsaturated machine, $|I_A| \propto |\phi_{lh}|$ and, given proportionality factors k_1 and k_2 ,

$$M_i = \frac{c_R}{2\pi\sqrt{2}} k_1 |I_A|^2 = \frac{c_R}{2\pi\sqrt{2}} k_2 |\phi_{lh}|^2 \tag{6.13}$$

therefore $M_i \propto |I_A|^2$. The armature current depends only on the load torque and not on the supply voltage. Because I_A is an alternating current, the torque pulsates at twice the mains frequency about the average value M_i and between extreme values zero and $2M_i$ (Figure 6.7). In a magnetically saturated machine, $|\phi_{lh}|$ stays approximately constant and $M_i \propto |I_A|$.

From eqn. 6.12, in a magnetically unsaturated machine the mechanical power is

$$P = 2\pi n M$$

$$P_i = \frac{c_R n}{\sqrt{2}} |\phi_{lh}| |I_A|$$

and from eqn. 6.13,

$$P_i = \frac{c_R n k_1}{\sqrt{2}} |I_A|^2 \tag{6.14}$$

The mechanical power P_m and the torque M at the output shaft are smaller on account of friction and fan losses.

Given friction torque M_R ,

$$M = M_i - M_R$$

Efficiency η is calculated from the net output power P_{ab} and the gross input power P_{zu} :

$$\eta = \frac{P_{ab}}{P_{zu}} = \frac{P}{|I_A| |U_A| \cos \varphi} = \frac{2\pi n M}{|I_A| |U_A| \cos \varphi} \tag{6.15}$$

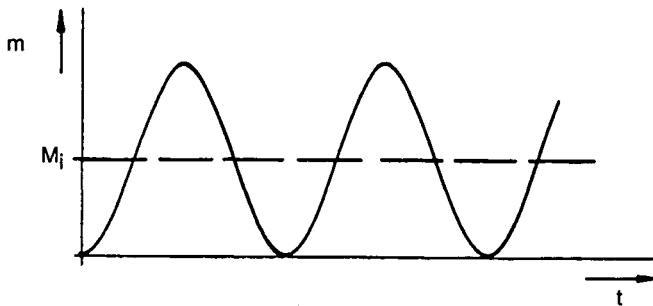


Figure 6.7 $m(t)$ of a universal motor

When the motor runs as a DC machine, with direct quantities I_A and ϕ_{lh} , torque

$$M_i = \frac{c_R k_1}{2\pi} I_A^2 \tag{6.16}$$

and mechanical power

$$P_i = c_R k_1 n I_A^2 \tag{6.17}$$

6.3.4 Commutation

The commutator and brush form a sliding contact and form a mechanical switch at whose contacts, particularly at the trailing edge, sparking occurs. Causes of sparking are, depending on the circumstances, heating at the point of contact owing to friction, excessive and uneven current loading through the brushes, mechanical vibration of the brushes through, for example, an uneven commutator, or too much play in the brush holders and, in every case, through incomplete commutation owing to electrically induced voltages in the commutating windings.

This commutation process will be explained at first for a DC machine. In Figure 6.8 the current distributions are shown before, during and after the commutation of a coil. The commutation current i_k changes in one commutator bar width b_k and with commutator circumferential speed v_k , and during the commutation period

$$t_k = \frac{b_k}{v_k} \tag{6.18}$$

from $+I/2$ to $-I/2$.

In an assumed resistanceless coil whose long sides lie in the magnetic neutral zone, this is a linear process (linear commutation) as shown in

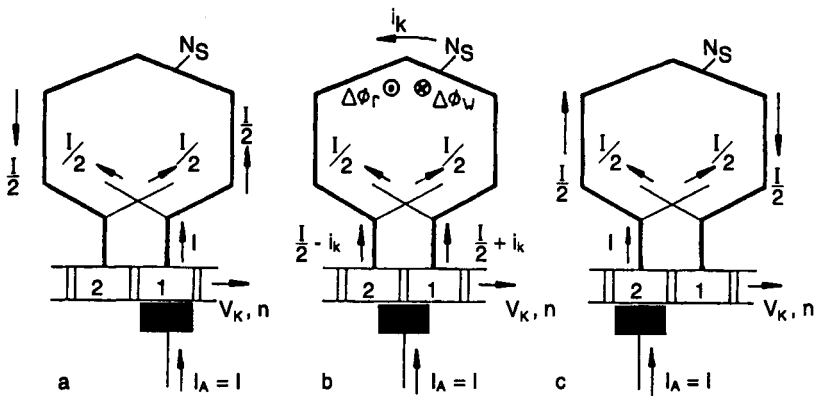


Figure 6.8 Winding currents in one armature coil
 a before; b during; c after commutation, and the flux changes $\Delta\phi$ inside the commutating coil with N_c turns.

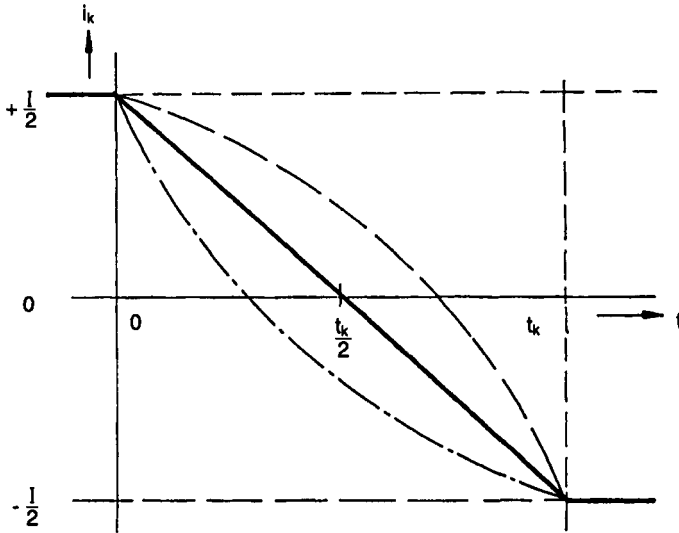


Figure 6.9 Current i_k in the commutating coil with
 ————— linear commutation
 - - - - - under-commutation
 - · - · - over-commutation

Figure 6.9. In reality there are stray inductances in the coils which lie in a ferromagnetic circuit and which are not negligible, so that a flux change $\Delta\phi_w$ occurs within the coil, which induces a voltage U_{qw} so that a current is induced that is shorted by the brushes and delays the change in i_k . Under-commutation occurs, during which the current density at the trailing edge of the brush is increased and sparking occurs at the instant of breaking contact between the brush and the commutator bar.

This effect is aggravated when, owing to uncompensated armature reaction, the load-dependent magnetic axis shifts relative to the geometrical neutral axis in a contra-rotation direction. A remedy is possible if the brush axis is shifted to coincide with the on-load magnetic neutral axis of the machine (see Figure 6.4). The angle β is about 15–30 ° and in the contra-rotation direction. This shift produces a flux change $\Delta\phi_r$ in the commutated winding which cancels $\Delta\phi_w$, or, in other words, a rotary generated voltage U_{qr} is induced in opposition to the commutation reactance voltage U_{qvw} . If U_{qr} is designed to be larger than U_{qvw} , then the resultant voltage induced in the commutating coil, that appears between the commutator bars where brush contact is made,

$$U_k = U_{qw} + U_{qr} \tag{6.19}$$

appears and is so directed that it supports (assists) the commutation. Over-commutation results (see Figure 6.9). The brush becomes loaded crosswise

between the commutator bars by the current generated from the contact voltage.

If the machine is driven from the AC mains at mains frequency, then, depending on the speed of rotation, there can be up to some hundreds of commutations per second. Let the sinusoidal current waveform be approximated by a series of level steps and be reflected in the horizontal axis as in Figure 6.10a. The sloping lines in Figure 6.10a depict the current flow through successively commutated armature winding elements. Figure 6.10b then depicts u_{qw} the voltages induced in these elements due to their leakage inductances. The fundamental component ($\nu=1$) of the commutation reactance voltage that appears between the brush contact points is

$$U_{qw} = -2 N_s l v \zeta A = -\text{const}_1 n I \tag{6.20}$$

where N_s is the number of turns per winding element, l is the armature length and v is the peripheral speed, A is the RMS armature ampere turns and $\zeta = 4-9 \times 10^{-6}$ Vs/Am is Pichelmayer's commutation factor.

The fundamental component of the generated voltage induced in the commutated winding owing to rotation is, in accordance with eqn. 6.5,

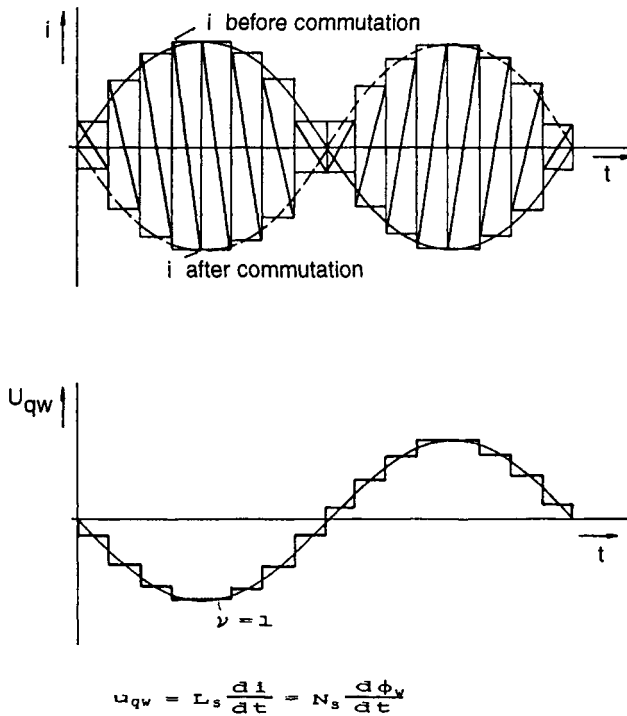


Figure 6.10 Induction of the commutation reactance voltage u_{qw} given a current which varies sinusoidally with time

$$\mathbf{U}_{qrs} = \frac{1}{\sqrt{2}} C_{RS} N_S b \Phi_1(\beta) = -\text{const}_2 n \mathbf{I} \quad (6.21)$$

Also, in the AC machine and in accordance with eqn. 6.6, the voltage induced in the commutated winding owing to transformer action is

$$\begin{aligned} \mathbf{U}_{qts} &= \frac{j}{\sqrt{2}} \omega N_S (\Phi_{th} \cos \beta + \Phi_{qh} \sin \beta) \\ &= j(\text{const}_3 + \text{const}_4) \mathbf{I} \end{aligned} \quad (6.22)$$

This voltage is independent of the speed of rotation.

The brush contact voltage is, in total,

$$\mathbf{U}_k = \mathbf{U}_{qv} + \mathbf{U}_{qrs} + \mathbf{U}_{qts} \quad (6.23)$$

\mathbf{U}_{qv} and \mathbf{U}_{qts} are capable of cancelling each other, as shown. However, for \mathbf{U}_{qrs} , which is displaced from the others by a 90° phase angle, no compensation is possible. This means that, in universal motors, which are not fitted with interpoles, brush contact voltage is determined mainly by the transformer action and to a lesser extent by the armature-reaction-dependent generated voltage. In accordance with eqn. 6.22, \mathbf{U}_{qts} can be influenced by the number of turns per winding element N_S and the excitation flux. A lower N_S necessitates a higher number of teeth and slots; lower flux means poorer utilisation of the machine volume.

Therefore it is necessary on economic grounds to accept a relatively high contact voltage U_k and limit the current in the commutating winding, bars and brush loop by means of resistance. Depending on brush quality, a value of U_k from 3 V to 6 V is chosen. It is only when $U_k < 1$ V that brush sparking is no longer visible. Universal motors always exhibit sparking. Sparking is irregular owing to the alternating commutating voltage change for successive commutating winding elements.

6.3.5 *Brushes*

Brushes used in universal motors should present, at a sufficiently high permissible current density, a relatively high specific contact resistance at and between the contact surfaces, and they should be relatively hard so that the products of sparking at the commutator are cleaned off.

To raise the resistance to short-circuit circumferential current through the brushes, a two-layer construction with an insulating film between them is used. Series motors to be driven from DC mains may be fitted with softer brushes with lower values of specific resistance. This is particularly the case for marine electrical systems, where the voltage is lower.

Important factors influencing brush life are loading owing to current density, sparking and friction at the contact surfaces, which is made worse by dust and low humidity.

As Figure 6.11 shows, mechanically related wear increases with brush pressure on the commutator, whereas electrically related current density wear decreases. There is therefore an optimum pair of parameters – maximum current density and corresponding brush pressure – declared by the manufacturer. Table 6.1 gives typical working data for various types of brushes.

When brushes are replaced, it is important to ensure that the radii of curvature of the brush face and the commutator are equal, i.e. that the brushes are bedded in.

Table 6.1 Permissible operating conditions for various brush types

Type	Current density, A/cm ²	Pressure, cN/cm ²	Specific resistance, Ω mm ² /m	Speed, m/s	Voltage drop per brush, V	
Hard carbon brushes	6–8	150–300	50–350	15–25	>1.5	AC motor
Graphite resin brushes	6–12	200–300	60–350	15–35	>1.5	
Electro-graphite brushes	10–16	160–300	15–100	40–60	0.75–1.5	DC motor
Metal graphite brushes	15–25	200–600	0.2–20	<30	0.75–1.5	

6.4 Operational performance

6.4.1 Operating characteristics

The torque–speed characteristic may be deduced from eqns. 6.7 and 6.11. Because all fluxes are proportional to the armature current I_A in a magnetically unsaturated machine, constants k_3 to k_6 may be defined

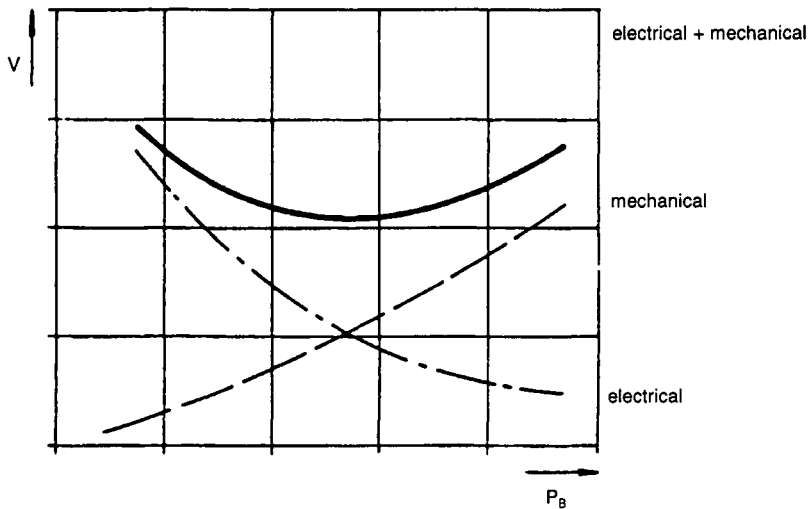


Figure 6.11 Rate of brush wear as a function of contact pressure p_B

$$\begin{aligned} |\Phi_{lh}| &= k_3 |\mathbf{I}_A| & |\Phi_{A\sigma}| &= k_5 |\mathbf{I}_A| \\ \text{and } |\Phi_{E\sigma}| &= k_4 |\mathbf{I}_A| & |\Phi_{\phi h}| &= k_6 |\mathbf{I}_A| \end{aligned} \tag{6.24}$$

$$\begin{aligned} n &= \frac{\sqrt{2}}{c_R k_3} \times \\ &\left[\sqrt{\frac{|U|^2 - c_R k_1}{2\sqrt{2}\pi M_i} - \left[\frac{\omega}{2\sqrt{2}} (N_E (k_3 + k_4) + N_A (k_5 + k_6 \cos \beta - k_3 \sin \beta)) \right]^2} \right. \\ &\left. - (R_A + R_E) - \frac{U_B \sqrt{c_R k_1}}{\sqrt{2\sqrt{2}\pi M_i}} \right] \end{aligned} \tag{6.25}$$

can be derived.

The speed n , therefore, depends on $1/\sqrt{M_i}$. Compared with the DC series motor, the AC motor runs more slowly on account of the term involving ω in eqn. 6.25. If the machine is to be supplied with DC, the field winding turns number must be increased with a supplementary winding.

Fig 6.12 shows n/n_N as a function of M_i/M_N on unified per-unit scales. In the absence of load torque, the speed can, depending on circumstances, become unacceptably high. In small machines the friction torque M_R limits the speed sufficiently.

From eqn. 6.13, Section 6.3.3, the armature current in an unsaturated machine is

$$|\mathbf{I}_A| = \sqrt{\frac{2\sqrt{2}\pi}{c_R k_1}} \times \sqrt{M_i} \tag{6.26}$$

Figure 6.12 shows $\frac{|\mathbf{I}_A|}{|\mathbf{I}_{AN}|}$ as a function of $\frac{M_i}{M_N}$.

Because iron saturation along the direct axis of the magnetic circuit increases progressively with load, the armature current for a required torque is greater than eqn. 6.26 would predict.

On account of the relatively high inductance of the field winding, the starting current and starting torque, at three to five times the full-load values, are comparatively small, so that direct switching is possible.

The power factor $\cos \phi$ depends on the load. At low speed, U_{qr} is small and \mathbf{I}_A , and the voltage drop that goes with it, is correspondingly large, so that the phase angle between \mathbf{U} and \mathbf{I}_A is relatively large. At high speed, U_{qr} is also large and the current falls and the voltage drop becomes smaller, so that ϕ also becomes smaller (see Figure 6.12).

When the machine is supplied with direct voltage (hence $\omega = 0$) and the phasors \mathbf{I}_A , \mathbf{U} , \mathbf{U}_B and $\phi/\sqrt{2}$ may be replaced in eqns. 6.25 and 6.26 with their DC equivalent values, we derive

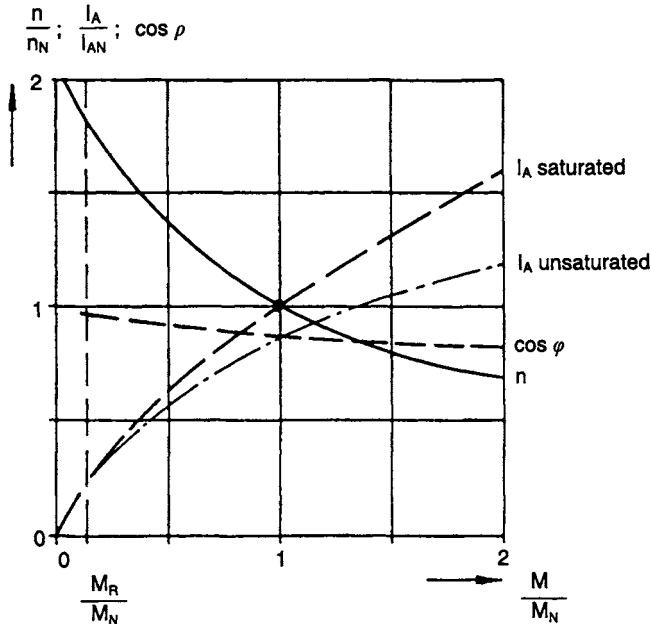


Figure 6.12 Working characteristics of a universal motor driven from the 50 Hz mains

The scales are per-unit using the rated values as the base

$$\text{speed } n = (U - U_B) \sqrt{\frac{k_i}{k_3^2 2\pi c_R}} \frac{1}{\sqrt{M_i}} - \frac{R_A + R_E}{c_R k_3} \quad (6.27)$$

and armature current

$$I_A = \sqrt{\frac{2\pi}{c_R k_1}} \times \sqrt{M_i} \quad (6.28)$$

6.4.2 Speed control

Eqn. 6.25 indicates that speed change can be achieved by adjusting the supply voltage U , the supply frequency f , the number of field winding turns N_E or the resistances R_E and R_A .

6.4.2.1 Variation of the terminal voltage U

The characteristics $n(M_i)$ for a range of terminal voltages are in accordance with Figure 6.13. The operating range is limited by the maximum allowable speed and the maximum allowable armature-current-derived heating during continuous running. This armature current is dependent on the load torque and not on the terminal voltage (see eqn. 6.26).

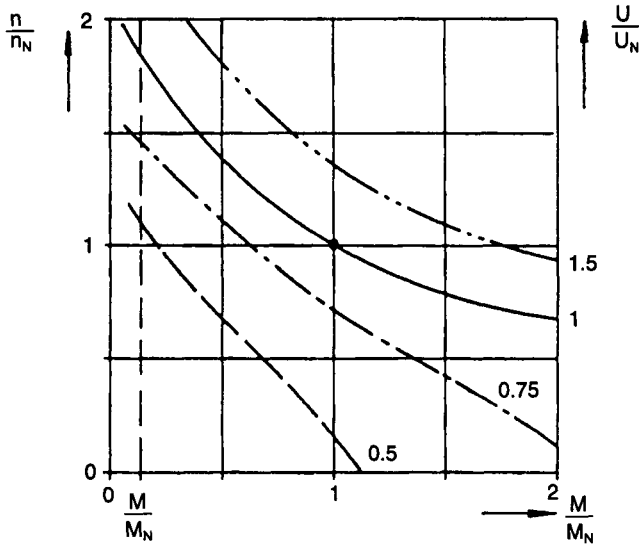


Figure 6.13 *Speed adjustment through supply voltage variation*

The terminal voltage may be controlled simply by the electronic circuit shown in Figure 6.14.

A triac T is placed between the motor and the mains supply and is controlled by a simple firing circuit. The charging time constant of an RC circuit may be adjusted by means of the variable resistor R.

When the capacitor voltage u_C becomes that of the firing voltage u_D of the diac D, the capacitor C discharges via the triac gate circuit. The triac fires and conducts so that the supply voltage is connected to the motor from this instant until the armature current becomes zero again, whereupon the triac goes open-circuit again.

This sequence is repeated for every half-cycle of the supply. By adjusting the firing instant (with R) the voltage-time integral of the applied voltage, and hence its RMS value, is controlled.

6.4.2.2 *Changing the supply frequency f*

As Figure 6.15 shows, increasing the supply frequency lowers the torque-speed characteristic. This effect is predictable from the term involving ω in eqn. 6.25. Currently available frequency changers are too expensive for economic speed control of motors.

6.4.2.3 *Changing the excitation flux ϕ_{lh} through field winding taps*

Changing the number of field coil turns N_E through tapping changes the excitation flux ϕ_E and therefore ϕ_{lh} as well as the constants k_1 , k_3 and k_4 in eqn. 6.25. With increasing excitation flux and constant torque load, the speed

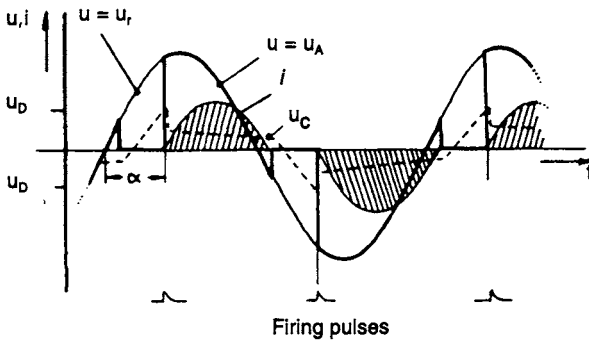
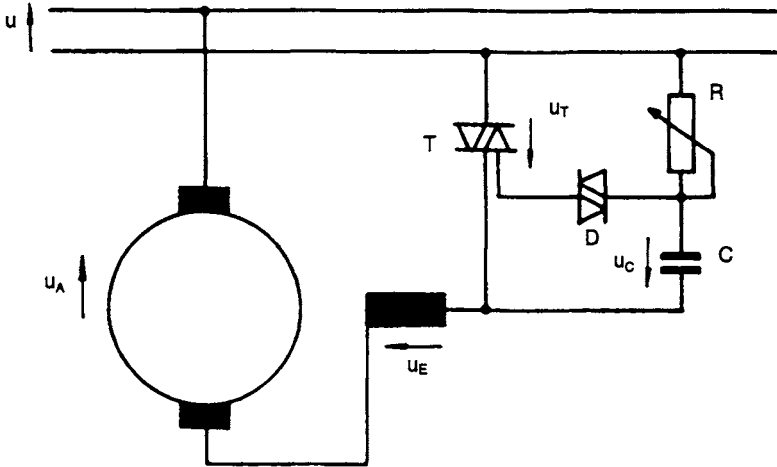


Figure 6.14 Circuit of an AC current controller and the time-dependent functions of motor winding voltage and current

- u_T = voltage across the triac
- u_A = voltage across the motor
- u_C = capacitor voltage
- α = firing angle
- i = motor current

falls off as shown in Figure 6.16. This provides a cost-effective means of achieving stepped speed control. Attention must be paid to the effect on armature current of tap-changing so that the maximum current is not exceeded when the motor is loaded.

6.4.2.4 Changing the series resistance $R_A + R_E$

By switching an extra series resistance R_S into the circuit the motor terminal voltage is reduced in a load-dependent manner. $I_A^2 R_S$ losses in this series

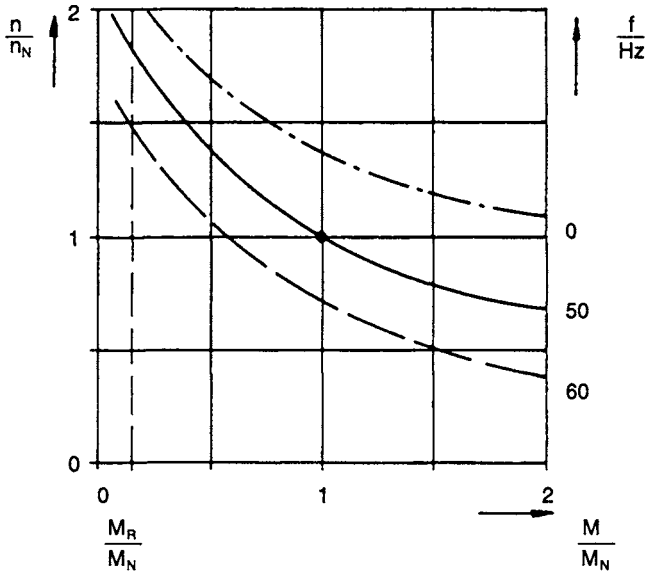


Figure 6.15 Speed changing by means of supply frequency variation

resistor lower the efficiency. Therefore, this form of control is only used for short periods during starting.

6.5 Radio-TV interference

The current transfer at the brush-commutator-bar interface happens as a result of travelling current pulses that punch through the surface patina and insulation film at the surfaces in contact. Consequently the contact voltage has a high wideband harmonic content. Also, wideband high frequency electromagnetic fields are caused by the brush contact sparking.

Voltage injection into the mains must be limited to acceptable levels by lowpass filters connected between the machine and the supply in the frequency range 0.15–30 MHz in accordance with the relevant standard specifications. As well as mains injection, there is radiation from the sparking in the frequency range 30–300 MHz to be controlled. This is only possible by careful design of the commutation systems and, where necessary, by metallic screening.

6.6 Applications

Mains powered universal motors are used, primarily, as direct drives for fast rotating low power appliances such as coffee mills, vacuum cleaners, fans or

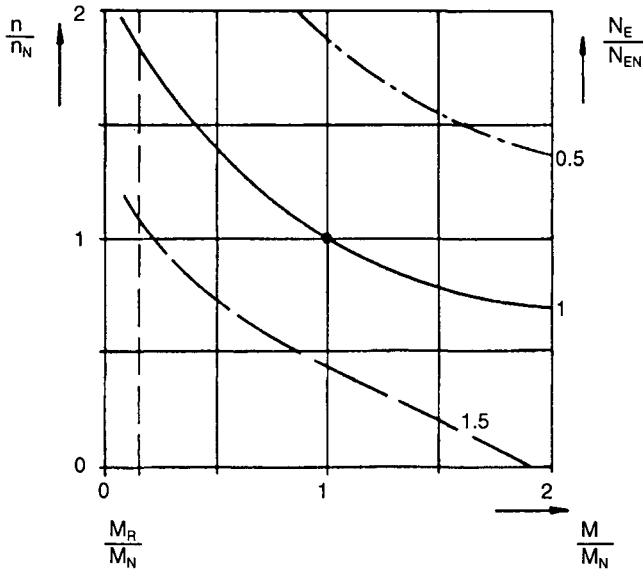


Figure 6.16 Speed changing by means of excitation flux variation

centrifuges. In other cases they are used in combination with mechanical reduction gears where high power together with low volume are demanded, such as in hand-held power tools, washing machines and household appliances. Not only do they have the advantage of small volume, owing to their high speed, but also of speed variation capability over a wide range and relatively high starting torque. Small direct voltage series motors find application in motor vehicles as starter motors. Note: virtually all small motors in vehicles are now permanent-magnet DC motors. About 50% of starters use series fields.

The design of the motor is usually adapted to the drive application. An important consideration with universal motors is the in-service life and its relation to commutation. Brush wear limits the uninterrupted running time of any apparatus driven by a universal motor. Table 6.2 indicates the brush lifetime in certain kinds of apparatus. Depending on circumstances, the commutator demands a strict maintenance routine for a motor.

Table 6.2 Brush lifetimes

Apparatus	Brush lifetime in hours
Teleprinter	2000 – 3000
Vacuum cleaners, pumps	700 – 1500
Hand-held food mixers	250 – 500
Coffee mills	50 – 100

Chapter 7
Direct current motors

Helmut Moczala

7.1 Basic principles

All DC motors utilise the force that results from a current-carrying conductor being in a magnetic field. Figure 7.1 shows a conductor with 'active length' l in a magnetic field with flux density \mathbf{B} and current $I = \Theta$ flowing through it. The force on the conductor is

$$\mathbf{F}_i = \Theta \mathbf{l} \times \mathbf{B} \quad (7.1a)$$

The current has the direction of the vector \mathbf{l} . If the conductor is replaced by a coil with N turns, the MMF becomes $\Theta = IN$.

The scalar equation for the magnitude of the force F_i is:

$$F_i = \Theta l B \quad (7.1b)$$

when \mathbf{l} and \mathbf{B} are at right angles to each other.

When the coil moves with velocity v in the direction of the force, the voltage

$$U_q = vNB \quad (7.2)$$

is induced in it.

Assuming that the resistance R of the coil is zero so that there is no loss of power, the source voltage U must equal the induced voltage U_q . Thus the velocity v is determined from eqn. 7.2.

From eqn. 7.1b the current in the conductor depends only on the force F_i exerted by it.

The power delivered by the source is

$$P_r = UI = (vNB)I$$

Rearranging the factors and applying eqn. 7.1 gives

$$P_r = UI = (INB)v = F_i v = P_m \quad (7.3)$$

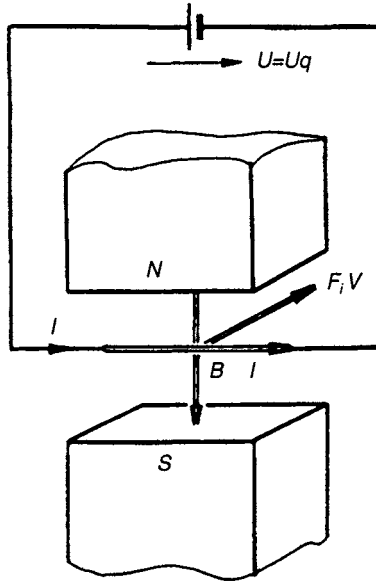


Figure 7.1 Force on a conductor in a magnetic field

The mechanical output power $P_m = F_i v$ from an ideal motor equals the power supplied from the source, and the efficiency is 100%. Of course, the efficiency is lower in practice because source voltage must exceed U_q by a voltage drop, and the ‘inner force’ F_i is not all available externally to the motor on account of unavoidable braking forces within the motor, such as friction.

7.2 Direct current linear motors without commutators

7.2.1 Operating performance

The current-carrying conductor in a magnetic field (Figure 7.1) is the mathematical model for the industrially produced linear motor of Figure 7.2b. This motor, comprising a moving coil 1, a permanent magnet 2 and a soft iron magnetic return path 3, could be regarded as a linear development of the familiar wide-angle moving coil meter (Figure 7.2).

Because of the braking force F_R in the motor, the available output force F is

$$F = F_i - F_R = INlB - F_R \tag{7.4}$$

F_R is mainly the friction between the moving coil and its track, but there are also other components such as hysteresis and eddy current losses.

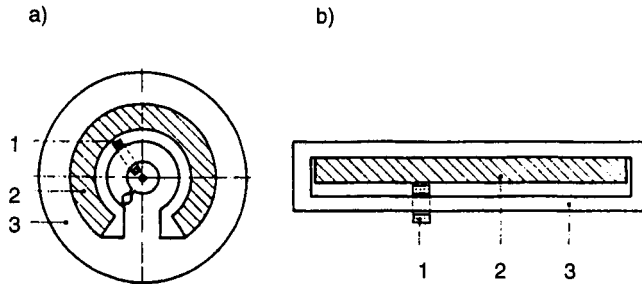


Figure 7.2 The familiar wide-angle moving coil meter (a) and the DC linear motor with moving coil (b)

Acceleration forces are, of course, not counted as part of F_R .
The function $I(F)$ is derived from

$$I = \frac{F_R + F}{NIB}$$

Under no-load static conditions ($F=0$), the no-load current is

$$I_0 = \frac{F_R}{NIB} \quad (7.5)$$

and so the working current I is

$$I = I_0 + \frac{F}{NIB} \quad (7.6)$$

Thus, the motor current increases linearly with the load force.

When the coil resistance is taken into account, the following relationship between the source voltage U and the motor parameters emerges:

$$U = U_q + IR = vNIB + IR \quad (7.7)$$

There is little point in deriving a constant velocity v from eqn. 7.7 because the linear motor is normally either stationary or accelerating. However, the starting force F_a when $v=0$ is interesting because it relates to acceleration. Starting current I_a is derived from

$$U = I_a R$$

It follows that

$$F_a = F_{in} - F_R = \frac{U}{R} NIB - F_R \quad (7.8)$$

7.2.2 Types of construction

The linear motor of Figure 7.2b has the disadvantage that the moving coil must have flexible supply leads. In comparison, Figure 7.3 shows a linear

motor with moving magnets (labelled 3). The coil is distributed along the soft-iron member 2.2 whilst the members 2.1 and 2.3 serve to provide return paths for the magnetic flux.

Eqns. 7.4–7.8 are applicable here for performance calculation provided N is understood to be the number of turns that lie within the influence of the permanent magnet airgap field.

This form of construction also has its disadvantages. In particular, the I^2R copper losses occur along the whole length of the winding, whereas only the turns between the magnets contribute to the force developed. The loss balance is therefore less favourable than in the moving coil linear motor. In addition, because of the large number of turns, saturation in the soft iron occurs for relatively low currents, and this leads to a loss of force around the middle of the motor. Eqn. 7.4 becomes invalid when saturation occurs. Finally, the sideways forces between the sliding magnets and the soft-iron members, resulting from a small off-centre misalignment, can become considerable and may not be disregarded. These forces demand a correspondingly robustly dimensioned track for the sliding magnet. Figure 7.4 shows another kind of linear motor which is characterised by moving permanent magnet 3 and two concentrated windings 1 and 2. The operation can be explained clearly in terms of forces of attraction and repulsion between the electromagnetic poles 11, 12, 21 and 22 of the stator and the permanent magnetic poles of the moving magnet 3.

Because here the coil windings are not directly in the permanent magnet field of the moving magnet, the equations used so far for force calculations –

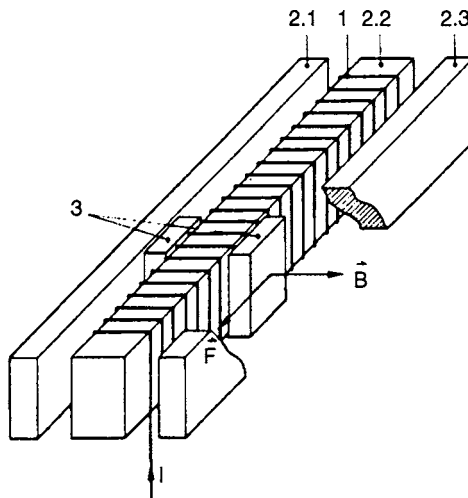


Figure 7.3 DC linear motor with two moving permanent magnets and a distributed stator winding

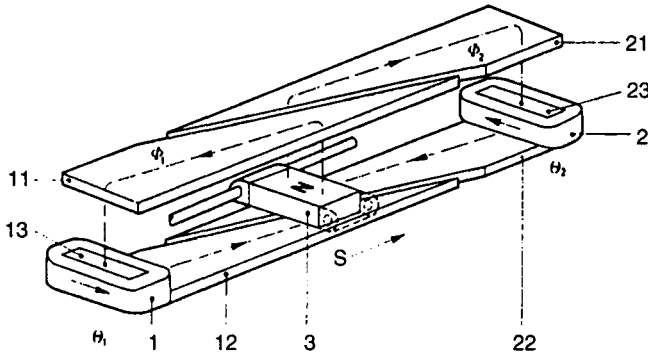


Figure 7.4 DC linear motor with moving permanent magnet and concentrated stator windings (poles 11 and 21 have been drawn vertically displaced)

1.1, for example – are not applicable here. A solution may be found, however, by application of the power-balance eqn. 7.3:

$$P_e = UI = F_i v = P_m$$

Transposing gives the ‘internal force’ F_i

$$F_i = \frac{UI}{v} \tag{7.9}$$

If U denotes the voltage across the two coils connected in series:

$$U = U_q = N \frac{d\phi_2}{dt} - N \frac{d\phi_1}{dt} \tag{7.10}$$

and substituting $v = ds/dt$, it follows that

$$F_i = \frac{\left(N \frac{d\phi_2}{dt} - N \frac{d\phi_1}{dt} \right) I}{\frac{ds}{dt}} = IN \left(\frac{d\phi_2}{dt} - \frac{d\phi_1}{ds} \right)$$

It is interesting to note that the force developed increases with the rate of change of coil flux with respect to magnet displacement.

The magnitudes of the coil fluxes ϕ_1 and ϕ_2 are dependent on A_1 and A_2 , the areas of pole surface covered by the armature magnet. Magnet movement in the direction of increasing s decreases the area A_1 facing poles 11 and 12 and increases the area A_2 facing poles 21 and 22.

Given that the airgap flux owing to the magnet is B ,

$$\phi_1 = BA_1 \quad \phi_2 = BA_2$$

The sum of areas A_1 and A_2 is (constant) A .

It follows that

$$F_i = IN \left(\frac{d}{ds} BA_2 - \frac{d}{ds} B(A - A_2) \right)$$

$$F_i = 2INB \frac{dA_2}{ds} \quad (7.11)$$

To obtain a force proportional to current for all magnet positions along its track, the pole contours must be such that dA_2/ds is independent of s , and remains constant. This condition may be met not only with tapered poles as drawn but also with stepped poles as shown in Figure 7.5, provided that the magnet length covers the length of the step.

7.3 Rotating direct current motors

Whilst DC linear motors are used only in modest numbers, rotary motors are produced in enormous numbers and find application in a wide range of situations.

7.3.1 *Principal construction*

The most usual construction (Figure 7.6) is characterised by the cylindrical rotor made up of iron stampings in whose slots winding 1 is seen. The stator is nearly always a pair of permanent magnets 3.1 and 3.2 for providing the field. Casing 4 has, amongst other things, the function of providing the magnetic return path.

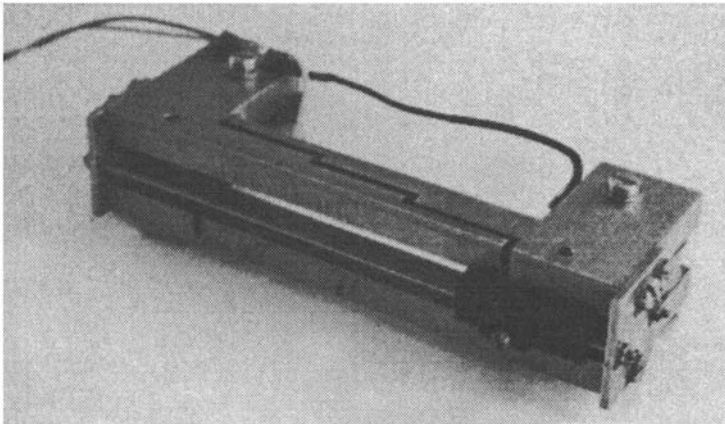


Figure 7.5 DC linear motor with permanent magnet concentrated stator windings and stepped poles

Armature force = 0.7 N

So that the conductors of the turning rotor always carry current in the proper direction for developing the torque, the commutator which turns with the rotor and the brushes 5.1 and 5.2 are needed for current reversal. The build-up of the winding as well as its connections to the commutators is shown clearly in Figure 7.7.

The armatures are machine wound, two coils being put on at the same time. The welded, soldered or crimped connections to the commutator bars are also made automatically during the winding process. This so-called H-winding gives good rotor dynamic balance. Figure 7.8 gives a good view of the motor construction.

7.3.2 Operating performance

Even when the individual coils lie in the rotor slots and not specifically in a field with airgap flux density B , the force calculations are in accordance with

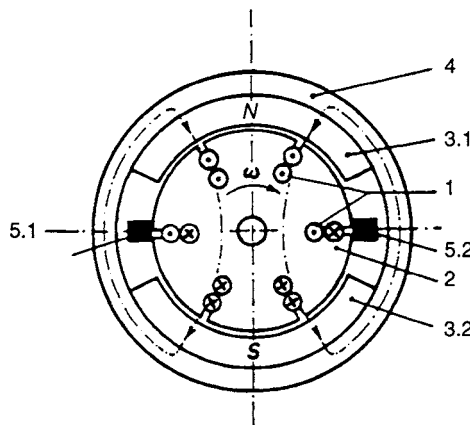


Figure 7.6 Principal construction of a DC motor with iron rotor and permanent magnet segments (cross-section)

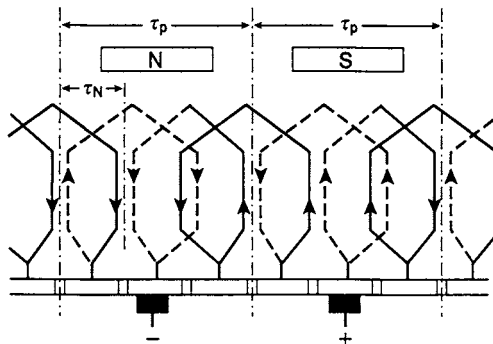


Figure 7.7 Winding and commutator of the DC motor of Figure 7.6 (developed view)

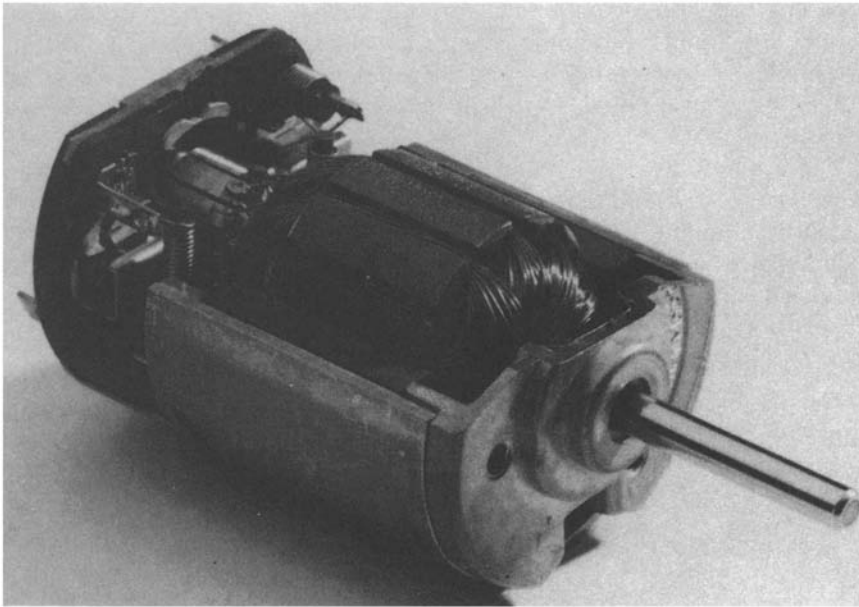


Figure 7.8 *Cut-open DC motor with cylindrical iron rotor (25 W, 4000 rev/min)*
(Courtesy: Bühler)

eqn. 7.1*b*. To calculate the ‘inner torque’ M_i of the motor, the torque components rF_N of the individual winding elements are added over the total number of slots z :

$$M_i = \sum_z rF_N \quad (7.12)$$

Because there are two parallel paths through the armature winding for the current I , the current flowing through each N_N turn winding is $I/2$ and the MMF is

$$\theta_N = \frac{I}{2} N_N \quad (7.13)$$

Applying eqn. 7.1*b* gives the torque M_i :

$$M_i = \sum_z r \frac{I}{2} N_N l B$$

Introducing the slot-pitch τ_N and rearranging gives

$$M_i = \frac{rIN_N}{2\tau_N} \sum_z l B \tau_N$$

Given an armature length l , the product $lB\tau_N$ represents the magnetic flux which enters and leaves one rotor slot, and it follows that

$$\sum_z lB\tau_N = 2\phi$$

Here, ϕ is the flux from the stator magnet that enters the rotor on one side and leaves from the other. The incoming and outgoing flux, together with their corresponding rotor MMFs, contribute equal parts to the total torque M_i .

It follows, therefore, that

$$M_i = I \frac{rN_N}{\tau_N} \phi \quad (7.14)$$

$$\text{Let } k = \frac{rN_N}{\tau_N}, \quad (7.15)$$

a motor constant, so that

$$M_i = Ik\phi \quad (7.16)$$

Given friction torque M_R within the motor, the torque available at the output shaft is

$$M = M_i - M_R = Ik\phi - M_R \quad (7.17)$$

When the load torque is M , the motor current I is

$$I = M_R \frac{1}{k\phi} + M \frac{1}{k\phi}$$

Off-load ($M = 0$) gives the no-load current:

$$I_0 = M_R \frac{1}{k\phi} \quad (7.18)$$

so that the simple form for the equation for motor current is

$$I = I_0 + M \frac{1}{k\phi} \quad (7.19)$$

Therefore, the motor current I increases linearly with the load torque M .

The induced voltage U_q measurable at the brushes of an externally driven unloaded motor can be derived from summing the components induced in the conductors in each slot. Eqn. 7.2 is applicable for the component voltage

$$U_{qN} = vN_N lB \quad (7.20)$$

Because of the parallel armature conducting paths, the summation takes place over one half of the slots

$$U_q = \sum_{z/2} r\omega N_N lB \quad (7.21)$$

The conductor speed v is calculated from the rotor angular velocity ω from the formula $v = r\omega$. Introducing the slot pitch τ_N and rearranging gives

$$U_q = \frac{r\omega N_N}{\tau_N} \sum_{z/2} lB\tau_N$$

For reasons already given,

$$\sum_{z/2} lB\tau_N = \phi$$

It follows that

$$U_q = \omega \frac{rN_N}{\tau_N} \phi = \omega k\phi \quad (7.22)$$

Taking armature resistance (R), voltage drop and brush contact drop (U_B) into consideration, the motor terminal voltage U becomes:

$$U = U_q + IR + U_B \quad (7.23)$$

Making substitutions from eqns. 7.22 and 7.19 gives

$$U = \omega k\phi + \left(I_0 + M \frac{1}{k\phi} \right) R + U_B$$

Rearranging, to make ω the subject, gives

$$\omega = \frac{U - U_B - \left(I_0 + M \frac{1}{k\phi} \right) R}{k\phi}$$

At no load ($M = 0$), the angular velocity ω_0 is

$$\omega_0 = \frac{U - U_B - I_0 R}{k\phi} \quad (7.24)$$

and the expression for ω becomes

$$\omega = \omega_0 - M \frac{R}{k^2 \phi^2} \quad (7.25)$$

This equation may be simplified further by introducing the starting torque M_a when $\omega = 0$:

$$0 = \omega_0 - M_a \frac{R}{k^2 \phi^2}$$

$$M_a = \omega_0 \frac{k^2 \phi^2}{R} = \left(\frac{U - U_B}{R} - I_0 \right) k\phi \quad (7.26)$$

from which eqn. 7.25 becomes

$$\omega = \omega_0 \left(1 - \frac{M}{M_a} \right) \quad (7.27)$$

The angular velocity falls linearly from ω_0 , when $M = 0$, as the load torque increases.

Figure 7.9 shows the characteristics $I(M)$ and $\omega(M)$, which correspond to eqns. 7.19 and 7.27, respectively. Extrapolation of the characteristics produces the point at which the armature current is zero and the friction torque M_R may be read off the M axis. The angular velocity extrapolates to ω_0^* at which the induced voltage U_q equals the supplied voltage U and at zero internal torque with zero armature current.

7.3.3 Armature reaction

The magnetic field in a DC motor is determined not only by the permanent magnets but also by the armature current. Figure 7.10 depicts the component fields owing to the permanent magnets (curve B) and to the armature current (B_A). Whilst the B -distribution depends on the permanent magnet material and the geometry of the magnetic circuit and may therefore be looked on as constant, the B_A field magnitude is proportional to the motor current. The triangular spatial distribution is derived on the presumption that the permanent magnet material has a μ_r of unity, and behaves as does air in the face of armature MMF. It follows that the armature current derived crossfield – it is displaced spatially from the permanent magnet field by 90° – plays a less significant role than would an electrically excited field in soft iron poles.

The resulting magnetic field B_p , the sum of the main field B and the armature crossfield B_A is characterised by two facts:

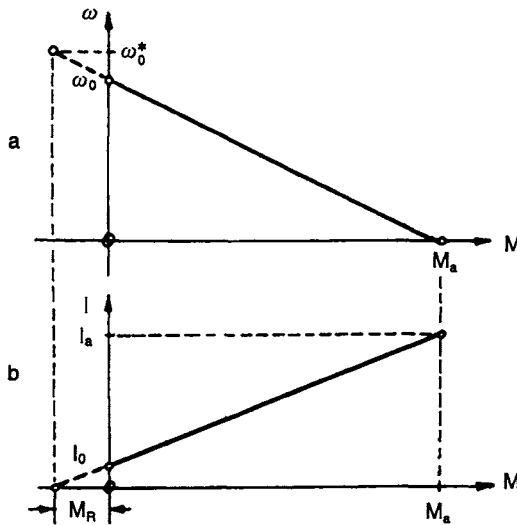


Figure 7.9 Characteristics of a DC motor
 a Angular velocity ω as a function of load torque M
 b Motor current I as a function of load torque M

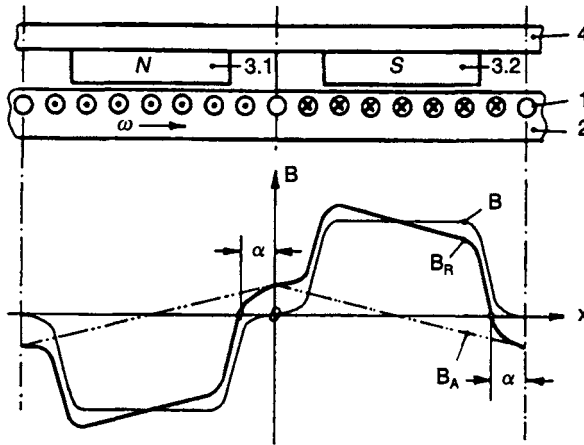


Figure 7.10 Magnetic field in the airgap of a DC motor (developed view)
 $B(x)$: field owing to the permanent magnets
 $B_A(x)$: field owing to the armature current
 $B_R(x)$: resultant magnetic field

- The neutral zone, which is characterised by $B_R = 0$, is displaced by an angle α relative to the permanent magnet axis and in the counter-rotation sense. This load-dependent displacement is discussed again in Section 7.3.4.
- The armature MMF causes demagnetisation along the trailing pole edges. High armature MMFs can cause permanent changes in the permanent magnet characteristics.

When permanent magnet materials with low coercive force are chosen, particular attention must be paid to starting conditions, especially when the motor is supplied with voltage in excess of the rated value. When a motor is reversed by means of reversing the supply voltage, it is good practice to bring the motor to a stop before reversing the supply voltage. Otherwise there is a strong possibility that the supply voltage and U_q are momentarily assisting, and a current equal to twice the normal starting current will flow.

7.3.4 Commutation

Commutation problems are less severe in DC motors than in universal motors because in DC motors there are no transformer effects involved.

Only two factors determine the voltage in the commutated winding:

- the voltage that is induced in the stray inductance of the coil by the current changing from $+I/2$ to $-I/2$, and

- the change of voltage that is induced by rotation because the commutating coil is not always in the neutral position. The situation of the commutating coil is determined by the brush position; the neutral zone changes position according to the armature current.

In low power DC motors, these voltage components do not have such an influence on the commutating that the recognised countermeasures – such as interpoles or brush shift – become necessary. Brush shift is fully effective, at only one working point and for one sense of rotation, in cancelling the two voltage components.

However, the mechanical criteria for good commutation should be sought after, including commutator irregularity of only a few μm and minimum play and vibration in the brush holders.

7.3.5 Speed control

From eqns. 7.24 and 7.25 the equation for the speed n of the motor is

$$\omega = 2\pi n = \frac{U - U_B - I_0 R}{k\phi} - M \frac{R}{k^2 \phi^2} \quad (7.28)$$

For a given load torque M there are two possibilities for adjusting the speed, namely:

- variation of the supply voltage U
- connecting a resistor R_{zu} in series with the motor.

Both methods have the effect of changing $U_q = \omega k \phi$. The implications of the methods are seen from Figs. 7.11 and 7.12. In Figure 7.11 the characteristics are displaced vertically but the gradients remain equal. The angular velocity ω_0^* at which the internal torque is zero is proportional to the supply voltage U , provided $U_B \ll U$. The subscript N denotes the rated value.

If the supply voltage must remain constant, $U = U_N$, the series resistance in the armature circuit changes the gradient of the characteristic (Figure 7.12). For a given load torque M , the reduction in angular velocity below ω_{0N}^* is proportional to the total armature circuit resistance ($R + R_{zu}$).

The ways in which electronic switching may control speed are discussed in Chapter 8.

7.3.6 Rotating direct current motor designs

The discussion so far has been around the standard form of rotating DC motor as depicted in Figs. 7.6 and 7.8. Next in this Chapter, variations on the standard design are discussed and finally other design concepts.

7.3.6.1 Motors with standard forms of construction

The characteristics of the standard design are the inner wound rotor

assembled from iron stampings, and the outer stator, the airgap flux between them normally being derived from permanent magnets. Possible variations are the number of rotor slots, the commutation arrangements, the permanent magnet layout and the number of pole-pairs.

Figure 7.13 depicts a particularly simple construction with only three slots – the so-called triple-T armature motor. Of particular interest is the 2-pole ring magnet stator. A comparison between a 4-pole and a 2-pole DC motor with the same power output (Figure 7.14) weighs heavily in favour of the 4-pole motor from the viewpoint of size and material content.

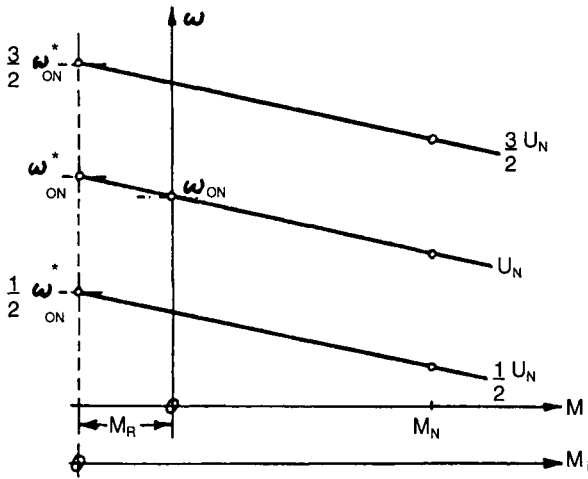


Figure 7.11 *Speed variation through changing the supply voltage U*
 U_N is the rated voltage

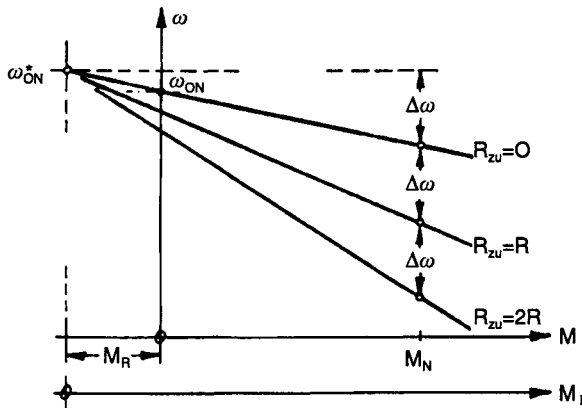


Figure 7.12 *Speed control through series resistance R_{zu} in the armature circuit*
 R = armature resistance

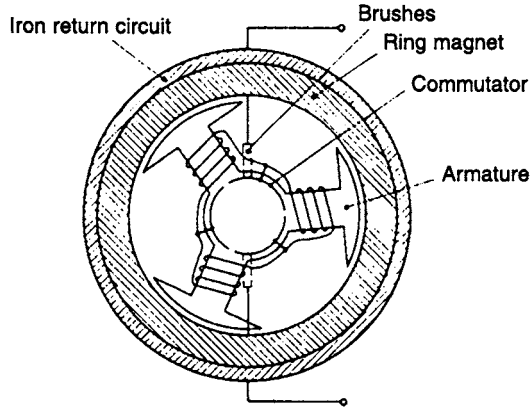


Figure 7.13 DC motor with triple-T armature and ring magnet

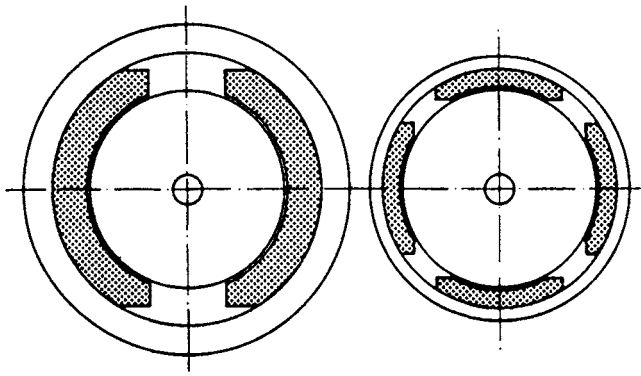


Figure 7.14 Sections of DC motors with the same power output, in 2-pole and 4-pole constructions

(Note: the fewer components and ease of manufacture of the 2-pole motor make it the preferred choice in small motors.)

7.3.6.2 Motors with flux concentration

The basic idea of these motors, for servosystems with high dynamic specifications, is the use of a small, low inertia long rotor which, owing to the high magnetic flux density in the airgap, is nevertheless capable of delivering a high torque output. In Figure 7.15 the magnetic circuit is shown in cross-section. The fluxes of two permanent magnets reach the rotor via each stator pole.

7.3.6.3 Motors with cup rotors

Compared with motors described so far, in which the slotted rotor iron assembly and its windings rotate together, motors having no iron in the rotors

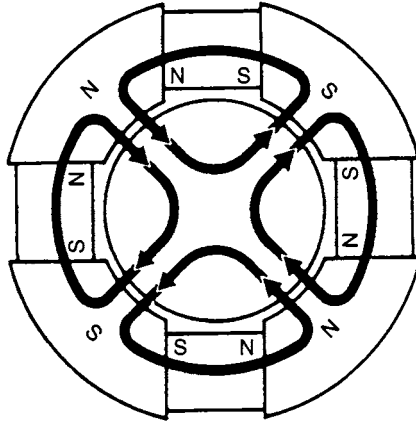


Figure 7.15 Concentration of the magnetic fluxes in a MINI-MINERTIA motor

display a number of advantages. In these, the armature windings, in disc or cup form, are self-supporting and rotate in the airgap of the stator magnet system.

In this kind of construction there is, of course, no iron loss, so that even at high angular velocity the loss torque M_R stays small. This implies that the efficiency can be high even when the load torque is small. Reluctance torques, resulting from interaction between the slotted iron rotor and the stator magnets in standard motor designs and which produce vibration torques, are also impossible. Finally, owing to the low winding inductances, the commutation problems are much smaller. Also, the low rotor moment of inertia is an advantage in mechanically demanding applications.

Figure 7.16 shows a longitudinal section through a motor with a cup rotor. In this motor the self-supporting skew winding (*c*) is of interest in that it possesses no winding overhang. In low power motors, multifinger, gold springs are used as brushes. Consequently the brush voltage drop U_b is practically zero.

In Figure 7.17 the construction of the skew armature winding can be seen. On account of the higher power, the commutation is conventional.

7.3.6.4 *Motors with disc rotors*

The disc rotor is an interesting variant of the iron-free rotor. The conductors are radial copper foil on each side of an insulating disc. (Note: printed circuit techniques are often used in low power motors, and stamped copper windings are used for higher powers.) Close to the shaft, the conductors become commutator segments. This makes possible a very large number of commutator segments. The torque is consequently extremely uniform and practically independent of the position of the rotor.

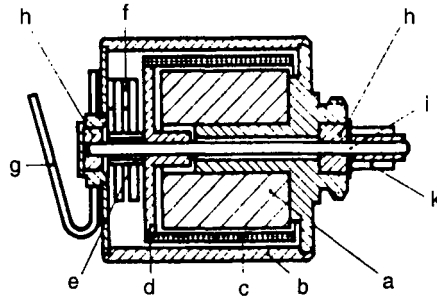


Figure 7.16 Section through a DC motor with cup armature
 a Permanent magnet; b iron return circuit; c rotor coil; d armature winding support plate; e commutator; f brushes; g connections; h sintered bearing; i rotor shaft; k drive pinion



Figure 7.17 Opened DC motor with cup rotor (20 W, 5000 rev/min)
 (Courtesy: Faulhaber)

Whilst the arrangement of disc rotor 3 together with the axially orientated permanent magnet system 1 and the brushes 4 in the casing can be seen in Figure 7.18, Figure 7.19 conveys, amongst other things, an impression of the construction of the rotor disc.

In other designs, e.g. those with encapsulated coils and a cylindrical commutator, the disc rotor is gaining recognition.

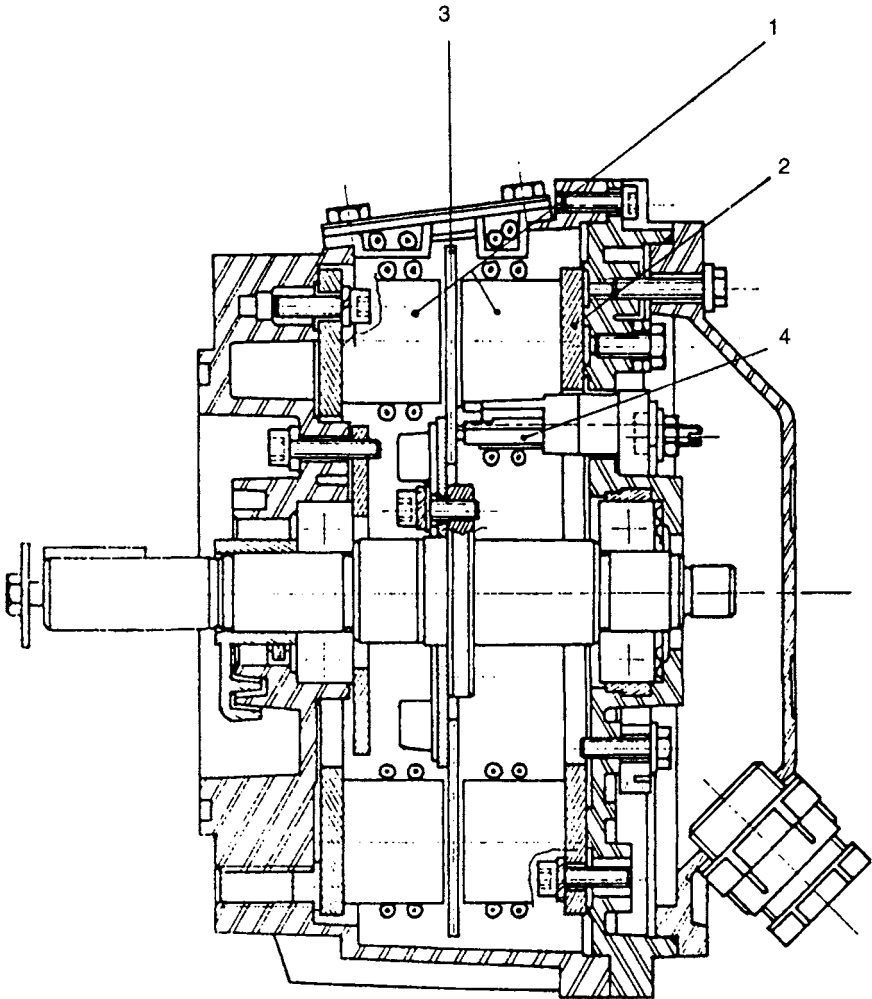
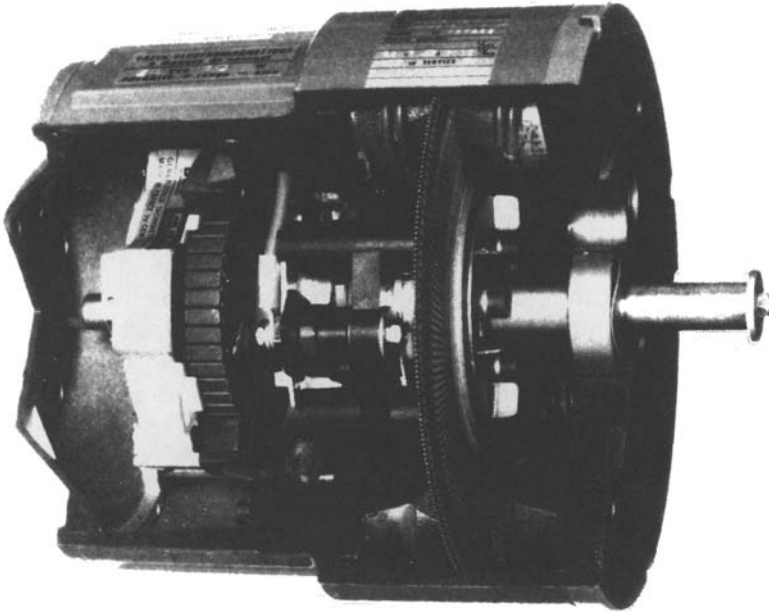


Figure 7.18 Section through a disc rotor motor
1 Multipole permanent magnet system
2 Iron flux return path
3 Disc rotor
4 Carbon brush



*Figure 7.19 Construction of a disc rotor motor with integrated tachometer (600 W, 3000 rev/min)
(Courtesy: BBC)*

7.4 Properties

The advantages of DC motors over rotating field motors are easily seen from the motor characteristics $\omega(M)$ and $I(M)$ (Figures 7.9 and 7.11):

- The motor current I increases linearly with load torque, so that a higher efficiency may be expected over the whole range of working.
- The motor has a higher starting torque M_a .
- The motor speed may be easily controlled by varying the supply voltage U .

A disadvantage compared with the rotating field motor is the limited brush lifetime. One thousand hours may be considered as typical. In certain special motors the brush lifetime is considerably more, but depends very much on the motor speed. In iron-free rotor motors and at speeds around 2000 rev/min the lifetime can be up to 10^4 h.

DC motors are made for a very wide power range. The nominal power of the smaller motors is of the order of 100 mW and, of the larger motors, several kW. Disc rotor motors with ratings up to 9 kW are available. In comparison, the power range of cup-rotor motors stops at about 100 W.

The speeds of DC motors are dependent on the supply voltage and the winding designs. Many motor types are listed with speeds around 3000 rev/min. The upper speed limit is around 20,000 rev/min.

The efficiencies of DC motors are high when compared with rotating field motors. Even the smaller motors can return an efficiency around 50% and the larger motors reach efficiencies of 80% and more. The efficiencies of iron-free rotor motors can be astonishingly high.

Any ripple in the motor torque is less than in single-phase rotating field motors. Iron-free rotor motors are particularly good in this respect because there are no reluctance torques that are associated with rotor teeth and slots. Uniformity of rotor torque depends heavily on the number of commutator bars. The triple-T armature is therefore not very good at all, whereas the disc rotor motor with its many commutator segments is hard to surpass.

7.5 Applications

DC motors are incorporated, of course, where direct voltage sources, e.g. in portable battery powered devices or in vehicles, are available. On account of their advantageous properties the range of application of the DC motor goes beyond these restricted boundaries.

When the supply is just AC, DC motors driven from controlled rectifiers are proving to be easier to manufacture and present fewer problems than universal motors. Drives with high dynamic response are generally provided with DC motors with series connected electronic switching for speed control or regulation. A series of special motors with power ratings up to 20 kW are available for these applications.

Many AC energised devices these days are fitted with semiconductor switching modules that require DC supplies. If motors are also necessary, DC motors are preferred because, for a given starting torque or power, they are smaller and lighter than rotating field motors and, because of their higher efficiency, do not cause as much heating in the device being driven.

Linear (performance characteristic) DC motors with iron-free rotors are particularly suitable for providing the torque and power input requirements of dynamic mechanisms. On account of there being no complicating iron losses there is a close linear relationship between torque and motor current over a wide range of torque, almost totally independent of speed, so that the torque requirement of the mechanism may be very accurately determined from the measured armature current and the motor characteristic $I(M)$.

Some hesitancy in installing DC linear motors is still very noticeable. This surely, is owing to the fact that linear motors must be connected directly to

their load devices without any intermediate gearing. To achieve the necessary forces and speeds, material usage is greater than with rotating motors and gearboxes. Commutatorless linear motors are beginning to be installed in x - y recorders and in sewing machines.

Chapter 8

Electronic circuits for small electric motors

Helmut Schock

8.1 Introduction

Controllable electrical drives are now almost without exception driven electronically. The continuing development of new components, as well as the steady reduction in the cost of electronics, gives the development engineer many possibilities for optimising his drive designs.

As well as reversibility of rotation and precise speed control, an electronic system offers the following facilities:

- protection against overload and overheating – the motor may therefore be smaller than would be dictated by unfavourable running conditions
- diagnosis and feedback in the control system. Sensors register mechanical and electrical parameters (e.g. a mechanically locked motor) and inform the processor.
- reduction of power losses through pulsed power delivery – conservation of energy is particularly important in battery powered equipment
- increased lifetime – achieved by replacing mechanical commutation with electronic switching (brushless DC motor – see Chapter 9). New motor types; the stepper motor is only useful in association with electronics.

The task of the electronics is control, regulation and driving of motors. A typical control system has the elements shown in Figure 8.1. In complex systems, the control is managed by a microcomputer. Given low motor powers, up to about 50 W, the controller and drive system can be one IC chip.

8.2 Active electronic components for driving motors

The electronic components for driving motors can be divided into three groups: diodes, thyristors and transistors.

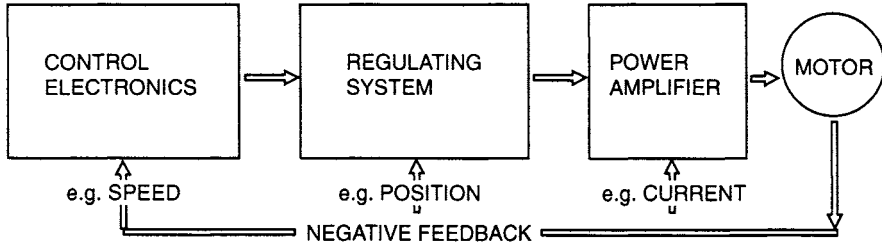


Figure 8.1 Control system

8.2.1 Diodes

Diodes are principally produced from silicon. They allow current to flow in one direction only. The voltage drop across a conducting diode is of the order of 0.7 V. Their main application is the rectification of alternating currents. In some applications, special diodes are brought into play, e.g. diodes with a low forward voltage drop (Schottky diodes) or fast switching diodes.

8.2.2 Thyristors

These components can work directly in AC circuits. Direct voltage thyristor circuits are expensive and complicated, and impractical in the small motor power range.

8.2.2.1 The thyristor

The thyristor is a controllable rectifier. It blocks current flow like a diode in both directions, but it can be switched on (fired) in one direction by means of a small external current driven through the control electrode (gate).

The conducting thyristor switches off (blocks current flow) only when current falls below the holding current level, at about 5–10% of the normal forward current as declared in the data sheets. In AC circuits this current cutoff occurs regularly as the alternating supply current passes through zero. In DC circuits, the thyristor current must be diverted through a parallel quenching circuit. The structure and characteristics of a thyristor are shown in Figure 8.2.

The thyristor may also be unintentionally fired by momentarily exceeding the anode to cathode breakdown voltage, or by too steep a rate of change of voltage. A remedy is to connect a series RC 'snubber' circuit branch in parallel with the thyristor. Thyristors are found in the highest power inverters. They switch voltages up to 6 kV and currents of some thousands of amperes.

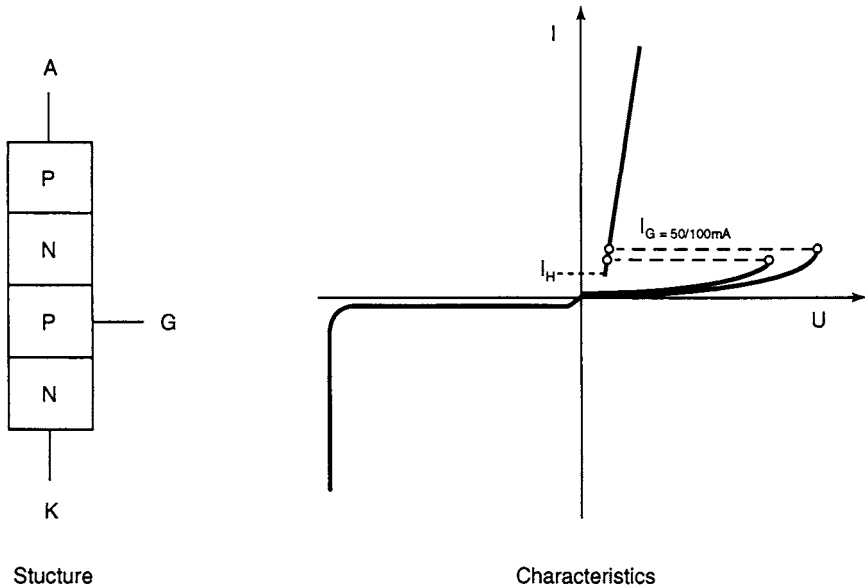


Figure 8.2 Structure and characteristics of the thyristor

8.2.2.2 GTO (gate turnoff thyristor)

These special thyristors for power electronics can be switched off via the control (gate) electrode. Because specified current gradients must be achieved and about 1/3 of the forward current must flow in the gate circuit, this kind of control is not too easy. GTOs are available with ratings of 500–4000 A and 4.5 kV breakdown voltage. Main applications are related to inverters for locomotives.

8.2.2.3 MCT (MOS controlled thyristor)

This is a new power switch, with input characteristics similar to MOSFET and thyristor output characteristics and is specified to work at around 50 A and 1500 V. The development, at the time of writing, is not completed. The main applications will be in inverters in the kW power range.

8.2.2.4 Triac, diac

Triac is short for 'triode for alternating current'. The triac comprises two antiparallel connected thyristors, with anodes A1 and A2 that are controlled from a common gate electrode. As Figure 8.3 indicates, the characteristics are extensively symmetrical. The triac can be triggered to pass current in either direction given an appropriately directed gate current. The necessary firing current depends on various circumstances.

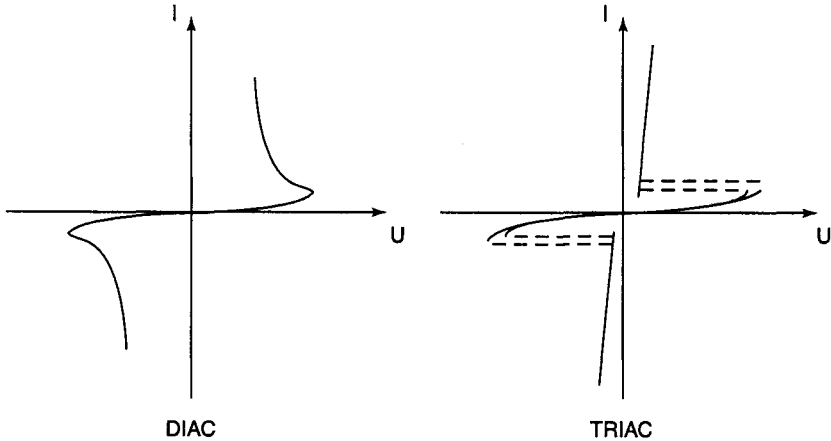


Figure 8.3 *Diac and triac characteristics*

Maximum currents and voltages switchable by triacs are appreciably less than for thyristors (~600–1000 V, 50 A). The triac is more susceptible to false firing owing to fast current and voltage transients. The use of an RC parallel snubber branch is always recommended.

Triacs find ready application as power controllers in consumer appliances with universal motors, because the number of circuit components is very small (vacuum cleaners, portable drills, etc.).

The diac has no control electrode. When the reverse breakdown voltage, about 20–40 V, is exceeded, the diode becomes instantly conducting. Diacs and unijunction transistors are used as cost-effective triggering components for triacs.

8.2.3 *Transistors*

8.2.3.1 *Bipolar transistors*

The bipolar transistor is a current controlled component. In power electronics, silicon transistors are used almost exclusively. The production spectrum ranges from small signal transistors in SMD (surface mounted device) packaging to power transistor modules with several transistors in one unit (1000 A/1700 V).

In the linear region, the collector current is proportional to the base current:

$$I_c \approx \beta I_b$$

The factor β lies between 10 and 100 for power transistors ($I_c > 1$ A) and can be as much as 800 for small signal transistors.

Figure 8.4 shows a typical set of characteristics for a bipolar transistor with the collector to emitter voltage V_{CE} as the horizontal axis and collector

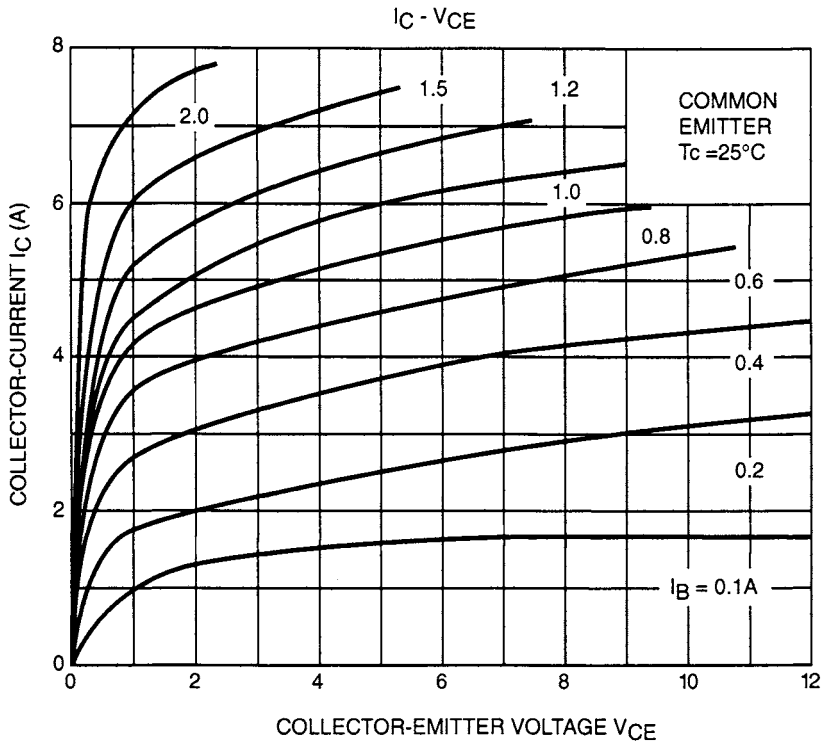


Figure 8.4 Characteristics of a transistor

current I_C as the vertical axis, each curve being for a given constant base current. The working region of the transistor is bounded by the maximum collector to emitter voltage $V_{CE\max}$, the maximum collector current $I_{C\max}$ and the maximum power dissipation. (Note: $V_{CE\max}$ and $I_{C\max}$ are not shown in Figure 8.4.)

In power electronics, the transistor is used principally as a switch. In this manner of working the load line exceeds the maximum power hyperbola when the working point switches between the cutoff and the conducting positions.

In the cutoff position only a very small current flows (a few μA). In the conducting position (when the base current is overdriven up to five times the necessary value) the collector to emitter saturation voltage is reduced to around 0.2–0.4 V. Overdrive reduces the switch-on time but increases the switch-off time.

Maximum values for collector current and voltage, with the switching time as parameter (the safe operating area) are given in the data sheets, and are shown in Figure 8.5. When inductive loads are being switched, the working point does not move along a straight line. During switch-on, the working point moves below the line connecting the starting and finishing points until

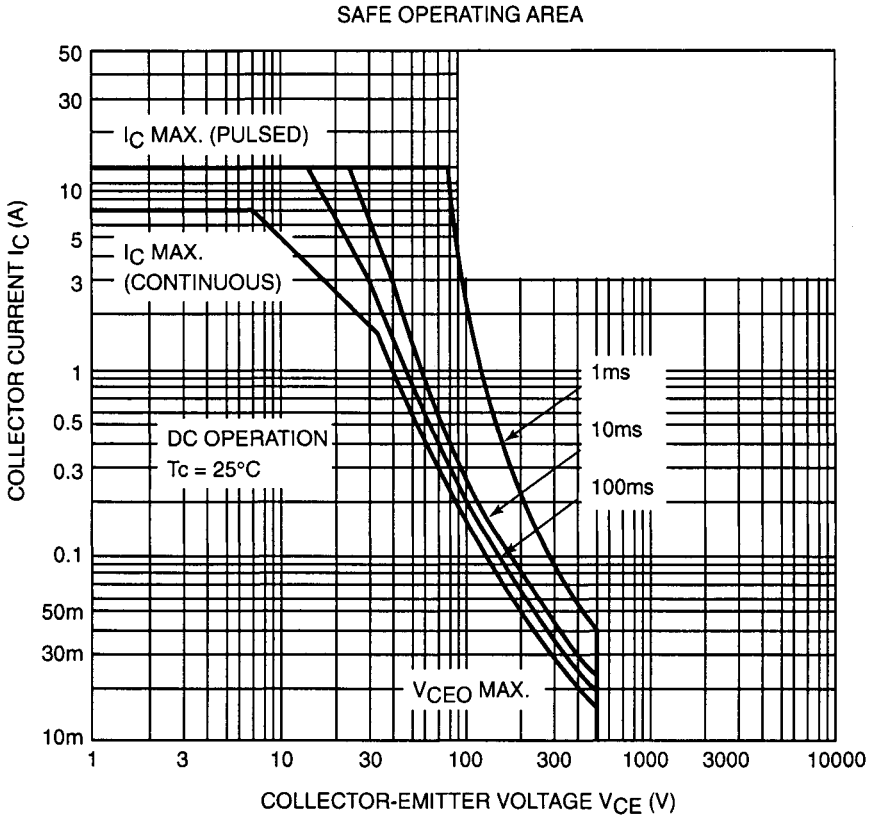


Figure 8.5 *Safe operating area*

the magnetic field builds up to its final value. During switch off, the induced voltage across the inductance can be very large, and this adds to the supply voltage. Therefore the use of a freewheel or bypass diode is absolutely necessary to protect the transistor from such high voltages (see Figure 8.6).

Switching losses during switch-on are relatively small compared with those in resistance load circuits. When inductive loads are switched off, collector current flows for a longer time, during which the collector voltage rises steeply and the losses are considerably greater.

The maximum switching frequency for power transistors with over 10 A collector current is about 10 kHz, at which low saturation voltage and high switching frequencies are mutually exclusive requirements.

8.2.3.2 *Unipolar (MOS) transistors*

In a field effect transistor the current between the source and drain electrodes is controlled by an electric field, a voltage. Depending on the type, only electron or hole current flow is involved. Amongst the various types

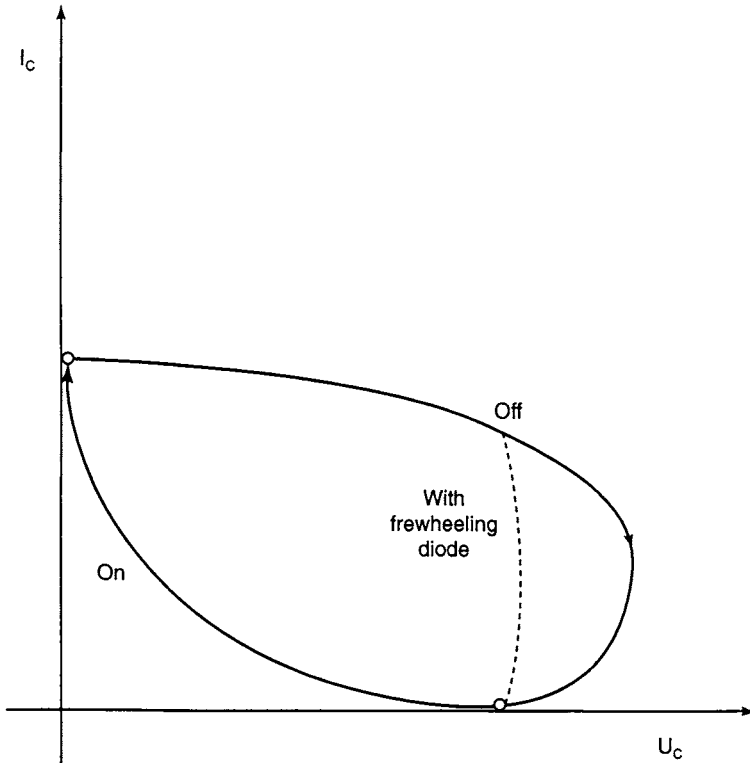


Figure 8.6 Switching inductive loads

available, the insulated layer FET, the MOSFET (metal oxide semiconductor FET) is preferred for power electronic applications in both n - and p -channel variants.

The features of the MOSFET are zero gate power, low switching time, simple parallel connection and low path resistances (bulk resistances). These are getting smaller from generation to generation through parallel connection of many individual transistors. The present state of the technology achieves up to 1.5 million transistors per square centimetre.

The maximum switching frequency is around 100 kHz and the bulk resistance for 60 V types is $\sim 5 \text{ m}\Omega$ and for 1000 V types $\sim 50 \text{ m}\Omega$. As the output characteristics of Figure 8.7 show, the MOSFET requires a gate to source voltage of over 5 V in order to switch, i.e. provide a low resistance path for drain – source current.

8.2.3.3 IGBT

The IGBT is a combination of a MOSFET input, giving a fast, simple and zero power input, and an output like that of a bipolar transistor, with low

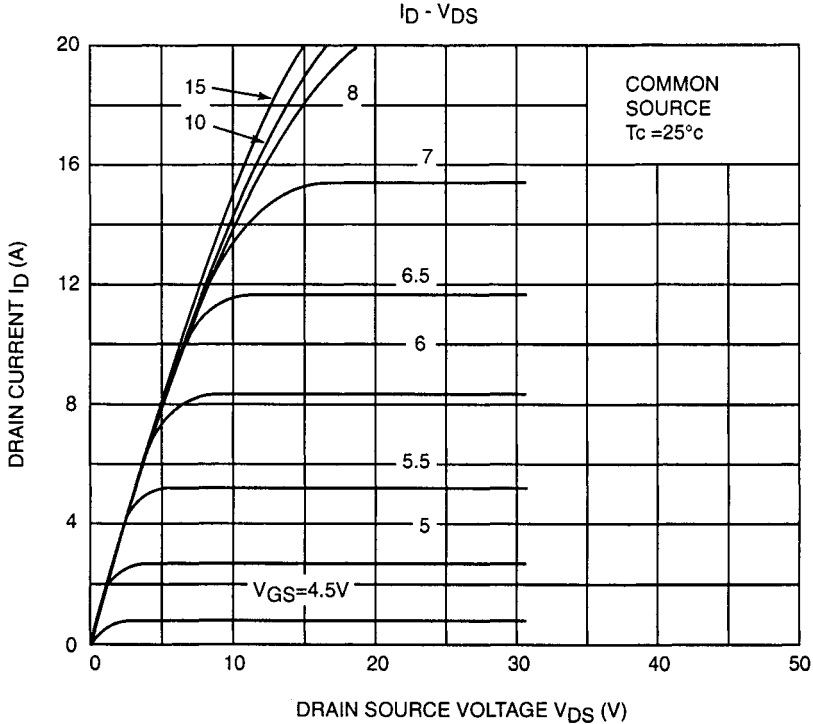


Figure 8.7 Output characteristics of a MOSFET

saturation voltage and a wide safe operating area. Through appropriate doping (ion implantation) it has been possible to raise the switching speed to 20 kHz.

Figure 8.8 shows the structure and equivalent circuit of an IGBT. It resembles the MOSFET with the exception of the p^+ doped substrate. In the conducting state supplementary charge carriers are injected through the substrate in the drain region of the MOSFET. Consequently the losses in the switched-on condition are reduced.

IGBTs are currently available for currents between 8 and 800 A and collector – emitter voltages between 600 and 1700 V. Compared with the MOSFET, the IGBT with the same power needs a smaller area of silicon and is therefore cheaper to manufacture.

Figure 8.9 shows an elegant form of an electrically isolated IGBT driver circuit. A special optocoupler, which can drive up to 500 mA, controls the IGBT directly. V_{CC} and V_{EE} are voltage sources around 12–15 V. When current flows through the LED, it illuminates the photodiode through a transparent plastic film with high potential isolation capability. This signal becomes amplified and controls the output stage. The isolation voltage of such an optocoupler lies around 5000 V.

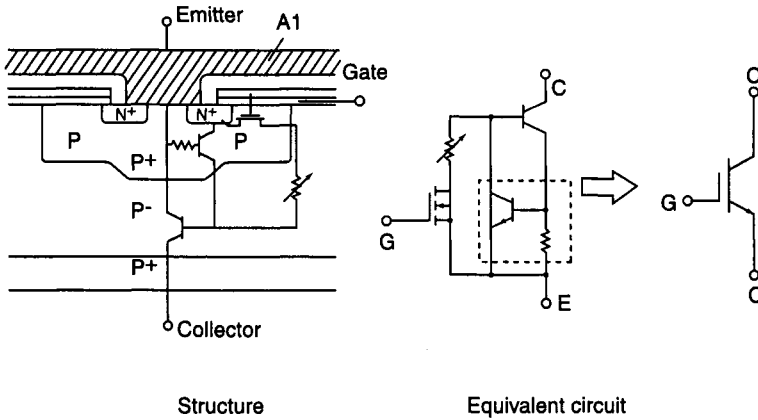


Figure 8.8 Structure and equivalent circuit of an IGBT

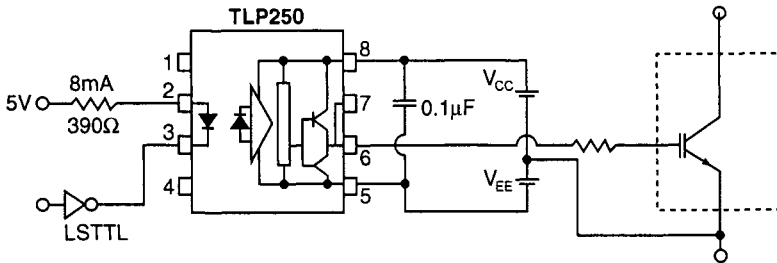


Figure 8.9 Driving an IGBT with an optocoupler
 Note: V_{CC} and V_{EE} must very often be electrically isolated from all other voltage sources in the system

8.2.4 Integrated circuits

We refer here to several active and passive components on one silicon chip and encapsulated into one package. Available integrated circuits include bipolar, MOS and mixed (bipolar + CMOS = BiCMOS) technologies. The wide range of off-the-shelf circuits for motor control may be divided roughly into control, regulation and power building blocks.

Microcomputers serve as control building blocks. Many modern types have special built-in functions specifically for motor control, for example a 3-phase generator. The control building blocks are specifically adapted to the motors to be controlled. Those for controlling brushless DC motors include preamplifiers for Hall sensors.

Integrated driver circuits can be installed directly as motor drivers in low voltage applications. Their operating range extends to around 40 V and 6 A. The catalogue of bridge circuit drivers and processors is very extensive. More

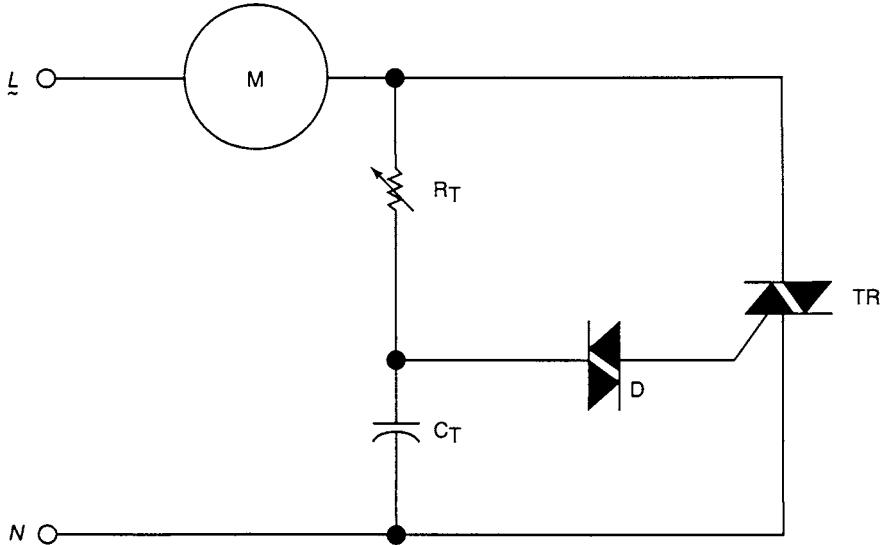


Figure 8.10 *Phase-shift control of a universal motor*

and more ‘intelligent’ chips are being developed and introduced – circuits that are protected against excess temperature, short-circuits and overload, and which report to a processor through the output terminals what the particular fault is.

8.3 Motor control

8.3.1 *Circuits with alternating voltage*

Phase-shift controlled firing with triacs has been the norm for a long time for medium power drives. Increasing demands for starting torque and constant speed have extended the use of transistors in firing control circuits. The most frequently used circuit is the controller for a universal motor using a triac, and has already been described fully in Section 6.4.2.

The circuit in Figure 8.10 is impressively simple with its minimal call on components, and finds application in domestic apparatus such as vacuum cleaners, portable drills, kitchen machines, etc. where the lowest prices come before all other considerations.

Three-phase motors are controlled with three triacs or antiparallel connected thyristor pairs (Figure 8.11). Exactly similar running characteristics are necessary in the three circuits to avoid the generation of direct voltage components, which would simply increase the losses. Special integrated firing circuits, e.g. TCA 780, ease this problem.

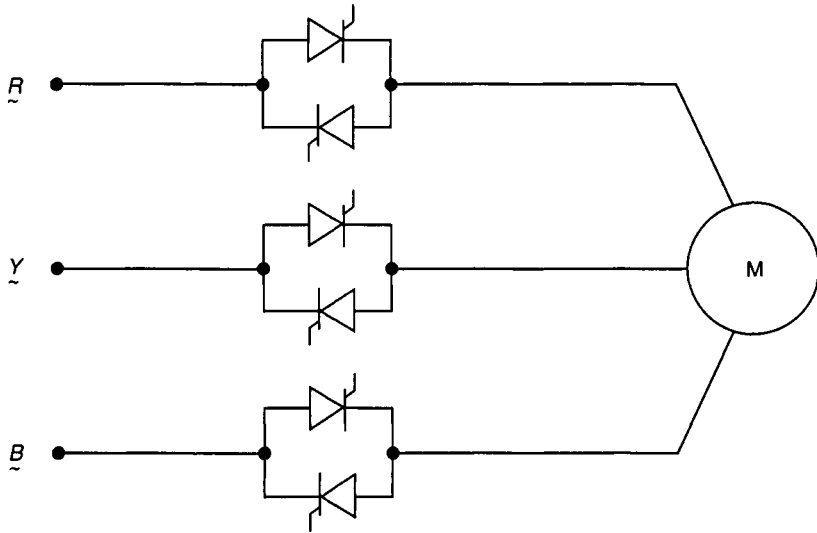


Figure 8.11 Phase-shift control of a 3-phase motor

8.3.2 Direct current circuits

DC energised circuits are gaining importance, because all types of motors can be controlled and regulated. Furthermore, faster, more easily driven, semiconductor switches – bipolar transistors, MOSFETs, IGBTs, etc. – may be utilised.

Linear circuits are used with small low voltage motors. Control is simple but there are higher losses in the driving circuit. Pulse power controllers are widespread. They improve the efficiency of battery-driven devices, and in mains-driven equipment there is less heat generated in the driving circuits.

1-quadrant control: In general, the torque–speed characteristics of a motor occupy four quadrants. Four-quadrant operation controls the motoring and braking characteristics in the clockwise and counter-clockwise senses. 1-quadrant control means that the motor rotates in one direction only, and only positive torque can be applied (braking comes only from the load).

In this case the motor is connected into the collector circuit of the transistor, as shown in Figure 8.12, and it rotates when the transistor is in the switched-on condition. When the transistor is switched off, any induced voltages resulting from motor reactance are clipped by the freewheel diode.

Direct current controller (chopper): If the speed in the above motor is to be changed, there are two possibilities:

- linear control of the motor current through transistor base current. The transistor collector – emitter voltage times the motor (transistor

collector) current causes severe heating in the transistor and energy loss from the supply

- pulse control. The transistor is switched on periodically. At the fully switched-on working point the power loss in the transistor is $U_{CE.SAT} \times I_M$. Whilst the transistor is switched off and absorbs practically no power, the freewheel diode diverts the motor current, which falls in an exponential manner (see Figure 8.13).

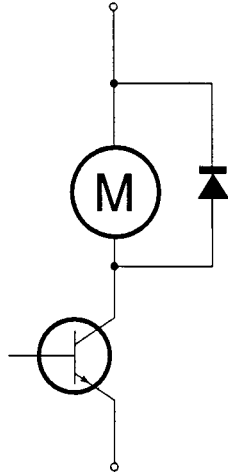


Figure 8.12 *1-quadrant drive for a DC motor*
The transistor forces acceleration. Braking comes from the load only

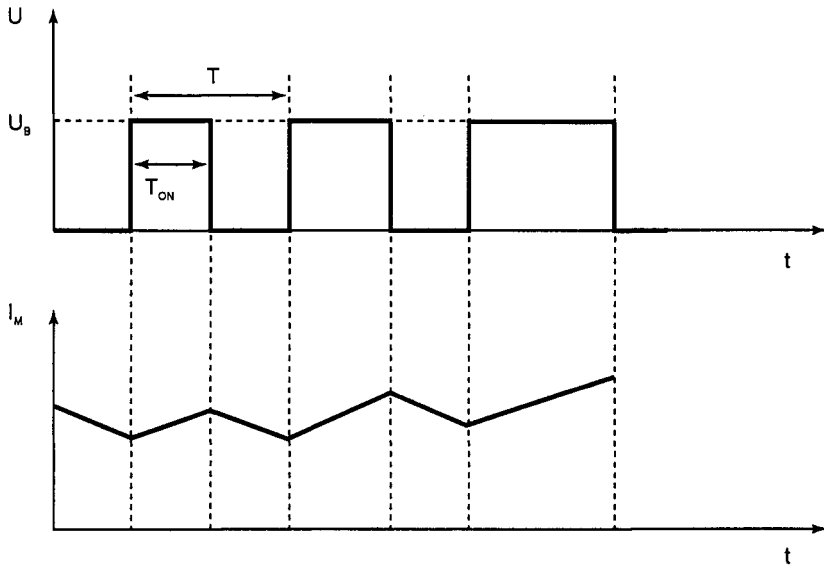


Figure 8.13 *Voltage and current relationships during chopping*

The average voltage applied to the motor, U_M , is

$$U_M = \frac{T_{ON}}{T} U_B$$

Variation of T_{ON} results in a proportional variation in U_M and hence control of motor speed over a wide range.

2-quadrant control: By extending the circuit of Figure 8.12 with a transistor in parallel with the motor, a 2-quadrant drive is achieved (Figure 8.14). When T_1 is cut off and T_2 is conducting, the motor is braked.

A simple method of selecting the direction of rotation of a small motor (< 10 W) is by using an operational amplifier with positive and negative supply voltages (Figure 8.15). These amplifiers are built to work at ± 30 V and can deliver up to 2 A current. Typical applications are video recorder and CD drives, in which the video cassettes and compact discs are electromechanically accepted and ejected.

4-quadrant drive: When a mirror image of the circuit of Figure 8.14 is added, the result is the so-called bridge circuit (Figure 8.16). By diagonal switching of transistors T_1/T_4 or, alternatively, T_3/T_2 , clockwise or counter-clockwise rotation is obtained.

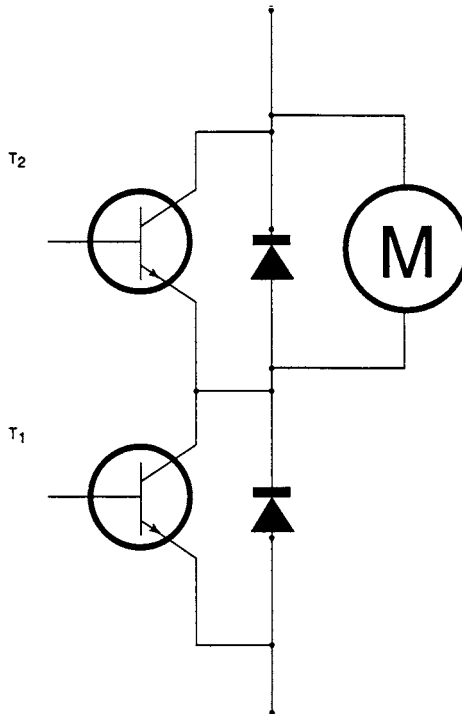


Figure 8.14 2-quadrant drive

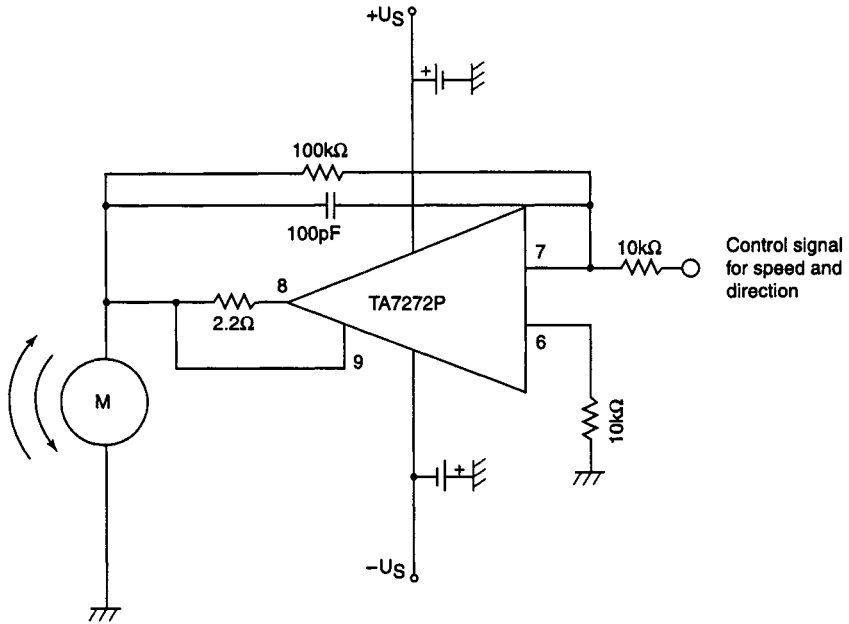


Figure 8.15 *Motor control using an operational amplifier*

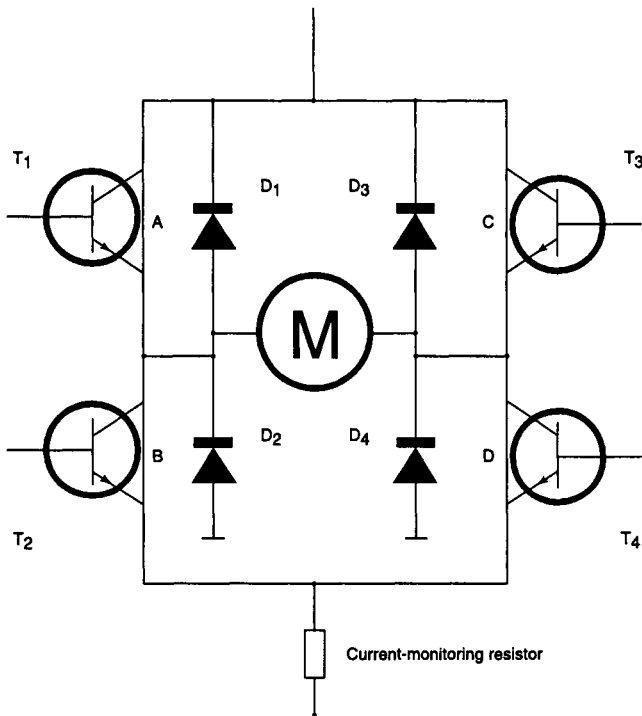


Figure 8.16 *4-quadrant drive bridge circuit*

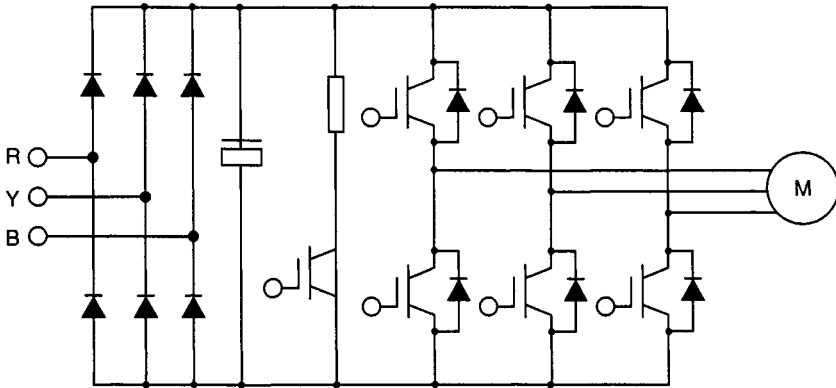


Figure 8.17 Speed controller for a 3-phase 4-quadrant motor drive

This circuit can also operate with pulse control, which may be applied to the upper pair, the lower pair or all four transistors. The freewheel diodes D_1 to D_4 ensure that whatever transistor or transistors get switched off, there is a path to carry the transient motor current. The power supply to the diode bridge must be capable, in the short term, of absorbing as well as delivering current.

3-phase controller in 4-quadrant mode: The speed of a synchronous or induction motor can be controlled over a wide range by varying the supply frequency. When a third column of two transistors is added to the circuit of Figure 8.16, the result is the circuit of Figure 8.17, which can deliver a variable frequency 3-phase supply to the motor.

Special modules are now available in all technologies (Bipolar, MOSFET, IGBT) which embody all six transistors and fast acting freewheel diodes in one block.

To avoid overloading the motors at low frequency, and to exploit the high frequencies, the supply voltage should increase in proportion to the frequency. Given a sinusoidally derived pulse width modulation gate supply chip, which produces low harmonic content sinusoidal motor current, this requirement can be met (Figure 8.18).

8.4 Examples

8.4.1 Control circuit for a bipolar two-winding stepper motor

TA8435H is an integrated circuit for driving a two-winding stepper motor. It includes a coding table for the generation of sinusoidal output currents that enable a microstep setting of the rotor. Furthermore, an oscillator for pulse width modulation, current limiting logic and two bridge circuits capable of

delivering 2 A output current each are built onto the chip. Figure 8.19 shows the block-schematic diagram. This component was developed for the purpose of driving the larger stepper motors in printers, photocopiers and scanners.

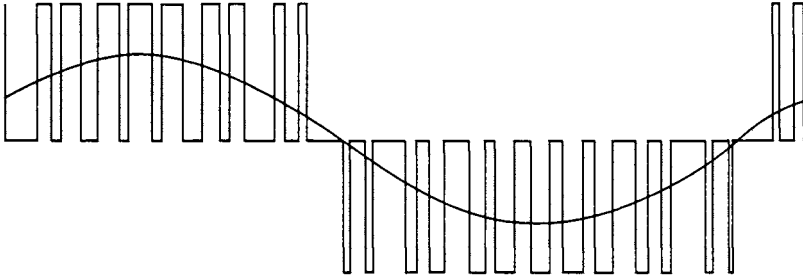


Figure 8.18 *Pulse width modulation waveform, containing a pure sinusoidal fundamental frequency*

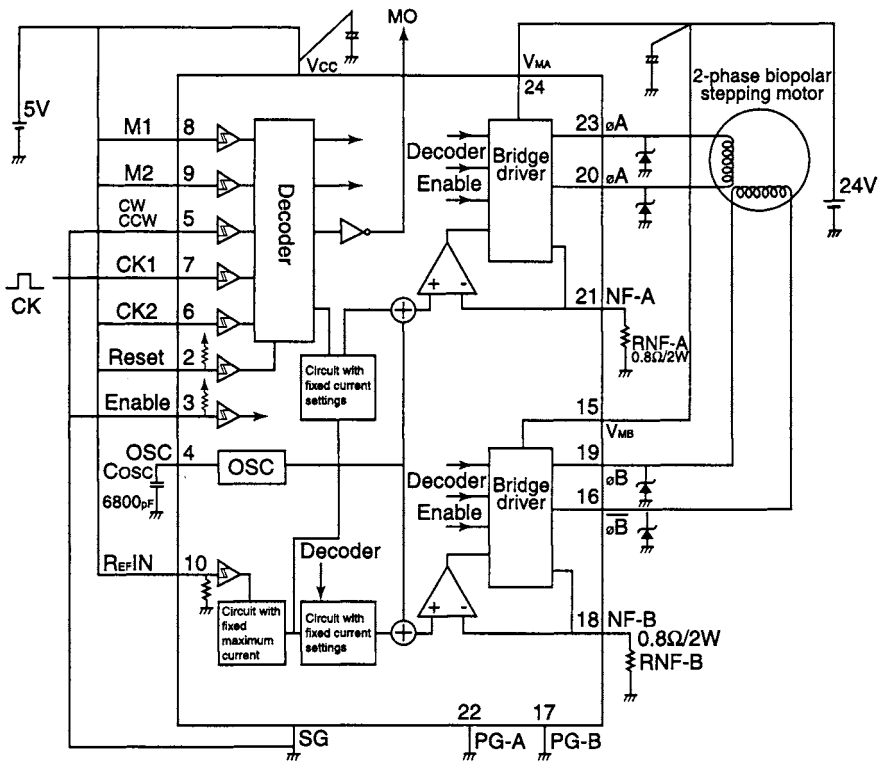


Figure 8.19 *Block-schematic diagram of the stepper motor chip TA8435H*

A microcomputer controller responds to input signals: Clock, Reset, Rotation (CW/CCW), and Enable. Inputs M1 and M2 determine the stepper action. When M1 and M2 are set at 5 V, the motor rotates with 32 steps per revolution; the synthesised sinusoidal currents are shown in Figure 8.20.

The output stages are constructed as bridge circuits. The maximum output current is 2 A. The emitters of the lower transistor pair in the bridge are connected to NF-A or NF-B. Output current monitoring resistors are provided so that the output current is limited to 2 A when the voltage drop across the resistor reaches about 0.7 V. The switching frequency can be changed to suit the motor by means of an external capacitor (C_{OSC}).

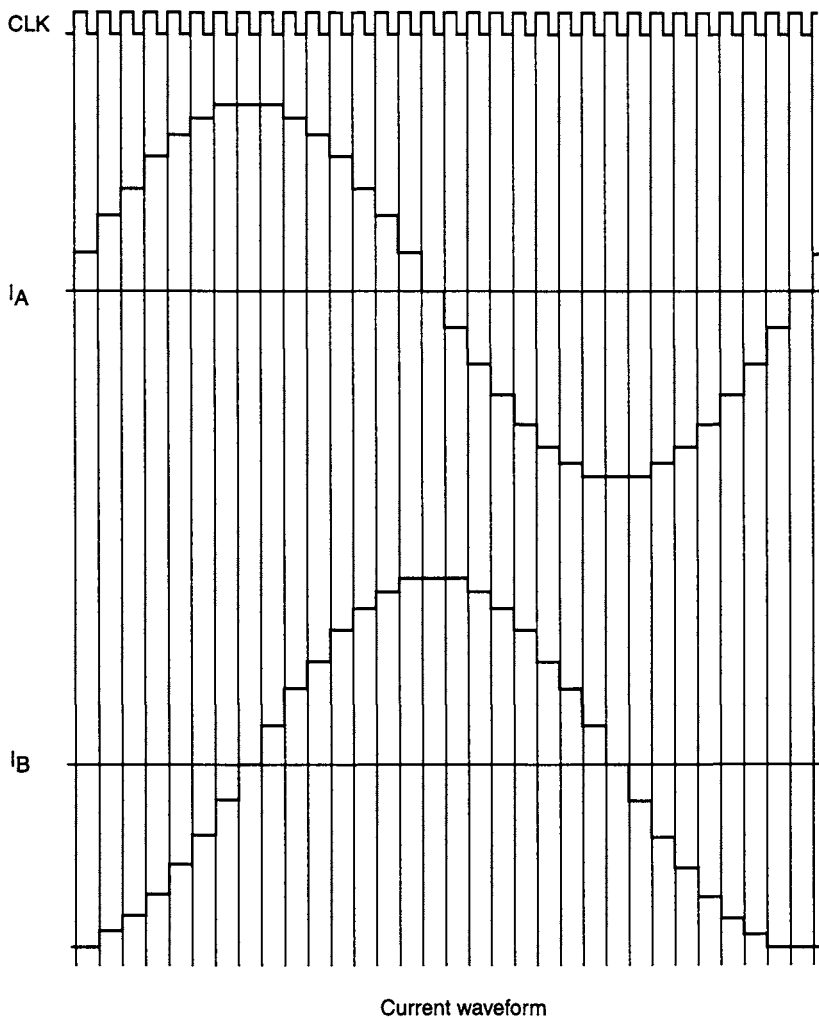


Figure 8.20 Output currents I_A and I_B of a microstep drive

8.4.2 Washing machine controller

In this instance, the conventional induction motor with capacitor was replaced with a brushless DC motor [5]. The block diagram of the motor controller is shown in Figure 8.21. The mains voltage is converted to direct voltage through a bridge rectifier. The 3-phase inverter comprised six transistors and six freewheel diodes in one integrated package.

The position and speed signals were taken from Hall sensors, amplified in the motor control chip and transferred to the microcomputer. This controlled the speed corresponding to the required programme, the type of wash and the weight of the load, which is proportional to the power transistor current. This current is monitored as the voltage across the common emitter resistance. In the case of overload, all transistors are cut off.

The lower transistors in the bridge circuit are switched directly and the upper transistors are controlled, at the same time, with pulse width modulation. The pulse width is determined by the microcomputer. The oscillator frequency is 16 kHz.

Switching each upper power transistor is achieved, as shown in Figure 8.22, by means of an isolated optocoupler. When current flows through LED D_1 , Tr_1 becomes conducting and about 40 mA flows into the base of the power transistor through R_{ex} . For as long as this current flows the capacitor C is charged over diodes D_2 , D_3 , D_4 . When no more current flows through the

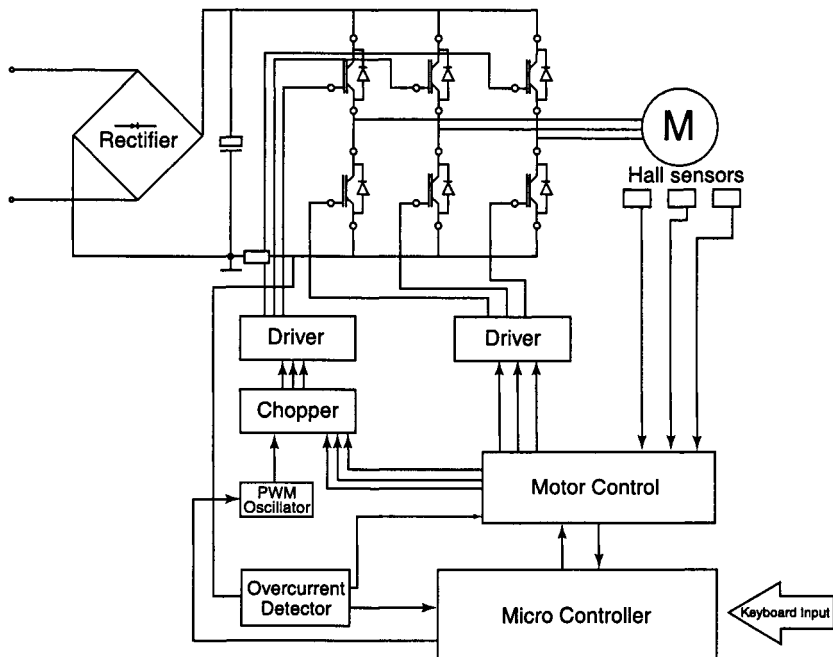


Figure 8.21 Block-schematic diagram of a washing machine controller

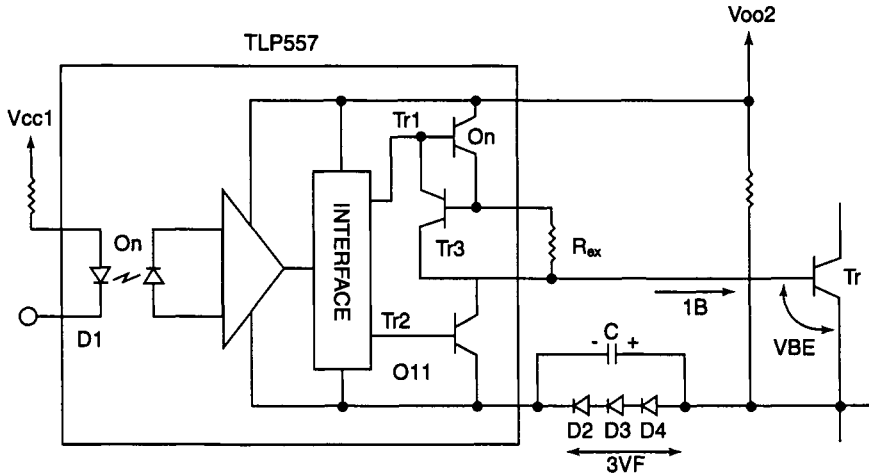


Figure 8.22 Power transistor driving circuit

LED, transistor Tr_2 conducts and the capacitor discharges over the base of the power transistor. The negative voltage between base and emitter shortens the switching time.

Compared with a similar machine model with a conventional motor, the motor power requirement decreases from 385 W to 290 W. Owing to a steady run-up for spinning, the new washing machine is quieter than the conventional model.

Chapter 9
Brushless direct current motors

Helmut Moczala

The classical DC motor, described in Chapter 7, is characterised by its mechanical commutation, comprising a rotating commutator and fixed brushes. The shortcomings of this system are:

- limited lifetime (around 10^3 h)
- unreliable contact, especially at low voltages
- electrical interference, and
- additional noise.

These disadvantages, in comparison to induction motors, led to the development of brushless DC motors, which combine the positive properties of DC motors together with the robustness of induction motors.

9.1 Technical solutions for brushless direct current motors

Solutions to the problem of driving a motor from a direct voltage supply without brushes are:

- combination of induction motor and constant frequency inverter
- combination of synchronous motor and constant frequency inverter
- an in-built electronic commutator in place of the conventional mechanical commutator.

In the power range up to 10 W, the first solution is excluded on account of the low efficiency of the induction motor. With constant inverter output frequency the motor speed is almost constant, but the starting torque is small compared with the classical DC motor. In the higher power range, the combination of inverter with induction motor is generally satisfactory.

Combining the synchronous motor and inverter results in higher efficiencies under certain working conditions, but the start and run-up

present special problems. Also, running is rough on account of the synchronous motor's tendency towards oscillation.

The expedient solution is therefore the substitution of the mechanical commutator with an electronic commutator whilst preserving the principles of the DC motor. This 'electronic commutator' must switch in the coils that develop the torque (and which have a fixed spatial distribution) by electronic means at the instants that the rotor is in the right position relative to those coils.

Motors which act in this manner have been described and named variously:

- brushless DC motors
- electronically commutated DC motors or DC motors with electronic commutation, and
- electronic motors.

This last description is the property of certain manufacturers and has more the character of a trade name.

The names 'commutatorless DC motors' and '3-phase synchronous motors', used particularly to name three-winding brushless DC motors, refer only to pure motors and are not concerned with the necessary commutating circuitry. These descriptions give rise to misunderstandings and should be treated with some reservation.

9.2 Principal construction and behaviour

Immediately after the arrival of the 'transistor', proposals sprang up for brushless DC motors. Figure 9.1 shows a particularly simple example. The rotating permanent magnet (2) induces an alternating voltage in the pick-up coil (4), which switches on the transistor during the positive half-cycles (base to emitter). The collector current in stator coil (1) together with the permanent magnet rotor develops a pulsating torque. Ignoring special applications, such as clock-chiming drives, this motor with a single phase stator winding is not particularly useful as it has to be set in motion by external mechanical means.

Therefore, in later developments, there were at least three spatially distributed sequentially energised stator coil windings, giving three-phase operation which ensured that there was some torque in all the rotor positions. On account of the cost of the electronic circuits the number of windings is generally limited to 3–6. The principal parts of the first brushless DC motor that was installed in numerous audio players are shown in Figure 9.2.

The three-phase stator winding comprises the minimum number of three coils spatially distributed at 120° relative to each other, 1, 2 and 3, which act on the 2-pole permanent magnet rotor 4. The control of transistors 5, 6

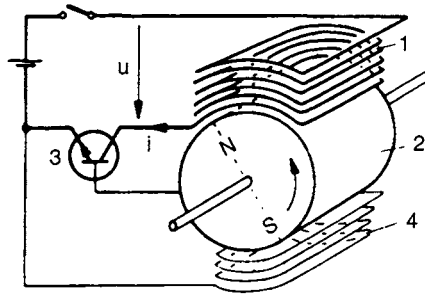


Figure 9.1 Brushless DC motor with a single phase stator winding

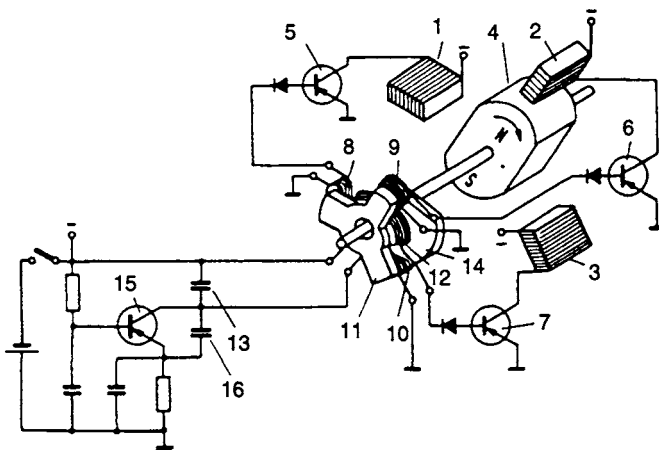


Figure 9.2 Brushless DC motor with auxiliary frequency transformer as position indicator

and 7 that connect the stator coils to the supply must, as in the classical DC motor, depend only on the rotor position and be independent of rotor speed if the motor is to be reliably self-starting.

The necessary stimuli for starting the motor are derived from the special auxiliary frequency transformer, which comprises the fixed core (11), the rotating segment (14), the primary coil (12) and the pick-up coils (8, 9 and 10).

The rotating segment (14), which is integral with the rotor, completes a transformer between the primary coil and each of the pick-up coils in turn. The alternating flux has a frequency of about 100 kHz. Transistor (15) provides the gain necessary for oscillation, the positive feedback component being capacitor (16) connected between its collector and emitter. With the rotating segment 14 in the position shown in Figure 9.2, coil (10) becomes

the main secondary winding of the transformer and transistor (7) becomes saturated on the negative half-cycles of this secondary winding voltage. Transistor (7)'s collector current energises coil (3), which then attracts the N-pole of the permanent magnet rotor.

Induction in coils (8) and (9) is much weaker and, therefore, when the rotating segment (14) is in the position shown, transistors (5) and (6) do not draw significant base currents. The magnitudes of the voltages induced in the secondary coils (8, 9 and 10) are entirely a function of the rotor position – segment 14 – and independent of the rotor speed.

Thus, there are no problems with starting and run-up.

The practical realisation of this motor (Figure 9.3) is characterised by the external cup rotor with the 2-pole ferrite magnet (4) and the inner stator with its three-phase winding lying in six slots; each phase winding comprises two component coils.

The similarity between brushless and conventional DC motors is apparent; except that the windings are spatially fixed and the field magnet rotates.

The fundamental equations of brushless DC motors, whose basic operation has been explained in the preceding paragraphs, may be derived from Figure 9.4. This is the circuit of the k th phase winding of the symmetrically constructed s -phase path motor winding together with its respective transistor Tr. (See Figure 9.9 for a description of the value of s which actually defines the number of current pulses per pair of poles.) R represents the resistance of the k th phase winding and L is its self inductance. M_k represents the mutual inductances with respect to the other phase windings.

By applying Kirchhoff's second law around the closed circuit, a differential equation is obtained:

$$i_k R + L \frac{di_k}{dt} + u_{Mk} + u_{qk} + u_{Tk} - U = 0 \tag{9.1}$$

where u_{Mk} is the mutual inductance voltage

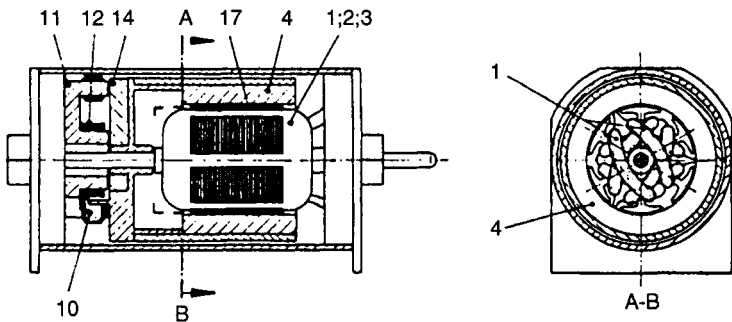


Figure 9.3 *Practical construction of the brushless DC motor with auxiliary frequency transformer*

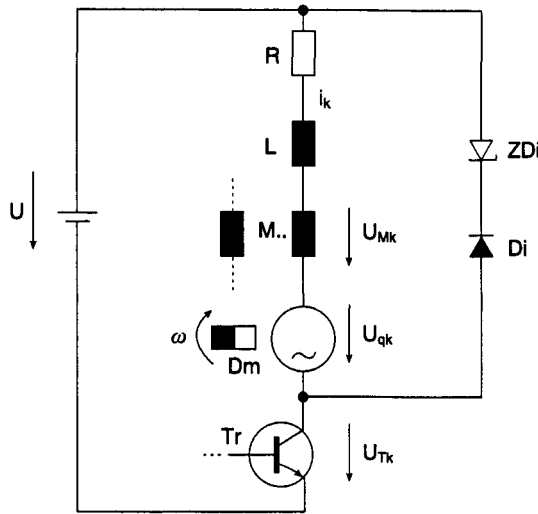


Figure 9.4 Equivalent circuit for one winding path

$$u_{Mk} = M_{1k} \frac{di_1}{dt} + M_{2k} \frac{di_2}{dt} + \dots + M_{sk} \frac{di_s}{dt} \quad k = 1, 2, \dots, s$$

The sum, u_{Mk} , becomes zero if either the mutual inductances are zero or if the currents in the mutually coupled circuit remain constant. Large changes of current only occur during the brief starting and stopping periods. Consequently, u_{Mk} is neglected.

u_{qk} results from the rotating permanent magnet Dm, and u_{Tk} is the control-dependent voltage across transistor Tr, and U is the supply voltage.

In the saturated condition, the transistor collector – emitter voltage is very small ($u_{Tk} \rightarrow 0$) so that eqn. 9.1 simplifies to

$$U = i_k R + L \frac{di_k}{dt} + u_{qk} \quad (9.1a)$$

When the transistor is saturated, the current i_k can flow through the coil only, because the diode prevents any current flow in the parallel path.

At first, in the slow speed starting phase, u_{qk} may be set at zero. When consideration is limited to the steady-state condition, in which $di_k/dt = 0$, the result is

$$i_k = U/R \quad (9.2)$$

Figure 9.5 shows the dependence of the winding current and the resultant torque on the rotor angular position, $\alpha = \omega t$, in a 2-pole motor with $s = 2, 3$ and 4 (see Figure 9.9). The torque, designated m_{ia} , is the instantaneous magnitude of the internal torque between stator and rotor during run-up.

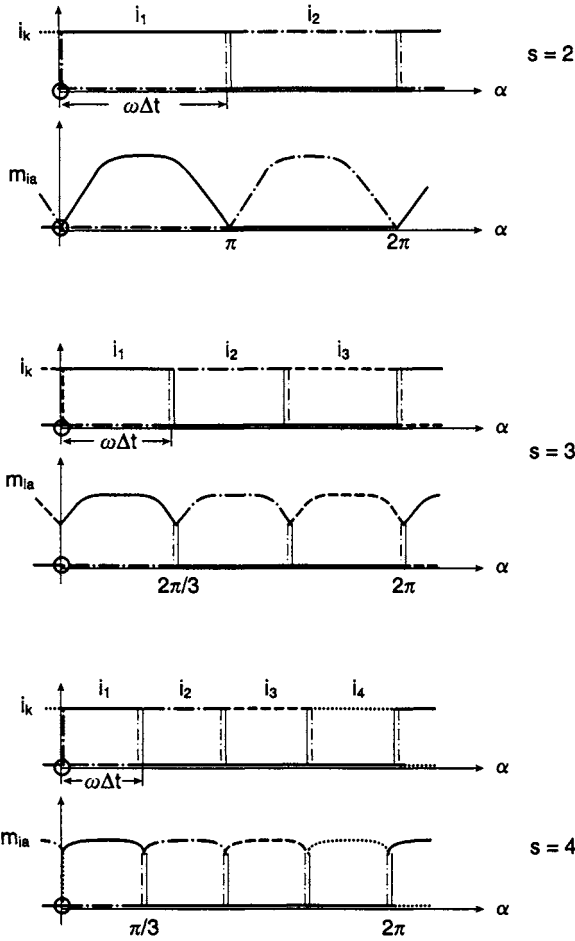


Figure 9.5 Phase winding current i_k and torque m_{ia} during start-up as a function of the rotor position α
 $s =$ number of phase coils

Figure 9.5 shows that the starting torque $m_{ia}(\alpha)$ has more ripple for a smaller number of stator phases. The angle of rotation, during which a transistor is saturated, $\omega\Delta t$, is chosen to be $2\pi/s$. So that there is torque present for every position of the rotor, it is necessary that

$$\omega\Delta t \geq 2\pi/s \tag{9.3}$$

Making Δt the subject produces

$$\Delta t \geq \frac{1}{sn} = \frac{T}{s} \tag{9.4}$$

in which n is the angular speed and T the period of one revolution at constant angular speed.

As Figure 9.5 shows, the single phase motor ($s = 2$), with current flowing in only one direction through a coil, develops zero torque for certain rotor positions. The motor would be incapable of starting from these positions unless special starting means were provided. Therefore, in general, the motor must be designed with $s \geq 3$.

During normal running at speed n the induced voltage u_{qk} in the stator phase coil must be taken into account in the differential eqn. 9.1.

Figure 9.6 shows, with broken lines, the phase winding current derived from the voltage difference $U - u_{qk}$ and the winding resistance R . The current curve takes the self-inductance into account giving the resultant exponential rise and decay with time constant L/R .

At cutoff in the transistor Tr , current i_k is diverted through the diode Di and the Zener diode ZDi and falls rapidly to zero. The Zener diode ZDi in Figure 9.4 is necessary, first, to ensure a rapid fall in i_k and, secondly, to prevent the induced voltage u_{qk} from driving a current through the diode Di when u_{qk} is negative.

To calculate the gross torque m_i in the k th phase winding, the power balance equation (see eqn. 7.3) is applicable:

$$P_{ek} = u_{qk} i_k = m_{ik} \omega = P_{mk}$$

$$m_{ik} = \frac{u_{qk} i_k}{\omega} \tag{9.5}$$

For the average value M_i of a motor with s stator phase coils,

$$M_i = \frac{1}{T} \sum_{k=1}^s \int_0^T m_{ik} dt \tag{9.6}$$

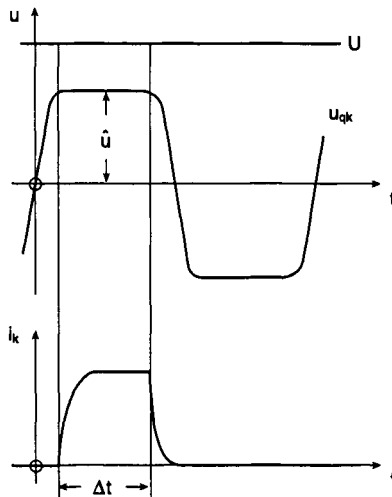


Figure 9.6 Time-dependent waveform of the induced voltage $u_{qk}(t)$ and phase coil current $i_k(t)$

Substituting for m_k from eqn. 9.5, and $\omega T = 2\pi$, gives:

$$M_i = \frac{1}{2\pi} \sum_{k=1}^s \int_0^T u_{qk} i_k dt \quad (9.7)$$

It may be accepted that each of the s phase windings make equal contributions in turn to the torque in a symmetrically constructed motor. It follows that

$$M_i = s \frac{1}{2\pi} \sum_{k=1}^s \int_0^T u_{qk} i_k dt \quad (9.8)$$

Progress towards an expression for M_i can only be made if the time-dependent functions $u_{qk}(t)$ and $i_k(t)$ are known. If it is accepted that, during the time that $i_k \neq 0$, the induced voltage u_{qk} is constant and equal to the maximum value \hat{u}_{qk} , it follows that

$$M_i = s \frac{1}{2\pi} \hat{u}_{qk} \int_0^T i_k dt \quad (9.9)$$

The average current I of the whole motor, i.e. the sum of the s phase winding currents, emerges as

$$I = \frac{1}{T} s \int_0^T i_k dt \quad (9.10)$$

The result for the average gross torque is therefore

$$M_i = I \frac{T \hat{u}_{qk}}{2\pi} \quad (9.11)$$

Here, as in an earlier chapter, we have a DC motor with permanent magnet excitation with its linear relationship between torque M_i and motor current I . The peak value \hat{u}_{qk} of the induced voltage is, according to Faraday's law of electromagnetic induction, dependent on the rate of change of flux and therefore the magnitude of the rotor flux Φ and the angular velocity ω of the rotating magnetic field:

$$\hat{u}_{qk} = \omega k \Phi \quad (9.12)$$

where k is a constant which depends on the geometry of the motor and the number of turns per winding. (Compare eqns. 7.15 and 7.22.)

Substituting for \hat{u}_{qk} from eqn. 9.12 into eqn. 9.11 gives

$$M_i = I \frac{T \omega k \Phi}{2\pi} = I k \Phi \quad (9.13)$$

The peak value \hat{u}_{qk} is less than the supply voltage U by about the amount IR .

Approximately,

$$U = \hat{u}_{\eta k} + IR \quad (9.14)$$

Taking into account that the available torque from the motor shaft M is smaller than the gross torque M_i by the friction torque M_R

$$M = M_i - M_R \quad (9.15)$$

The correspondence with eqns. 7.12–7.15 is complete, showing that the brushless DC motor is nothing other than a DC motor with a permanent magnet field whose commutation is electronic instead of mechanical.

Figure 9.7 shows the well known characteristics $\omega(M)$ and $I(M)$ of these motors.

9.3 Types of construction

There are, of course, various possibilities for matching DC motors with electronic commutation to the requirements of the driven device. The survey begins with the different basic constructions that can be fitted with various windings and electronic circuits. Variations on these themes are discussed, and finally a number of examples of manufacture are given.

9.3.1 Design variants

Figure 9.8 shows the various design configurations of brushless DC motors with rotating and linear armature motion.

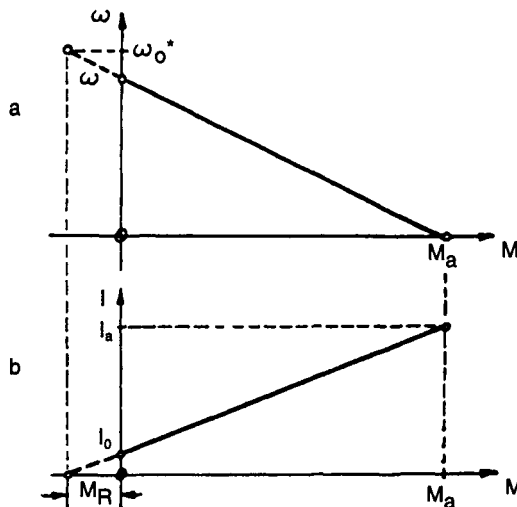


Figure 9.7 Characteristics of the brushless DC motor (replica of Figure 7.9)

a Angular velocity ω as a function of torque M
 b Motor current I as a function of torque M

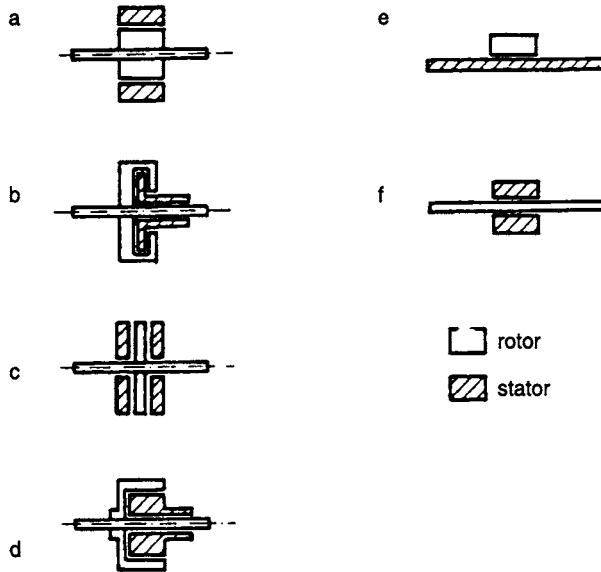


Figure 9.8 Design variants of brushless DC motors

a inner rotor motor; *b* disc stator motor; *c* disc rotor motor; *d* outer rotor motor; *e* long stator linear motor; *f* short stator linear motor

A frequently occurring arrangement is the cylindrical inner-rotor variant, surrounded by the wound stator (*a*). Rotors in variants (*b*) and (*d*) have particularly high moments of inertia. Whereas in the disc-stator type (*b*) only the iron-free airgap winding is fixed and the permanent magnet together with its supporting structure and back iron rotate, in type (*d*) only the cup-shaped permanent magnet fixed to the shaft rotates. In comparison the disc-rotor type (*c*), in which only a disc shaped axially magnetised permanent magnet rotates, has a low moment of inertia.

Type (*e*) is a long-stator linear motor, which is characterised by its lightweight armature. In this motor the maximum possible movement can be only slightly less than the length of the stator, whereas in type (*f*) the length of the motor can be as much as twice the attainable movement.

9.3.2 Motor windings and energising circuits

The most frequently encountered motor winding circuits with their energising circuits are collected together in Figure 9.9. Circuit (*b*) has two coils ($s = 2$) and the current flows in one direction only through each of the coils. The same effect can be achieved with just one coil in a four-transistor bridge as shown in circuit (*a*). Circuit (*a*) has the advantage of all power bridge circuits that for a given copper content and heat loss in the coils a torque which is $\sqrt{2}$ times that in (*b*) is achieved.

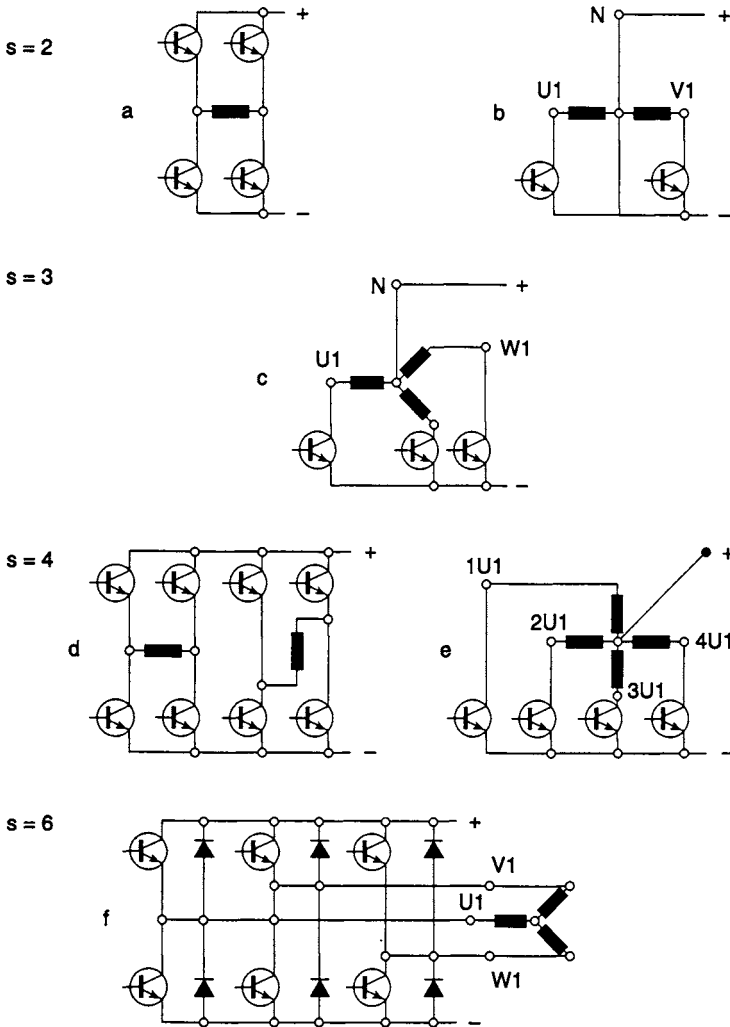


Figure 9.9 Motor windings with various numbers of coils and halfwave or full wave switching arrangements giving a range of values of s , the number of current pulses per pole pair

- a $s = 2$ single phase, full wave inverter driving one coil
- b $s = 2$ single phase, half wave inverter driving two coils
Both of these give effectively single phase operation.
- c $s = 3$ three phase, half wave inverter driving three coils connected in star with neutral connected to positive terminal of battery
- d $s = 4$ two phase, each phase fed by full wave inverter
- e $s = 4$ four phase windings connected to common positive feed, half wave inverter feeding each phase
- f $s = 6$ three phase, full wave inverter feeding three coils
The value of s is the number of pulses of torque-producing current per revolution (for a two-pole motor)

Neither circuit (a) nor (b) can guarantee starting without auxiliary equipment because of the zero values in the torque-rotor angle characteristic. Circuit (c) is the minimal circuit ($s = 3$) for reliable starting and running. There is, however, appreciable ripple on the torque/rotor angle characteristic.

A more uniform torque characteristic can be achieved from four stator coils energised as in circuit (e). The comparable circuit (d) has the advantage already mentioned of higher torque for the same copper mass and heat loss. The need for double the number of transistors in circuit (d) is not a problem because reasonably priced double-bridge power stage integrated circuits are available.

Circuit (f) whose three coils pass currents in both directions is gaining importance. This circuit combines the advantages of requiring fewer power transistors than circuit (d), providing a uniform torque and good utilisation of copper in the coils.

The diodes shown in (f) connected in anti-parallel with the transistor collector-emitter paths prevent a sudden interruption of coil currents following transistor cutoff. Dangerous voltage transients are thus avoided. The equally necessary protection in circuits (a)–(e) is not shown on the diagrams.

In the power stages of the 'electronic commutator' the preferred device for switching is the transistor. Assistance in selecting the appropriate types is to be found in Section 8.2.2.

9.3.3 Position indicators

Besides the carrier frequency transformer described above, there are other more modern possibilities for determining the rotor magnet's position. Obvious contenders are:

- Hall generators
- Magneto-resistive sensors
- Magnetic diodes.

All the position indicators mentioned respond only to the magnetic field, the output being independent of the angular velocity, and therefore fulfill the requirements for a start from rest.

Rotor position sensing is possible by means of fixed stator coils, in which the rotating magnet induces voltages. Even the coils which are there for producing the torque can perform this second function. These coils produce, of course, the required signals only when the rotor is turning – see the system in Figure 9.1. In such cases there must be an assisted start, e.g. in the form of a mechanical starting commutator with brushes that retract at speed owing to centrifugal forces. Alternatively, the motor could be started up as a stepper motor with increasing step rate until the speed is sufficient to produce the induced voltages mentioned above.

Finally, the possibility of optosensitive devices for indicating rotor position should be considered.

9.3.4 Speed setting and control

As can be seen from eqns. 9.12 and 9.14, the angular velocity ω and speed n of the brushless DC motor can be adjusted by means of changing the supply voltage U .

If only a constant direct voltage supply is available, reduction of speed can be achieved by means of a series resistor which achieves voltage reduction at the motor, by a voltage divider, a transistor or a DC chopper with its attendant low heat losses.

The same effect can also be achieved using the full supply voltage, but with some voltage being absorbed by appropriate control of the transistors in the stator coil circuits. When the transistors are not fully saturated, then the resultant power loss, which arises as a consequence of the voltage drop, must be allowed for in the design. The increased power loss can be avoided if the switching frequency is high compared with the motor speed. Variations in switch-on/switch-off time can be used to control the average voltage that is applied to the winding. Current interruptions must be prevented by means of fast acting freewheel diodes.

Regulating the speed presupposes a means of measuring the speed, together with a regulator that operates in the manner described above on the motor winding voltages. The motor speed can be measured by means of an AC tachometer generator whose induced voltage magnitude or frequency is a measure of the speed. An exact setting of the motor speed is achieved when the tachometer's frequency and phase angle are the same as those of the reference signal generator. Integrated circuit components are available to fulfil these somewhat demanding requirements.

In certain circumstances, the speed signal may be read directly from a brushless DC motor because the rotating magnet and fixed coil windings are already there. Where individual coils are not connected in bridge circuits, they are connected to the voltage source for less than half a period. Figure 9.10 shows a way in which the induced voltages in the coils which are not carrying current producing torque may be used to indicate speed.

The AC tachometer action is most easily explained for the case of a four-winding star-connected motor (Figure 9.10 extended to include four coils and four transistors). The rotor north pole passes coils 1, 2, 3 and 4 in that order. As the N-pole passes coil 1, the S-pole passes coil 3. The induced voltages in the four coils (U_{cs} = voltage at transistor collector with respect to the star point) are 1 (-), 2 (0), 3 (+) and 4 (0). At this time transistor 1 is conducting and the others are not. The voltage induced in coil 3 charges capacitor C via diode D_3 . The remaining diodes are all reverse-biased and nonconducting. As the magnet rotates, each coil injects a pulse of charge into the capacitor in turn. The capacitance of C is a compromise, large enough to provide adequate smoothing, and small enough to discharge through the

measuring circuit (not shown) as the motor speed falls. For simplicity, the use of transistor current chopping with consequent inductive voltage transients which are damped by freewheel diodes has been omitted.

9.4 Motor designs and constructions

9.4.1 Internal rotor motors with airgap windings

Motors of this type appeared early in the development history of brushless DC motors. They were characterised by a cylindrical 2-pole permanent magnet rotor (2), with a four-coil winding (1), which was located in the airgap between the rotor and a concentric slotless iron stator (3). (see Figure 9.11).

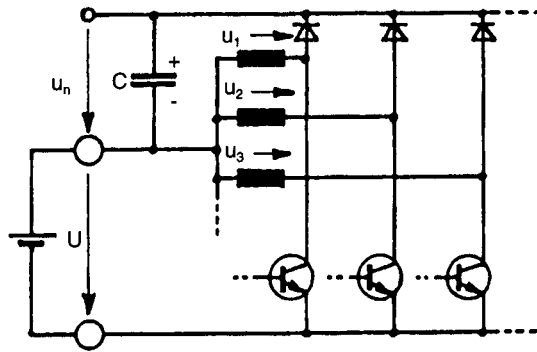


Figure 9.10 Circuit for obtaining the tachometer voltage u_n from the motor winding

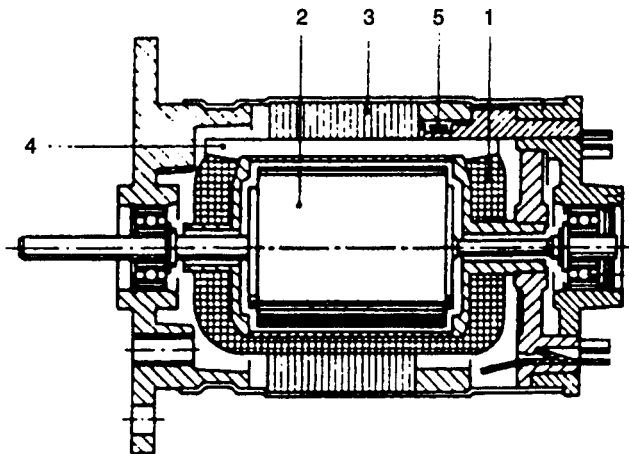


Figure 9.11 Longitudinal section through an internal rotor motor with an airgap winding

The two Hall-effect generators (5) are installed in an extended airgap outside the winding. The winding carrier is the plastic 'cage' (4). The magnetic winding axes of the coil pairs are at right angles and the two Hall-effect generators are fixed spatially at 90° from each other.

Thus, as shown in Figure 9.12, each Hall generator 5.1 and 5.2 controls the current in a pair of diametrically opposed stator coils. When, say, Hall generator 5.1 detects the N- or S-pole of the rotor, one or other of transistors 7.1 and 7.2 is energised. At the same time, Hall generator 5.2 detects no pole and generates no voltage. Thus only one of the four coils 1.1–1.4 is energised at any instant. Current flows through each stator coil in turn as the rotor turns through 90° , during which full torque is developed. Transfer of current flow from one coil to the next occurs without any interruption in the motor current, so that torque continues to be developed in the rotor during the current transfer phases.

The tachometer voltage u_n , needed for speed control, is derived through four diodes in the manner described at the end of Section 9.3.

The comparison of reference and tachometer voltages takes place in transistor 9 of Figure 9.12 in that the speed, i.e. u_n , adjusts until the network comprising resistors 10–14 applies the 'correct' base-emitter voltage to transistor 9. The voltage at the collector of transistor 9 determines the current through transistor 8. This current flows through one transistor 7 which provides the base-emitter voltage of one transistor 6. The transistor 6 energises its coil 1 and develops voltage u_n via a diode, and the control loop is closed.

The base-emitter voltage of transistor 9 is temperature-dependent, and thus the temperature-dependent resistor 12 is included to give compensation. Speed setting is achieved by adjusting resistor 14.

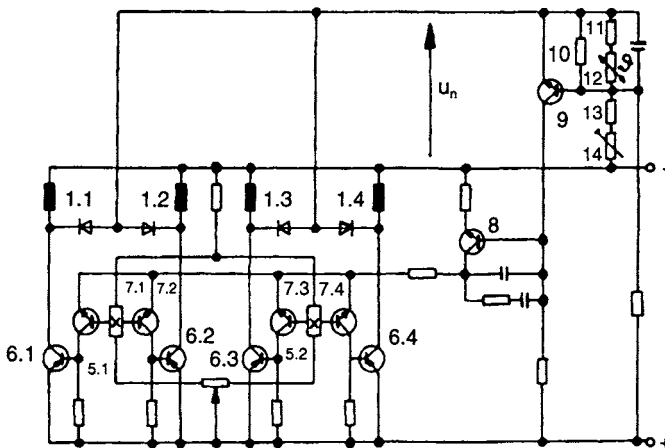


Figure 9.12 Circuit diagram of a four-coil inner-rotor motor with an airgap winding

The winding which lies in the airgap between the rotor and the slotless iron-stator has a particularly low stray inductance. Consequently, fast winding current switching is possible and, with it, high rotor speed. In addition, because of the absence of reluctance torques, particularly smooth running is achieved, and this type of winding is found in many brushless DC motors.

Figure 9.13 is a photograph of a motor of the type just described. Such motors can also be switched using special electronic commutating circuitry, which dispenses with rotor position sensors. In these, the stator windings are not only used to develop the torque and possibly the tachometer voltage, but are also used for switching the power transistors. (Another arrangement was described in Figure 9.10.)

In the circuit of Figure 9.14, the voltages across stator coils 1, 2 and 3 are phase-shifted by the RC networks (e.g. 21, 12, 33 and 43) and fed to the base-input terminals of the two-stage transistor amplifiers which energise the stator coils appropriately. This 'phase shift oscillator' action works only when the rotor is running and is inducing voltages in the stator coils.

During starting, the electronic circuit runs as a three-stage multivibrator whose sweep frequency is determined by the phase-shift networks. A pulsed stator field which 'rotates' is achieved, and the motor runs as a stepper motor, and changes over to the mode described in the previous paragraph when the induced voltages in the coils have sufficient magnitude. A prerequisite for a reliable start and run-up is a careful and correct electronic circuit design that takes the load – in particular the torque for accelerating the rotating masses – into account.

Modern developments are giving new approaches towards enabling the control described above to be achieved without the need for supplementary

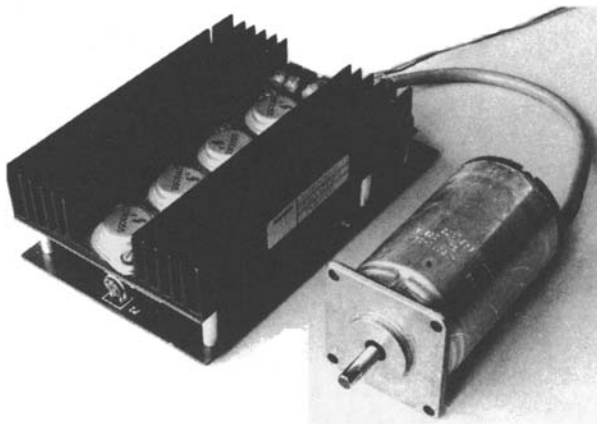


Figure 9.13 Four-coil brushless DC motor with electronic control
(32 W, 6000 rev/min)
(Courtesy: Siemens)

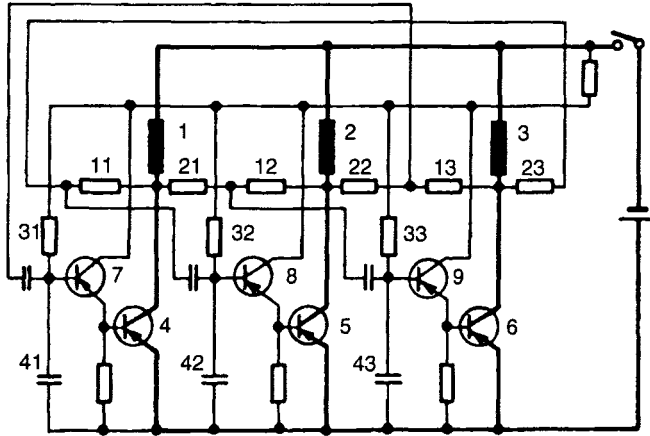


Figure 9.14 Circuit diagram of a brushless DC motor with control through phase-shifter sections

position indicators. Here, too, starting is achieved by impulsing the stator coils to turn the rotor until the necessary induced voltages appear. An integrated circuit detects the instants at which the three-stator coil induced voltages pass through zero. This occurs during the period when the coil current is zero, i.e. when the current in the one direction has been switched off and the current in the reverse direction has not yet been switched on. Given the instants at which the voltages pass through zero, the ICs determine the timing for switching the power transistors on and off.

The ICs described above are capable of controlling various motors in full-wave circuits such as that of Figure 9.9*f*. They also provide protection circuits for the power transistors and offer possibilities of extracting information about the rotor speed and position.

9.4.2 Internal rotor motor with slotted stator

Slotted stators, with which higher magnetic fluxes in the magnetic circuit are achieved owing to the small airgap, are preferred for higher power motors. For a given amount of material and winding heat loss, these motors deliver higher torques than those with airgap windings. Especially high power per volume is achieved by the use of high quality permanent magnet materials, e.g. samarium-cobalt alloys (samarium is a rare-earth element: at.no. 62; at.wt. 150.35).

Figure 9.15 shows the cross-section of a motor of this kind with a 4-pole rotor. The winding is made up of three coil groups (Figure 9.16) and is energised through three half-bridge circuits as shown in Figure 9.9*f*. In this way a good utilisation of active winding copper is achieved with a small number of power transistors, and this leads to a higher power output with a better efficiency.

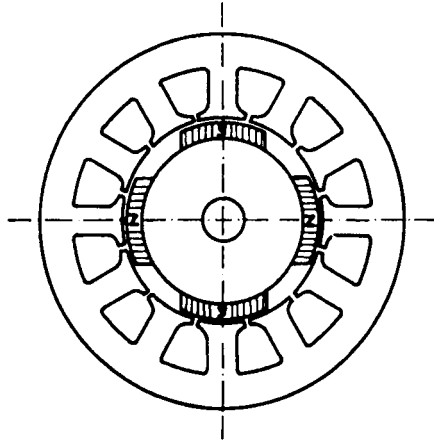


Figure 9.15 *Stator stamping and 4-pole rotor of a brushless DC motor*

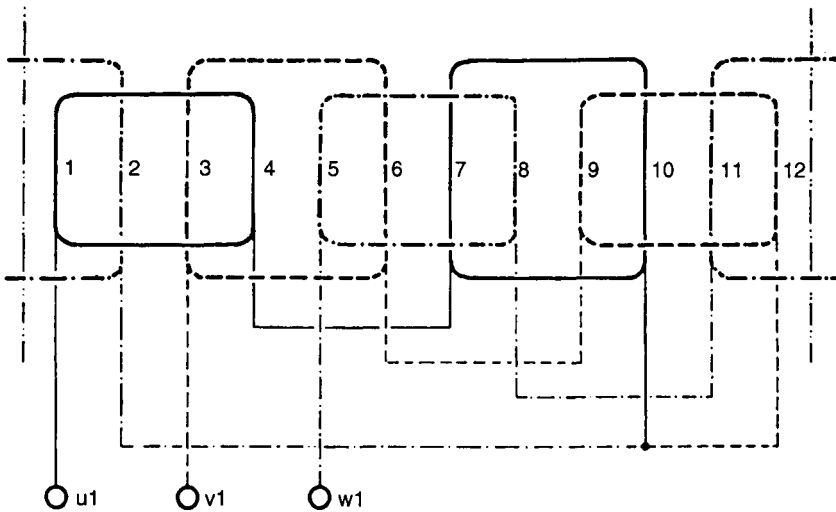


Figure 9.16 *12-slot winding with three-coil groups in star connection for a brushless DC motor*

Also the developed torque is quite uniform, because by reason of overlapping in the switching there are 24 separate current impulses per turn of the rotor. This is in line with the performance of high quality DC motors with mechanical commutators. The motor described above is shown dismantled in Figure 9.17. Higher power motors with more than four poles are also used.

There are integrated circuits available that process signals from Hall-effect generators located in the airgap for controlling power transistors. There are,

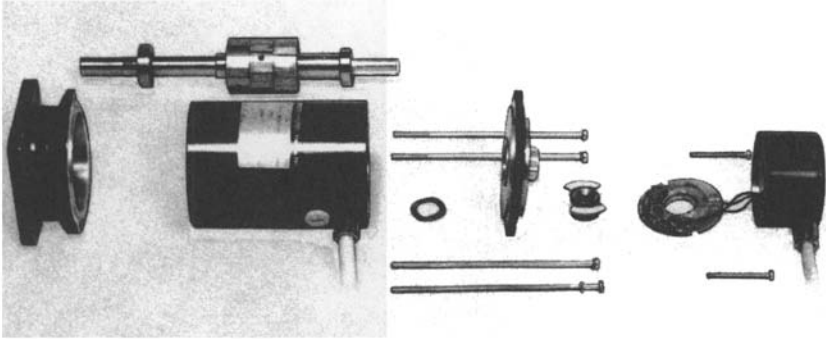


Figure 9.17 Dismantled brushless DC motor with slotted stator.
(320 W, 4000 rev/min)
Position indication is by photoelectric devices (right of picture)
(Courtesy: Groschopp)

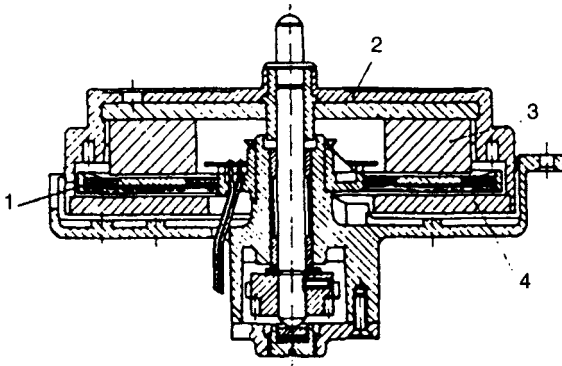


Figure 9.18 Section through a brushless DC motor for direct drive of a gramophone turntable

of course, reluctance torques between the rotor poles and the slotted stator. These torques can, nevertheless, be counteracted by skewing the stator slots or off-setting the rotor magnets against each other.

9.4.3 Motors with disc stators

Figure 9.18 shows an example that was designed for the direct drive of gramophone turntables. Stator 1 has an iron-free construction and is composed of a four-coil winding. Together with the 8-pole magnetised rotor, 16 disc-shaped component coils are required that are arranged at half a pole pitch from each other in two layers.

Rotor assembly (2) makes possible the application of easily manufactured ferrite magnets (3) grain-orientated and magnetised in the axial direction. Of

interest is that the back iron (4) turns with the rotor magnet so that there are no hysteresis or eddy current losses. This arrangement also increases the rotor moment of inertia, which must be advantageous for driving the turntable at constant speed directly from the motor.

Two Hall generators are used in this motor which signal the rotor position, and thus the electronic circuit is very similar to that of Figure 9.12. Throwing a switch in the electronic circuit can select speeds of 33.3 and 45 rev/min. The motor of Figure 9.19 with a permanent magnet disc rotor and airgap coils was designed for driving magnetic disc stores. Six stator coils arranged as three pairs are set opposite the 8-pole rotor. Torque is developed by the interaction between the coils of one winding and four of the eight rotor poles.

Position indication in this extremely flat motor ('pancake design') is by three Hall generators situated inside the coil cluster.

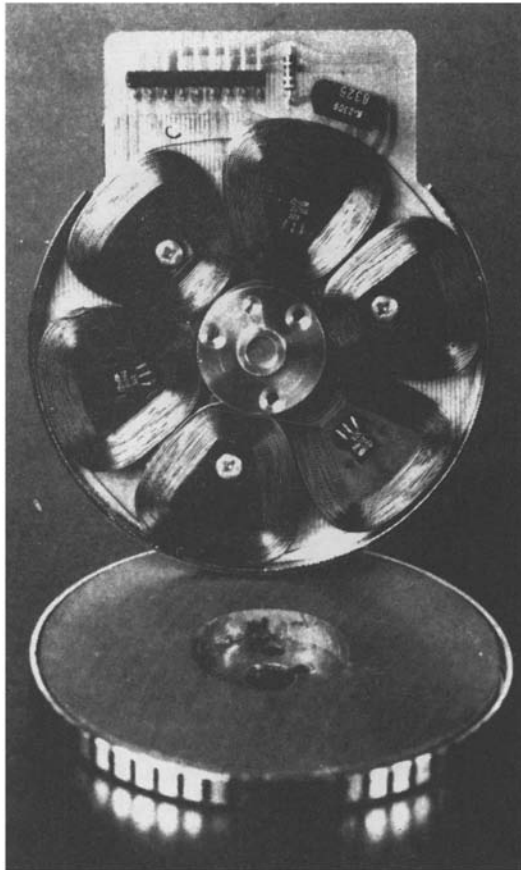


Figure 9.19 Brushless DC motor for direct drive of disc stores
The rotor is removed to give a view of the coils in the ironless stator.
(Courtesy: Bühler)

9.4.4 Two-coil motors

Reducing the number of coils to $s = 2$ (Figure 9.9b) reduces the cost of the motor and of the electronic circuit. However, as is evident from Figure 9.5 ($m_{is}(\alpha)$), certain special measures must be taken during starting.

Figure 9.20 shows the circuit of a two-coil motor whose coils are energised from the power supply using two power transistors. The signals to these transistors, which depend upon the rotor position, are derived in the known manner from the Hall generator (9).

In Figure 9.21 the curve $m_{is}(\alpha)$ is seen to be a pulsed torque with contributions from the currents in both coils. With an eye towards efficiency, a relatively large pause occurs between these current pulses, because the rotor position during these pauses is unfavourable for the production of torque.

To avoid the situation in which zero torque is developed for certain rotor positions, auxiliary soft magnetic poles are placed in the stator, which interact with the magnetic rotor and develop the reluctance torque m_{iw} .

Figure 9.22 shows an example of a 2-pole brushless DC motor, in which narrowing of the airgaps takes care of the required supplementary torque m_{iw} .

The effect of this arrangement is shown graphically in Figure 9.21; in addition to the torque $m_{is}(\alpha)$ derived from the stator coil currents there is also periodic torque resulting from the presence of soft iron poles. The sum of these torques, $m_i = m_{is} + m_{iw}$, is not zero for any rotor position, and the change in torque is considerably less than with m_{is} on its own.

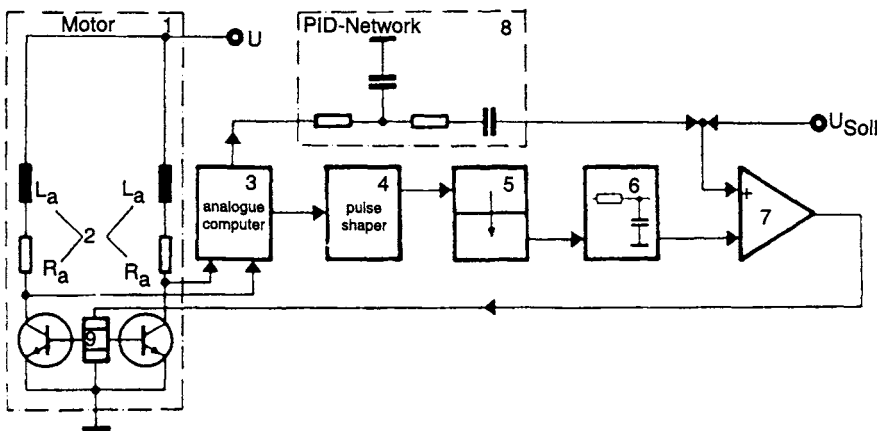


Figure 9.20 Block circuit diagram of a speed-controlled two-coil motor

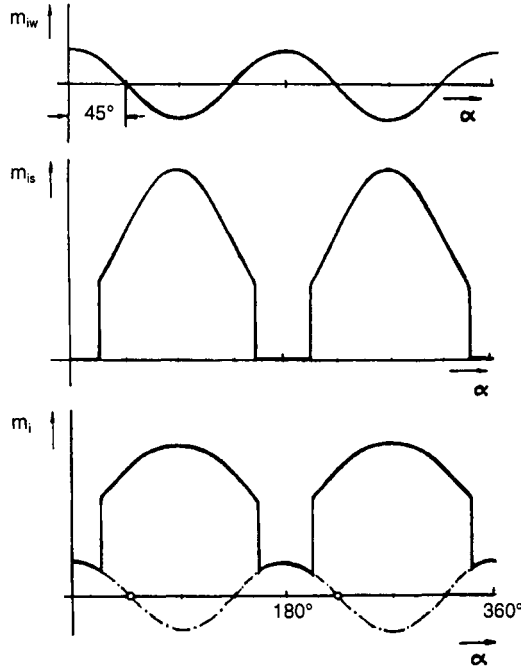


Figure 9.21 Torque components m_{iw} and m_{is} and the total torque m_i of a two-coil motor as a function of the rotor position α

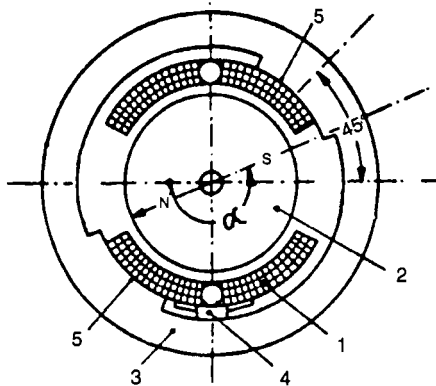


Figure 9.22 Cross-section through a two-coil motor

Figure 9.23 shows the practical form of a motor based on these principles (this is the playback motor in a cassette recorder whose construction is similar to that of the gramophone turntable motor of Figure 9.18):

- 3 is the ironless stator winding
- 4 soft back iron, which rotates with 5
- 5 rotating permanent magnet
- 6 soft iron pole which provides reluctance torque m_{iw} in the 6-pole motor.

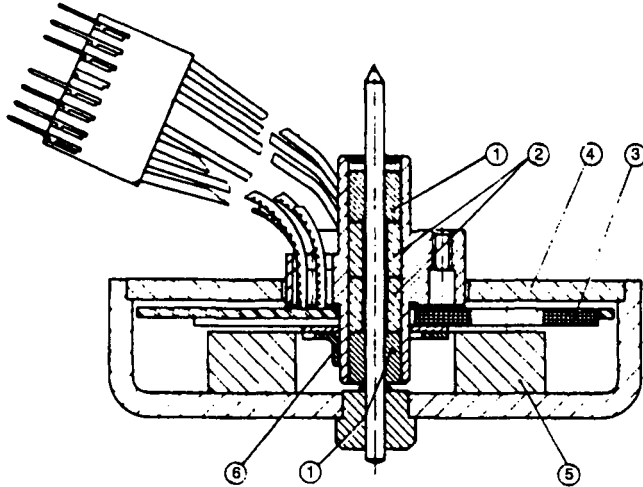


Figure 9.23 Two-coil motor for directly driving the playback shaft of a cassette recorder

The electronic circuit necessary for speed control is given in block-schematic form in Figure 9.20. Motor speed is defined in terms of the frequency of the induced voltage in the stator coil and is converted by electronic means into a proportional direct voltage. The comparison of reference and feedback voltage takes place in the operational amplifier (7), which in turn affects the current through the Hall-effect generator.

Figure 9.24 shows a two-winding motor fitted with an external rotor. The variations in the stator airgap contour, necessary for the production of the reluctance torques, are not difficult to see here.

9.4.5 Linear motors

There has been no lack of effort towards producing brushless DC linear motors, but this has not yet resulted in large-scale application, for economic reasons. The linear motor in Figure 9.25 is characterised by its multipole stator magnet system comprising permanent magnets 3, and the back irons 4.1 and 4.2. Coils 1.1 and 1.2, together with the position indicators, make up, for the most part, the armature. The armature coils are energised with currents of opposite sign by the electronic commutating circuits, which in turn are controlled by the position indicators. Because of the limited armature movement, its current supply comes in via flexible leads, i.e. without any sliding contacts.

The armature of another linear motor model (Figure 9.26) comprises nothing more than a permanent magnet block (4) magnetised at 90° to its direction of movement, so that supply leads are not required. The 'upper pole' (N) of the permanent magnet armature slides past the adjacent stator poles 11, 21 and 31, and similarly for the lower pole (S) and the stator poles

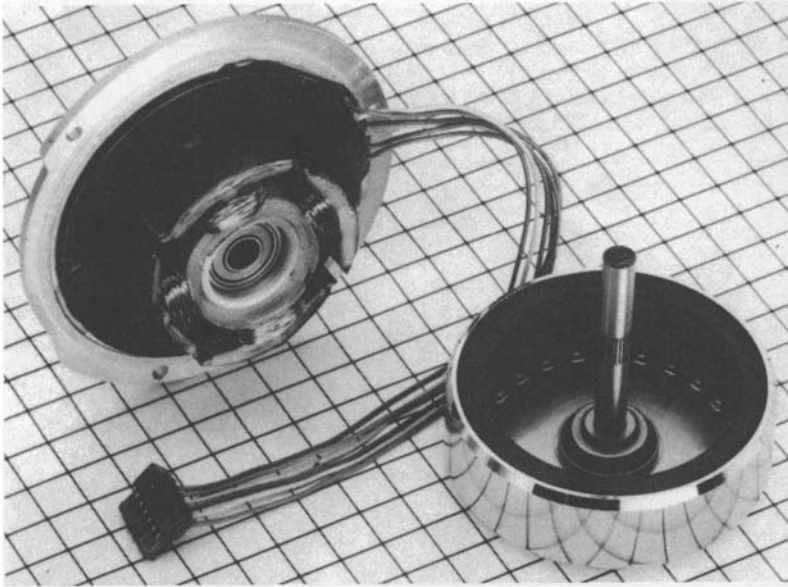


Figure 9.24 *Stator and external rotor of a 4-pole two-winding motor (5.6 W, 3600 rev/min) (Courtesy: Papst)*

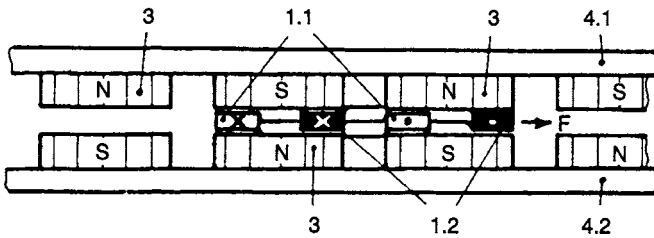


Figure 9.25 *Brushless DC linear motor with armature coils and long stator*

12, 22 and 32. Fluxes Φ_1 linking coil 1, and similarly Φ_2 linking coil 2, are the results of (i) the permanent magnet armature and (ii) the ampere turns Θ_1 and Θ_2 owing to the currents in coils 1 and 2, respectively. Fluxes Φ_1 and Φ_2 are highly variable but always in one direction. This fact has led to the designation 'common-pole motors'.

Given the stator coil ampere turns Θ_1 and Θ_2 as shown, Φ_1 is less than the permanent magnet component of flux and Φ_2 is greater. This results in a force being applied to the armature in the direction of increasing s . The directions of Θ_1 and Θ_2 are determined by the position detector (24) signalling to the power electronic circuits. Meanwhile there is no current in coil 3.

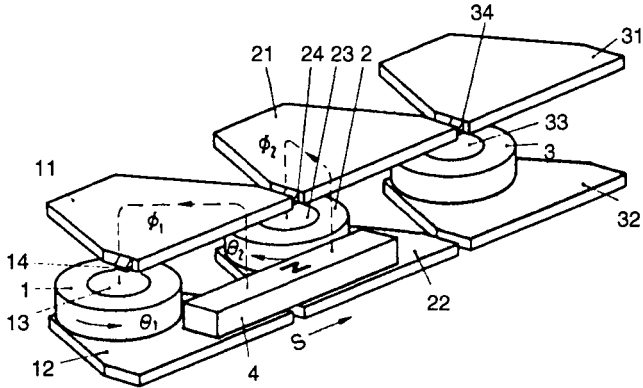


Figure 9.26 Brushless DC linear motor with common-pole armature
Pole pieces 11, 21 and 31 are shown displaced vertically upwards

When the right end of the armature arrives under the position indicator (34), by which time the push from coil 1 is fading and the pull from coil 2 is practically zero, the current through coil 2 is switched off and an equal current in the same sense is passed through coil 3. The field of coil 3 then pulls the armature in the direction of increasing s .

The armature (4) is somewhat longer than the edges of the keeper plates 11, 21 and 31. Therefore, by the time the left end of the armature passes under position indicator 24, the pull exerted by coil 3 is well established. At this instant, position indicator 24 causes the electronics to switch off the current through coil 1 and pass an equal current in the same sense through coil 2. Coil 2 then contributes push to the armature movement.

Armature 4 being longer than the keeper plates ensures that, for all positions of the armature and states of the position indicators, at least one coil is energised and exerts a force on the armature in the correct direction, including when the current is being commutated from one coil to another.

Reversal of the armature direction of travel is achieved by reversing the coil currents in all situations. Just as for the motor shown in Figure 9.25, this is a matter of changing the logic coupling between the position indicators and the power transistors. Because the position indicators are located in a unidirectional field emanating from the armature it is only necessary (and sufficient) for the position indicators to detect the presence of a magnetic field and not its direction or polarity. Magneto-resistive sensors may be used without magnetic bias, for example.

The 'common pole' motor may be extended to any length by adding more stages to the three shown in Figure 9.26. This is a considerable capital expense, but the energy demand is confined to the two coils operating on the armature at any given instant.

Considerations of designing DC linear motors with the highest possible armature force and with minimum demand for material led to the

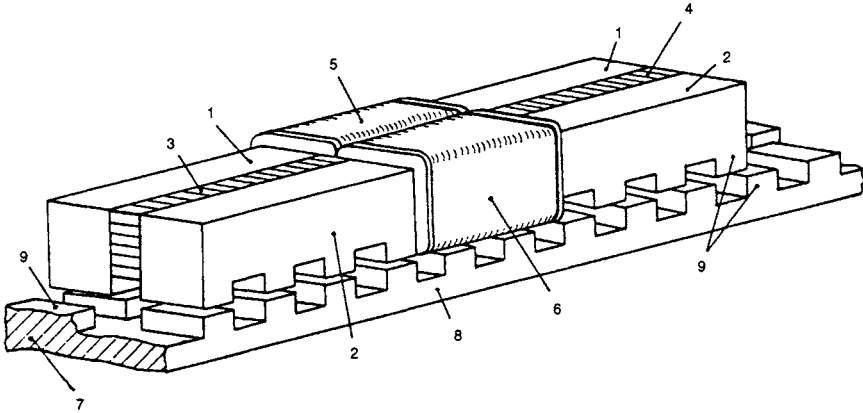


Figure 9.27 *Direct current linear motor with pole teeth (pole-group or linear hybrid stepper motor)*

conception of the pole-group (linear hybrid stepper) motor as shown in Figure 9.27.

The active armature of this motor comprises the two iron-formed parts, 1 and 2, the coils 5 and 6, and permanent magnets 3 and 4, while stator 7 is made of passive soft iron. The high forces come about on account of the sets of uniform armature and stator teeth (9), the action being similar to that in a stepper motor.

The magnetic circuit energised by the coils comprises some parallel paths over the teeth, so that flux changes in individual teeth add up to a larger total $d\phi/ds$ which, as explained in Section 7.2.2, is decisive for the magnitude of the force developed.

The coils, 5 and 6, are connected into electronic commutating circuits in the customary manner, and are controlled by the necessary position indicators that are not shown in the drawing.

9.5 Properties

The measured characteristics $n(M)$ and $I(M)$, speed/torque and current/torque given in Figure 9.28 of a brushless DC motor as shown in Figure 9.11, are in accordance with the theoretical considerations of Section 9.2.

The efficiency η (Figure 9.28) peaks around the working point – $M_N = 1$ Ncm, $n_N = 6000$ rev/min and $P_N = 6.28$ W – at a value of $\sim 50\%$. This value can also be achieved with smaller motors (~ 1 W), but with some difficulty.

One reason for what is poor efficiency for a DC motor is the copper loss, which is linked to the irregular current flow in the individual coils. In bridge-connected circuits in which current flows through the coils in both directions, and for a greater proportion of the total time, and when high

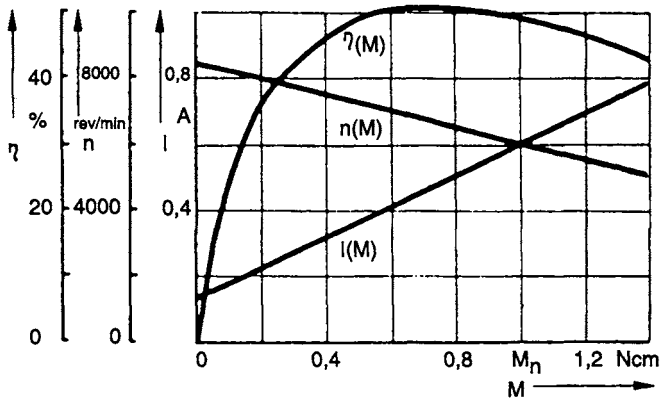


Figure 9.28 Measured characteristics of a brushless DC motor: motor current I , speed n and efficiency η as functions of the torque M

quality permanent magnetic materials are used, the efficiency is substantially improved. In larger motors, with samarium–cobalt magnets, the efficiency can exceed 80%.

The starting torques of brushless DC motors are high, as they are in classical DC motors, but there is more torque ripple which depends on the rotor position, and is particularly high in simple motors with low coil numbers.

Brushless DC motors come in a range of designs, and have power ratings up to and beyond 2×10^5 W. Whilst, in most cases, the motors on offer have speeds less than 10^4 rev/min, there are motors which can rotate at up to 10^5 rev/min. Brushless DC motors have characteristics and performance specifications similar to those of classical DC motors, but they also have the following interesting features:

- The lifetime of brushless DC motors is very high, even at high running speeds, and is limited only by the bearing life ($>10^4$ h), just as in induction or synchronous motors.
- Brushless DC motors are very reliable on account of their having no mechanical sliding contacts. All the components used undergo no changes with time, so that the motors retain their characteristics during their running lifetimes.
- The absence of a commutator makes radio suppression components unnecessary.
- They are quieter running than classical DC motors.
- Brushless DC motors can be made to have good speed regulation without great additional cost, and also at a number of switchable electronically controlled speeds.

These positive properties must be paid for because of the need for electronic

circuits, which results in higher unit costs than for conventional motors. These extra costs are, however, offset by a reduction in subsequent maintenance costs, and the elimination of the cost of radio suppression components.

In those applications where the brushless DC motor can now perform the tasks which hitherto required stepper motors, or inverter-powered synchronous or asynchronous motors, the brushless DC motor is now offering the cheapest drive concept.

9.6 Applications

Brushless DC motors are called into service in DC powered apparatus, where classical motors with mechanical commutation are not acceptable on account of their limited brush lifetime. In the larger electronic systems, for example those which are powered from a central rectifier, a cooling fan is required with a long life to remove the heat generated. To eliminate the need to provide a separate AC supply for such a fan, brushless DC motors are installed.

A broad application spectrum for brushless DC motors is offered by portable, battery or accumulator powered appliances which do not have AC mains. Only measuring instruments with plotters, dictation machines, tape and gramophone disc players are mentioned here. In these devices, the brushless DC motor plays a role not only because of its reliability and durability but also because excellent speed control – at a number of selectable speeds – is possible without excessive extra expense. This removes the need for reversible mechanical gearboxes that were necessary for the establishment of various speeds, for printing paper or sound recording, when using motors that can only rotate at constant speed.

Apparatus other than purely battery-powered portable equipment is gaining importance, e.g. that which can be energised from a variety of sources: the AC mains, a vehicle DC system or from an individual DC supply independent of the mains. In principle, these are devices which can be supplied from an external mains-energised 12 V DC power adapter, a dictation machine being an example.

Their advantages, when added together, make brushless DC motors so attractive that they are finding applications in the province of what were purely AC equipments, e.g. tape recorders and CD players. Owing to the higher efficiencies of brushless DC motors compared with AC induction or synchronous motors, they cause less heating in the devices being driven. Finally, they are smaller and lighter. They are also capable of being energised from mains supplies of various frequencies without any change of speed occurring as happens with induction or synchronous motors. Thus, a piece of equipment can be exported to European markets (50 Hz mains) and to the North American market (60 Hz mains).

In many drives, where speed changes are required, brushless DC motors may be used to advantage. Because classical DC motors are excluded from certain applications from the outset on account of their limited brush life and uncertain reliability, only stepper motors, induction or synchronous motors have been considered so far. Stepper motors, however, present problems with starting and at high speeds, and induction or synchronous motors demand expensive auxiliary equipment if speed-changing is required.

By adding to the electronic circuits of brushless DC motors, it is possible to change the motor characteristics in ways already described. It is now also possible to produce high power four-quadrant motor drives which are capable of wide speed variations whilst maintaining good efficiency throughout. In contrast to the classical DC motor, holding torque at zero speed can be achieved in a simple manner, in that a direct current can be routed through a stator coil winding independently of any electronic commutation.

The possibilities described above have led to numerous drives using brushless DC motors, e.g. peripheral drives in data processing systems, copiers with numerous speed stages, and in precision mechanical drive systems.

A new and interesting application spectrum lies in the field of industrial drives, where there is a trend towards controllable individual drives. Brushless DC motors are being installed in automatic measurement installations, robots and some machine tools. Their advantages over classical DC motors in explosive atmospheres are obvious. In new very high speed spinning applications there is a requirement for motors with very high speeds (up to 100,000 rev/min). Here, also, the brushless DC motor has advantages over the inverter-driven induction or synchronous motor. Difficulties occur in induction motors during acceleration and deceleration owing to rotor heat losses. Conventional DC motors are excluded from the beginning owing to limited brush life, high rotor losses and rotary speed limits imposed by the wound armature and commutator. High speed brushless DC motors must be fitted with special bearings; of course, magnetic bearings and air bearings provide practical solutions to this problem.

9.7 Outlook

Design philosophy for industrial drives which use brushless DC motors is moving towards developing the electronic circuitry to meet increasing demands for new applications. The inclusion of high quality permanent magnet materials characterises the trend as well as the increasing application of integrated circuits and very high power transistor modules. There is also the possibility of reducing the cost of brushless DC motors considerably. The single coil motor of Figure 9.1 involves the least cost. This motor's pulsating torque makes it comparable with the shaded-pole motor for powers up to 100 W which has replaced it in many applications. Better starting

characteristics are achieved by the motor shown in Figure 9.29 with its specially formed soft-iron poles (5) and additional permanent magnet poles (6) located in the stator (3). Figure 9.30*a* shows the soft-iron pole torque component m_{iw} as a function of α . The permanent magnet pole torque m_{id} (Figure 9.30*b*) is added to torque m_{iw} when there is zero motor current.

The total no-current torque $m_{iw} + m_{id}$ is shown in Figure 9.30*c*, and the stable no-current no-torque rotor angle is shown in Figure 9.29 and as 1 in Figure 9.30*c*.

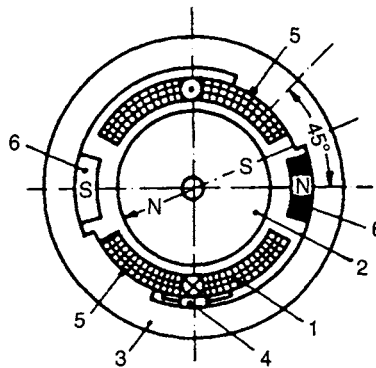


Figure 9.29 *Cross-section of a single-winding brushless DC motor*
The rotor is in the stable off-load, no-current position

When the motor current is switched on, component m_{is} (Figure 9.30*d*) is added to the torque, giving $m_i = m_{is} + m_{iw} + m_{id}$ (Figure 9.30*e*) and the motor turns and accelerates under the influence of a varying but strongly unidirectional torque. The use of the single-winding motor just described is acceptable in drive systems up to power levels of ~ 100 W.

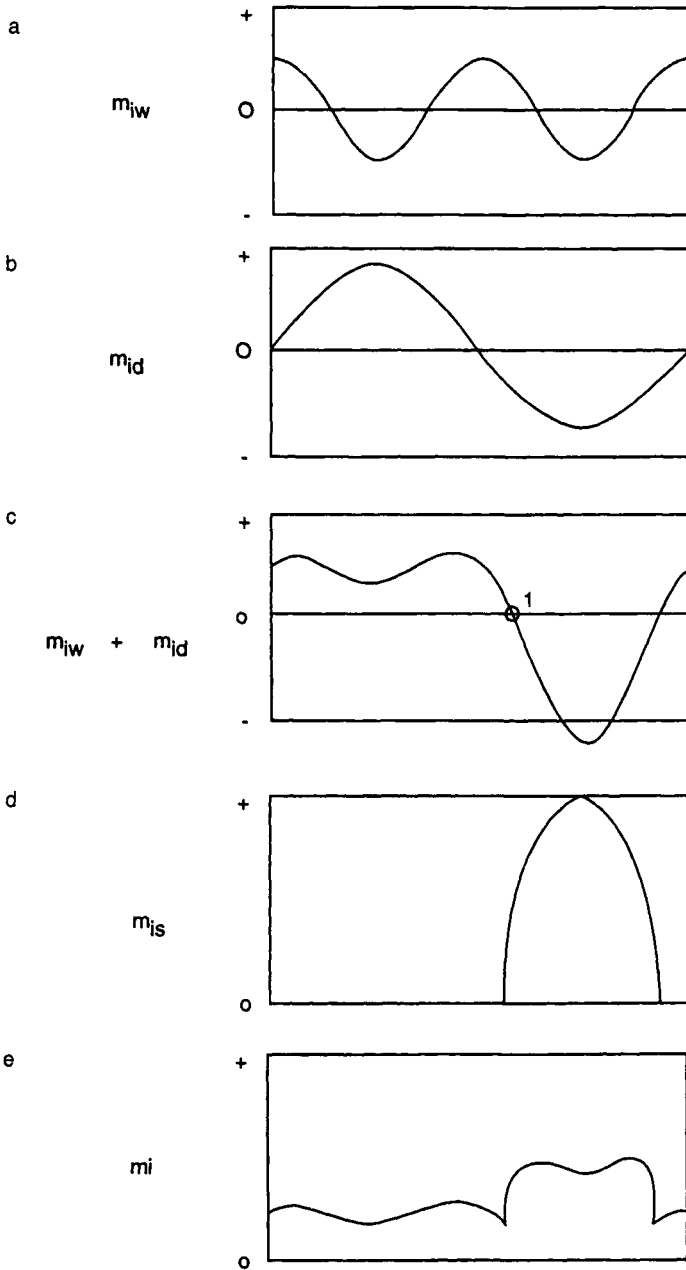


Figure 9.30 Component torques m_{iw} , m_{id} , $m_{iw} + m_{id}$, m_{is} and gross torque m_i as a function of rotor position α

Brushless DC motors with reluctance rotors are being developed alongside those with permanent magnet rotors described above. Figure 9.31 shows one such motor with a 6-pole rotor whose active material is simply soft iron. Through cyclic switching of the stator coils 1–4 by means of semiconductor switches S1, S2, etc. the rotor is set in motion.

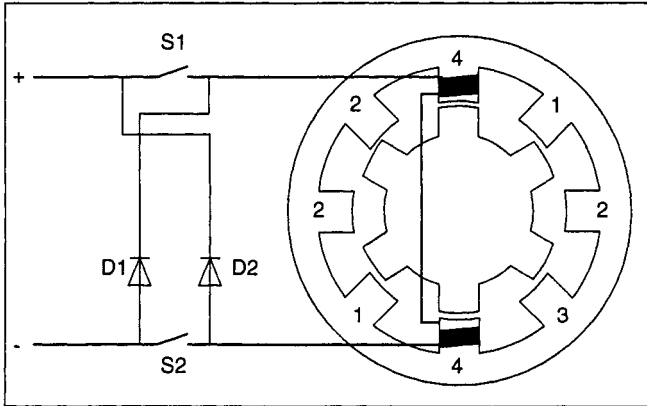


Figure 9.31 Switched reluctance motor
 1 ... 4 stator pole pairs
 S1, S2 semiconductor switches
 D1, D2 freewheel diodes

Chapter 10
**Stepper motors –
principles and applications**

H. Krauss

10.1 Introduction

There are several types of stepper motor currently available, with permanent magnet or soft-iron rotors, and there are hybrids. Permanent magnet stepper motors have found the widest application because they have good dynamic and static characteristics and a relatively high efficiency. Also, they have a static holding torque when not energised, which the soft-iron rotor motor does not have. A further advantage is that they have good damping. Therefore the following discussion is limited to stepper motors with permanent magnets and to hybrid motors.

The characteristic property of the stepper motor is the step-by-step turning of the motor shaft. One complete turn of the shaft is made up from an exactly specified number of steps, which is determined by the motor design. This property meets the requirement for operating directly from digital signals. The stepper motor can thus be the bridge between digital information and incremental mechanical displacement. If a stepper motor drive is to be secure and interference-free, certain fundamental points must be taken into account.

Drive systems with stepper motors bring together the following properties:

- 1 precise step-by-step positioning – without feedback – following a predetermined number of control pulses
- 2 high torque at low speeds, and with single steps
- 3 in a powered standstill condition a large holding torque with self-locking.

Problems occur in stepper motor drives during starting, accelerating, decelerating and stopping, and these are associated with the dynamic structure of the drive.

In stepper motor drive systems attention must therefore always be paid to the characteristics of the stepper motor itself, the mechanical system to be

driven and the necessary electronic control circuits, because all three together determine the dynamic structure of the system.

Position setting drives can be effected without feedback, i.e. with open loop control. Then there are none of the problems of closed loop control, particularly that of instability. But stepper motors are also found in closed loops and, in certain applications, produce very good results.

A 2-phase stepper motor can cause oscillation problems when operated at and around its natural resonant frequency, in which case damping must be incorporated somehow. Further, there are transients during stopping which result from the dynamic properties of the motor and its load and from the control circuits. If at the design stage of a system with stepper motors certain fundamental points are taken into account, the dynamic problem can be largely overcome and a neat dynamically excellent drive system can be built up that fully justifies the cost of the electronic controls.

10.2 Modes of operation

10.2.1 Principle of function

The mode of operation of a stepper motor may be explained as a simple example of the 2-phase principle (Figure 10.1). Two possibilities for the

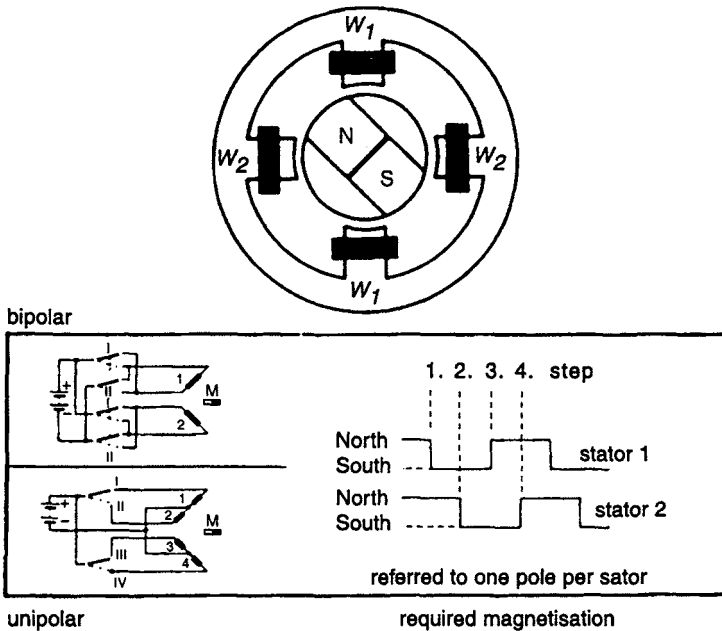


Figure 10.1 Schematic construction and two ways of switching a stepper motor (See also Figure 10.21)

excitation of windings W1 and W2 are discussed: bipolar, in which winding W1 and similarly W2, comprises one coil distributed over two poles; and unipolar, in which W1, and similarly W2, is made up of two component coils. Nowadays the excitation switching is by means of electronic circuits, which generate a rotating sequence of control pulses.

Figure 10.2 shows the static torque/rotor angle curves for the situations:

- I current through coils W1 only
- II current through coils W2 only
- I' reversed current through coils W1 only
- I+II equal currents through coils W1 and W2 simultaneously
- I'+II reversed current through W1 and normal current through W2.

The last two curves show that, when the current in one stator coil, say W1, is reversed, the torque/angle curve shifts by 90° and the rotor turns 90° to the next statically stable position.

Figure 10.3 shows this same action in another way, with the rotor and stators linearly developed and the stators separated.

10.2.2 Static performance of stepper motors

10.2.2.1 Static torque curve

The static torque curve of a stepper motor is one of its more important characteristics. This curve is obtained by turning the rotor through the angle ϕ and measuring the torque necessary for holding the rotor at that angle. As an example, we choose a 2-phase motor with only one stator winding being energised. In this case the rotor positions itself as shown in Figure 10.4, the rotor S poles standing under the stator N poles. In Figure 10.4 only one S pole has been shown for simplicity.

To bring the rotor out of its stable alignment an increasing torque must be applied. The torque/angle curve approximates closely to the first quarter of a sine curve. The peak value M_K is the pull-out torque of the motor, and ϕ_K is the pull-out angle.

If the load torque on the motor shaft exceeds M_K , then the motor turns through the unstable region and stops at the next stable point if, meanwhile,

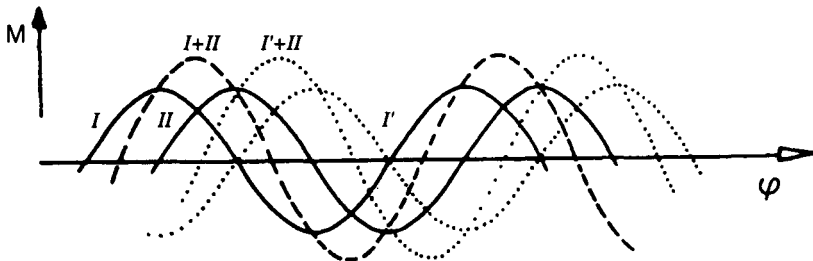


Figure 10.2 Composition of the static torque curves

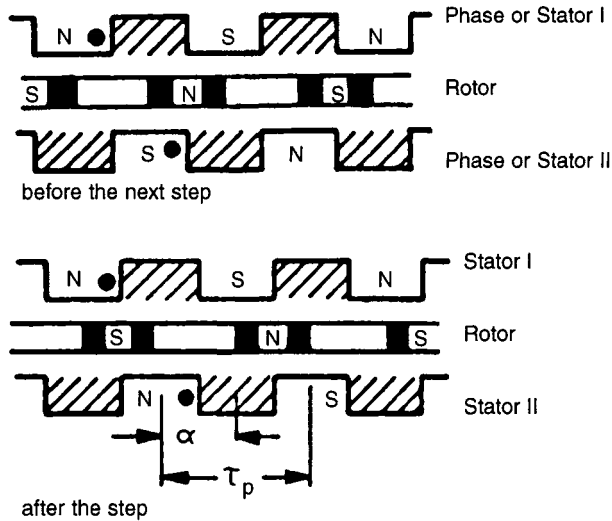


Figure 10.3 *Developed view of the two stators and rotor ring*

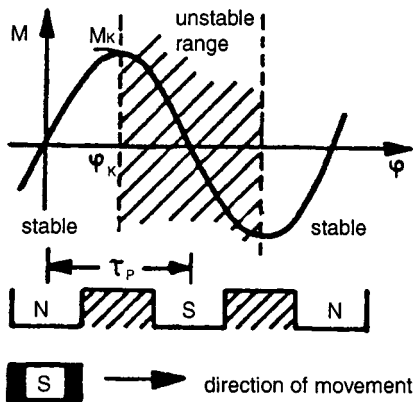


Figure 10.4 *Schematic development of a static torque curve*

the load torque has fallen below M_k . If not, the rotor continues to turn in a lumpy fashion and accelerates to an unpredictable speed. The situation is similar when both phases are energised.

The static torque curve for the whole motor is obtained by the addition of curves for the individual stator windings (phases) of torque as a function of displacement angle ϕ . Fig 10.5 shows the addition in a 2-phase motor. Figure 10.6 shows the addition in a 5-phase motor. The important difference in both curves is the contribution of the individual phases to the peak value M_H of the static torque curve of the whole motor.

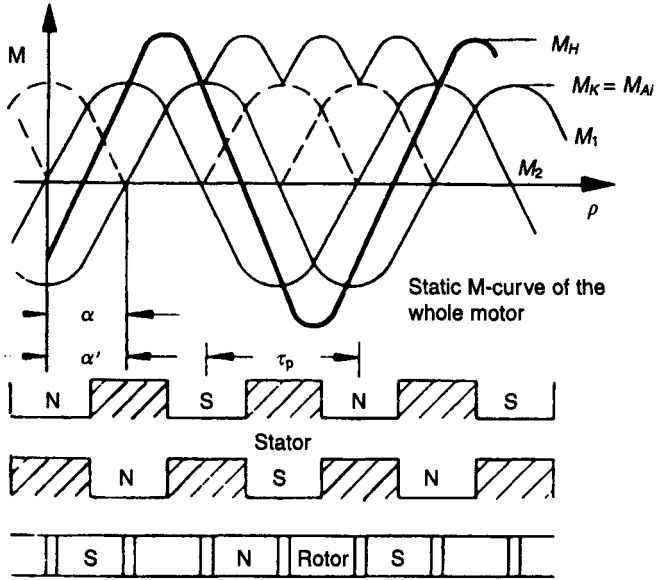


Figure 10.5 Static torque curve in a 2-phase motor

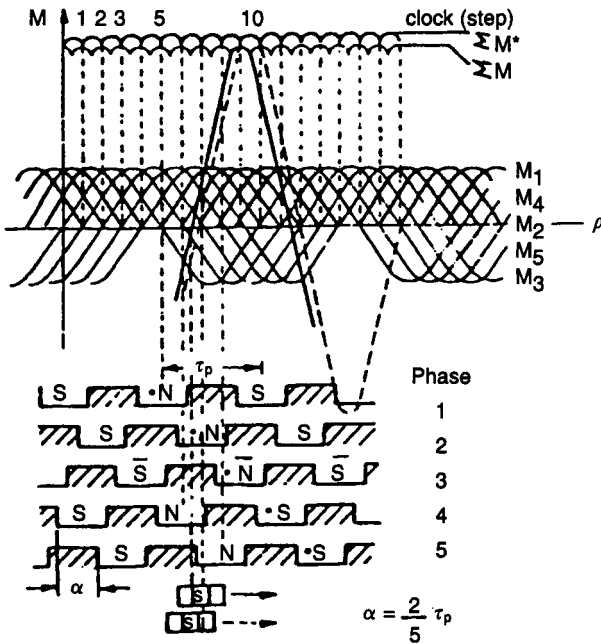


Figure 10.6 Static torque curve in a 5-phase motor

In a 5-phase motor there is very little difference in M_H if either four or five phases are energised simultaneously. The contrast between this and the 2-phase case is clearly seen.

The relationship between the motor's holding torque and its pull-out torque in a single stator is:

$$\begin{array}{ll} \text{in 2-phase motors} & M_H = \sqrt{2} M_K \\ \text{in 5-phase motors} & M_H \approx 3.1 M_K \end{array}$$

The static torque characteristic dictates the entire motor performance. The M -curves run through the negative torque region as well as the positive. Under stepper drive control, it is necessary that only positive torques are developed. The sequence, direction and timing of the stator coil currents are specified to achieve this. Whenever the M -curve of an individual coil would cross zero there must be a reversal in the direction of current flow. The static M -curve as a function of α then proceeds as a pulsating torque, as is shown in Figs. 10.5 and 10.6. For the 5-phase motor, M_1 – M_5 are the component torques from the five stator phases. ΣM^* is the holding torque obtained when five phases are energised and ΣM is when four phases are energised.

The mathematically inclined reader will enjoy confirming that the peak value of torque for five energised phases is

$$M_H = \{1 + 2 \sin(90^\circ - 36^\circ) + 2 \sin(90^\circ - 72^\circ)\} M_K = 3.24 M_K$$

and for four energised phases is

$$M_H = \{2 \sin(90^\circ - 18^\circ) + 2 \sin(90^\circ - 54^\circ)\} M_K = 3.08 M_K$$

10.2.2.2 Step angle accuracy

When the M -curves of the individual stator windings all have the same form and peak value, the step angle in both loaded and unloaded rotor conditions is the same as the design value. When the M -curves are dissimilar, angular discrepancies occur. Figure 10.7 shows an (exaggerated) example of unequal peaks M_{K1} and M_{K2} in a 2-phase motor and the resultant unequal angles between the cusps of the combined torque/angle curve. In a 2-phase motor the angular change after each pair of steps is always the same amount. Similarly, the angular increment of the rotor of a 5-phase motor after five steps is consistent. Small angular errors can occur owing to manufacturing tolerances, some positive and some negative and adding up to zero around the complete stator.

It is possible to adjust the individual phase coil currents externally in such a way that the motor angular steps are equal. However, the designer/user must be very careful to make sure that current trimming does not introduce new unknown errors in the angles.

On the other hand, controlled unequal currents in phases 1 and 2 may be used for fine-setting the rotor between the normal step positions. Any rotor setting angle between $\varphi = 0$ and $\varphi = \alpha$ may be achieved. It is also possible to

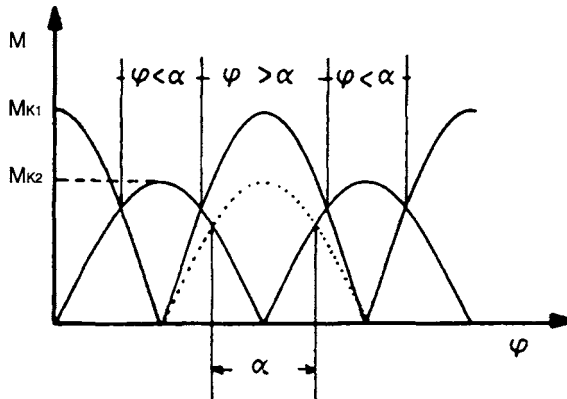


Figure 10.7 Static M -curve with unequal peak values

achieve discrete intermediate rotor positions by means of appropriate partial phase current switching.

Step angle accuracy and static load angle are related. The 'load angle' is the consequence of a static load on the motor shaft. This causes a 'load angle error' depending upon the nature of the load. There are two cases to be considered:

- 1 If a motor should take n steps and the load torque is applied (or changes) during the process, then the rotation $n\alpha$ is altered by an amount β . Depending upon the sense of the load torque, β may be positive or negative.
- 2 If rotation in one sense produces an error angle β and then both the sense of rotation and the load torque are reversed, the error in the angle then traversed is 2β . This is always the case with friction loads. This problem must be taken into account during the building of a system and, as necessary and where possible, eliminated.

A further point in relation to step angle accuracy is that differences can occur between the rotor positions of a motor with energised or unenergised stator coils. Depending upon the rotor permanent magnet distribution, the unenergised motor has a static torque curve with peak value M_s , self-holding torque. The unenergised torque curve, however, has double the (spatial) frequency of that of the M -curve of the energised motor.

The above paragraph is best appreciated when read with one eye on Figure 10.8.

If the rotor in Figure 10.8 is in a position A or C before stator energising takes place, then the energising causes no movement of the rotor. However, if the rotor is in the stable position B before energising, subsequent energising puts the rotor into an unstable state and it jumps two steps to the left or to the right depending on the direction of the load torque. It is therefore recommended that, in a drive system containing a stepper motor,

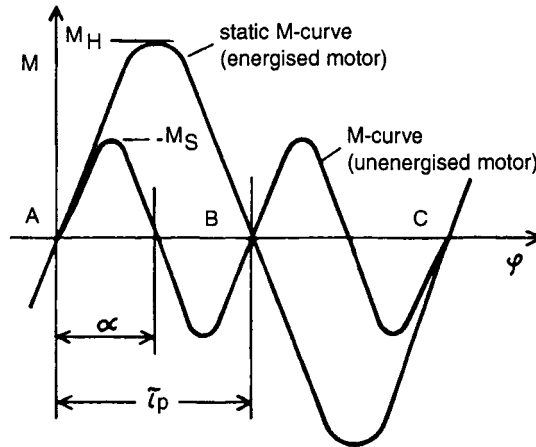


Figure 10.8 Comparison of the static M-curve with energised and unenergised stator

the motor is never left in the unenergised condition after ending a work cycle.

10.2.3 Dynamic performance

10.2.3.1 Torque/step frequency performance

The maximum torque obtainable at the shaft is the holding torque M_H . The motor shaft may be loaded with torque M_H at standstill only. During stepping, the load torque may not exceed the level of the cusps, known as M_{Ai} in Figure 10.5. These are the lowest points of the combined torque/angle curve. Even M_{Ai} cannot be fully achieved on account of friction torque in the motor.

When the stepping frequency is low, the kinetic energy of the motor and its load is insufficient to carry the motor through the trough in the torque curve, so that, as is depicted in Figure 10.9, the available torque depends upon the stepping frequency. 5-phase motors do not present the same problem and the torque is constant at low stepping frequency as the ripple on the pulsating torque curve is small. Figure 10.11 gives a comparison between two measured curves of this kind: for a 2-phase motor and for a comparable 5-phase motor. The broken curve relates to a 5-phase motor running at the same speed as the 2-phase motor.

On account of the finite rate of current change in the stator coils (determined by the time constants of the motor windings and their drive circuits) and of rotor-induced voltages, the torque falls off with increasing stepper frequency. The curve thus obtained is the in-service limiting torque curve. If the stepper frequency is increased beyond the boundary of the curve, then the motor falls out of step and comes to a standstill.

To bring the stepper motor into motion, its moment of inertia must be accelerated. The torque stepper frequency curve therefore falls into two zones: starting and accelerating. (The accelerating range is usually referred to as the 'slew' range of operation.) The starting zone is given for the motor alone without the external load referred moment of inertia.

Within the given starting torque boundary curve, and taking the given friction load into account, it is possible to get the motor started from standstill with an appropriate stepper frequency, without its falling out of step.

As Figure 10.9 shows, the starting zone diminishes as the load moment of inertia increases. Figure 10.10 shows the relationship between maximum permissible load moment of inertia and the stepping frequency. With these curves it is easy to determine the starting frequency for a given moment of inertia and from this the approximate starting performance.

A working point inside the acceleration zone can only be achieved by means of a steadily increasing stepping frequency (beginning at a frequency from within the starting zone). Whilst the inertial masses are being accelerated (moment of inertia = J) a torque M_b is needed throughout the acceleration zone.

The equations are $M_b = Jd\omega/dt$ and $M_b = M_{Bm} - M_{Am}$ (without external load torque M_L).

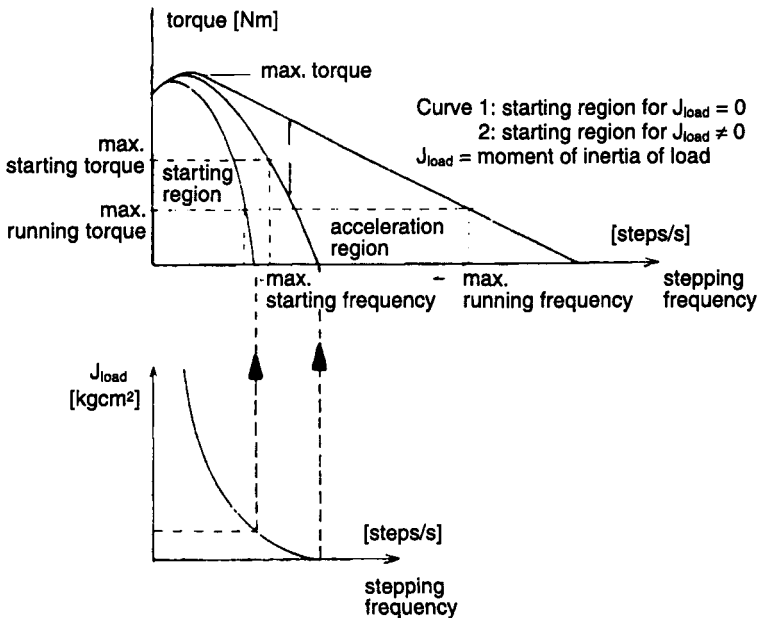


Figure 10.9 Torque as a function of stepping frequency and some important definitions

Figure 10.10 Maximum permissible load moment of inertia as a function of stepping frequency for correct start and stop performance

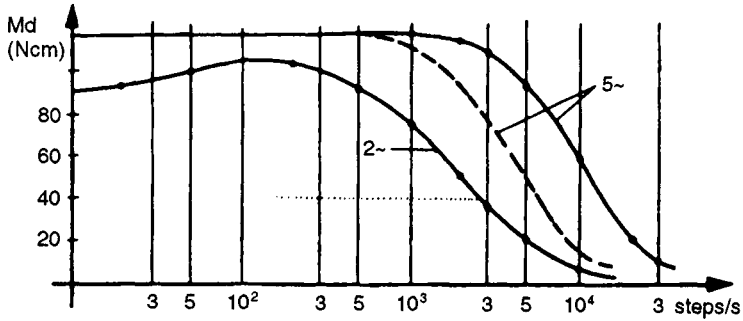


Figure 10.11 Torque measured as a function of frequency for a 2-phase motor and a comparable 5-phase motor

10.2.3.2 Acceleration and braking

For a given load torque M_L and moment of inertia J the stepping frequency f_1 in the starting zone may not jump abruptly to f_2 in the accelerating zone because the motor could fall out of step. Figure 10.12 shows the basic action sequence. When the starting frequency is f_1 , torque M_{b1} is available. This torque diminishes to M_{b2} at f_2 . There are several possibilities for using the available torque M_b , which falls off with increasing stepping frequency (Figure 10.13). Two cases are examined here more closely: the full usage of M_b and the usage of just M_{b2} .

Full utilisation of M_b : To simplify the analysis and applying the Figure 10.12 data, the following assumptions are made. The frequency f_2 shall equal the

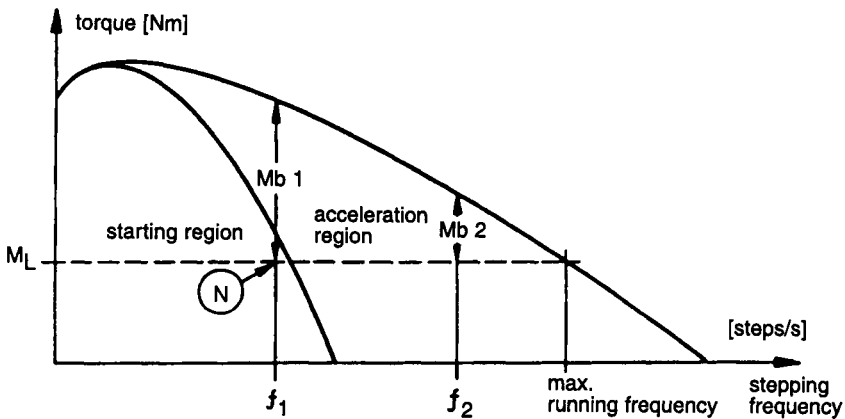


Figure 10.12 Principal representation of the acceleration of a motor loaded with torque M_L
Stepping frequency increases from f_1 to f_2

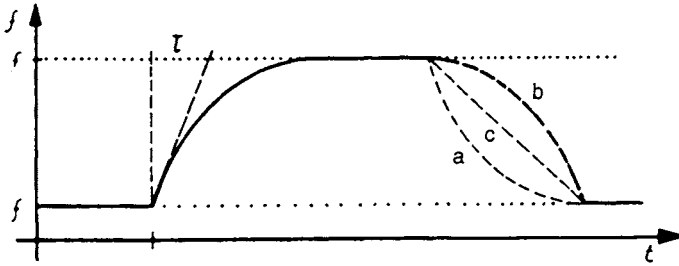


Figure 10.13 Stepping frequency as a function of time during acceleration and braking

maximum running frequency and consequently $M_{b2} = 0$. The change of torque as a function of stepping frequency between f_1 and f_2 may be considered to be linear. A closer approximation using a parabola is not necessary.

Let the point N be the starting point for the following analysis. Under these conditions the acceleration can be calculated with the help of the following differential equations:

$$M_{b1} \left(1 - \frac{f}{f_2} \right) = J \frac{\pi \alpha^\circ}{180^\circ} \frac{df}{dt}$$

in the range of validity $0 < f < f_2$, where $f = 0$ when $t = 0$ (N being the starting point).

The solution is $f = f_2 \{ 1 - \exp(-t/\Gamma) \}$, where

$$\Gamma = \frac{J \pi \alpha^\circ f_2}{180^\circ M_{b1}}$$

This is an exponential function that is easily realised in an electrical circuit. If the simplification $M_{b2} = 0$ for the purposes of simplifying the analysis were applied in practice, the motor would, theoretically, never stop. Therefore some remaining M_{b2} must be retained.

Utilisation of M_{b2} alone: For various reasons present practice is to strive for linear acceleration and braking. This, however, permits only the use of $M_{b2} = M_{b \min}$ (Figure 10.12). Braking and acceleration may then be calculated in the same way because the only difference between them is the algebraic sign. In many cases, external friction plays a part, in that it assists braking and hinders acceleration.

Let

$$f = f_0 \pm \frac{df}{dt} t$$

where f_0 is the stepping frequency used as a reference. The maximum possible rate of change of frequency is derived from

$$\frac{df}{dt} \leq \frac{M_{\min}}{J} \frac{180^\circ}{\pi\alpha^\circ}$$

If a change from linear acceleration to linear braking is called for, without a pause at constant velocity and constant stepping frequency, the condition

$$\frac{df}{dt} \leq \frac{1}{2} \frac{M_{\min}}{J} \frac{180^\circ}{\pi\alpha^\circ}$$

must be met.

Note that the largest frequency change occurs when the motor reverses from its normal direction of rotation. This reversing region normally lies beneath the starting region. In some situations rotor hunting may be exploited in order to achieve reversal during negative acceleration. By this means reversing can be achieved in the starting region as well.

The above note becomes clearer after the discussion on Figure 10.19 has been read.

10.2.3.3 *Optimal frequency for average velocities*

The requirement in the majority of drives is to achieve the highest possible average speed. For the stepper motor this means making a definite number of steps in the minimum possible time t_A . When the number of steps is high, it is clear that as high a stepping frequency as possible is the objective. This is not the case, however, for low and medium step numbers. As is seen from Figure 10.14, given linear acceleration and braking, the condition

$$\frac{df}{dt} \leq \frac{M_{b\min}}{J} \frac{180^\circ}{\pi\alpha^\circ}$$

must be met.

In many cases the decrease in torque may be taken to be a linear function of the stepping frequency to a good degree of approximation (Figure 10.15).

The company 'Berger' publishes Figure 10.15 for its 5-phase stepper motor RDM 596/50. As can be seen, in the frequency range $f_m > f_0$ (f_0 is dependent

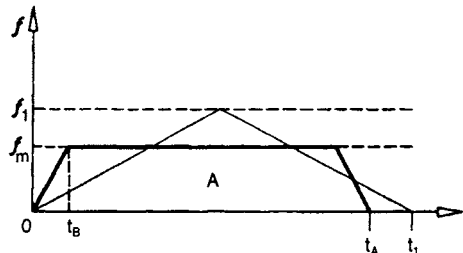


Figure 10.14 *Example of linear acceleration of a stepper motor*

$$f_1 = 8 \text{ kHz with } M_{b\min} = 3 \text{ N cm}$$

$$f_m = 5 \text{ kHz with } M_{b\min} = 9 \text{ N cm}$$

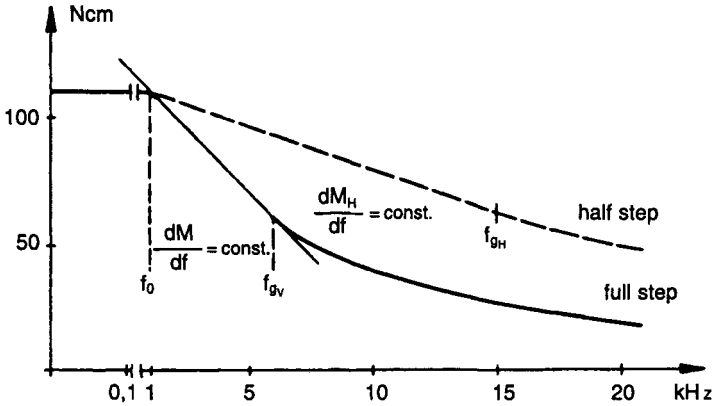


Figure 10.15 Representation of torque M as a function of the stepping frequency with an approximately linear fall-off in torque for motor type RDM 596/50

on the motor and can, for instance, be zero) the following equations are applicable for the torque M_b :

$$M_b = M_0 - K(f_m - f_0)$$

in which $K = dM/df = \text{constant}$.

Given the following substitutions:

$$B = J \frac{\pi \alpha^\circ}{180^\circ} \quad (J = \text{total rotor plus load moment of inertia})$$

$$C = M_0 + Kf_0$$

$A = \text{the path length in steps}$

the stepping frequency f_m for which the average velocity is a maximum is calculated to be

$$f_m = \frac{ACK - \sqrt{ABC^3}}{AK^2 - BC}$$

and the time t_A taken for these steps is

$$t_A = \frac{A}{f_m} + \frac{f_m B}{C - Kf_m}$$

These relationships are applicable to the situation in which the motor is started from rest and is stopped after taking A steps.

Convenient units are

Torque M in $N\text{cm}$

Moment of inertia J in $N\text{cm}^2$.

The acceleration and braking times are often of interest, and they may both be derived from the same equation. When the acceleration is linear,

$$M_b = M_0 - K = (f_m - f_0)$$

and the acceleration time t_h from $f = 0$ to $f = f_m$ is

$$t_{h \text{ lin}} = J \frac{\pi \alpha^\circ}{180^\circ} \frac{1}{M_{b \text{ min}}} f_m$$

The decelerating time is smaller because $M_{b \text{ min}}$ is increased by the external friction torque, when this is assisting the braking. In general, the acceleration time between $f = f_1$ and $f = f_2$ is expressed as

$$t_{h \text{ lin}} = J \frac{\pi \alpha^\circ}{180^\circ} \frac{1}{M_{b \text{ min}}} (f_2 - f_1)$$

When acceleration between $f = f_1$ and $f = f_2$ follows an exponential function by exploiting the total reverse torque in the acceleration mode and assuming that $dM_b/df = \text{constant}$, it follows that

$$t_{h \text{ exp}} = J \frac{\pi \alpha^\circ}{180^\circ} \frac{f_2 - f_1}{M_1 - M_2} \ln(M_1 / M_2)$$

where M_b at $f_1 = M_1$ and M_b at $f_2 = M_2$.

Suitable units are J in N cm s^2 , M in N cm . Approximating $g \simeq 1000 \text{ cm s}^{-2}$ gives $1 \text{ kg cm}^2 = 0.01 \text{ N cm s}^2$.

10.2.3.4 Single step and step sequence

Every stepper motor with its rotor moment of inertia and its magnetic turning forces may be considered as a damped oscillating system with a low damping factor. Hence, oscillations can occur and these are superimposed on the stepping motion.

When the motor is driven with single steps (Figure 10.20) the damped oscillations occur at every step. Depending on the stepping frequency, the oscillations so generated contribute negative and positive accelerations into the rotor. With high stepping frequencies the rotor shaft turns practically continuously. Figs. 10.17 and 10.18 show a few examples of the shaft movement of a stepper motor. Figure 10.17 shows the first six steps of a rotor shaft with various loadings. Curve 1 shows its progression off load. Curve 4 is when the motor has a friction torque load which is 40% of the full load torque. Curve 3 is when there is a relatively high external inertia torque and curve 2 is when there is also friction load torque present.

The static load angles have been left out in the determination of these curves. As Figure 10.16 shows, loading causes an 'error angle'. For a pure load torque this angle is very small, but it can be large during acceleration when there is an inertia torque. This 'error angle' is also called the 'dynamic load angle ρ '. It is necessary to distinguish between the ideal dynamic load angle

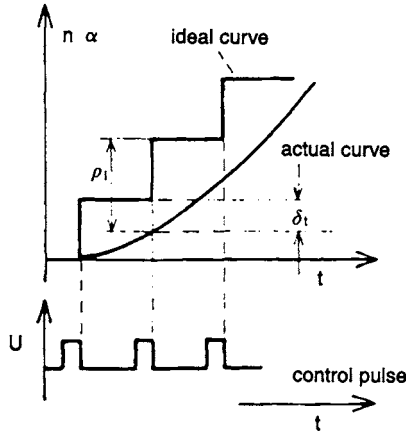


Figure 10.16 Schematic response

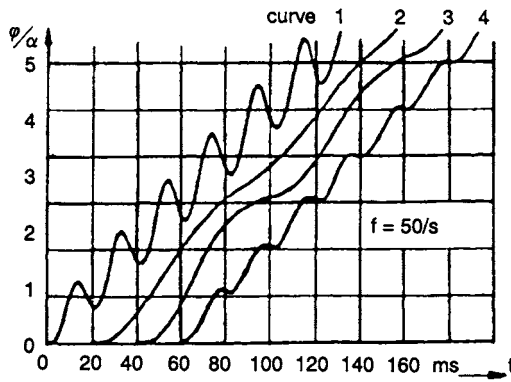


Figure 10.17 Six steps with various loadings

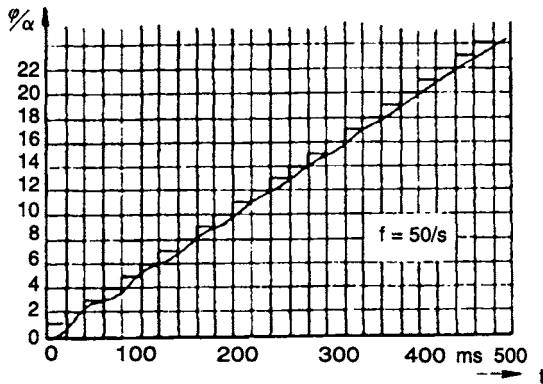


Figure 10.18 24 steps

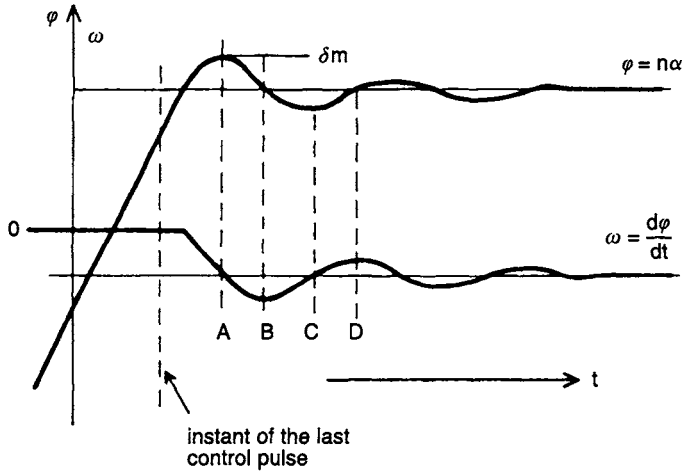


Figure 10.19 *Transient behaviour after the last step*

ρ_i and the expected load angle ρ_l (Figure 10.16). Often, this load angle can only be determined during the acceleration phase of the first step (Figure 10.17). What is important for the designer is that, after the n th control pulse, the angle traversed is only $n\alpha - \rho_l$.

The behaviour of the motor after the n th step is of particular interest. Figure 10.19 shows the oscillation of the rotor around the final position after the last step. The oscillation has the resonant frequency of the motor-load system. The maximum overshoot angle ρ_m depends on the instantaneous stepping frequency (speed), the rotor position, the static torque and the load. If the magnitude of ρ_m approaches that of the pull-out angle of the static torque curve (two steps for a 2-phase motor and five steps for a 5-phase motor), then the motors can go out of synchronism. Particularly unfavourable conditions are for an unloaded 2-phase motor and a stepper frequency at the resonance frequency or a harmonic.

With increasing excitation frequency the damping ratio of the system decreases with dependence on high internal circuit resistance. In 5-phase motors a drive at resonance frequency without auxiliary damping means is possible.

Use can be made of the fact that the load moment of inertia can influence the resonant frequency and the damping factor of the system.

10.2.3.5 *Stopping the stepper motor*

In many drive systems with stepper motors, auxiliary damping is unnecessary because there is sufficient already in the load. It may, however, be necessary to reduce the relatively long oscillating transient on stopping or, better, to remove it altogether.

It may be that, during this damped oscillatory 'tail', a new movement needs to be initiated. If friction proves insufficient, then an extra damping mechanism can be included, but then the entire dynamic performance and not just the oscillatory 'tail' would be affected. A further possibility for damping could be that a motor intended for unipolar circuitry could be energised in a bipolar manner. The unused coils could then be used to provide good auxiliary damping by means of continuously or intermittently (e.g. during stopping) short-circuiting these windings.

If the overshoot angle ρ_m is approximately equal to the step angle, then the overshoot angle can be reduced or sometimes completely eliminated. The rotor angle of turn as a function of time is illustrated schematically in Figure 10.19.

If the last pulse is applied at instant of time A (Figure 10.19), the rotor runs straight to its end position without any overshoot. Time B would be best if reversal were required, and time D for an immediate restart in the same sense of rotation.

The conditions for an oscillation-free stop are that (Figure 10.20):

- (i) the last control pulse is delayed until the instant at which the rotor reaches its first overshoot position following the penultimate control pulse ($n - 1$), and
- (ii) the first overshoot position coincides with a stable rotor position and the target position of the rotor.

The last control pulse then fixes the rotor in the required position.

In principle, it is possible to time the last two or three impulses so that no overshoot occurs. In the case of a 5-phase motor it may happen that the last impulse must involve more steps, because an overshoot of more than one step

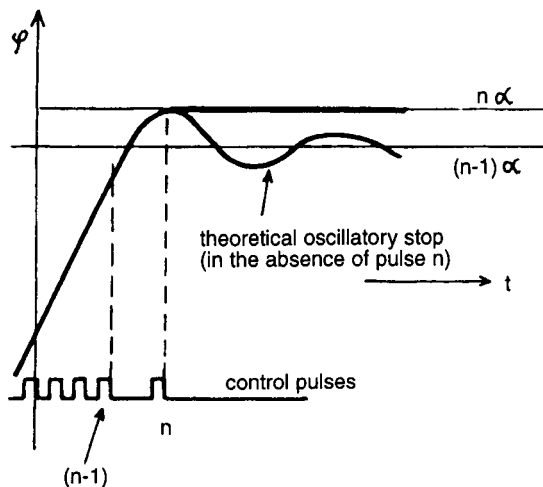


Figure 10.20 Transient behaviour given a delayed last step impulse

is possible. In every case, however, in which the first overshoot occurs close to a step position, timing the last impulse to correspond with this rotor position considerably improves the motor's stopping transient performance.

10.3 Electrical control circuitry

10.3.1 Methods of control

The torque/stepping frequency performance of the motors is highly dependent on the control circuits. Therefore in the following analysis the fundamental types, unipolar-drive and bipolar-drive, are discussed (Figure 10.21). Particular attention is drawn to the fact that the manufacturers' published motor characteristics apply only when the motor is connected in the accompanying drive circuit.

10.3.1.1 Unipolar drive

In the unipolar drive circuit each phase comprises two separate coils. The end of one coil connected to the start of the other coil represents the midpoint of the winding and it is connected firmly to one terminal of the

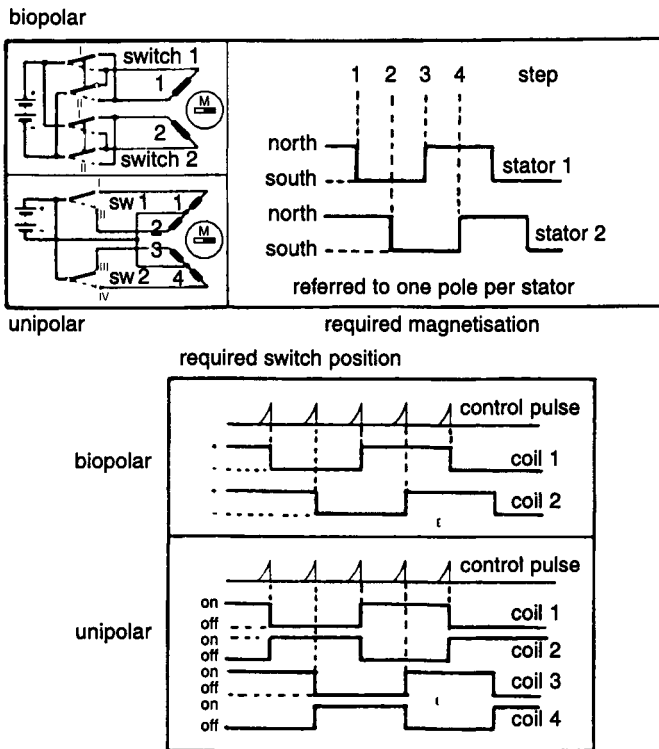


Figure 10.21 *Unipolar and bipolar drive*

power supply. The open ends of the coils are connected alternately to the other terminal of the power supply via the electronic equivalent of a single-pole changeover switch (see sw 1 and sw 2 in Figure 10.21).

As Figure 10.21 shows, only one phase is switched per switching operation or step. For example, when unipole sw 1 changes from position I to position II, a reversal in the magnetic field controlled by the winding takes place. In order to realise this switching electronically, two output-transistors per phase are necessary.

Two circuits showing the principle of unipolar drive switching along with the appropriate switch status at each step are shown in Figure 10.22. In this circuit each stator phase has a winding with two identical elements. Only one winding element carries current at a given instant. Because only half the volume of copper is in use at any one time the power to weight ratio of the motor is low. Four switching transistors are necessary.

An interesting variant, particularly suited to low power stepper motors, is shown in Figure 10.23. Two advantages from the bipolar and unipolar circuits are combined, namely a single coil per phase and only four switches. The necessary resistors do not represent an unreasonable initial extra cost. The extra I^2R loss, however, is considerable and the efficiency is very low.

10.3.1.2 Bipolar drive

In the bipolar controlled circuit each phase possesses just one energising coil. Thus there must be provision for changing the voltage at both ends of the coil. Hence four transistors are required per phase for switching.

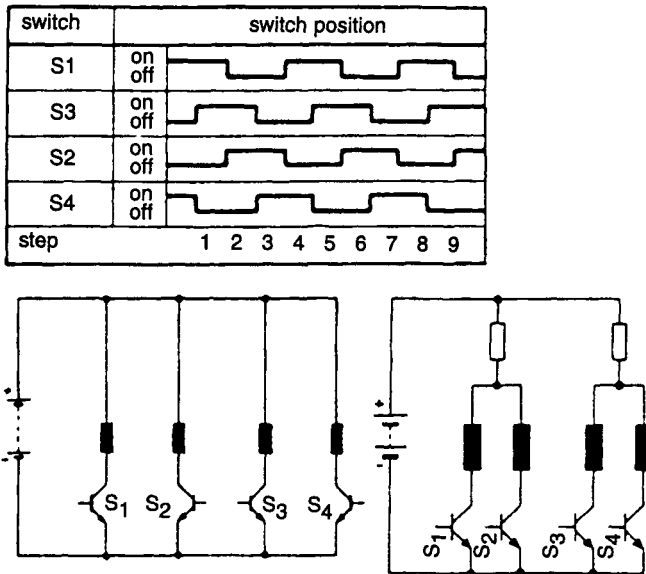


Figure 10.22 Unipolar drive circuit principle

The principles of the bipolar control circuit and the corresponding switching states are illustrated in Figure 10.24. The circuit contains only one coil (two connected in parallel for a lower inductance) per stator phase. Thus the total volume of copper is employed for developing the magnetic field. The resultant inductance is large, however. To achieve an acceptable time constant, resistance must be connected in series with the inductive stator windings. By this means the flux build-up is accelerated and the torque is maintained up to higher stepping frequencies. Eight power switching transistors are needed in the circuit.

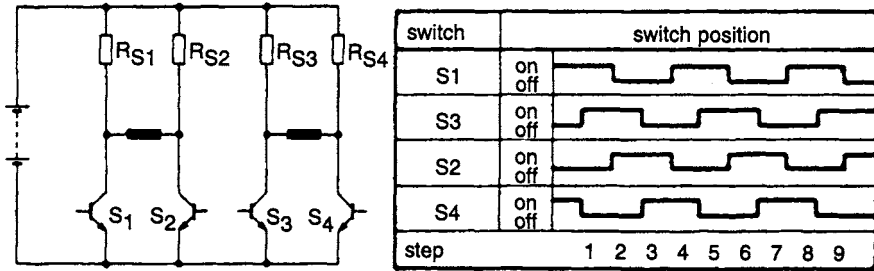
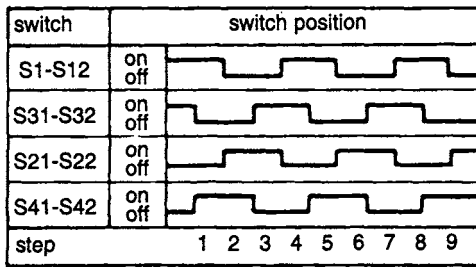


Figure 10.23 *Low power drive circuit*



(full step)

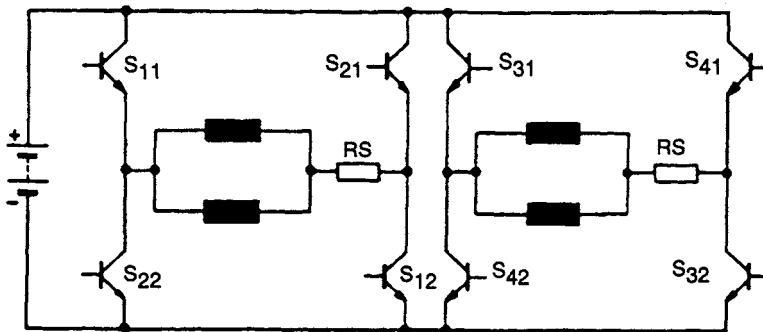


Figure 10.24 *Basic circuit for bipolar control*

10.3.1.3 Five-phase motor drive

Because the difference in peak holding torque is small, whether four or five phases are energised, a comparatively simple bipolar drive circuit, as shown in Figure 10.25, is effective. The five phases are connected in a closed ring and each node is connected to the midpoint of a two-transistor cascade circuit. At any instant, only four out of the five coils are simultaneously energised for full-step operation. The holding torque for a full-step drive $M_{f5} = 3.08 M_{\max}$ and that for a half-step drive $M_{h5} = 3.24 M_{\max}$. Attention is drawn to the similarity between these equations and those at the end of Section 10.2.2.1.

It is worth mentioning that the nonexcited coil out of five has both ends connected to the plus or minus terminal of the power supply via conducting transistors and is thus effectively short-circuited. This short-circuited coil contributes usefully to the damping, whether or not there is a resistor connected in series.

10.3.2 Semiconductor power switch with inductive load

To switch the individual phases, power switches are necessary, which still comprise only transistors. Both bipolar and MOS transistors are applied to this task. The torque/speed performance is highly dependent on the speed at which the stored magnetic field energy can be built up and removed. The switching transistor characteristics play an important part here.

Current in the coils changes, according to the normal rules of inductive circuits, in an exponential manner, to which the applicable equation is

$$i = \frac{U}{R} \left[1 - \exp(-t/T) \right]$$

where

$$T = \frac{L_w}{R_w} = \frac{\text{coil inductance}}{\text{coil resistance}}$$

Because the switch is in series with the coil, the transistor switching with its accompanying freewheel diodes has an influence on the torque-stepping frequency performance. To drive the windings, therefore, a principal aim is to provide a circuit which delivers the fastest possible build-up of current, which means that it should have very high internal resistance. This is not always achievable on economic grounds, and a compromise must be arrived at. However, if a fall-off of torque at higher stepping frequencies is to be avoided, current forcing through the coils should be attempted.

In all transistor switches with inductive loads there is the problem of the switching-off transient, which often exceeds the peak instantaneous voltage parameter of the transistor. Protection circuits are then necessary, and these have a damping effect on the motor because they increase the time constants of the coil circuits in which they are working. Some examples of overvoltage protection are shown in Figure 10.26.

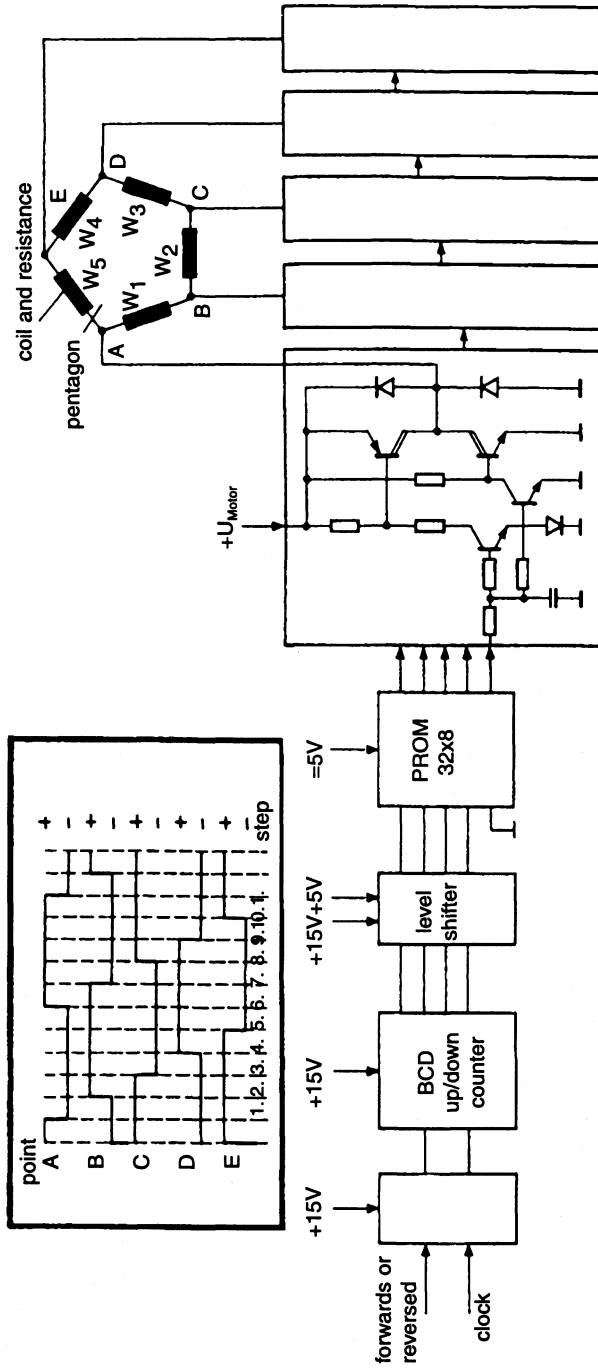


Figure 10.25 Full step 5-phase motor drive circuit

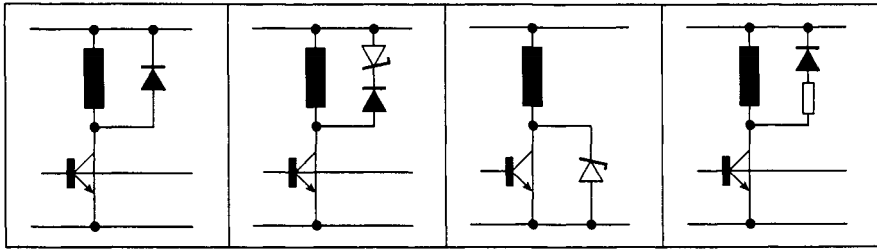


Figure 10.26 Transistor switching circuits, inductively loaded and with protection against overvoltage

Furthermore, the switching-off times of the transistors must be considered. Depending on the phase difference between switch-off voltage and switch-off current, the power dissipation peaks can become very large. These can destroy the transistor by driving it into the secondary breakdown mode. Transistors must be operated within the 'safe operating area'. MOS transistors can be advantageous here.

10.3.3 Control circuits

10.3.3.1 Switching stages

Switching stages may be built up from normal (bipolar) or from MOS transistors. Each transistor type has its advantages and disadvantages. Bipolar transistors have high switching losses and need a higher input power but have a lower on-state dissipation.

MOS (unipolar) transistors have lower switching losses and do not suffer from secondary breakdown. The input power required is low but they have higher on-state dissipation. In many circuits their parasitic diode works disadvantageously.

The basic circuits using bipolar transistors are discussed. These circuits can, of course, be modified to suit MOS transistors.

Figure 10.27 shows a simple circuit with no extra features. It does not deviate from the customary transistor switching circuit, except for the addition of the diode peak voltage limiting components. The Zener diode D_z in series with D_1 is effective only when the inductive-coil switch-off voltage exceeds the Zener inverse turn-on voltage U_z . For voltages less than U_z , the motor coil time constant remains low (see equation $i = f(t)$ in Section 10.3.2). Figure 10.28 shows part of a bilevel circuit which works more economically than a circuit with series resistance. It requires two voltages U_1 and U_2 , however. U_2 becomes effective at the instant at which the higher voltage U_1 is switched out by a signal from SWS. This occurs when the winding current reaches a predetermined value.

Another form of drive is the 'transistor chopper', the essentials of which are depicted in Figure 10.29. In this circuit a relatively high voltage is applied

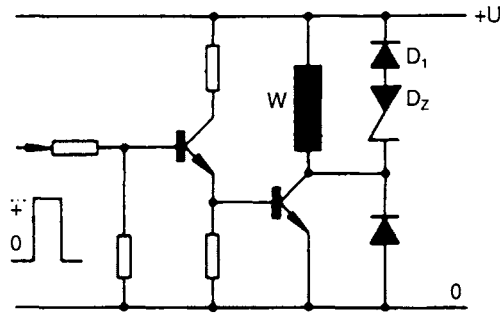


Figure 10.27 *Basic circuit for driving a stepper motor stator coil*

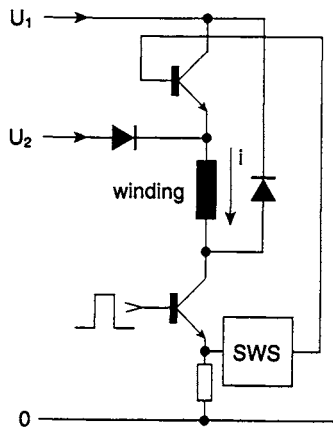


Figure 10.28 *Bilevel circuit*

as a series of impulses in such a manner that the maximum designated coil current is not exceeded, so that no thermal overloading occurs in the motor.

For low power and medium power motors, supply from a constant current source is possible and acceptable, along the lines of Figure 10.30. The circuit has the same effect as a large series resistor. Of course, the circuit requires a second higher voltage rail U_2 , which, together with storage capacitor C , presents a sufficiently large voltage at the instant of 'firing'. In the steady state U_1 is operative. In this way the power loss dissipation can be reduced considerably, which would otherwise have to be absorbed by the transistor.

Many semiconductor component manufacturers offer integrated circuit stepper motor drives.

For example:

VALVO	SAA 1027
Siemens	TCA 1560/61
SGS	L292, L293, L298

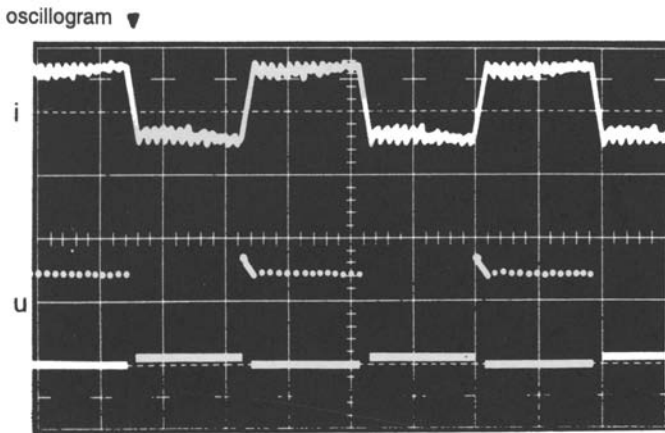
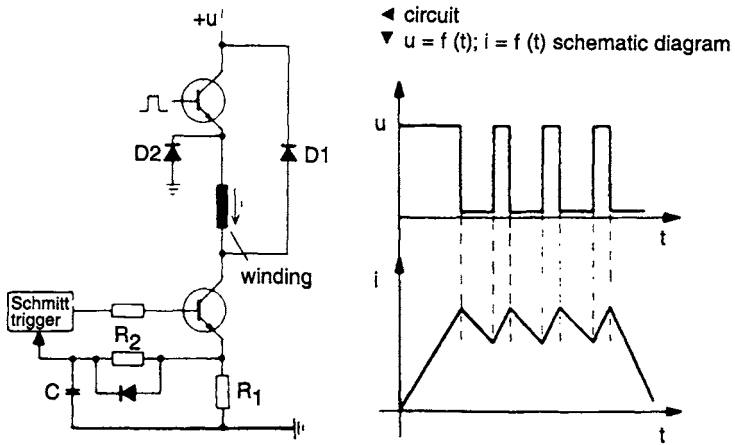


Figure 10.29 Switching control circuit for a stepper motor

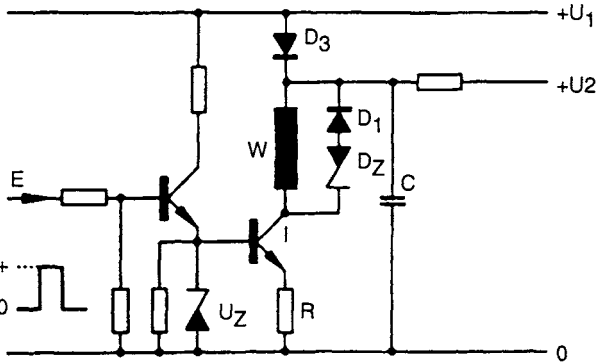


Figure 10.30 Constant current source for driving low-power motors

L292 is particularly interesting insofar as an analogue input signal enables a continuous adjustment of output current. Many innovations may be expected.

10.3.3.2 Circuits for producing the switching sequences

As already explained, each stator coil must be energised via a switch and in sequence. This is achieved by means of a ring counter. The counter is so designed that an auxiliary input signal reverses the sequence of counting and thus reverses the sense of rotation of the motor.

In a 2-phase motor with a four-part cycle this is particularly easy to arrange, as the basic circuit for unipolar control of Figure 10.31 shows. An integrated circuit is available for this switching function with sufficient built-in capability for driving small motors. Correspondingly, a 5-step ring counter is needed for energising a 5-phase motor (Figure 10.25).

With the circuit elements described so far it is possible to build up a basic drive circuit for stepper motors, as shown in Figure 10.32. It is worth mentioning that separate power supplies for the motor and the control electronics are recommended.

10.3.3.3 Control circuits for acceleration and braking

Various demands are made on the control function generator depending upon the motor's duty. For starting and stopping only, a fixed frequency generator suffices. For motor acceleration and braking, acceleration and

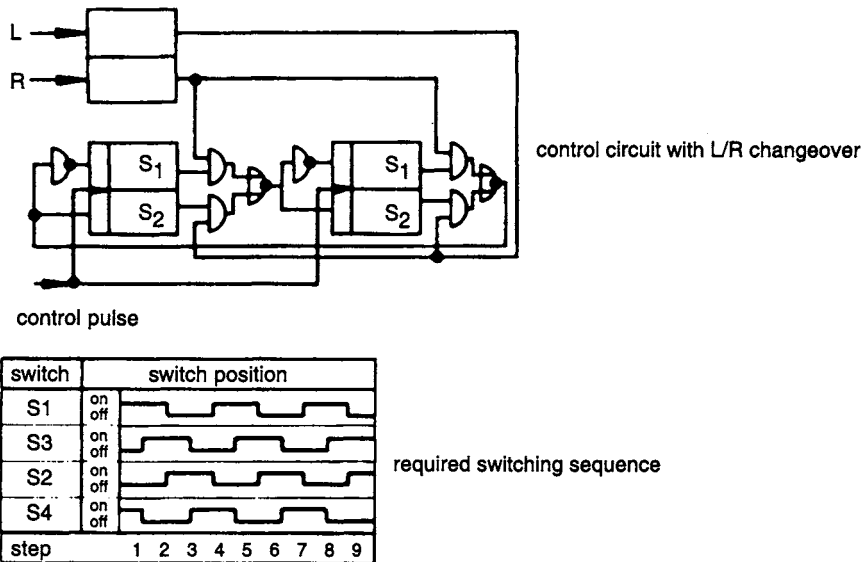


Figure 10.31 *Circuit for unipolar drive of a 2-phase stepper motor*

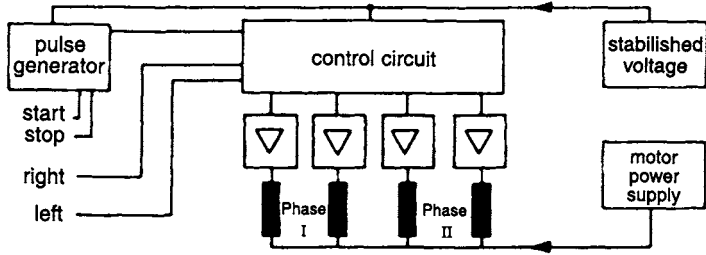


Figure 10.32 Basic circuit for stepper motor drive

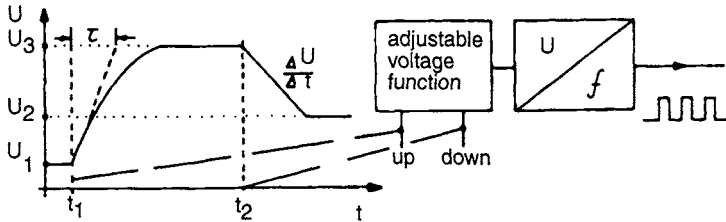


Figure 10.33 Schematic representation of a variable frequency generator for accelerating and braking a stepper motor

deceleration of the generator frequency is necessary. To this end an analogue voltage/time function generator may be used to drive a linear voltage/frequency converter. At instant t_1 a voltage function must start from a preset value U_1 and increase in a linear or exponential manner to voltage U_3 . At a second instant t_2 the voltage function must start falling – generally in a linear manner – and arrive at U_2 . Thus the values of t_2 and $\Delta U/\Delta t$ must be preset in the function generator. The scheme is shown diagrammatically in Figure 10.33.

10.3.3.4 Digital step sequence control

Because a stepper motor is driven digitally there are now many possibilities for applying LSI (large scale integration) ASICs or microprocessors for control. The microprocessor offers greater flexibility but the ASIC (application-specific integrated circuit) is faster and more compact. In many duty cycles the load and the path are predetermined and a simpler control system with a counter and stored programme chip is applicable. An $n \times 4$ bit store is sufficient for these applications and it may be programmed as a ROM from which a pulse sequence for start, accelerate, run, decelerate and stop without overshoot may be derived.

A schematic diagram is given in Figure 10.34. The timing code is built up from the frequency of the control generator. The switching conditions for the motor phases can be built directly from the bit structure of the chosen words.

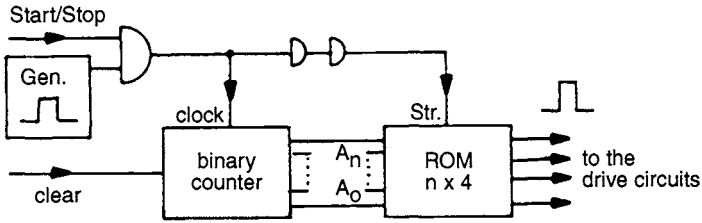


Figure 10.34 Schematic circuit for storing a step sequence by means of a ROM

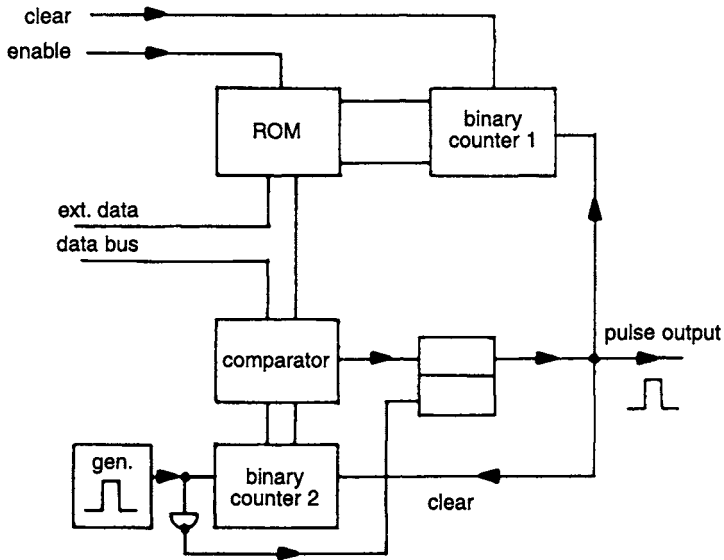


Figure 10.35 Circuit for the generation of an arbitrary pulse sequence

The required word length is related to the number of motor phases. The circuit is appropriate for short step sequences. For longer step sequences it is better to use a circuit in which the time code is stored in a ROM (read only memory).

Figure 10.35 shows one such circuit. In this circuit the times are given in binary form. These can be stored in a ROM or fed in externally. The generator determines the highest stepping frequency. The functioning of the circuit rests on the fact that the content of counter 1 is compared with a given timer word. When equality is achieved a control pulse is outputted. The content of counter 2 is increased by one, at which the word for the next time interval is applied to the comparator. In the following impulse pause of the generator, counter 1 is set to zero, and the cycle is repeated.

10.3.3.5 Stepper motor with closed-loop drive

When the load on a stepper motor is constant, the step sequence can be easily designed to suit the systems dynamics characteristics, and be specified. This is not possible with varying loads. It may become possible if the stepper motor operates in a closed loop, i.e. with feedback. Figure 10.36 shows one such arrangement. A generator with the highest required stepping frequency is compared with the signal from an encoder using an AND gate. A following pulse is then only passed to the electronic system when the encoder signals its arrival at the valid instantaneous step position. In this way the optimal acceleration independent of the load is achieved. If this pulse sequence is recorded and stored it can then be used in reverse order for optimum braking. The increased cost and complication is justified by the improved results.

10.3.3.6 Step division – microstep drive

In this form of drive use is made of the fact that the rotor can assume any steady-state position within a step if the currents flowing in the two phases are continuously adjustable. One special case is when one phase is fully excited and the other not at all. If the current in one phase is increased in small steps and the current in the other phase is similarly decreased, then the result is microstep drive.

If the motor torque is to remain constant and if the step is to be subdivided into equal-magnitude microsteps, then the currents in phase 1 and phase 2 must be in accordance with the following relationships:

$$I_1 = I \sin \frac{n\pi}{2k} \quad I_2 = I \cos \frac{n\pi}{2k}$$

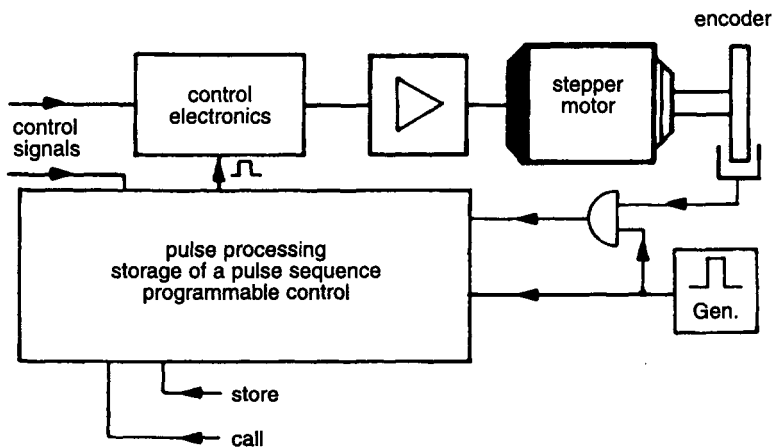


Figure 10.36 Stepper motor in 'closed-loop drive'

where n is the number of microsteps to be moved, k is the number of microsteps in a full step and I is the nominal current for a phase. The premises are that the torque/shaft angle curve is sinusoidal and that the stator phases are displaced by 90 electrical degrees. Figure 10.37 indicates the process for $k = 3$.

The demands on the electronic circuitry are considerable as the block diagram, of Figure 10.38 shows. The circuit brings together the following various advantages, and thus finds frequent application:

- The pulsating torque curve has a low ripple content.
- Mechanical resonances are less apparent.
- The noise level is lower.
- Positional accuracy is better.

Under 'positional accuracy' it is to be noted that the microsteps have nothing like the accuracy of those of a high resolution motor, whose full-step accuracy is mainly determined by the manufacturing tolerances. Depending on the

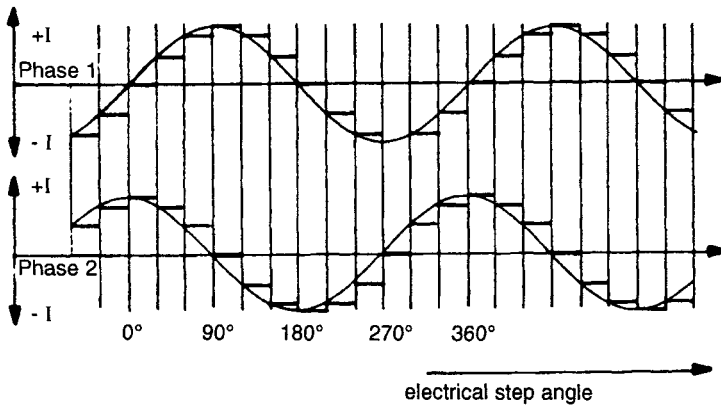


Figure 10.37 *Currents in the two phases for microstepping*

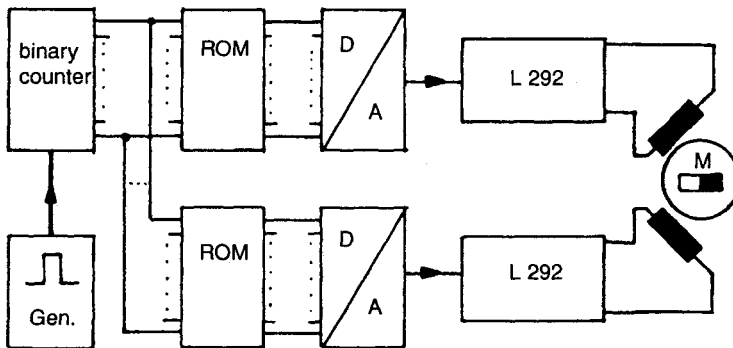


Figure 10.38 *Block diagram for a microstep drive*

sort of drive, only the holding torque of one fully energised phase is available. If the construction of the motor permits, the maximum current per phase may be increased and thus also the torque, because the heat losses are smaller than for a full-step drive.

It must also be noted that the switching frequencies for motors with small step angles and large step division can become very high. This can lead to problems in the power circuits.

10.4 Basic system for stepper motor drives

10.4.1 Drives with the facilities of acceleration, braking, variable stepping frequency and reversibility

Circuits of this kind make possible the build-up of drive systems which can be controlled by specified signals during running (Figure 10.39). The external signals can be derived from sensors, e.g. microswitches, photoelectric devices or proximity switches.

The stepping frequency is switchable between f_0 and f_w , in that the changeover results from the prescribed function. Other stepping frequencies derived from external sources are possible. A programmed frequency generator may also be used, but the expense and complication can be considerable.

10.4.2 Positioning drive in combination with a counter

This is as for the circuit of Section 10.4.1 but with preselection of the required path (Figure 10.40). In this circuit a stop signal can be obtained from a preselection counter. With this a definite preselected number of steps or preselected positions with one step accuracy can be achieved over a programmable preselection. Here an advanced signal is often necessary before the motor reaches its preselected position so that braking can be

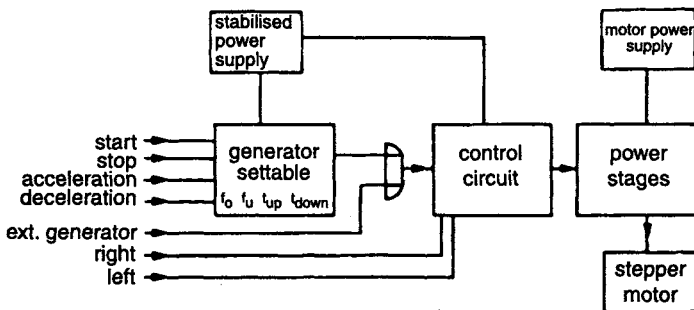


Figure 10.39 Basic circuit discussed in Section 10.4.1

applied. The acceleration programme can be combined with the start signal. It is therefore appropriate to equip the counter with two preselection options.

10.4.3 Drive with step frequency variation via a voltage/frequency converter

This circuit (Figure 10.41) enables the construction of a drive system whose stepping speed can be adjusted directly from an analogue voltage. Thus a special circuit for accelerating and decelerating becomes unnecessary because these can be derived directly from the input voltage. Depending upon the resolution of the voltage/frequency converter, the stepping frequency can be varied over a wide range, which makes possible an excellent match to the dynamic structure of the system to be driven. For example, in a servodrive a bridge voltage can be applied to speed control. A balance point is arrived at and with it automatic braking of the motor, whilst the drive torque remains constant.

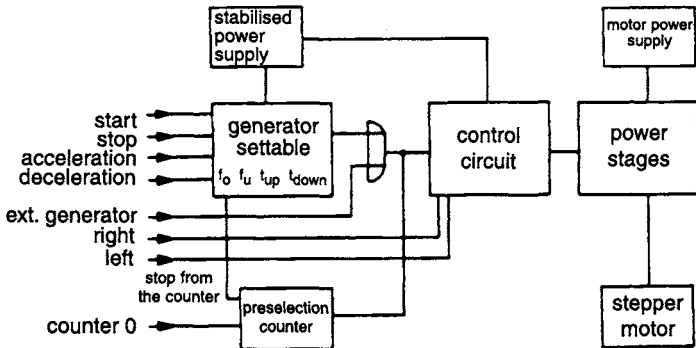


Figure 10.40 Basic circuit discussed in Section 10.4.2

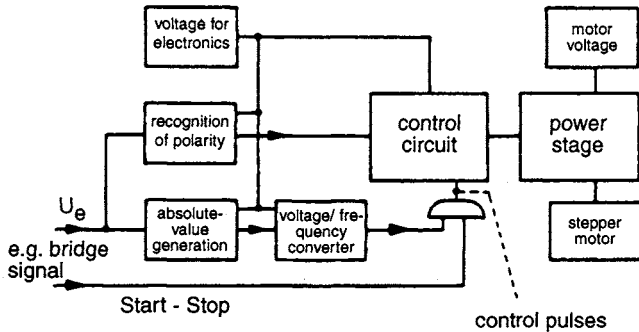


Figure 10.41 Basic circuit for the drive of Section 10.4.3

10.4.4 Drive with microprocessor control

The introduction of microprocessors into stepper motor control systems offers many possibilities. As an example the control of a stepper motor over a prescribed path and with variable speed is described diagrammatically in Figure 10.42. This variant has great flexibility and the drive parameters can be varied practically at will in a simple manner, within the limits of the motors capabilities, from an input unit.

The data for the stipulation of a path for distance (frequency changes, maximum frequency and start frequency) are called up into one data block. At each step an interrupt is applied at the MPU and checked for whether the prescribed number of pulses for stepper motor control has been transferred. To control the acceleration and braking sequences, an external timer is introduced, in which the required frequency changes are called up in the time interval of an interrupt. The frequency changes for acceleration and braking are approximated in a staircase fashion.

10.5 Choice criteria for stepper motors

10.5.1 Forms of construction

10.5.1.1 Two-stator motor

The photographs of Figure 10.43 give a view of a two-stator motor with eight pole pairs. The 90° displacement does not occur in the stator, but by appropriate orientation of the two separate permanent ring magnets of the

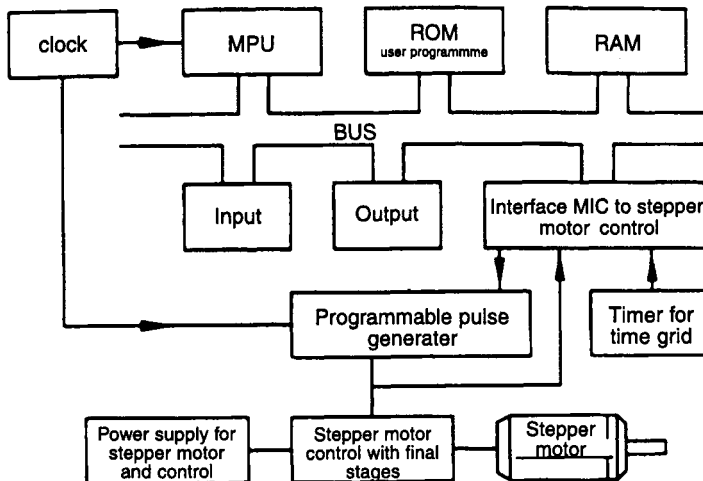


Figure 10.42 System for controlling a stepper motor with a microprocessor: flexible adaptation of speed to the prescribed path

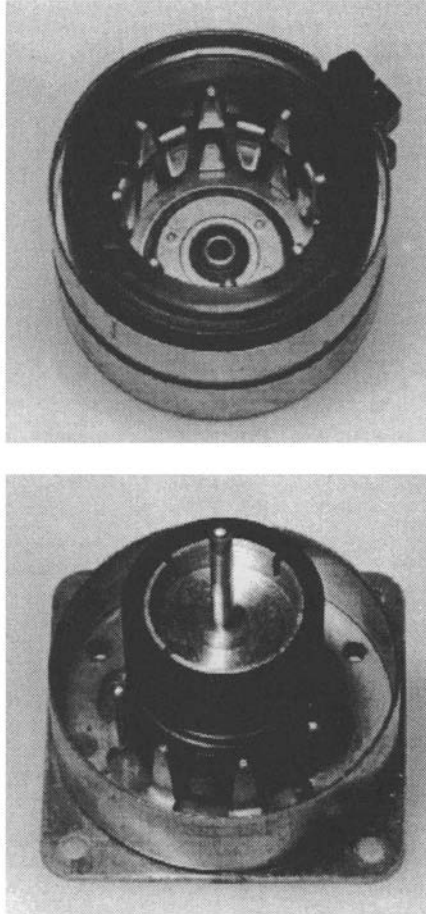


Figure 10.43 Two-stator motor

rotor. Each of the two individual stators is made up of a pair of interlaced crown-rings surrounding a toroidal coil winding. Depending on the direction of current flow, one set of crown teeth have north poles and the second set have south poles.

10.5.1.2 Hybrid stepper motor

In this motor the laminated stator has eight salient poles each with five teeth, and each pole carries an energising coil (see Figure 10.44). The eight coils are so connected and switched that a 2-phase winding is realised (alternate poles are one phase). The rotor comprises a cylindrical permanent magnet with its axis coinciding with the rotor shaft. Soft-iron pole shoes at each end of the permanent magnet take the form of two identical toothed wheels which have the appearance of spur gears. This form of stepper motor is

known as a 'hybrid' as it combines the attributes of the 'reluctance' and 'permanent magnet' arrangements.

The teeth of the 2-pole shoes are displaced circumferentially by half a tooth pitch, i.e. by 90 electrical degrees (see Figure 10.44). The teeth of one pole shoe are entirely north poles and those of the other entirely south poles. Step-by-step switching of this 2-phase motor is achieved as in the two-stator motor by sequential current reversals in the two phases.

Figure 10.44 shows the stator and rotor construction of one such motor. The stator poles with five teeth each are easily recognisable, as are the two toothed rotor pole wheels with 90° electrical displacement.

A wide choice of 2-phase motor types is at the user's disposal. Motors with this construction are suitable for systems with 'average' dynamic specification, e.g. for tracking a floppy disc, for the type wheel or roller of a printer. It must be noted that instabilities can occur around the natural frequency of the motor, so that auxiliary damping is called for.

There is a choice between motors of average and coarse resolution. The following table gives a rough overview of the range of types:

Resolution	Average	Coarse (small motors)
Step angle	0.9° or 1.8°	7.5–22.5°
Maximum stepping frequency	~20 kHz	~1.5 kHz
Torque	20–1200 N cm	0.4–60 N cm

10.5.1.3 Construction of a 5-phase hybrid stepper motor

A 5-phase motor may, in principle, be constructed like a 2-phase motor using a 'unipole' rotor. The five separate windings, each with two coils, are distributed on ten main pole shoes, each with four teeth separated by three

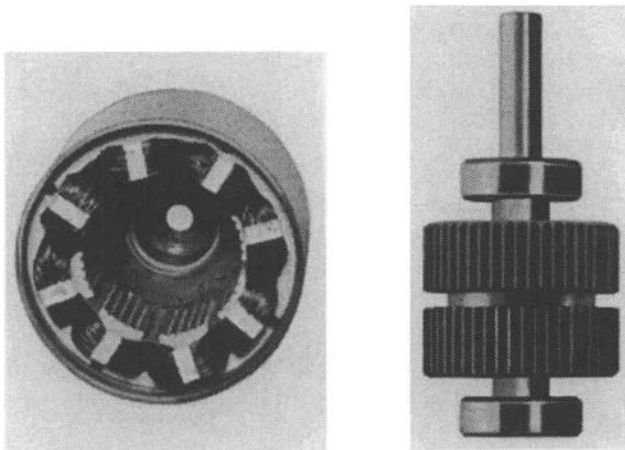


Figure 10.44 Hybrid stepper motor

slots. The rotor is similar to that of the 2-phase motor. With this arrangement there are 500 uniformly distributed steps per rotor evolution, giving a step angle of 0.72° . The basic construction of the 5-phase motor is shown in Figure 10.45.

That there are 500 step positions for the rotor of the 5-phase motor of the drawing, Figure 10.45, may be argued as follows. The ten stator poles are not distributed uniformly around the circle. The angle between pole centres is generally τ_p and exceptionally τ_p' such that

$$4\tau_p + \tau_p' = 180^\circ$$

We coin the word 'steppi' to mean an angle equal to $1/500$ of a complete turn, and give it the symbol s superscript, so that $1^s = 0.72^\circ$. It follows that $4\tau_p + \tau_p' = 250^s$ where τ_p and τ_p' must be integral multiples of 1^s .

Possible solutions are:

τ_p	49^s	48^s	47^s	46^s
τ_p'	54^s	58^s	62^s	66^s

Inspection of the drawing, Figure 10.45, and the fact that 1 rotor tooth pitch = $500^s/50 = 10^s$, suggests that: $\tau_p = 46^s$, $\tau_p' = 66^s$ is the solution.

Given the above distribution of stator poles, it is a straightforward matter to show that there is a minimum reluctance position for the rotor at each 1^s interval. Motors with this construction possess excellent dynamic properties and enable applications beyond the scope of 2-phase motors. Advantages of a 5-phase system are:

- step angle $0.72^\circ/0.36^\circ$
- torque 20 – 700 N cm
- high resolution 500 or 1000 steps per rotation without gearing
- no pronounced resonances
- with appropriate electrical inputs, greater system damping (makes auxiliary damping unnecessary)
- high start/stop and running frequencies
- running frequencies up to 50 kHz.

10.5.1.4 Disc magnet stepper motors

A very interesting construction is the disc magnet stepper motor with two phases from the Portescap Co. This motor possesses excellent dynamic characteristics. This rests on the fact that the rotor is made up of thin axially magnetised discs. Thus the rotor moment of inertia is extremely small. Figure 10.46 shows such a stepper motor with a section removed.

By means of a special magnetising technique very small steps are achieved. According to type they range from 6° to 1.8° . The absolute angular errors amount to $\pm 6\%$ for the 6° step angle in two phases and $\pm 2\%$ for the 1.8° . The stepper motor with 1.8° step angle and two phases supplied with nominal current develops a torque of typical magnitude 570 nNm.

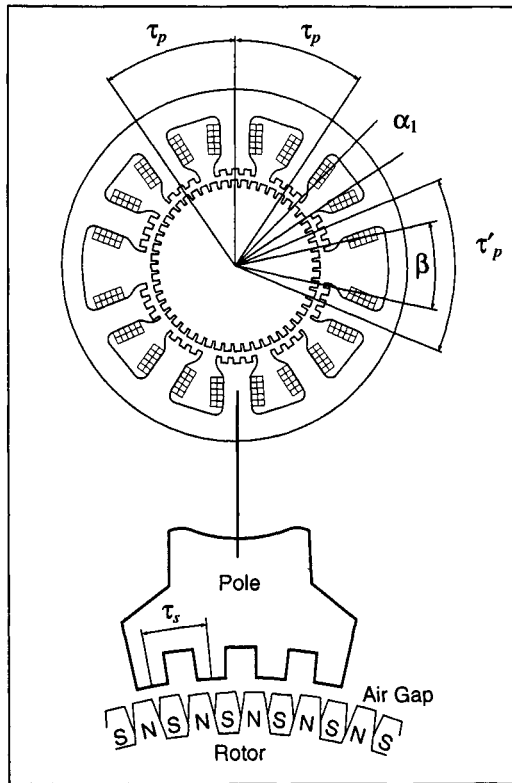
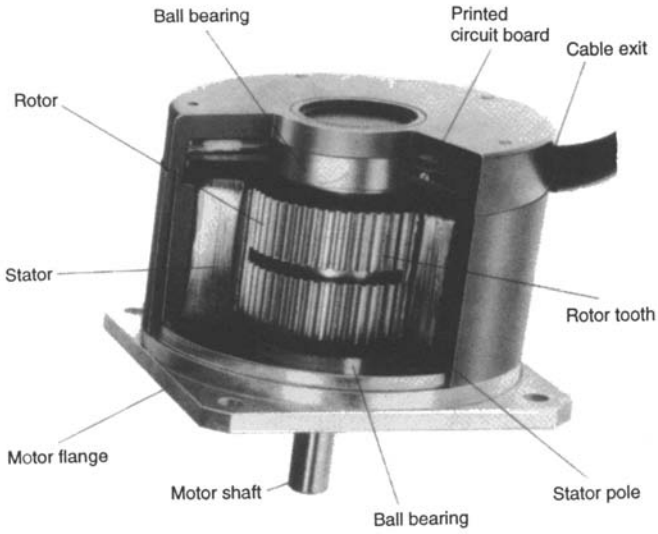


Figure 10.45 Construction of a 5-phase motor

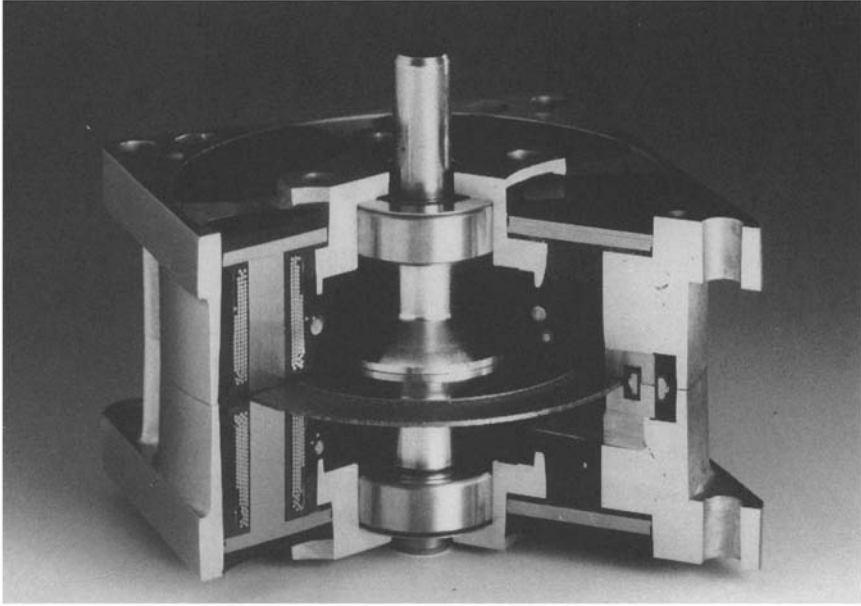


Figure 10.46 *Disc magnet stepper motor (Portescap Co.)*

10.5.2 *Example of choosing a stepper motor*

In choosing a stepper motor the following five points must be taken together and consequently known exactly: external load torque, external moment of inertia, acceleration time, running speed and braking time. In many cases a means for traversing a path in the shortest possible time is sought. This is particularly so for short paths. Then, shorter acceleration and braking times instead of short time movements with high stepping frequencies (which can only be reached after longer acceleration and braking times) often lead to better solutions.

Additional conditions, e.g. oscillation-free stopping, make compromises necessary. In practice, the question normally presents itself in a form such that the user chooses a motor whose internal torque for a given load torque permits the required stepping frequency and with it adequate excess torque to meet the start and stop conditions. In the following numerical example, the calculations test whether the motor can meet the necessary conditions concerning acceleration and braking times.

The calculations proceed as follows. The following data are given:

External moment of inertia	$J_{ex} = 0.03 \text{ N cm s}^2$
External friction load torque	$M_L = 40 \text{ N cm}$

A motor shaft speed of 600 rev/min is required. Acceleration shall be from rest. The motor shall be run at optimum power rating. Minimum acceleration

and braking times are required. This last requirement brings with it a high torque value M_1 (Figure 10.47).

The specific conditions together point to the choice of a 5-phase motor RDM 596/50 with a step angle of 0.72° with constant current drive. This motor has a rotor moment of inertia of $J_{\text{Rot}} = 0.007 \text{ N cm s}^2$, something which must be taken into account later on. Figure 10.47 shows the loading conditions.

The motor selected can undoubtedly be stopped by the given load when the stepper frequency is 100 Hz (Figure 10.47, 5-phase motor, mass moment of inertia as a function of stepping frequency). Owing to the external load torque the braking performance is improved but the acceleration is worsened. The start frequency must be appreciably less than 100 Hz. This is of no consequence in the present case as starting is from rest and $f_1 = 0$. The run-up and braking times can be derived from the formulas already discussed in Section 10.2.2.3. Acceleration and braking times can be derived from the same formula, as it is only a matter of reversing the procedures.

In our example we calculate the acceleration time in two stages. Because M_1 remains constant up to the point K in Figure 10.47, the frequency is accelerated from 100 Hz in a linear manner. After point K and up to a stepping frequency of $f_2 = 5000 \text{ Hz}$ the acceleration function is exponential (linear approximation $M(f)$).

During the braking period the external friction torque assists. Braking is applied appropriately until the possible stop frequency and then the motor stops and holds.

External and motor moments of inertia total 0.037 N cm s^2 . The run-up time from 0 to 1000 Hz (see Section 10.2.2.3) is $t_{h1} = 6.64 \times 10^{-3} \text{ s}$ and from 1000 Hz to 5000 Hz is $t_{h2} = 39.4 \times 10^{-3} \text{ s}$, and $t_h = t_{h1} + t_{h2} = 46.04 \times 10^{-3} \text{ s}$.

Calculation of the braking torque comes from $M_{br} = M_3 + M_L$ (see Figure 10.47) because friction torque assists braking. We derive for $M_{br} = 110 \text{ N cm}$ and, from this value, the braking time

$$t_{br} = 16.9 \times 10^{-3} \text{ s}$$

The calculated values meet the specified task adequately, so the chosen motor may be used. If the values are not satisfied, other means need to be examined. It may be that a half-step drive meets the given requirements. If there is no other solution, then the next motor up the power scale must be considered. If the calculated values seem to be too favourable it is worth trying a lower power motor.

10.6 Summary of important stepper motor concepts

Definitions must sometimes be reciprocal, i.e. are described with the aid of other definitions in the group. When this occurs, the other 'definition words' are emphasised.

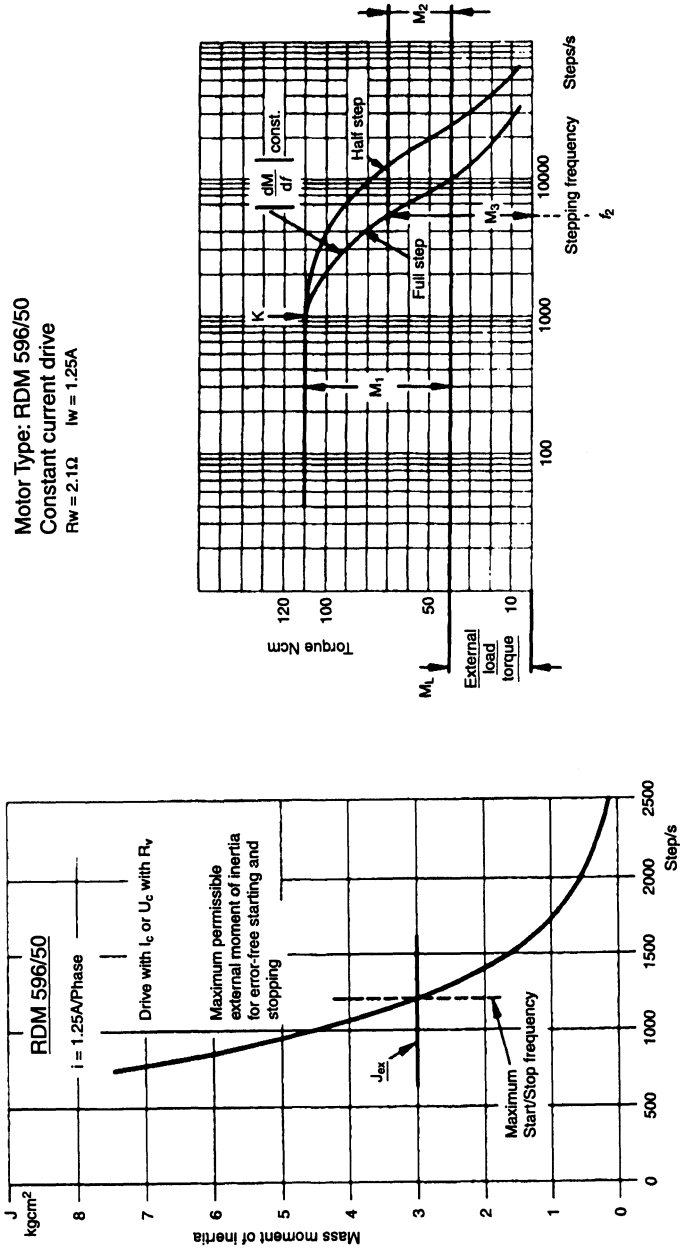


Figure 10.47 Showing the load distribution in the accompanying example

1. *Step*

The event whereby the motor shaft turns through the *step angle* from one stable *magnetic rest state* to the next.

Symbol: z Unit: ./ (i.e. zero unit)

2. *Step angle*

The specified angle through which the motor shaft turns per drive impulse.

Symbol: α Unit: $^{\circ}$

3. *Stepping frequency*

The number of *steps* that the motor shaft makes per second when the *drive frequency* is constant.

Symbol: f_2 Unit: step/s

4. *Drive frequency*

The pulse frequency with which the motor is driven. This frequency corresponds to the *stepping frequency* when the motor is running without step errors.

Symbol: f_2 Unit: pulses/s

5. *Rotation speed*

Motor turns/minute, calculated from $(\text{stepping frequency} \times \text{step angle} \times 60) / 360^{\circ}$

Symbol: n Unit: rev/min

6. *Phase, number of phases (applied to a motor winding)*

Ref DIN 40.108

Symbol: m

7. *Magnetic rest state*

The position that the rotor assumes when the motor is energised and the static load torque is zero.

Symbol: ./ Unit: ./

8. *System angle tolerance per step*

Greatest positive or negative static angular deviation from the specified *step angle* that can occur when the rotor steps from one *magnetic rest state* to the next.

Symbol: $\Delta\alpha_s$ Unit: $^{\circ}$

9. *Greatest system angle deviation*

Greatest static angle deviation of a *magnetic rest state*, relative to the appropriate integral multiple of the specified *step angle*, that can occur in one complete turn of the rotor starting from a defined rotor position.

Symbol: $\Delta\alpha_m$ Unit: $^{\circ}$

10. *Static torque*

The maximum static torque that can be applied to an unenergised motor before it starts continuous rotation.

Symbol: M_s Unit: N cm

11. *Holding torque*

The maximum static torque that can be applied to an energised motor before it starts continuous rotation.

Symbol: M_H Unit: N cm

12. *Static load angle*

The angle between the position of a rotor loaded with static torque and the unloaded position (*magnetic rest state*) when the motor is energised with the specified direct (zero frequency) current.

Symbol: β Unit: $^\circ$

13. *Start – stop region (also known as the ‘slew’ region)*

The operating area in which the motor and its specified rigidly coupled load can run without a step error occurring.

14. *Acceleration region*

The operating area in which the motor and its specified rigidly coupled load can run in one direction of rotation without a step error occurring but nevertheless cannot start or stop without step errors.

15. *No-load running*

The drive state in which the motor is loaded with neither an external torque nor with a rigidly coupled inertial load.

16. *Maximum starting frequency*

Greatest drive frequency that can be applied to a motor with no load such that it can start and run without a step error occurring.

Symbol: f_{Am} Unit: pulse/s

17. *Starting frequency*

Greatest frequency with which the motor with a specified load, comprising friction and rigidly coupled inertia, can be started without a step error occurring.

Symbol: f_{Am} Unit: pulse/s

18. *Starting torque*

The maximum load torque against which a motor with a specified rigidly coupled inertial load and a given drive frequency can be started without a step error occurring.

Symbol: M_{Am} Unit: N cm

19. *Maximum torque*

The greatest load torque against which a motor with no externally coupled inertia can be driven.

Symbol: M_m Unit: N cm

20. *Maximum drive frequency*

Maximum drive frequency at which the motor can be driven off-load in one direction of rotation without a step error occurring, but cannot be started or stopped with this frequency.

Symbol: f_{Bom} Unit: pulse/s

21. *Drive frequency limit*

Greatest frequency with which a motor with a specified load comprising friction torque and an acceleration torque for a rigidly coupled inertia can be driven in one direction of rotation without a step error occurring but nevertheless cannot be started or stopped in synchronism with this frequency.

Symbol: f_{Bm} Unit: pulse/s

22. *Drive torque limit*

The highest load torque with which the motor can run when it has a specified rigidly coupled inertia and is to be driven in one rotation sense from a specified drive frequency without a step error occurring.

Symbol: M_{Bm} Unit: N cm

23. *Dynamic load angle*

The angle between the present instantaneous position of the rotor and that of the *magnetic rest state* determined by the most recent drive pulse.

Symbol: γ Unit: $^\circ$

24. *Maximum overshoot angle*

The largest angle between the furthest position reached by the rotor under specified loading conditions and the *magnetic rest state* determined by the last pulse in the drive pulse sequence.

Symbol: γ Unit: $^\circ$

Chapter 11
Measurements in small drive systems

Jürgen Draeger

11.1 Introduction

To achieve the desired characteristics in a drive it is necessary to know the electrical and mechanical data of its individual parts, including their unwanted properties such as heating, vibration, noise and interference field generation. Figure 11.1 shows the breakdown – source, motor and load – of a drive system and the flow of power together with the following set of quantities that should be determined:

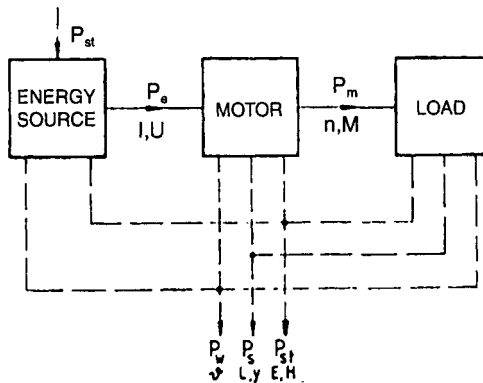


Figure 11.1 Power flow in a drive system

- P_e = electrical power
- P_{st} = disturbance field power
- P_m = mechanical power
- P_w = heating power
- P_s = vibration power

I	current
U	voltage
n	speed of rotation
M	torque
ϑ	temperature
y	vibration
L	noise level
E, H	electrical and magnetic disturbance fields.

Measurement of these quantities – except for noise level and vibration, which are treated in Chapter 12 – is discussed in this chapter.

11.2 Sampling functions

If an arbitrary function $F(t)$ contains all frequencies up to f_g , then the function may be expressed completely by the following Fourier series:

$$F(t) = \sum_{v=-\infty}^{v=+\infty} F\left(\frac{v}{2f_g}\right) \frac{\sin(2\pi f_g t - v\pi)}{2\pi f_g t - v\pi} \quad (11.1)$$

This series is called a cardinal series. In practice, f_g is chosen such that the energy content of the components $f > f_g$ is negligible compared with the total signal energy. Because the numbers v are all integers, eqn. 11.1 shows that the function must be known at equidistant time intervals,

$$\Delta t = \frac{1}{2f_g} = \frac{T_g}{2} \quad (11.2)$$

This means that it is only necessary to sample a time-dependent function at regular intervals $T_g/2$ in order to know it completely.

The statement of eqn. 11.2 is the essence of Shannon's sampling theorem, as follows.

If $F(t)$ is band limited by upper frequency f_g and $F(t)$ is sampled at regular intervals of $\Delta t = 1/2f_g = T_g/2$, then the function $F(t)$ may be completely determined from the samples.

In practice this means that the sampling frequency f_a must be at least double the highest frequency f_g in $F(t)$. Figure 11.2 shows examples of a function $F(t)$ being sampled by impulsing and by a carrier frequency.

Depending on their form, sampling pulses produce the frequencies contained in the original function $F(t)$, side frequency bands centred about f_a and integral multiples of f_a (Figure 11.3). The information about $F(t)$ is contained fully in the frequency band $f \leq f_g$. When measurements are being made, frequencies $f > f_g$ must be filtered out. Thus it is necessary that $f_a \geq 2f_g$ so that frequencies in the sidebands are not interpreted as information. Practical filter design considerations rule that the sampling frequency should be from $3f_g$ to $5f_g$. The short sampling periods cause the

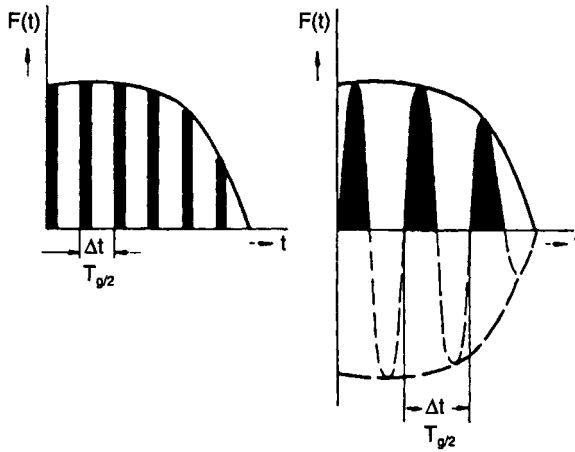


Figure 11.2 Function $F(t)$
 a Impulse sampled
 b Carrier frequency sampled (half-wave rectification)

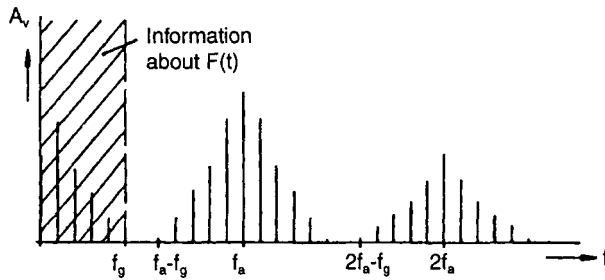


Figure 11.3 Frequency spectrum of the amplitudes A_v by sampling the function $F(t)$ at frequency f_a

power measured to be much smaller than that in the original signal. Therefore it is sometimes necessary to have amplifiers in the measuring system.

11.3 Current, voltage, power

The accuracy of simultaneous measurements of the current i and the voltage u depends on the internal resistances R_i and R_u of the measuring instruments and their relationship to the impedance of the motor Z_M .

If meters with the highest possible R_u and lowest possible R_i are used, then the circuit of Figure 11.4 is deemed appropriate. The ammeter overstates the current i by the amount

$$+i \frac{Z_M}{R_u} \tag{11.3}$$

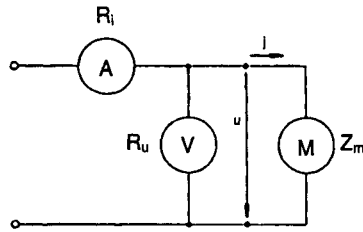


Figure 11.4 *Current and voltage measurement*

Therefore $R_u \gg Z_M$ is desirable. Moving coil instruments indicate the average values, whereas moving iron instruments indicate the RMS values.

When instruments with digital readouts are used for measuring the RMS values of signals with a harmonic or direct component content, it is particularly necessary to ensure that they are genuine RMS instruments.

For graphical registration of the measured quantities, a direct-coupled operational amplifier may be connected in parallel with the measuring instrument or across a calibrated resistor. The amplifier output is then used to drive a recorder or plotter or, after further processing, produce a digital equivalent for direct read-out or as an input to a computer. Time-dependent graphical representation of measured quantities may also be achieved by means of an appropriate oscilloscope, which may be analogue or digital and have a built-in plotter. Some selection of the sampling frequency may be called for, in accordance with Section 11.2.

When analogue signals are digitised, the analogue functions $F(t)$ are converted into staircase functions $F^*(t)$ in accordance with Figure 11.5. The accuracy of the measurement is related to the number of steps in the staircase, i.e. on the analogue to digital conversion circuitry and its bit resolution. The accuracy of an A/D converter for a number of bit resolution capabilities is given in Table 11.1.

Table 11.1 *Grading and accuracy of A/D converters with various bit numbers*

Bits	Steps	Accuracy, %
8	256	0.4
10	1024	0.1
12	4096	0.025
16	65 536	0.0015

The same considerations are applicable to power measurement. Current and voltage circuits for current and voltage measurement are set up as shown in Figure 11.4. Power is indicated by means of an analogue multiplier that performs the operation $p = ui$, or a power measuring loop if the power as a function of time must be indicated.

If the functions are in digital format, time-dependent and with harmonics, then FFT (fast Fourier transformation) analysis may be used to transform the information from the time domain to the frequency domain. The frequency components are indicated over a wide range in quasi-real time. An example for an intermittent current with harmonic content is shown in Figure 11.6.

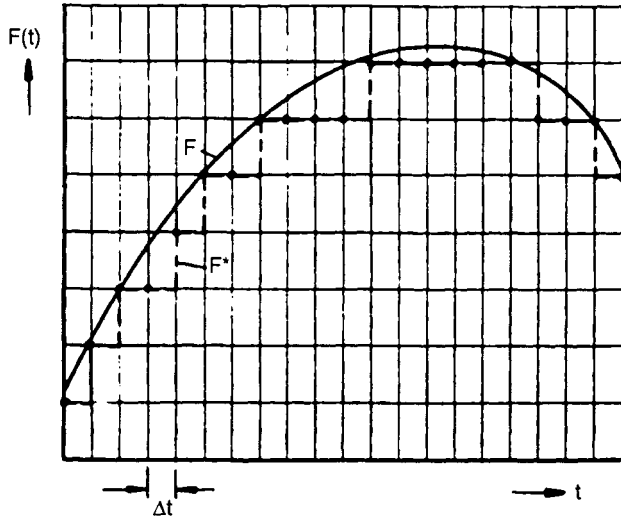


Figure 11.5 Conversion of a continuous function $F(t)$ into a staircase function $F^*(t)$ with sampling intervals Δt

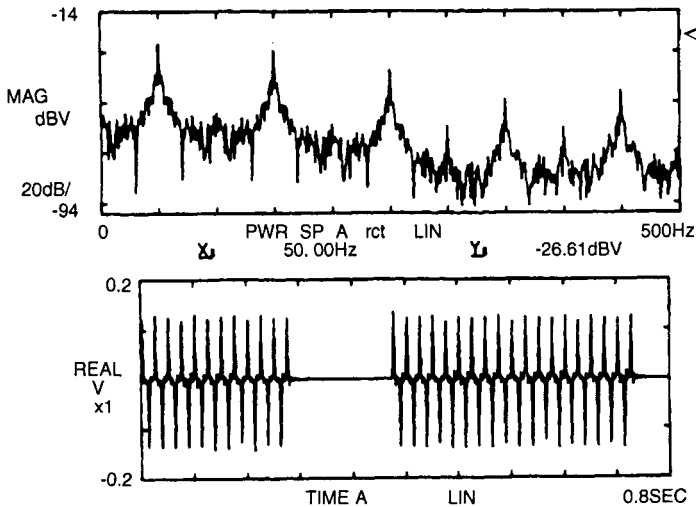


Figure 11.6 Intermittent current in the time and frequency domains

11.4 Speed of rotation

11.4.1 Analogue speed measurement

Speed measurement is in fact measurement of the angular velocity ω , from which the speed $n = \omega/2\pi$ is derived. In analogue methods an analogue signal proportional to the speed is generated directly by a rotor turning at that speed. Electric fields (voltages) are developed in accordance with the law of induction and appear as direct or alternating voltages from DC or AC tachometers. Alternatively, eddy currents developed in extended conductors induce alternating voltages in Hall sensors, magnetoresistors or induction coils. A summary of the structure and function of analogue tachometers is given in Table 11.2.

The tachometers described here are suitable for connection to a direct reading electrical instrument or to a plotter, the voltage being made direct by means of rectifiers where necessary. (It is important to note the 0.3–0.7 V forward voltage drop in a semiconductor diode which can cause a significant zero error.)

According to the sampling theorem (Section 11.2), a time-dependent function can be rebuilt adequately and accurately when the sampling frequency f_a is at least twice that of the highest frequency to be measured. Consequently, the highest measurable frequencies that can be derived from AC tachometers is dependent on the frequencies of the induced voltages and, in some circumstances, on the speed of rotation.

Inductances, capacitances and also mechanical resilience in the measuring system delay the readout. The resulting measurement error during dynamic measurements should not exceed 3 dB, i.e. a loss of 30%, at the upper signal frequency f_g . Eddy current tachometers are particularly suitable for dynamic measurements. Homopolar generators are also suitable provided that brush contact related disturbances can be kept sufficiently small.

The performance of all electrical equipment is temperature-dependent owing to the temperature coefficient of resistance of the conductors. For Cu or Al the figure is about 0.4%/K, for manganin 0.004%/K and for constantan –0.003%/K. The linearity error of the devices discussed above lies between 0.02 and 1%.

Power is needed for generating the analogue signals and it must frequently come from the machine being investigated and, in the case of a small machine or drive, this amount of power is far from negligible.

In such cases it is highly recommended that the measurements be made by contact-free incremental tachometers so that the energy for the measurement is not taken from the motor being tested.

11.4.2 Incremental rotation measurement

In incremental transducers, the number of pulses is used to determine the speed, i.e. the angular velocity. Only the number of pulses per unit time and not their form is significant. Therefore, incremental transducers are not

Table 11.2 Analogue tachometers

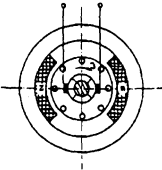
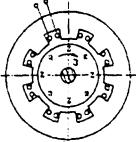
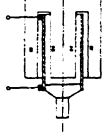
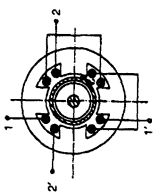
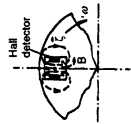
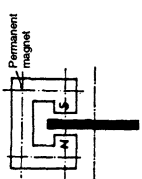
Type	Construction/operation	Signal $\chi =$ various	Speed, rev/min	f_n Hz	Remarks
1. DC tachometer 	Permanent magnet stator field excitation, wound rotor with mechanical commutator. During rotation an alternating voltage is induced in the rotor and rectified by the commutator	Direct voltage with ripple $\dot{u} = \chi (0.1-100) \text{ V}$	up to 10,000 small tachometers ($P < 0.5 \text{ W}$) up to 20,000	$\omega/2\pi = n$	Brush lifetime $\approx 20,000 \text{ h}$. In small tachometers, metal brushes with low brush voltage drop are used.
2. AC tachometer 	Permanent magnet rotor, wound stator: $p = 6-8$, $p_{\text{max}} = 30$. During rotation alternating voltages are induced in the stator windings.	Alternating voltage $U = \chi (1-100) \text{ V}$	up to 50,000	$p\omega/2\pi = pn$	Increasing linearity error at higher speeds owing to frequency-dependent stator resistance.
3. Homopolar generator 	Conducting nonferromagnetic cylindrical rotor. Homopolar magnetised permanent magnet stator. During rotation direct voltage is induced in the cylinder and taken off via slip-rings.	Pure direct voltage $\dot{u} = \frac{10 \text{ mV}}{1000 \text{ rev/min}}$	up to 50,000		Extremely low internal resistance ($R \approx 1 \text{ m}\Omega$). Accordingly, large currents are possible. Some brush noise voltage may interfere with low-level signals. Particularly suitable for dynamic measurements.

Table 11.2 Continued

Type	Construction/operation	Signal χ = various	Speed, rev/min	f_p , Hz	Remarks
4. Eddy current tachometer	2 double coil stator windings displaced spatially by 90°, fixed ferromagnetic cylindrical core. Nonferromagnetic conducting rotor in the airgap. Coil system 1 is excited with χ (0.1–100) V at 50–400 Hz (exceptionally up to 10 kHz). During rotation, currents are induced in the rotor, whose magnetic fields induce an alternating voltage in coil system 2 at the excitation frequency f_1 .	Alternating voltage $U = \chi(0.1-10)V$ $U = 1000 \text{ rev/min}$	up to 20,000	$\leq 1/2f_1$	Owing to geometric asymmetry, a voltage $U \approx 10\text{--}150 \text{ mV}$ appears at standstill. Suitable for precision measurement systems and for dynamic measurements.
4.1 Alternating field tachometer					
4.2 Direct field tachometer	The rotor is a conducting nonferromagnetic disc. A permanent magnet stator generates a spatially bounded magnetic field. During rotation an eddy current density field appears in the disc, and is sensed by magnetic field dependent resistors or Hall-effect detectors.	Direct voltage $\dot{u} \approx \frac{10 \text{ mV}}{1000 \text{ rev/min}}$	up to 10,000	Limited by the mechanical construction to about 3 kHz.	Suitable for dynamic measurements.
					
					

temperature-dependent. Their outputs may be transmitted over long lines without any need for compensation. No physical contacts are involved and thus no power is extracted from the machine being tested.

A disadvantage is that the measured value can only be an average value, and there is a delay between the measurement and the readout. This must be taken into account if any kind of dynamic measurement is being contemplated.

If during the period of measurement Δt the number of pulses counted is ΔZ , and given that the number of pulses per revolution is m , it follows that

$$\bar{n} = \frac{1}{m} \frac{\Delta Z}{\Delta t} \quad \text{or} \quad \bar{\omega} = \frac{2\pi}{m} \frac{\Delta Z}{\Delta t} \quad (11.4)$$

\bar{n} may be determined by counting the number of pulses received during a prescribed time interval (say 1 s) or by measuring the time interval between two consecutive pulses. It is less complicated and less expensive to count the number of pulses ΔZ received in a fixed time Δt . The measurement error can be up to ± 1 pulse (the noninteger value being rounded up or down to the nearest integer). The measurement error is

$$\Delta \bar{n} = \frac{1}{m \Delta t}$$

and the relative measurement error is

$$\frac{\Delta \bar{n}}{\bar{n}} = \frac{1}{\bar{n} m \Delta t} \quad (11.5)$$

For a given constant Δt , the relative error is inversely proportional to the speed. It may be kept small by making m large. The measurement error can be smaller than 0.1%. Dynamic measurements can, in accordance with the sampling theorem, be made up to the boundary frequency

$$f_g = \frac{1}{2 \Delta t} \quad (11.6)$$

f_g depends on the measurement interval Δt .

From eqn. 11.5 for the relative error of measurement,

$$f_g = \frac{1}{2} \bar{n} m \frac{\Delta \bar{n}}{\bar{n}} \quad (11.7)$$

Therefore, the boundary frequency and the relative error of measurement are proportional. Small errors of measurement and higher boundary frequencies, i.e. good dynamic measuring characteristics, are possible when m is large.

When dynamic speed measurements are being made (i.e. during acceleration or deceleration), a dynamic measuring error F_{dyn} appears. Figure 11.7 shows as an example a linear speed ramp between initial value n_0 and final value n_f .

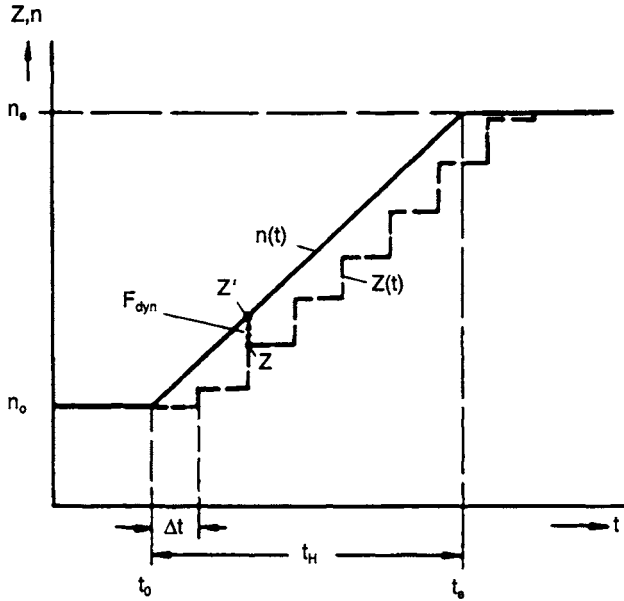


Figure 11.7 Dynamic error $F_{dyn} = (Z' - Z)/m$

Given the run-up time t_H , the equation for speed is

$$n(t) = n_0 + (n_e - n_0) \frac{t}{t_H} = n_0 + \Delta n \frac{t}{t_H} \tag{11.8}$$

where $\Delta n = n_e - n_0$.

As there are m pulses per revolution, the indicated (counted) number of pulses between instants t_0 and $t_0 + \Delta t$ is

$$Z(\Delta t) = m \int_{t_0}^{t_0 + \Delta t} n(t) dt = m \int_{t_0}^{t_0 + \Delta t} \left(n_0 + \Delta n \frac{t}{t_H} \right) dt \tag{11.9}$$

which becomes

$$Z(\Delta t) = m \left(n_0 \Delta t + \frac{\Delta n}{2t_H} (2t_0 \Delta t + \Delta t^2) \right) \tag{11.10}$$

The actual (true) speed at time $t_0 + \Delta t$ is

$$n(t_0 + \Delta t) = n_0 + \Delta n \frac{t_0 + \Delta t}{t_H} \tag{11.11}$$

and the true pulse count should be

$$Z'(\Delta t) = m \int_{t_0}^{t_0 + \Delta t} \left(n_0 + \Delta n \frac{t_0 + \Delta t}{t_H} \right) dt \tag{11.12}$$

or

$$Z'(\Delta t) = m \left(n_0 + \Delta n \frac{t_0 + \Delta t}{t_H} \right) \Delta t \quad (11.13)$$

Thus, the dynamic error in the measured speed is

$$F_{\text{dyn}} = \frac{Z' - Z}{m} = \frac{\Delta n}{2t_H} \Delta t^2 \quad (11.14)$$

F_{dyn} is small for

- small changes in speed Δn
- long run-up times t_H and
- short measuring time intervals Δt .

The normally encountered pulse generators are described in principle in Table 11.3. One-off measurements on fixed speed machines, or on machines with inaccessible shaft ends, may be made using a discharge tube stroboscope. Any bright, reflecting or salient feature of the machine's rotor may be illuminated by a variable frequency stroboscope lamp. When the rotor speed and strobe frequency correspond, the illuminated part(s) seem to stay in the same place. The machine appears to have stopped. The direct measurement is ambiguous because this effect occurs when the machine speed is any integral multiple of the strobe frequency.

When two adjacent 'standstill' frequencies f_1 and f_2 are read off, and the rotor has m equally spaced markers around its circumference, the speed is then

$$n = \frac{1}{m} \frac{f_1 f_2}{f_1 - f_2}$$

This procedure is applicable for speeds from 100 to 60,000 rev/min. It is not suitable for dynamic measurement, but small departures between motor and strobe speed make dynamic phenomena (e.g. rotor oscillations) observable.

In all the methods discussed above, the digital measurements may be transformed into direct voltage signals by means of a DAC (digital to analogue converter).

11.5 Torque

Many methods of measuring the torque M have been developed. Some are restricted to laboratory research work. Torque measurement is particularly useful in plant supervision systems and it is also used in regulating systems. The methods are grouped roughly as follows:

- total loss methods in which the power developed by the machine being tested is absorbed by the measuring system

Table 11.3 *Incremental tachometers*

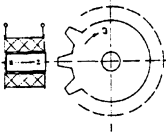
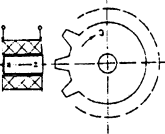
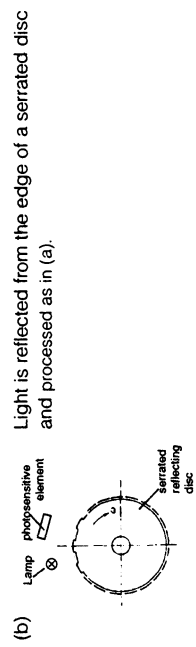
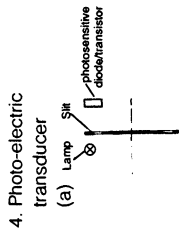
Type	Construction/operation	Signal	Speed, rev/min	Remarks
1. Electromagnetic transducer	<p>A spur gear, made of ferromagnetic material, is mounted on the shaft of the machine being tested. The coil is fixed and has a permanent magnetic core. During rotation, reluctance changes and resultant flux changes induce an alternating voltage in the coil.</p> 	<p>$u_a(t)$ is an alternating voltage with a waveform depending on the gear tooth profile.</p>	<p>10–30,000 up to 120,000 in special circumstances</p>	<p>The normal form is shown The teeth may also project axially</p>
(a)				
(b)	<p>A permanent magnetic spur gear with alternating polarity teeth is mounted on the shaft of the machine being tested. The coil is fixed and has a ferromagnetic core. During rotation the alternating polarity poles induce an alternating voltage in the coil.</p> 	<p>$\dot{u} \approx 0.01-1$ V and is dependent on the speed.</p>		<p>Not usable in a ferromagnetic dusty environment.</p>
2. Magnetic transducer	<p>The toothed wheel is the same as that for (b). The pick-off is a Hall generator or magnetoresistor firmly attached to a fixed pole shoe. The Hall-effect voltage or the change of magnetic resistance is proportional to the wheel-position dependent magnetic flux density B.</p>	<p>$u_a(t)$ is an alternating voltage dependent on the tooth profile. $\dot{u} = \chi \times 0.1$ V and is independent of speed.</p>	<p>as 1</p>	<p>Because $\dot{u} = \text{constant}$, it is particularly suitable for low and for high speeds.</p>

Table 11.3 Continued

Type	Construction/operation	Signal	Speed, rev/min	Remarks
3. Capacitive transducer	Change in capacity results, in accordance with changes in A or h in the formula $C = \epsilon A/h$, during rotation. Capacitance changes involve corresponding fluctuations in charge and hence current flow.	An alternating voltage dependent on the tooth profile.	as 1	An external voltage supply is necessary. Not used in dielectric dusty environments.
4. Photo-electric transducer	A disc with holes or slits rotates in front of a visible or infra-red light source, and generates voltage pulses in a light-sensitive component.	Voltage pulses.	Up to 100,000	At higher speed/impulse rates, dynamic measurements are possible on account of the shorter measuring intervals. The number of slits is normally up to 1000, but up to 36,000 is possible. In dusty atmospheres the measuring transducer must be totally enclosed. The slit accuracy can be 10 μm . Position indication using coded slits is possible.



- direct methods, in which the torque between the motor and load is measured in a transducer with as little power loss as possible
- indirect methods, in which the torque is derived from measurements of other system quantities in a basic low-loss measuring system.

The most frequently encountered methods under the above three headings are discussed briefly below.

11.5.1 Total loss methods

Torque may be measured very simply by means of a rope brake as shown in Figure 11.8. A wheel with radius R has the rope wrapped around one half turn. On rotation the motor output power is absorbed as heat in the wheel owing to the friction.

The tensions at the two ends of the rope (F_2 and F_1) are measured by spring balances, and the torque is

$$M = R(F_2 - F_1) \quad (11.15)$$

Automatic recording is difficult for this method.

In the eddy current brake (Figure 11.9) a large electrically conducting rotor which runs within the field of a DC electromagnet, is coupled to the motor (see Figure 11.9). The electromagnet is mounted in bearings and is restrained from rotating by a mechanical weighing machine. Torque is derived from the spring force and/or weights needed for the restraint.

As the characteristic curves of the eddy current brake show (Figure 11.10), the torque developed at low speeds is low, and it is zero at standstill.

For low speed and standstill torque measurements, torque may be measured by using the hysteresis loss in permanent magnetic materials, i.e. the remanence effect. The braking torque is principally as a consequence of magnetic cycling in the rotor. Figure 11.11 shows the corresponding torque-speed characteristics.

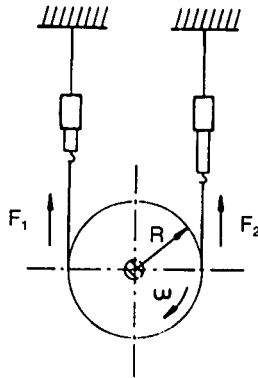


Figure 11.8 *Rope brake*

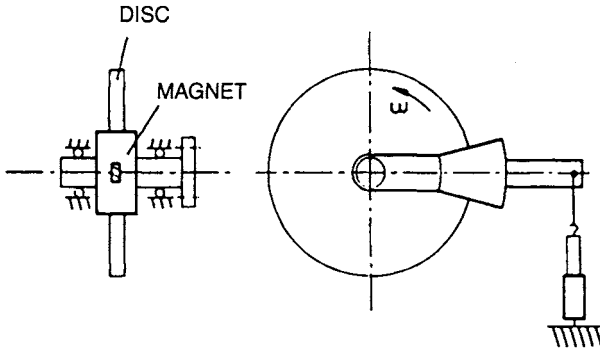


Figure 11.9 Eddy current brake

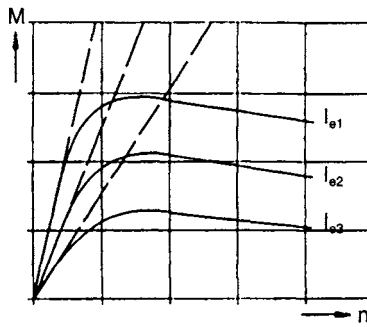


Figure 11.10 $M(n)$ of the eddy current brake for various electromagnet currents I_e
 — ferromagnetic rotor (disc)
 - - - nonferromagnetic rotor (disc)

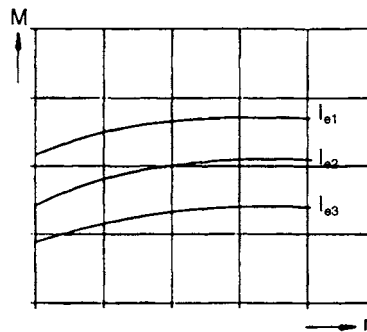


Figure 11.11 $M(n)$ of the hysteresis/remanence brake for various electromagnet currents

Total loss methods are only suitable for laboratory tests and not for plant supervision.

11.5.2 Direct methods

It is usual to measure the torque between the output shaft of the motor and the input shaft of the load. Use is made of the fact that any shaft twists through an angle that is proportional to the applied torque.

For a definitive measurement a relatively thin shaft (~0.8 mm diameter) acts as the sensor of a torque transducer (Figure 11.12) mounted between the motor shaft and the load. The shaft twists through an angle $\sim 0.5^\circ\text{--}1^\circ$ at the rated torque. In relatively thick shafts, the mechanical torsion can be converted to a voltage by means of resistance strain gauges bonded to the shaft and connected into full or half Wheatstone bridge circuits. The bridge circuit is energised by a supply of a few volts and several kHz from an oscillator. The supply is transferred to the bridge via slip-rings or via a transformer whose primary winding is fixed and whose secondary winding rotates with the shaft. The guidelines of Section 11.2 are applicable for dynamic measurements: the carrier frequency should be at least 3–5 times that of the maximum frequencies being measured. Carrier frequencies are normally from 1 to 10 kHz and, for dynamic measurements, can extend to 500 kHz.

The bridge is balanced when the torque is zero. The torque-dependent unbalanced signal of a few millivolts is transferred over slip-rings or by transformer action to a tuned amplifier to, for example, an analogue recorder or to an analogue to digital converter for further processing. In the case of fine – small-diameter – measuring shafts, the resistance strain gauges are replaced by variable inductances (moving core or variable mutual inductance) or, less frequently, by variable capacitors. A photoelectric relative movement detector is also possible. Such rotating torque transducers with a sensitivity of 0.1 N cm rated torque are manufactured. They can rotate at speeds up to 12,000 rev/min and, when provided with oil-mist bearing lubrication, up to 40,000 rev/min.

The relatively thin measuring shaft is a soft torsional spring between the rotating masses of the motor and the load. Consequently, torsional resonance occurs at some point along the range of measurement. The expected mechanical resonance frequency f_r , when the shaft's stiffness is c_d (torque/angle) and the moments of inertia of the motor and the load are J_M and J_L , respectively, is (when the influence of damping is neglected)

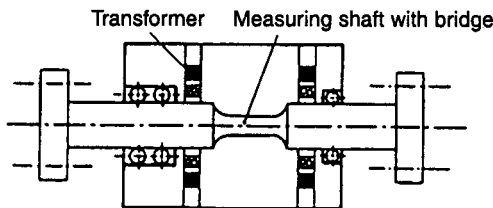


Figure 11.12 *The essentials of torque transducer construction*

$$f_r = \frac{1}{2\pi} \sqrt{\left(\frac{1}{J_M} + \frac{1}{J_T}\right) c_d} \tag{11.16}$$

When the static deflection angle in the shaft ($\Delta\alpha_{st}$ when $f = 0$) is compared with $\Delta\alpha$ when an oscillating torque of the same magnitude as the static torque is applied, the function $\Delta\alpha/\Delta\alpha_{st}$ as shown in Figure 11.13 is derived. Thus, at frequencies around resonance and above, the shaft torsion $\Delta\alpha$ is a very bad representation of the torque M . In systems with low damping factor, a correction factor k as shown in Figure 11.14 may be applied. k is, effectively, the reciprocal of α/α_{st} of Figure 11.13.

The measuring shaft can easily be overloaded.

If the vibration torque of a motor is to be measured, J_T must be chosen such that $J_T \gg J_M$. Then

$$f_r = \frac{1}{2\pi} \sqrt{\frac{c_d}{J_M}} \tag{11.17}$$

Because readings at frequencies approaching resonance are inaccurate, the measuring shaft must be chosen such that its resonant frequency is much higher than the motor vibration torque frequency. Particular attention must be paid to the torsional stiffness of the couplings.

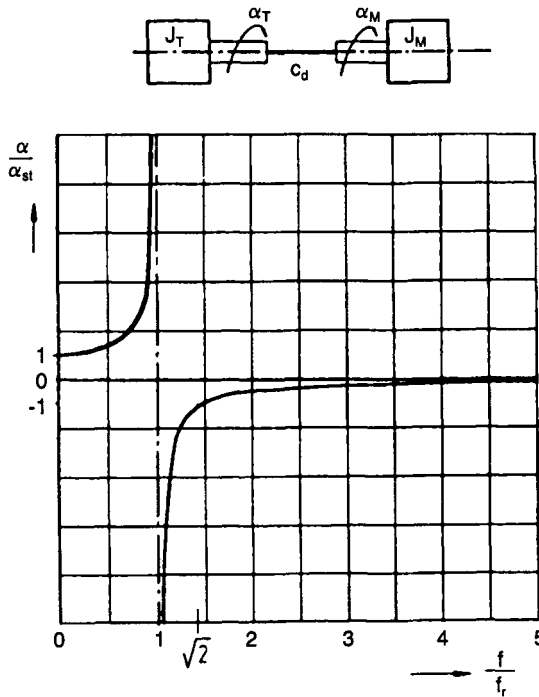


Figure 11.13 $\Delta\alpha/\Delta\alpha_{st}(f)$ of a torsional resonant system with two rotating masses

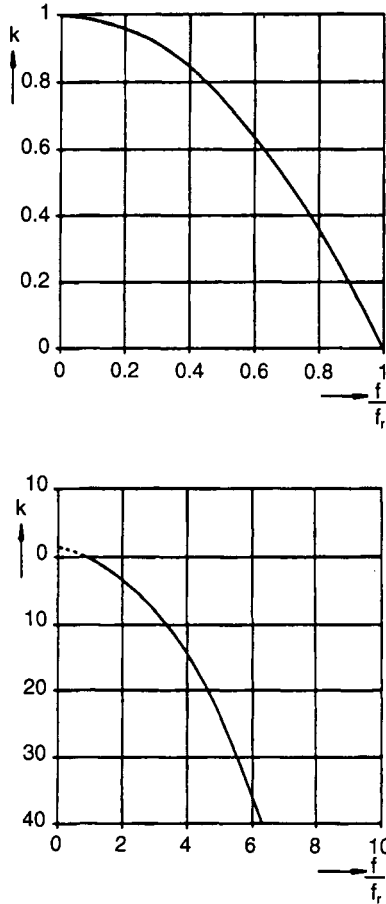


Figure 11.14 Correction factor $k(f/f_r) = \Delta\alpha_{st}/\alpha$

Rotor torque is balanced by an equal and opposite torque in the stator. Therefore, torque may also be measured on the stator by means of supporting the frame mountings on quartz pressure sensors (piezoelectric effect). In this case there are no significant linear or angular displacements involved and a high degree of accuracy is possible. Care must be taken to ensure that the points of attachment are free from mechanical vibrations and other disturbances.

Very small average torques, up to about 0.01 N cm, are measurable when the motor stator is restrained by a torsional transducer. Alternatively, stator frame extensions can be fitted with resistance strain gauges at their points of attachment. The same problems involving vibrations occur.

In the test bay, the speed/torque characteristic during run-up is mostly recorded automatically. The results may not be over valued owing to system

vibrations during the acceleration. This means that the run-up must be protracted so that the angular acceleration can be kept constant. This can be achieved satisfactorily by coupling the test machine to a relatively large fully controllable (four-quadrant) machine, or more simply by fitting a suitable flywheel.

11.5.3 Indirect methods

In the case of independently excited DC motors, there is a strong linear relationship between armature current and torque. Therefore, it suffices to measure the current or the voltage drop across a calibrated series resistor to determine the torque. This method may also be used with other motors, where the speed/torque characteristic is single-valued. Because the relationship between current and torque must be known in advance, this method is only applicable to plant supervision.

An inexpensive way of measuring torque starts with deriving the speed/time curve during run-up. Given motor torque M and moment of inertia J_M , the dynamic torque/angular acceleration law is

$$M = J_M 2\pi \frac{dn}{dt} \quad \text{or} \quad \frac{dn}{dt} = \frac{M}{2\pi J_M} \quad (11.18)$$

where n is the speed and t is the time at which the speed has reached n . Because J_M is constant, $M \propto dn/dt$. If the function $n(t)$ is known, then M can be derived by differentiating this function with respect to the time (see Figure 11.15). It is the acceleration torque that is being measured. Therefore, in machines in which the friction torque M_R is not negligible, this M_R must be known and the total torque must be corrected by this amount. A prerequisite for accurate measurement is that a fast recording instrument (e.g. a storage oscilloscope) is available. Vibration torques cannot be picked up by this method of measurement.

The necessary upper frequency limit of the speed measuring system is derived approximately from the run-up time:

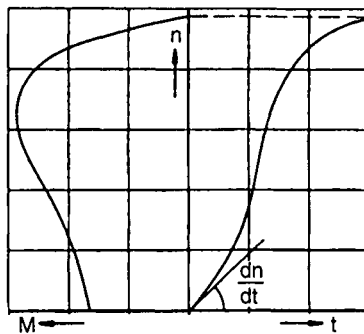


Figure 11.15 Derivation of $M(n)$ from $n(t)$

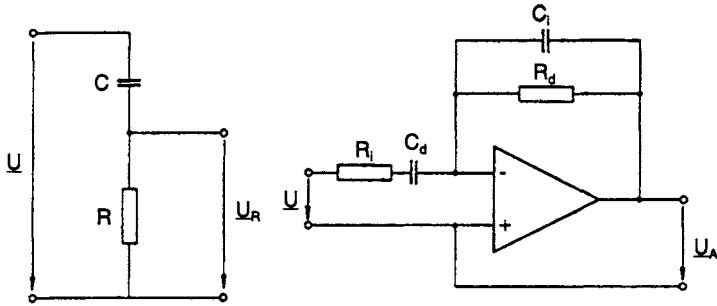


Figure 11.16 *Simple differentiating circuits*
a passive; b active

$$f_g = \frac{1}{t_H} \quad \text{or} \quad \omega_g = \frac{2\pi}{t_H} \tag{11.19}$$

Differentiation with respect to time can either be done digitally via a calculator or by means of a simple passive CR circuit, or by an active op-amp differentiating circuit as shown in Figure 11.16.

Given the input voltage U as shown in Figure 11.16a, the output voltage U_R is derived from:

$$U_R = U \left(\frac{R}{R + 1/j\omega C} \right) = \frac{j\omega RC}{1 + j\omega RC} U \tag{11.20}$$

Let U be derived from the speed n , such that $U = Kn$; and replacing $j\omega n$ with dn/dt gives

$$U_R = KRC \frac{dn}{dt} \frac{1}{1 + j\omega RC}$$

This equation simplifies to $U_R \sim dn/dt$ for frequencies below the boundary frequency $\omega_g = 2\pi f_g$.

For the circuit Figure 11.16b and the conditions $\omega R_i C_i \ll 1$, $\omega R_d C_i \ll 1$ and $\omega R_i C_d \ll 1$,

$$\frac{U_A}{U} = -j\omega R_d C_d \quad \text{or} \quad U_A = -R_d C_d K \frac{dn}{dt}$$

C_i and R_i give the circuit lowpass properties.

In this way the specified values for R and C are chosen.

11.6 Mechanical power

The mechanical power P_m is derived from $P_m = 2\pi nM$. Speed n and torque M are measured as proportional direct voltages by the methods discussed in

Sections 11.4 and 11.5. The necessary multiplication of the two voltages is then effected simply in an analogue multiplier chip.

11.7 Temperature

The thermal performance of a system is an important consideration in the planning of layouts and running conditions. In general, winding temperatures are derived by observing changes in resistance in a DC circuit test. If specific regions within a winding must be examined, e.g. in winding end turns, or in slots, or other parts, temperatures must be measured, so thermocouples are usual.

The thermocouples are usually iron–constantan with a sensitivity of 5.37 mV/100 K or copper–constantan with sensitivity 4.25 mV/100 K. The reference temperature is most conveniently that of melting ice (0°C) in a thermos flask. On account of the possible conductivity of the water, the thermocouples are placed in thin-walled oil-filled tubes. It is also possible to hold the reference temperature source at 0°C by application of the Peltier effect or, in the case of measuring higher temperatures, to hold the reference temperature point at a steady 50°C above ambient temperature.

Direct-reading thermocouple meters are calibrated with 10 Ω or 20 Ω total loop resistance (symbol e.g. $\langle 10$). If the loop resistance is lower, then it should be ‘padded’ to the specified value. More accurate measurements are made by using comparator, zero current circuits, and are thus independent of the connecting conductor lengths. For multi-point measurement and for time-dependent temperature measurement, the thermocouple elements are connected to an appropriate compensated recorder.

11.8 Interference field strength

Accurate interference field strength measurement can be achieved by placing measuring equipment at the source and at the affected area. Qualitative judgement of the effects of screening can be adequately achieved by simply observing the induced voltage in a search coil on an oscilloscope.

Chapter 12

Vibration and noise problems in small drives

Jürgen Draeger

12.1 Introduction

An electric motor, with its magnetically generated parasitic torques, magnetostriction, radial forces of attraction, rotor imbalance and turbulent air flow, is a source of noise and vibration which is transferred via its mountings and couplings to its surroundings. Reduction of vibration transfer and noise propagation in a drive is seen as a figure of merit. It is therefore necessary as a part of quality assessment and control to measure noise and vibration.

The following discussion will therefore concentrate on:

- the definition of sound field quantities
- oscillation measurement
- noise measurement
- vibration excitation and propagation, and also
- vibration and noise reduction.

12.2 Sound field quantities

When parts of an elastic medium are caused to vibrate, then these vibrations are propagated as pressure waves through the medium and, owing to redistribution at boundaries, the waves penetrate into neighbouring media. The pressure waves constitute an acoustic field which spreads out at the speed of sound in the medium. The speed of sound depends on molecular coupling and is dependent on the material. Typical values at 20°C are in air: 343 ms⁻¹, in water: 1440 ms⁻¹ and in steel: 5850 ms⁻¹.

Pressure wave propagation in air and liquid is entirely longitudinal. Solid materials contract transversely when they are stretched and hence transverse waves appear as well and, depending on the excitation, also torsional waves.

Pressure variations in the acoustic field from 2×10^{-5} to 60 Nm^{-2} superimposed on the static pressure (e.g. $1.101325 \times 10^5 \text{ Nm}^{-2}$ for standard atmospheric pressure) and at frequencies between 16 Hz and 20 kHz are recognised by the human ear as:

- tone, when the pressure variations are purely sinusoidal
- musical sound, when harmonically related tones are superimposed, and
- noise, when there is a broadband random set of frequencies.

So that the acoustic field may be discussed and analysed, the variables s = particle displacement, v = particle velocity and p = pressure variation are introduced. Given these, the acoustic power density I may be determined.

For simplicity, the discussion is restricted to one dimension, i.e. to a plane wave normal to the direction of propagation and remote from the source.

The movement of the wave in the x -direction is derived by considering the state of the slice of the medium as shown in Figure 12.1. The net force on the slice, in the direction of x , is

$$pA - \left(pA + \frac{\partial p}{\partial x} \Delta x A \right) = - \frac{\partial p}{\partial x} \Delta x A$$

The mass of the slice is $\rho \Delta x A$.

In accordance with Newton's second law:

$$\text{Force} = \text{Mass} \times \text{Acceleration}$$

it follows that

$$- \frac{\partial p}{\partial x} \Delta x A = \rho \Delta x A \times \frac{\partial^2 s}{\partial t^2} \tag{12.1}$$

or

$$- \frac{\partial p}{\partial x} = \rho \frac{\partial^2 s}{\partial t^2} = \rho \frac{\partial v}{\partial t} \tag{12.2}$$

In the case of a sinusoidal tone, variables s , v and p may be replaced by phasors \mathbf{s} , \mathbf{v} and \mathbf{p} , and the operation $\partial/\partial t$ may be expressed as multiplication by $j\omega$, giving

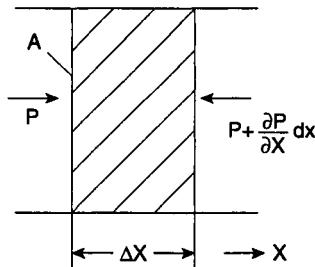


Figure 12.1 *Acoustic pressures on an element of mass*

$$-\frac{\partial \mathbf{p}}{\partial x} = -\omega^2 \rho \mathbf{s} - j\omega \rho \mathbf{v} \quad (12.3)$$

In particular $\mathbf{v} = j\omega \mathbf{s}$, and the particle displacement lags the particle velocity by 90° .

From eqn. 12.3 and given that $\mathbf{s} = s \exp(-j \omega x/c)$ where c is the speed of sound,

$$\begin{aligned} \mathbf{p} &= \omega^2 \rho s \int \exp\left(-j\omega \frac{x}{c}\right) dx \\ \mathbf{p} &= j\omega \rho c \mathbf{s} \end{aligned} \quad (12.4)$$

The pressure is 90° phase advanced on the particle displacement, and is in phase with the particle velocity. It follows that the acoustic power density is

$$I = |\mathbf{p}| |\mathbf{v}| = \omega^2 s^2 \rho c \quad (12.5)$$

It should be noted that the RMS value of s is used in this equation. The threshold of acoustic power density, for it to be audible at $f = 1$ kHz, is $I_0 = 10^{-12} \text{ Wm}^{-2}$.

The relationship, sound pressure/particle velocity, is a constant for a given medium and is expressed as:

$$Z_0 = \frac{\mathbf{p}}{\mathbf{v}} = \rho c \quad (12.6)$$

and is called the acoustic impedance. It governs the reflection of sound waves at interfaces. For air at standard atmospheric pressure $Z_0 = 408 \text{ Nsm}^{-3}$.

When a plane sound wave arrives at the plane surface connecting two media with different acoustic impedances, Z_{01} and Z_{02} , reflection occurs, with reflection factor

$$r = \frac{Z_{02} - Z_{01}}{Z_{02} + Z_{01}} \quad (12.7)$$

This is the relationship between reflected and incident wave pressure. Power density is proportional to the square of the pressure. The proportion of incident power that is reflected is

$$\kappa = \left(\frac{Z_{02} - Z_{01}}{Z_{02} + Z_{01}} \right)^2 \quad (12.8)$$

The sensitivity of the human ear to sound pressure extends over seven decades, and direct comparisons of pressure or power density produce very large numbers. Therefore these quantities are expressed in logarithmic form as ratios, the reference level being the 1 kHz threshold values of $p_0 = 2 \times 10^{-5} \text{ Nm}^{-2}$ and $I_0 = 10^{-12} \text{ Wm}^{-2}$. The sound level L has the unit Bel (B) defined as

$$L = \log \frac{I}{I_0} B \quad \left(\log \frac{I}{I_0} = \log_{10} \frac{I}{I_0} \right) \quad (12.9)$$

or, because $I \approx p^2$,

$$L = \log \left(\frac{p}{p_0} \right)^2 B \quad (12.10)$$

It is usual to express the interval between two levels in the smaller unit, the decibel. Thus

$$L = 10 \log \frac{I}{I_0} = 20 \log \frac{p}{p_0} \text{ dB} \quad (12.11)$$

for example, when $p = p_0$, $L = 0$, and when $p = 10^7 p_0$, $L = 140$ dB.

Because of the logarithmic way of representation, a doubling of the acoustic power does not imply a doubling of the sound level. Furthermore, the rise in sound level is independent of the starting point, and

$$\Delta L = 10 \log \frac{2I}{I_0} - 10 \log \frac{I}{I_0} = 10 \log 2 = 3 \text{ dB} \quad (12.12)$$

When several sources of sound are working together, the resultant sound level at the point of observation is

$$L_{\text{ges}} = 10 \log \frac{\sum I_v}{I_0} \quad (12.13)$$

Thus, the influence of a single noise source with $L < 0.5$ dB is negligibly small when it is more than 9 dB quieter than the rest of the noise. This means, for example, that the disturbance caused by the noise-measuring equipment must lie at least 9 dB below the level of the noise being measured.

To access the total acoustic power emission from a source in given surroundings, the applicable formula is

$$P = \int_S I dS \quad (12.14)$$

in which S is the closed surface surrounding the power source. The acoustic power level L_w is defined as

$$L_w = 10 \log \frac{P}{P_0} \text{ dB} \quad (12.15)$$

where $P_0 = 10^{-12}$ W.

L_w , and consequently the radiated acoustic power

$$P = P_0 10^{\frac{L_w}{10}} \quad (12.16)$$

may be determined from measurements when the sound level is measured at as many points as possible on a defined closed surface S around the source.

Then

$$L_w = 10 \log \frac{\frac{1}{v} \sum I_v}{I_0} + 10 \log \frac{S}{S_0} \text{ dB}$$

where $S_0 = 1 \text{ m}^2$.

12.3 Subjective sensitivity to noise

To create a hearing stimulus, a minimum acoustic pressure is necessary and its magnitude must increase at the lower frequencies. The sensitivity of the ear, therefore, increases with frequency at first. This means that two tones at different frequencies but with the same acoustic power give different impressions of loudness. The impression of the loudness is also dependent on the acoustic power level. A measure of the subjective impression of the loudness, is the phon. By general agreement the physically measured power density and the subjective loudness scales coincide at frequency 1000 Hz. Through tests on many people, the curves of equal loudness, as shown in Figure 12.2, as functions of frequency and power density, have been recorded. From these we can see, for example, that a 100 Hz tone compared with a 1000 Hz tone at ~50 phon has an extra power density of about 8 dB, which means that the acoustic intensity is 6.3 times larger.

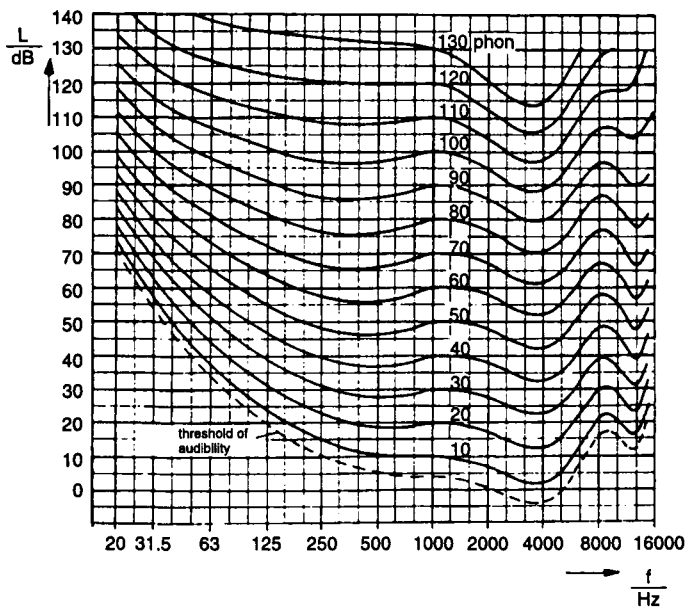


Figure 12.2 Curves of equal loudness level for pure tones

From 40 phon upwards, an increase in loudness of 10 phon is interpreted subjectively as a doubling in loudness. Two equally loud sound sources acting together, therefore, are not interpreted as a doubling in the loudness. A linear relationship between loudness sensitivity and the scale of measurement is given in the loudness unit N sones. The unit sone, $N = 1$, is set at 40 phons and N doubles for each increase of 10 phons. The relationship between loudness sensitivity and loudness is shown in Figure 12.3.

12.4 Noise measurement

The double dependence of loudness level on acoustic pressure and frequency leads to difficulties in the construction of measuring equipment. To simplify matters, a constant displacement independent of frequency is assumed to exist between any two phon curves. Also, to relate measuring equipment readings and human ear response, three measuring ranges, A , B and C are specified and their corresponding weighting curves are defined as shown in Figure 12.4.

Appropriate weighting filters, in the form of electrical networks, are then included in the measuring system, and selected by switching. Curve A corresponds to the phon range up to 60 phon, curve B covers the range 60–90 phon, and curve C is for loudness values beyond 90 phon. When the phon range is known definitely, the appropriate weighting curve can be selected. Curve A is used exclusively for motor loudness measurements, independent of the noise level.

Capacitor microphones are the normal sound measurement transducers. Because of their high internal impedance, they are connected directly to an impedance changing preamplifier.

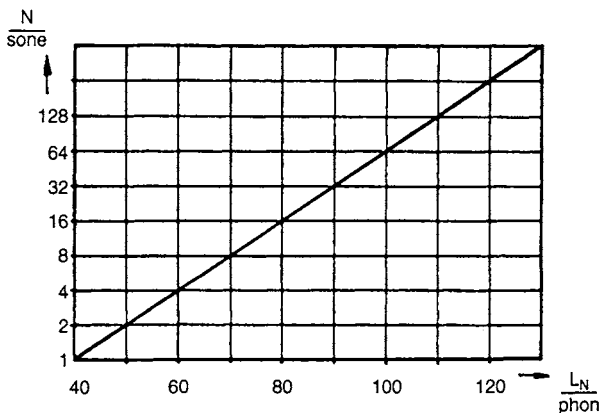


Figure 12.3 Loudness N as a function of the loudness level L_N

Figure 12.5 shows a perspective cutaway view of a capacitor microphone capsule with direct voltage polarisation. Pressure variations cause proportional membrane movement relative to the reference electrode and corresponding capacitance and charge variations.

Taking distortion and mechanical strength into account, microphone membranes can range in diameter from 25 mm (1") for measurements to 145 dB and 18 kHz, to 3 mm (1/8") for measurements to 170 dB and

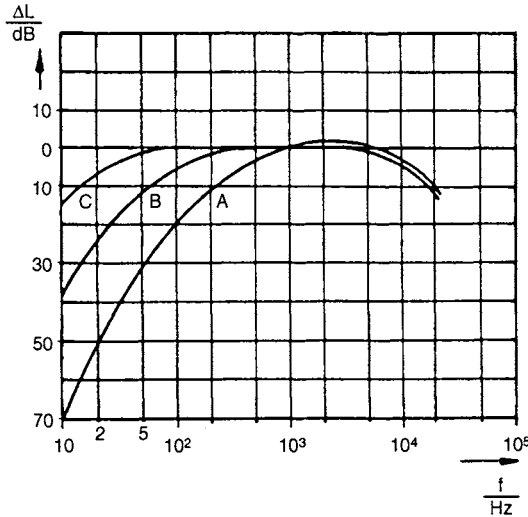


Figure 12.4 Weighting curves for measuring perceived loudness in measuring apparatus in accordance with DIN 45633

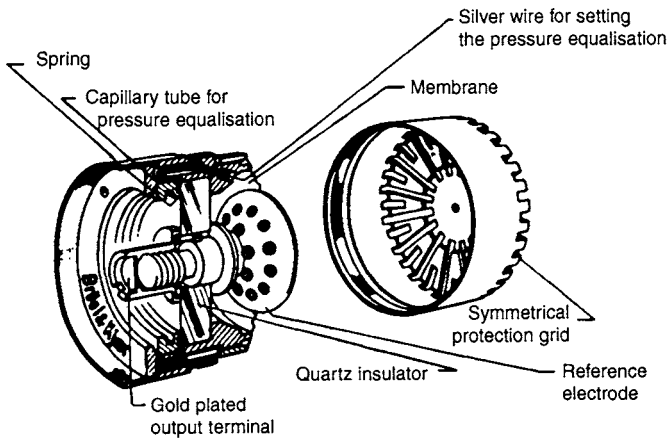


Figure 12.5 Cross-section view of a microphone capsule (Courtesy: Brüel & Kjaer)

140 kHz. Moving coil microphones may be used for simpler measurement purposes. They have the advantage of a low source impedance but are somewhat frequency-dependent. Piezoelectric microphones have particularly uniform frequency/sensitivity characteristics but are easily permanently damaged by overload.

Every microphone distorts the acoustic field in which it is placed, mainly owing to reflections at wavelengths corresponding to the microphone's dimensions, in particular the diaphragm diameter. Therefore, the slimmest possible microphones should be used for high frequency measurements. Microphone sensitivity decreases with decreasing diameter.

In a sound level meter the microphone signal is amplified, weighted, and can be separated into its component frequencies (frequency bands) with in-built or external filters. A simple evaluation is possible by recording the magnitudes on a plotter.

Tape recorders provide a convenient means for reproducing the sounds at will. Sound level measurements may be carried out in anechoic rooms, as shown in Figure 12.6, or – when the objects are small – in cabins with specially treated surfaces. The background noise level must be at least 10 dB below the noise to be measured.

Noise power measurements may be measured in rooms with hard reflective surfaces or in any room with a known reverberation time. Meaningful measurement procedures for the purposes of testing to a specification are laid down in the appropriate national standards (BSS, NBS, DIN, etc.). Microphones being used for measuring purposes, together with their processing equipment, must be calibrated from time to time against laboratory standards (e.g. piston microphone).

12.5 Vibration (oscillation) measurement

Vibration measurement takes the form of structural-borne noise measurement by means of piezoelectric accelerometers. Figure 12.7 shows cutaway views of two different accelerometers in which seismic masses produce acceleration-derived pressure variations in piezoelectric crystals, which in turn produce proportional measurable electric fields at the crystal surfaces.

The lowest measurable frequency in a transducer for measurements in small drives with a mass of 0.7–30 g is ~0.1 Hz, and its resonant frequency lies between 25 and 85 kHz. Attachment to the point of measurement is by adhesive, screws or magnetic feet. A preamplifier is directly connected to the high impedance transducer. The signal is then passed via coaxial cable to amplifying equipment which includes integrators for deriving velocity and displacement at the input.

An adequate frequency analysis of the vibration source being examined is achieved by in-built or external octave or third-octave bandpass filters.



Figure 12.6 Anechoic room

Vibration measurements are normally carried out in order to assess the types of vibration and to determine their resonant frequencies and their transmission. To this end, the various resonances (modes) may be determined with the aid of FFT and mode analysis in a single series of measurements. In addition, a number of impacts are applied to a network of input points and the effects measured at the hammer head as well as the vibration accelerations in the excited modes at a fixed reference point. Both measured values at the various excited resonance frequencies are processed in a computer and displayed as natural resonant frequencies on a monitor.

Particular interest is taken in the examination of vibration transmission from the feet of a motor and the mounting points on, say, the bedplate between which some form of vibration absorption device is fitted. The amplitudes and relative phase of the two vibrations need to be determined. This is achieved with two vibration accelerometers whose outputs are filtered down to two harmonic signals at the same frequency. The two signals may then be compared on a two-beam oscilloscope, or applied to the X and Y

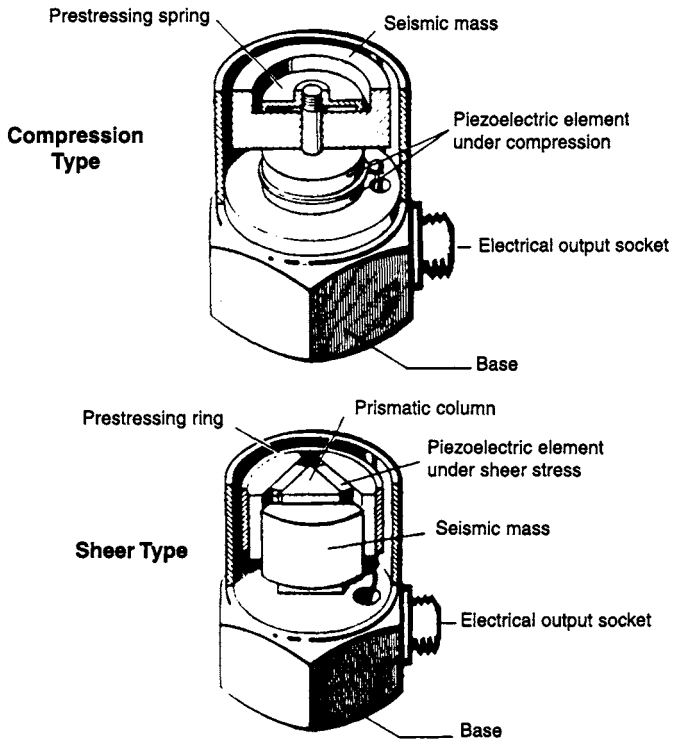


Figure 12.7 Cross-section pictures of acceleration transducers
(Courtesy: Brüel & Kjaer)

deflection inputs of a single-beam oscilloscope to produce the Lissajous figure ellipse, from which the relative amplitudes and phase angle may be determined.

From Figure 12.8,

$$\frac{a}{b} = \sin \varphi$$

or
$$\varphi = \sin^{-1} \frac{a}{b}$$

When:

$$\varphi = 0, \pi, \dots,$$

the figure is a straight line; when

$$\varphi = \frac{\pi}{2}, \frac{3\pi}{2}, \dots$$

(resonance) the figure is an ellipse whose major and minor axes lie on the X and Y axes.

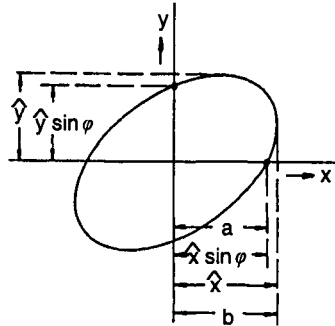


Figure 12.8 Determination of the phase shift from a Lissajous figure

12.6 Vibration and noise excitation

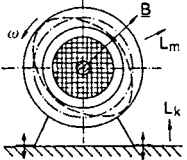
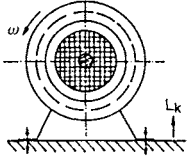
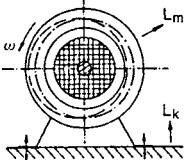
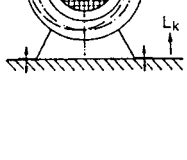
Causes of noise generation in electrical apparatus are deformations and angular oscillations in the motor and its load, which are transferred to neighbouring structures through couplings. In some circumstances, fans add to the noise. Their origins – through radial forces of attraction in the airgap, vibrating torques which are developed electrically or in the driven load, magnetostrictive induced changes in dimensions, imperfect dynamic balance, brush vibrations and bearing noises – are many and various. Causes and effects are listed and described in Table 12.1.

The radiation properties of a noise generator are strongly influenced by the possibility of pressure equalisation tangential to the generator's outer surface. They are dependent on the forms of vibrations from the source and the relationships between the wavelengths λ of the sounds generated and the dimensions L_u of the generator's surroundings. Figure 12.9 shows the vibration modes of order r (r being the number of nodal axes) of a cylindrical vibrator. Pressure balance occurs at the nodal point between pressure maxima and minima. Therefore the noise resulting from flexural vibrations in a freely suspended motor is very little. The situation is less favourable when the noise-radiating surface of the driven load is significantly increased by coupling to a larger structure or by a relatively large outer case area.

The motor housing as well as the components that are mechanically coupled to the motor, with their various elasticities and mass distributions, form a configuration susceptible to mechanical vibrations. Any correspondence between the vibration frequencies generated and the natural vibration modes of a flexible system, whether approximate or exact, results in greatly increased vibration amplitudes and consequently a clear increase in the noise radiated through resonances, as is shown in Figure 12.10.

In the resonance region, the phase relationship of a vibrating damped system relative to the excitation, rises steadily from $\varphi = 0$ below the resonant frequency f_r to $\varphi = \pi$ above the resonant frequency. At the resonant frequency f_r , $\varphi = \pi/2$.

Table 12.1 Noise excitation and its causes

Cause	Resultant noise	Deformation
1 Radial tensile forces	Periodic stator deformation. Dependent on speed and number of poles. Excitation of L_m and L_k over the foot mountings.	
2 (a) Electrically developed vibrating torques (elliptic rotating field or ripple current)	Periodic concentric torsion in the motor frame, dependent on speed and ripple current frequency in DC machines. In AC machines, the torques are at double the mains frequency. Excitation of L_m over the foot mountings	
(b) Vibrating torques owing to uneven load torque	Vibrations in sympathy	
3 Magnetostriction	Periodic stator deformation owing to magnetostrictive strains. Excitation of L_m and L_k	
4 Imbalance	Periodic frame displacement dependent on speed. L_m and L_k via the foot mountings	
5 Bearings	Bearing vibrations, only partially dependent on speed. Transmission as structural borne noise as L_m in the machine in general and as L_k over the bearing housings. $f = 1-10$ kHz	
6 Brushes	Brush vibrations transmitted via the brush holders as structural borne noise into the machine in general, and as L_k via the bearing housings. Characterised by the product of speed and number of commutator bars. In general, only partially dependent on speed and in the frequency range 600-16,000 kHz.	
7 Fan	Development of air-borne noise at the fan as L_m . Speed-dependent. $f = 200-6000$ Hz	
8 Slots	Siren noise L_m owing to turbulent air flow. Frequency = speed \times number of slots	

L_m = sound level radiated from the motor

L_k = sound level from the structures connected to the motor

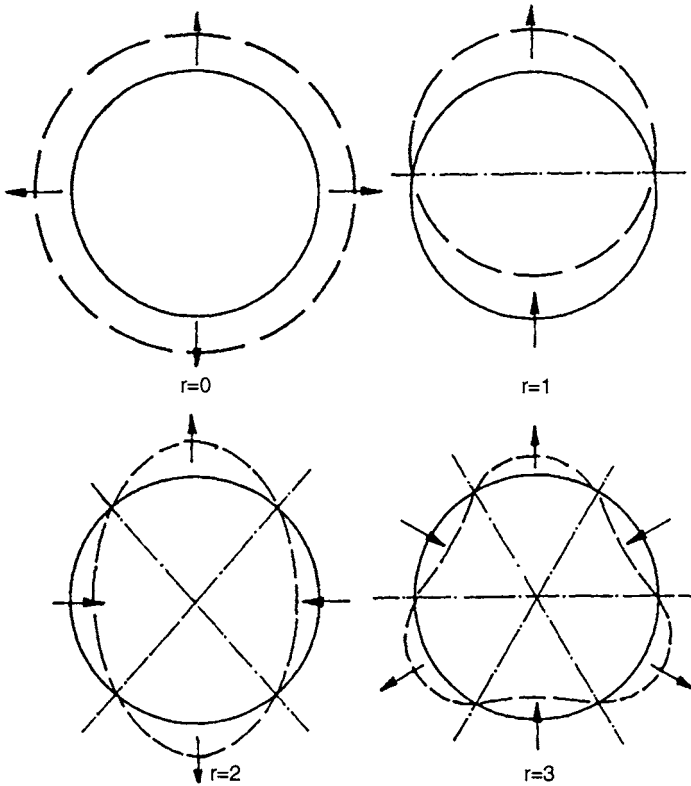


Figure 12.9 Vibration modes of a cylindrical radiator

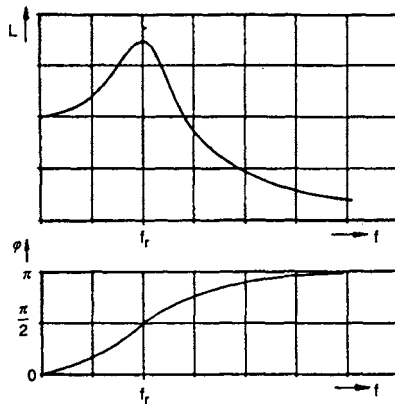


Figure 12.10 Noise increase of a simple damped vibrator and its phase angle ϕ relative to its excitation at resonance

12.7 Vibration and noise reduction

12.7.1 *Methods at the noise source*

All considerations regarding the manufacture of a low noise drive begin at the noise source, first with the selection of a suitably dimensioned motor and then with special attention to noise generating component parts.

For every type of machine an effective way of reducing causes 1–3 of Table 12.1 is to keep the airgap and stator fluxes as low as possible. This leads, however, to relatively large machine dimensions. Vibration torques induced in the motor are avoided through the choice of machine in which the torque developed is independent of the rotor position. This is achieved with a symmetrical polyphase supply connected to a symmetrically built multiphase induction motor, and to almost the same extent in a DC machine whose number of slots is not too small. It is not so successfully achieved in a single-phase c-sar induction motor which runs symmetrically at one working point only, nor for a brushless DC motor on account of its limited number of stator coils. Where ball bearings must be used instead of plain bearings, the use of specially selected low noise bearings must be considered.

Commutator noise may be reduced by chamfering the commutator bar edges and ensuring that the brush mass/spring system is excited at well below its mechanical resonant frequency. It is very difficult to limit the airspeed-dependent airborne noise generated in motor fans.

All measures taken at the noise source demand an increase in the quantity and quality of the construction materials. Such measures are generally expensive and require (in as far as the choice of machine and its noise-generating parts – for example, the commutator – permits) further noise-reducing means of preventing the sound from spreading. When such supplementary means of noise reduction become necessary, it is often more economical to replace what appears to be a bargain-priced motor by a more expensive but better one. An example is the replacement of a less than ideal shaded-pole motor in an audio recorder by a simply controlled single-winding commutatorless motor for the same purpose.

Supplementary means of preventing the spread of noise are discussed in the following sections.

12.7.2 *Insulation and vibration isolation*

Techniques by which the reduction of radiated noise or vibration energy results in no conversion of mechanical energy into another form of energy are called insulation.

As discussed in Section 12.2, a reflection of sound energy occurs at the interface between two media with acoustic impedances Z_{02} and Z_{01} in accordance with the power reflection factor (eqn. 12.8)

$$\kappa = \left(\frac{Z_{02} - Z_{01}}{Z_{02} + Z_{01}} \right)^2 \quad (12.17)$$

when $Z_{01} \neq Z_{02}$.

κ is large when $Z_{02} \gg Z_{01}$ or $Z_{02} \gg Z_{01}$.

In accordance with eqn. 12.6,

$$Z_0 = \rho c \quad (12.18)$$

so suitably heavy walls (steel, stone, etc.) around an airspace or a soft layer (air, elastic padding) around a solid filled space act as sound barriers.

The factor for sound insulation R depends on the relationship between the energy incident on an interface and that which penetrates into the adjacent medium:

$$R = 10 \log \frac{1}{1 - \kappa} \text{ dB} \quad (12.19)$$

At, for instance, an air-steel interface, for which

$$Z_{0, \text{air}} = 408 \text{ Nsm}^{-3} \quad Z_{0, \text{steel}} = 45.6 \times 10^6 \text{ Nsm}^{-3}$$

$$\kappa = 0.999964$$

and hence $R = 44.4$ dB.

The thickness d of the insulating (steel) wall is usually much less than the wavelength λ of the incident sound waves ($d \ll \lambda$), so that the wall vibrates practically in phase with the sound (simple wall). In this case the wall can be considered as a homogenous vibrating mass which has mass M per unit of surface area. The resulting factor for sound insulation for an arbitrarily deep air compartment in front of the wall is shown in Figure 12.11 as $R(f)$ with M given as a parameter. The quoted values are not achieved in practice because:

- a thin flexible wall experiences vibration modes that reduce the sound insulation considerably
- an in-phase vibrating wall together with the vibration source and the intervening airspace form an oscillatory spring mass system which produces resonance effects.

These negative influences on the effectiveness of the insulation may be extensively countered by the use of flexible heavy walls with large internal damping (plastic, rubber with metal inserts, sandwich plates) and by the deepest possible air compartments. The factor for sound insulation when the spring stiffness of the air compartment between the noise source and the insulating wall cannot be neglected, assuming that damping may be neglected, is:

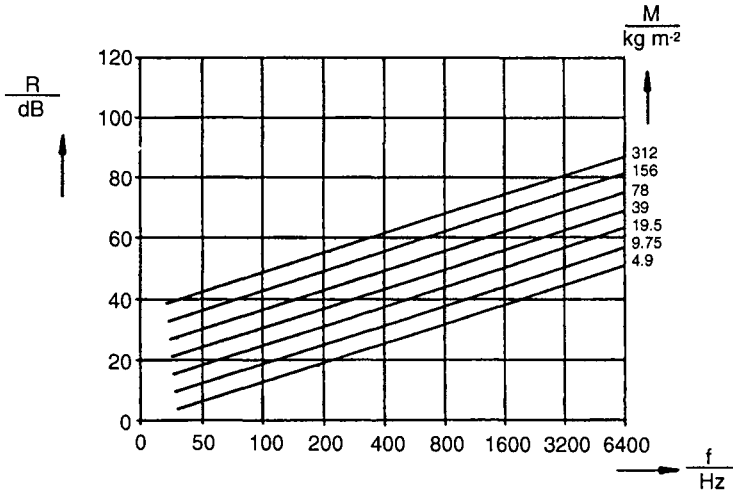


Figure 12.11 The factor for sound insulation $R(f)$ of a simple wall with M as a parameter

$$R = 20 \log \left[\left| 1 - \left(\frac{f}{f_r} \right)^2 \right| \right] \text{ dB} \tag{12.20}$$

where the resonant frequency f_r is

$$f_r = \frac{1}{2\pi} \sqrt{\frac{c^2 \rho_L}{Ml}} \tag{12.21}$$

where ρ_L is the specific density of air, c is the velocity of sound in air and l is the distance between the noise source and the insulating wall.

In Figure 12.12 the function $R(f/f_r)$ of eqn. 12.20 is shown graphically. Furthermore the dimensions of small drives are generally so small compared with the wavelengths of the vibration tones that the machine parts vibrate in phase both radially and tangentially. Thus the stator and rotor of a machine may be considered to be homogenous masses, each with its moment of inertia J , the tangential vibration torques transmitting vibrations to their surroundings, the stator via its mountings and the shaft to the load.

If appropriate elastic elements (rubber buffers, springs) are installed between the motor and its bedplate and its load, the components beyond these elastic couplings are for the most part insulated (vibration insulation).

An appreciation of the effect of vibration insulating coupling members with torsional stiffness C_d is gained from Figure 12.13. J_M can be the moment of inertia of the motor rotor and J_T that of the load, or J_M can be the moment of inertia of the motor stator and J_T the effective moment of inertia of the

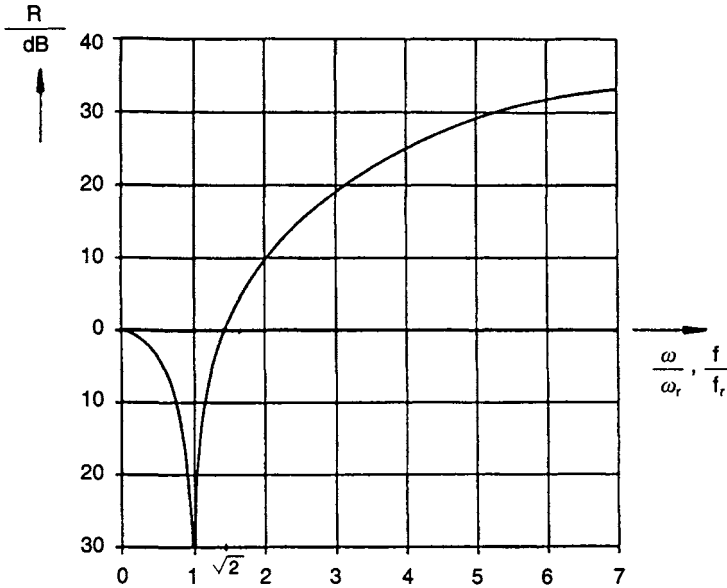


Figure 12.12 Sound insulation $R\left(\frac{f}{f_r}\right), R\left(\frac{\omega}{\omega_r}\right)$

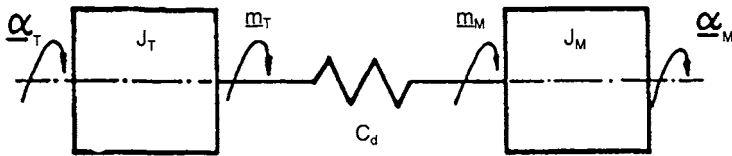


Figure 12.13 Equivalent mechanical system for the induced vibrations in a 2-mass system

structure to which the stator is connected via its mountings. If the system is undamped, then the relation between the vibrating torque m_T developed in the load and the vibrating torque m_M generated by the motor at angular velocity $\omega = 2\pi f$ is

$$\frac{m_T}{m_M} = \frac{C_d}{J_M \omega_r^2} \frac{1}{1 - \left(\frac{\omega}{\omega_r}\right)^2} \tag{12.22}$$

where

$$\omega_r = \sqrt{C_d \left(\frac{1}{J_M} + \frac{1}{J_T}\right)} \tag{12.23}$$

is the natural frequency of the system. Figure 12.14 shows the function

$$\frac{m_T}{m_M} \left(\frac{\omega}{\omega_r} \right)$$

of eqn. 12.22 in graphical form. The transmitted vibration is seen to be small when $\omega \gg \omega_r$. This means that ω_r must be as small as possible. This requirement is met when the couplings are soft (C_d small) and the coupled moment of inertia J_T is large. Note that the ordinates (vertical axis functions) of the graphs of Figure 12.12 and Figure 12.14 have inverse (reciprocal) properties.

For example, when $\omega \approx 5\omega_r$ the load excitation is reduced by about 27 dB. If the motor derived vibrating torques are speed-dependent, then, in a low frequency tuned system when the system is accelerating through the resonance point, greatly increased vibrations are transmitted and result in high noise levels. Therefore it becomes necessary to use damped elastic members in such cases (rubber elements, all metal dampers, no steel springs). Then, for a given damping coefficient, the resonant frequency is less noticeable.

12.7.3 Sound damping

Techniques that convert sound and vibration energy into thermal energy are called damping. They provide sound reduction particularly in enclosed rooms and along ducts (e.g. for cooling).

So that the sound energy can penetrate into the sound-absorbing material, the material's acoustic impedance should not be more than twice that of air. The proportion of incident acoustic power α that is absorbed is related to the power reflection factor κ by the equation

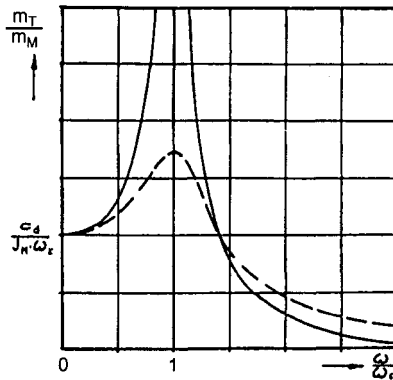


Figure 12.14 $\frac{m_T}{m_M} \left(\frac{\omega}{\omega_r} \right)$
 — without damping
 - - - with damping

$$\alpha = 1 - \kappa \quad (12.24)$$

The term α includes that proportion of the power that penetrates through the damping layer. The relationship between the penetrating power intensity I_p and the incident power I_i is defined as

$$\tau = \frac{I_p}{I_i} \quad (12.25)$$

Finally, the sound dissipation level

$$\delta = \alpha - \tau \quad (12.26)$$

is taken into account for deriving the energy conversion equation. This is now

$$\kappa + \tau + \delta = 1 \quad (12.27)$$

In sound-absorbing material the heat arises owing to deformation and internal friction and to external friction with vibrating air in the structure of porous materials. Normally porous foam or mineral fibre materials are used. If sound absorption is to be reasonably successful, the thickness of the damping layer should be of the order of a quarter of the wavelength of the incident sound. At the very least, the damping layer must be where the air particle velocity is greatest, i.e. at a quarter of a wavelength $\lambda/4$ from a reflecting wall, as the standing wave pattern of Figure 12.15 shows.

Low frequency sound damping measures, therefore, demand a lot of space. Low frequency vibrations can be reduced effectively. If one takes care of large amplitudes by means of the resonant effects of friction within the vibrating media, the damping effect is increased.

If openings are unavoidable, then for broadband radiated audio spectra, damping layers can be placed along the length of the ducts as shown in Figure 12.16. The opening width W must not exceed the wavelength λ of the sound components, which must be damped effectively. Where necessary the channel must be subdivided by damping layers. The diagram in Figure 12.16 shows the frequency spectra outside a channel with various damping means as examples. When the opening width W is too large, the damping is ineffective at higher frequencies.

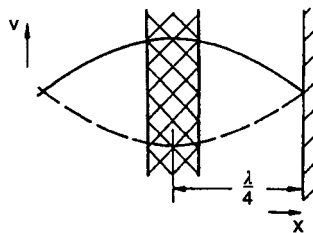


Figure 12.15 Positioning an absorbing layer in front of a wall

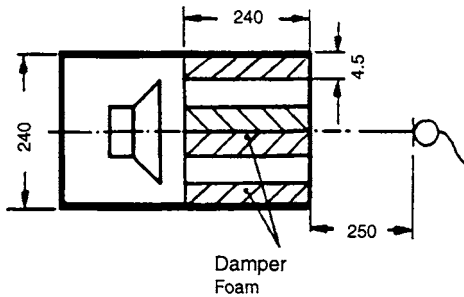
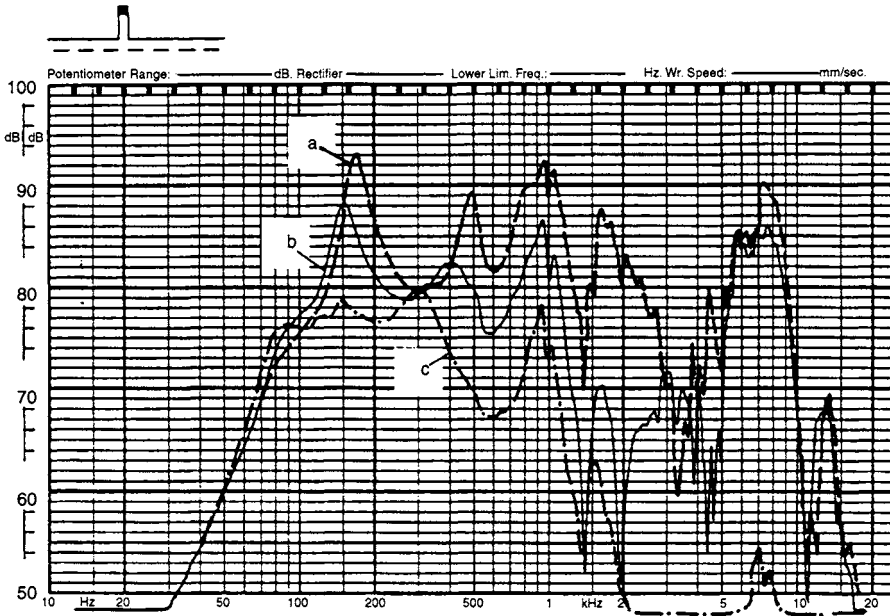


Figure 12.16 Frequency response of a sound-filled channel
a Without damping material
b With wall insulation
c With wall insulation also on a channel divider

If the sound propagated along the channel is narrowband or a single tone, then its walls may be lined with Helmholtz resonators as illustrated in Figure 12.17. They comprise relatively large air compartments working as springs and are open to the channel via long fine-bored holes. The relatively incompressible air in the bored holes acts as a link, forming a vibrating system with the air compartment acting as the spring. The vibration is in antiphase with the excitation at frequencies above resonance. Consequently, as Figure 12.17 shows, an effective reduction in sound level is achieved through sound pressure interference. If the walls are lined with damping material as well, the noise reduction becomes broadband.

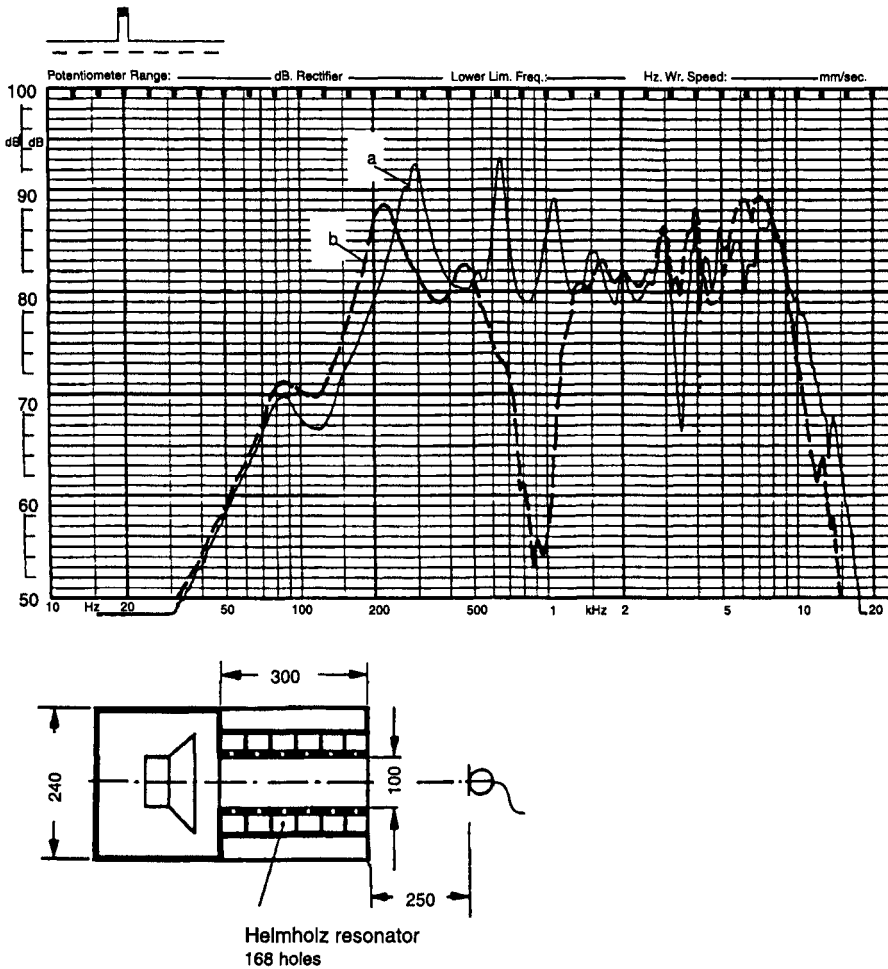


Figure 12.17 Frequency response of a lined channel
 a Without Helmholtz resonators
 b With Helmholtz resonators

12.7.4 Technical solutions

After the choice of the motor for a drive application has been made, the measures for reducing noise and vibrations are principally as follows:

- mounting the drive on the heaviest and stiffest possible frame
- correct angular mounting on the frame plate so that the vibration stimulus is in the plane of the plate and not at right angles to it
- avoidance of resonance excitations from parts of the machine construction (e.g. stator stamping shape) by the introduction of connecting bridges in large-area parts or by the inclusion of supplementary masses (e.g. antivibration coatings).

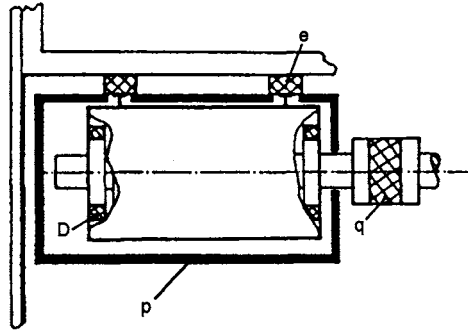


Figure 12.18 *Motor isolation*

- interruption of the structural vibration paths by using insulation and damping between the drive and the surrounding structures in accordance with Figure 12.18.
- (a) Casings are connected to the support structures by elastic elements (*e*) with internal damping (rubber, plastic). The natural frequency of the motor mass/spring system should be below one-fifth of the lowest exciting frequency.
- (b) The motor is elastically coupled (*q*) to its load (spring couplings, rubber or plastic tube, rubber bands). For specific 'below-resonance' applications it can become necessary to increase the rotating mass of the load through the addition of flywheels (record players, film apparatus). In some cases, where vibrating torques developed in the load are transferred back to the motor, the additional rotating mass should be coupled to the motor side of the drive.
- (c) When it is not possible to use low noise plain bearings, the ball bearings may be mounted elastically (*D*) in the bearing housing. In machines with small airgaps (induction motors) this is not possible.
- (d) If necessary, the motor or the complete drive may be totally enclosed (*p*) by relatively heavy sound-insulating material. The inner wall of the capsule can be lined with damping material in order to reduce standing waves.
The capsule should be connected to the motor in a vibration-free manner.

Further points to be noted are:

- When brushes are used, the vibration frequency of the brush mass/retaining spring system should be sufficiently low.
- The space surrounding the drive should be closed as far as possible with sound damping material. Ideally, flexibly soft or damped plates (sandwich plates) should be used.

- When openings are necessary, for cooling, for example, sound-absorbing materials can be laid parallel with the air flow.
- Large hollow spaces should be provided with surface coverings to absorb the standing waves.

In small drive applications, effective solutions are greatly influenced by design solutions for larger drives, and are correspondingly many and various.

Index

- accuracy of A/D conversion 244
- accuracy of measurement 244
- acoustic power 266
- actuator 14
- airgap 104
- airgap
 - extension 68
 - width 24
- alternating field 18, 20
 - tachometer 247
- analogue speed measurement 246
- analogue to digital converter 244
- anechoic room 271
- angular velocity 6
- armature
 - current 110, 115
 - reaction 106, 133
 - winding 105
- auxiliary phase current 52f

- balancing (two phases) 39
- basic equations of the brushless
 - DC motor 168f
- bilevel circuit 220
- bipolar control switching 215
- boundary frequency 242, 249
- bridge circuit 158
- brush
 - lifetime 121
 - sparking 111
 - types 115
 - voltage drop 108
 - wear 115
- brushes 115
- brushless DC linear motor
 - with moving coil 188
 - with unipole armature 189
- brushless DC motor 165
 - lifetime 191
 - with auxiliary frequency transformer 167
 - with single-coil stator winding 167
- capacitive transducer 253
- capacitor
 - microphone 269
 - motor 39
 - start motor 46, 59, 60
 - voltage 41, 53
- carrier frequency 256
- central heating circulating pump 1
- characteristics
 - of the brushless DC motor 173
 - of the DC motor 133
- circular rotating field 20
- closed-loop operation 225
- coil former 77
- commutation 111
 - current 111
 - duration 111
 - problems in DC motors 134
- commutator 103, 106, 111
 - bars 103
- commutator machine 103

- contact voltage 113, 114
- correction factor 257
- csar motor
 - three windings 46, 55
 - two windings 46f, 52
- current behaviour 29
- current reversal voltage (commutation) 111, 114

- damping 265
- DC linear motor
 - with armature coil 125
 - with permanent magnet armature and concentrated stator winding 127
 - with permanent magnet armature and distributed stator winding 126
 - with pole teeth 190
 - without commutator 125
- DC motor
 - with cup rotor 139
 - with cylindrical iron rotor and permanent magnet shells 129
 - with triple-T armature 137
- DC tachometer 247
- design variations on brushless DC motors 173
- differentiating circuit 260
- direct drive for disc stores 184
- direct field tachometer 247
- direct methods 254
- direction of rotation 56
- discharge pump 76
- discharge tube stroboscope 251
- double capacitor motor 41, 46, 61
- driven device 5
- dust extractor hood 78
- dynamic
 - basic law 260
 - measurement error 249
 - speed measurement 249

- eddy current
 - brake 255
 - tachometer 248
- efficiency 59, 73f, 110
- electromagnetic transducer 252

- electronic component 145
- elliptic rotating field 20, 28, 47
- equivalent circuit 30, 107
 - for a winding element 169
 - of the series motor 107
- equivalent magnitudes 30
- evaluation curve 269
- externally started motor 37

- FFT analysis 245, 271
- field components 18
- field distribution 67f
- field effect transistor (FET) 150
- field excitation winding 106
- force on a conductor in a magnetic field 124
- four coil brushless DC motor 180
- Fourier series 242
- frequency changer 24
- frequency spectrum 243

- gramophone, disc direct drive 183

- harmonic field torque 69
- harmonic fields 67f
- heat power 8
- Helmholz resonator 283
- hysteresis angle 89

- IGBT 147
- impulse hammer 271
- incremental speed measuring methods 246
- indirect methods 259
- induction
 - distribution 18, 106
 - machine 18
 - motor 17
- input voltage selection (series-parallel connections) 77
- integrated circuit 153
- interference field strength measurement 261
- interference level 266
- internal rotor
 - with airgap winding 178
 - with slotted stator 181
- inverse rotating field 29
- iron losses 73

- Kloss formula 28
- leakage flux 66, 74
 - bridge 70
- linear motor
 - with long stator 15
 - with short stator 15
- Lissajous figure 273
- longitudinal axis 107
- loss distribution 73
- loudness 269
- loudness level 268
- magnetic field transducer 252
- main phase current 51f
- main pole 66
- measurement errors 249f, 257
- measurement field 250
- measuring
 - motor 142
 - time 249
 - torque 251
- mechanical power 25, 108, 260
 - drawn from the shaft 5
- microstep
 - control 159
 - drive 225
- modal analysis 271
- moment of inertia 6
- motor
 - efficiency 5
 - speed 5
 - vibration torque 259
 - windings with varying coil numbers 175
 - with disc rotor 138
 - with flux concentration 138
 - with resistive auxiliary phase coil 38
- motors with disc stators 183
- multicoil winding 21
- natural vibration mode 271
- neutral zone 106, 111
- noise
 - excitation 273
 - measurement 268
 - reduction 276
 - sensitivity 267
- off-load run-up acceleration 259
- oil-burner motor 1
- operating characteristics 51, 70, 115
 - of a squirrel cage induction motor 32
 - of a universal motor 115
- operating performance 51, 72
- oscillation form 275
- oscillation free halt 213
- overcommutation 112
- particle displacement 265
- particle velocity 265
- permanent magnet 83
 - material 84
 - circuit 83
- phase changer 24
- phase-shift control 154
- phasor diagram of a loaded universal motor 109
- phon 267
- photocopiers 64
- photoelectric transducer 253
- plastic coil former 77
- pole, distribution 19
- pole-pair number 18,103
- position indicator 176
- power
 - data 71
 - distribution 25
 - factor 116
- pressure sensor 258
- primary current diagram 31
- production quantities of small motors 5
- production value of electric motors 4
- PTC (positive temperature coefficient) resistors 57
- pull-out (stall)
 - slip 28
 - torque 28
- radiated acoustic power 266
- radio and TV interference
 - suppression 120
- reflection coefficient 365, 277
- reflection factor 265

- refrigerating apparatus 77
- reluctance rotor 90
- resistive auxiliary phase motor 46, 59
- resonance 273
- resonant frequency 257, 278
- RMS value 244
- rotating field 18f
- rotating field speed 24
- rotor resistance 75
- rotor rotating field power 25
- run-up 258

- saddle torque 27
- sampling
 - frequency 242
 - theorem 242, 246
- secondary winding 77
- self-holding torque 203
- shaded pole 65f
 - contour 76
 - motor stampings 69
 - resistance 76
- short-circuit rotor motor 24
- Siemosyn motor 90
- single-phase
 - capacitor motor 1
 - motor 37
 - synchronous motor with shaded poles 94
- slip 25
- slip-ring rotor motor 24
- small motor function principles 11
- sound
 - absorption coefficient 281
 - alternating pressure 265
 - characteristic impedance 265
 - dissipation coefficient 281
 - field magnitude 264
 - insulation 276f
 - intensity 265
 - level 265
 - transmission coefficient 280
- space vector 19
- speed
 - control 176
 - of sound 263
 - setting 117, 135, 176
 - possibility 34
- spinner 78
- split casing 61
- staircase function 244
- starting torque 27, 38, 41, 72
- static load angle 203
- static torque curve 199
- stator rotating field power 25
- Steinmetz circuit 42, 55
- step angle division 225
- structural-borne noise microphone 272
- switching control drive 219
- symmetrical components 48f
- symmetrical drive 51
- synchronous motor
 - types 81, 90
 - with external hysteresis rotor 96
 - with hysteresis rotor 88
 - with permanent magnet rotors and capacitor auxiliary phase 91
 - with permanent magnet rotors 85

- tachometer 247
- temperature 261
- temperature coefficient 246
- thermo element 261
- threshold value 265f
- thyristor 146
- torque 6, 109
 - development 25
 - during run-up 170
 - saddle 74
 - transducer 256
- torque–speed characteristic 115
- torsion measuring shaft 259
- torsional resonance 256
- total loss methods 254
- transformation ratio 39
- transistor 148f
- transverse axis 107
- travelling wave motor 14
- two-coil motor 185
- two-level winding 103
- two-pole alternating field synchronous motor 96
- under commutation 112

- unipolar
 - control circuit 214
 - generator 247
- universal motor 103

- vibrating torque 29, 41, 72
 - at double the mains frequency 50
- vibration
 - excitation 273
 - isolation 51, 76, 276, 278
 - isolation methods 278

- measurement 271
- reduction 276
- torque 38
- voltage change 70

- washing machine drive 61
- winding and commutator of a DC motor 129
- winding conformity 74
- winding path current 26, 29
- winding tapping 77

SMALL ELECTRIC MOTORS

Users of small electric motors face the difficult task of selecting the best motor for their particular drive application. The technical requirements of the drive, the level of safety needed and the cost factor must all be considered. The choice is made more difficult by the continuous arrival of newly developed types of motor. This book, a translation from German, aims to help those involved in specifying, developing, manufacturing and marketing small motors by reporting the current state of the art.

The various types of motor, together with their differing characteristics and their relationship to small drives are covered. Developments such as brushless DC motors and stepper motors are discussed, as well as the use of electronic control which widens the spectrum of small motor applications. Also covered are measurement and noise problems.

This book will be of interest to engineers, physicists and technicians involved in the design, manufacture and application of small motors in the laboratory, the factory and in service.

The Institution of Electrical Engineers
Michael Faraday House, Six Hills Way
Stevenage, Herts., SG1 2AY
United Kingdom

ISBN 0 85296 921 X

Printed in the United Kingdom

